CHEMICAL REVIEWS

Review

pubs.acs.org/CR

Tropospheric Aqueous-Phase Chemistry: Kinetics, Mechanisms, and Its Coupling to a Changing Gas Phase

Hartmut Herrmann,* Thomas Schaefer, Andreas Tilgner, Sarah A. Styler, Christian Weller, Monique Teich, and Tobias Otto

Atmospheric Chemistry Department (ACD), Leibniz Institute for Tropospheric Research (TROPOS), Permoserstraße 15, 04318 Leipzig, Germany

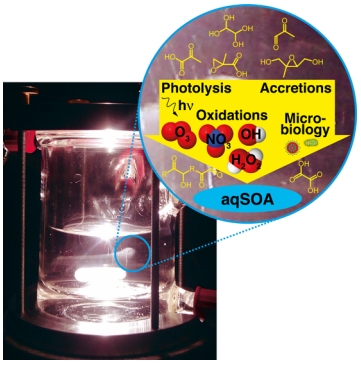

CONTENTS

Special Issue: 2015 Chemistry in Climate

Received: August 15, 2014
Published: May 7, 2015

DOI: 10.1021/cr500447k
Chem. Rev. 2015, 115, 4259−4334

1. INTRODUCTION AND OVERVIEW OF THE FIELD

This Review aims to summarize the current understanding of bulk tropospheric aqueous-phase chemistry. Because a complete review of all developments in this area would be impossible, the present contribution focuses on the compilation of kinetic data and the discussion of mechanistic and analytical information, emphasizing studies performed since the last overviews of this topic, which were published in 2010[1] and 2011.[2]

Short discussions of links to field studies and modeling are included, but these areas are not extensively reviewed here; for aqueous-phase modeling the reader is referred to the contribution of Ervens in this issue of *Chemical Reviews*. Similarly, interfacial processes are not the subject of this contribution as they are treated in the contribution by George et al. Uptake of gas-phase species into liquids will be treated by referencing to very recent other review material in this area.

In the following, a very condensed historic sketch of the development of the field of this Review, atmospheric aqueous-phase chemistry, is given; the authors hope that this, together with the cited references, will be helpful for those entering into the field. This area of research has developed rapidly since the early 1980s, when the landmark review of Graedel and Weschler[3] appeared. At that time, aqueous-phase chemistry was identified to conclude acid generation, as hydrogen peroxide and ozone are generated by active gas-phase chemistry, which then efficiently oxidize most SO_2 in cloud droplets as outlined by Calvert et al. in their 1985 key *Nature* paper.[4] The corresponding chemical mechanisms RADM2, RACM, and RACM2 have been very widely used; see Goliff et al. (2013) and references therein.[5] In this context, many aqueous-phase studies focused on the multiphase oxidation of sulfur from fossil fuel combustion, which, to a large extent, occurs in cloud droplets. Sulfur oxidation has been well-summarized by Brandt and van Eldik.[6] There are still many open questions regarding sulfate production under very polluted conditions, such as those met in China.[7] Current studies discuss whether aerosol chemical conversions, perhaps with contributions from transition metal ion (TMI) chemistry, might take place and contribute to particle sulfate formation.[7−9] This brief illustration is to show that very basic questions in atmospheric research are not fully understood, even if they have extreme environmental consequences. According to the scope of the present volume, the science field of aqueous and multiphase atmospheric chemistry needs to strive to reach better process understanding. Only this will lead to the development of predictive capabilities as necessary when pollution of the atmosphere might represent a threat to human health and the intactness of ecosystems while our planet, as a whole, undergoes substantial changes.

Early efforts in modeling tropospheric aqueous-phase chemistry were undertaken by D. Jacob and the group of M. Hoffmann,[10] initially in the context of California fog. Later, less specific systems such as remote clouds[11] were treated. At that time, in the later 1980s, various detailed aqueous-phase chemistry studies of inorganic systems, often with radicals as oxidants, were undertaken. Slowly, a focus on the behavior of organic compounds in atmospheric aqueous-phase chemistry developed, starting by adding organic "inhibitors" that were observed to shorten the kinetic chain length in the radical-induced sulfur(IV) oxidation.[6,12] These studies continued into the early 1990s in both the U.S. and Europe. Two reviews,

DOI: 10.1021/cr500447k
Chem. Rev. 2015, 115, 4259−4334

which appeared at nearly the same time, then gave overviews of the state of the art in the field, with emphasis on laboratory radical kinetic measurements.[13,14] Shortly after this, the multiphase formation of organic acids[15] was discussed, and heterogeneous and multiphase[16] atmospheric chemistry were clearly discriminated and then more widely recognized. After the early pioneering studies of Jacob[10,11] as well as Chameides and Davis,[17,18] other aqueous-phase models were created in the second half of the 1990s leading to current multiphase modeling. Since the end of the 1990s, aqueous-phase chemistry has made its way into the leading textbook monographs about atmospheric chemistry.[19−21]

Aqueous-phase laboratory studies and model development continued, often based on radical chemical kinetic concepts, but in the 2000s, some new aspects went into the focus of research. More analytical methods were applied to aqueous-phase systems, and, by means of these methods, more information on products being formed was obtained besides the pure kinetic information that often existed already. This kind of work was pioneered by a number of groups often located in the U.S., including, but not restricted to, those of B. Turpin, A. Carlton, K. Altieri, D. deHaan, and F. McNeill, as well as in Europe with B. Nozière, A. Monod, M. Claeys, I. Grgic, and their co-workers, collaborators, and other groups as well. These product studies, often performed in a time-resolved manner, added a very important and much needed facet to our understanding of aqueous-phase chemistry.

The kinetic and mechanistic laboratory investigations of nonradical reactions have gained increasing attention besides radical reactions. It is suggested that these reactions be divided into (i) reactions of the nonradical oxidants, that is, H_2O_2 and O_3, (ii) so-called organic accretion reactions, and (iii) other reactions such as hydrolysis reactions or nucleophilic substitutions. Organic accretion reactions consider a number of different reaction types such as aldol reactions, acetal and hemiacetal formation, and other oligomerizations as well as polymerizations where smaller molecules combine, for example, under the formation of C−C bonds or C−O−C bond sequences, leading to the formation of high molecular weight compounds. Accretion reactions are not exclusively nonradical processes; they can also be linked to or initiated by radical reactions or photolytic processes. Moreover, it should be noted that there is a new interest in aqueous-phase photochemistry both with regards to simple systems and with regard to the interaction of SOA compounds with light. Photochemistry might actually both compensate for some of the SOA formation taking place, due to the production of smaller and more volatile compounds, and contribute to the formation of SOA compounds, for example, through the production of less volatile oligomers.[22−25]

The area of work on accretion reactions has been very active over the last 15 years and hence is the topic of three major sections of this Review: section 4 (photochemistry), section 6 (nonradical reactions), and section 7 (main systems of current interest). These sections extend the scope of this Review beyond treating mainly radical aqueous-phase chemistry; the authors have tried to produce a coherent view on these parts of aqueous-phase chemistry together with the others.

Kinetic and mechanistic studies should be brought together; it is a continuing struggle of the scientific community to develop a unified view of the chemical mechanisms and kinetics that lead to the observed, identified, and quantified products in the atmospheric aqueous phase, which can then to be used for descriptive as well as for predictive modeling. Ultimately, the development of chemical schemes in atmospheric chemistry should then enable comparisons to real-world measurements. This should hold for aqueous-phase and multiphase mechanisms, and hence reference is given to a very profound review on organics in aqueous-phase systems such as fogs and clouds that has recently been published by Herckes et al.[26] Besides this, the reader interested in aqueous-phase field findings is referred to some key publications by Collett, his coauthors, and others.[27−30] It should be noted that the present contribution cannot intend to treat multiphase field experiments comprehensively; however, the authors have treated links to field work at selected places, especially for the inorganic systems of section 7.1, the epoxide section 7.2.3 and the organosulfate section 7.2.4.

In the more recent past, the influence of different reaction conditions as they are encountered in the dilute systems present in tropospheric clouds and the extremely concentrated, high-ionic-strength electrolyte solutions that exist in aqueous aerosol particles has emerged as a research focus, often again via product studies such as those performed by B. Turpin's group, for example, Lim et al. (2010).[31] Comparisons of products being formed under diluted cloudwater conditions with those obtained in the presence of higher concentrations of reactants as they exist under aqueous aerosol conditions have sometimes led to the opinion that a completely different chemistry is taking place in these two regimes; the authors of the present overview intend to call for an integrative view here. Not all of the chemistry under the one regime of conditions and concentrations is totally different from the other regime; rather, differences in concentrations of reactants and, eventually, oxidants, as well as other conditions such as ionic strength and pH, lead to different outcomes of the chemical mechanistic schemes. Hence, it would not be correct to state that totally diverse chemical mechanisms are needed. In fact, it is regarded as a goal of multiphase chemistry mechanism development to use one mechanism, the performance of which is good enough to simulate aqueous chemistry under both aerosol and cloud conditions as well. No fine-tuning of mechanisms for either regime should be necessary, and proper laboratory studies lay the ground for the advanced mechanistic descriptions needed here.

For the whole field of tropospheric aqueous-phase chemistry, a number of reviews and book chapters have been published in the past 15 years.[32−36] Material contained in these overviews will, of course, not be discussed again here. For a newcomer to the field, it is suggested to study these earlier key publications. Luckily, a certain development can be seen; aqueous-phase chemistry studies are an important part of today's atmospheric chemistry research as a whole.

Within section 2 of the present overview, some recent experimental developments of interest will be reviewed. Within section 3, the conditions in and differences between aqueous aerosol, fog, and cloud chemistry are collected and compared. This section includes a discussion of "switching reactions", which are especially sensitive to changing conditions. Photochemical reactions occurring in tropospheric bulk aqueous systems are treated in section 4 as a continuation from the recently published contribution by George et al.[37] and as a follow-up of our 2007 overview paper.[34] Radical reactions are summarized and reviewed in section 5, and nonradical oxidation reactions are reviewed in section 6, which aims to continue from the state of science as detailed by Hallquist et

DOI: 10.1021/cr500447k
Chem. Rev. 2015, 115, 4259−4334

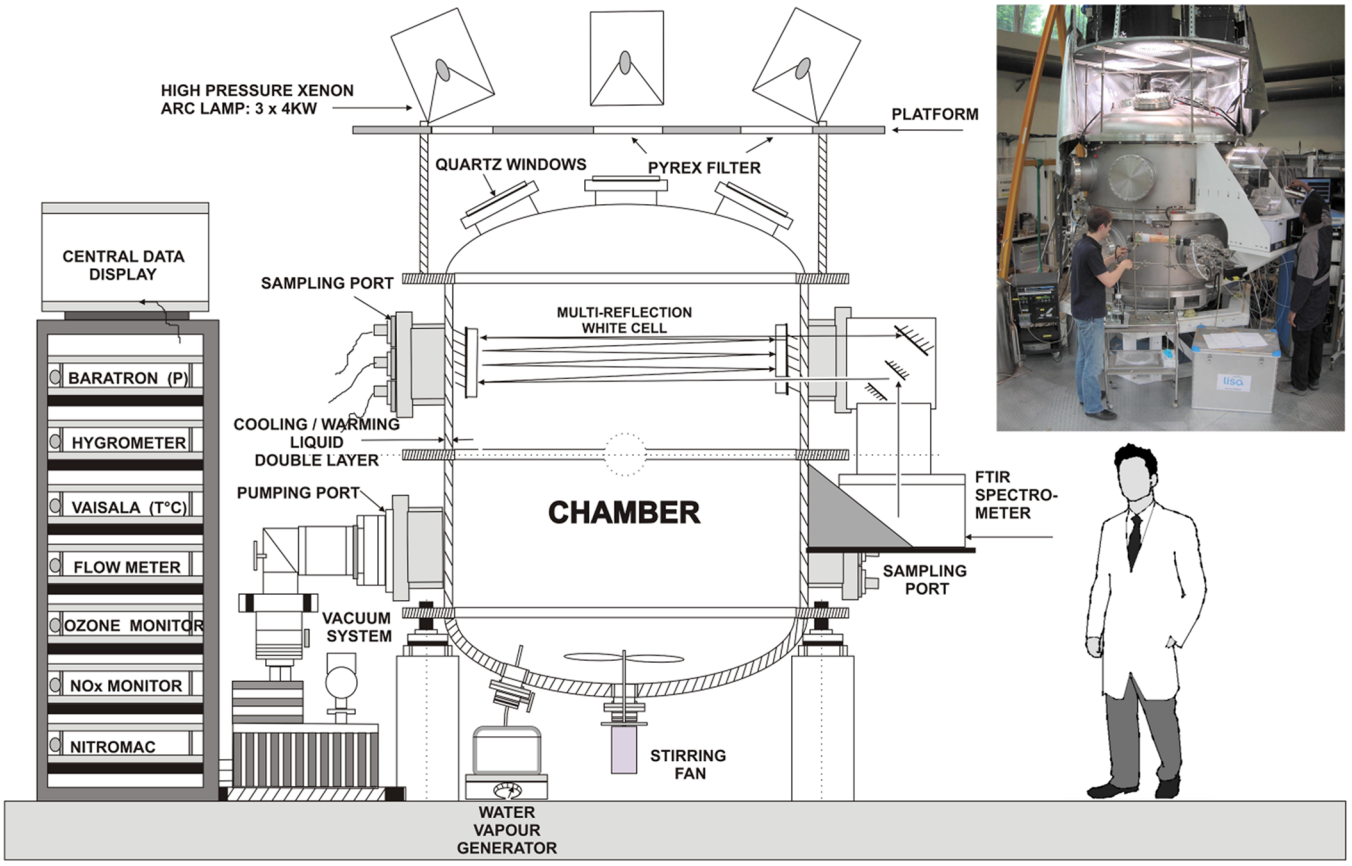

Figure 1. Instrumentation of the CESAM chamber at LISA in Paris. Inset: A picture of the installation (printed with personal permission from J. F. Doussin).

al.[38] in 2009. Section 7 presents the main systems of current interest in the field. Section 8 provides a very brief overview of the influence of microbiology on tropospheric aqueous-phase chemistry. Finally, section 9 discusses the effects of a changing atmosphere, and a conclusion and outlook are presented in section 10.

2. EXPERIMENTAL METHODS

This section provides a discussion of experimental developments regarded as important for the recent development of the field, and aims to serve as a follow-up to the overview of experimental techniques presented in Herrmann (2003).[12] However, because of limitations in this volume, a full comprehensive overview of all experimental laboratory techniques that can be applied to better understand atmospheric aqueous-phase processes cannot be provided. Instead, the reader should refer to key references, reviews, and more comprehensive treatments, which are available in the literature.

2.1. Chambers for Cloud and Aerosol Studies

Simulation chambers can be used for the study of cloud and aerosol chemistry. In the following, some recently emerging experimental approaches are discussed. It should be noted that many simulation chambers have the potential to be used for the investigation of aqueous aerosol chemistry, provided that the relative humidity (RH) in the chamber can be increased to a level at which a considerable mass fraction of the aerosol particles to be investigated consists of liquid water. Many of the chambers currently in operation, the EUROCHAMP2 consortium (http://www.eurochamp.org/) or, as a single example, the chamber at UNC (http://www.unc.edu/~kamens/chamber.shtml), and other installations like this may hence be used for such studies as well.

2.1.1. Cloud Chamber Studies. Interestingly, there is a tendency to apply "aerosol chambers" to the study of cloud reactions. Pioneering studies are currently being performed on this "warm cloud case" in the CESAM chamber installation at LISA in Paris, France, which is shown in Figure 1.[39]

In short, liquid water droplets are introduced into the chamber in operation, and then the effects of the presence of an ensemble of these droplets in the system are monitored. Droplet introduction is performed via two different procedures: (i) adiabatic pumping and (ii) water vapor injection from a heated pressurized reactor up to saturation.[39] At the AIDA chamber in Karlsruhe, Germany, liquid droplet formation is achieved by adiabatic pumping.[40] Studies in this chamber, however, concentrate on lower temperatures and thus mainly ice clouds. A new Japanese chamber for cloud studies has recently been reported;[41] despite new experimental possibilities, however, this installation will most likely be applied more to meteorological rather than to chemical research. It remains a technical challenge to apply reaction chambers to the study of cloud droplet chemistry, but new approaches are to be expected here in the future.

It should be mentioned that at the CERN facility, the CLOUD experiment has been performed, which is centered around a reaction chamber that has the potential to be used for multiphase chemistry studies in addition to studies on nucleation. Schnitzhofer et al. have recently described the

DOI: 10.1021/cr500447k
Chem. Rev. 2015, 115, 4259−4334

identification of organics, which might lead the way to multiphase studies in the future.[42]

2.1.2. Aqueous Aerosol Chamber Studies. In addition to being used aerosol for cloud experiments, aerosol chambers are currently increasingly operated under nondry conditions. Higher, relative humidities in chambers lead to the presence of aerosol liquid water (hereafter addressed as ALW) in the aerosol particles subject to study. A wealth of reactions occur in this medium, which, under the controlled conditions of such experiments, represents an aqueous strong electrolyte with ionic strengths surely above 5 M and often above 10 M. Using this experimental strategy, aqueous aerosol chemical conversions can be studied (i) with real dispersed particles and (ii) under the such extreme electrolyte conditions that are encountered in the real environment but that are difficult to mimic in bulk experiments because often the model electrolytes tend to disturb detection.

One prominent example of the contribution of chamber studies to our understanding of aqueous particle chemistry is the research on organosulfates (OS) derived from isoprene or monoterpenes with key steps of chemical conversions occurring within water-containing aerosol particles. Early key publications, such as those of Surratt et al.[43] and Iinuma et al.,[44] demonstrate the usefulness of chamber studies in elucidating nonradical OS formation pathways, while, for example, Schindelka et al.[45] studied OS formation via radical reactions; OS formation will be reviewed later in much more detail in section 7.2.4.

A series of three chamber studies of the multiphase processing of isoprene oxidation products has been published by the group of A. Monod.[46−48] These studies are also a good example of the value of combining aqueous-phase laboratory experiments with chamber work. In this new approach, proxy aerosol material produced in bulk aqueous-phase experiments was then dispersed into the chamber to be further investigated.

As reported by Kampf et al.,[49] chamber experiments have also proven useful in the study of the well-known salting-in of organics, which might also occur for glyoxal uptake into atmospheric sulfate particles. Clearly, many more contributions have used chambers to study aqueous particle chemistry, but, in the course of this Review, it will not be possible to always treat the applied experimental method.

Similarly to the work described above, it has been proven very useful to couple bulk-phase laboratory investigations with complementary chamber studies, which has actually been done in quite diverse studies, such as for cloud droplet photochemistry by Bateman et al.,[23] glyoxal multiphase oxidation by Lee et al.,[50] and aqueous photochemistry of high-NO_x isoprene SOA by Nguyen et al.[51]

It is expected that aqueous aerosol chamber studies, both alone and in combination with other laboratory work, for example, bulk aqueous phase studies, will gain even more attention in the future. This development has the potential to be very helpful, as, first, both the bulk and the chamber studies lead to complementary results. Second, the results of the chamber studies, which are usually viewed as "simulation studies", can be viewed as more realistic than aqueous-phase bulk experiments alone; possible differences have just been discussed by Daumit et al.[52] Third, chamber studies can then be compared to results from field campaigns as well. Hence, aqueous aerosol chamber investigations are beginning to become a tool to study the aqueous-phase reactions relevant for aerosol chemistry under realistic conditions not accessible using bulk aqueous-phase chemistry methods.

2.2. Analytical Techniques

2.2.1. Transfer-MS and ESI-MS. One key factor that has enabled major progress in the area of product studies related to aqueous-phase chemistry, and especially SOA production, has been not only the development of mass-spectrometric methods, including ESI-MS techniques and, most recently, chemical ionization mass spectrometry (CIMS), but also the development of nonstandard techniques for the transfer of analytes from aqueous solutions into MS instruments intended for gas-phase analysis.

How can these techniques be applied to aqueous-phase chemical reactions? A variety of transfer techniques have been developed and successfully applied in this area. In principle, a solution containing the reaction products is atomized, that is, dispersed into fine droplets, and this dispersion is then passed over a heating tube to evaporate the product molecules of interest. In this way, the analytes can be transferred into the gas phase and then be analyzed with CIMS. Such transfer-CIMS has been successfully applied in many studies, including those by Sareen et al.,[53,54] Schwier et al.,[55] Li et al.,[56] J. Abbatt and his group,[57−60] and the group of T. Hoffmann.[61]

In the case of organic accretion reactions, much of the work now available is based on sophisticated analytical techniques, such as those outlined above, but kinetic information is not always provided. Kinetic studies require time-resolved measurements, so any single analysis must not be too time-consuming or complicated. MS-based analysis directly coupled to reactors has been already introduced some time ago and has already been discussed in one of our last reviews, especially with the way-leading work of Poulain et al.,[62] and such time-resolved analysis with a coupled analysis of a reaction solution by an ESI-MS has since then been applied, for example, by Altieri et al.,[24,63] Kirkland et al.,[64] Lim et al.,[31,65] Tan et al.,[66−68] and Perri et al.,[69,70] and their co-workers and collaborators. It should be noted that ESI-analysis might lead to oligomer-like compounds in the course of MS-analysis,[71] so care should be taken in the application of this technique to the analysis of oligomers, for example, those formed in accretion reactions (see section 6.2).

Finally, it should be noted that care must be taken in the application of these online techniques, especially with regards to quantification. According to Bateman et al.,[72] methanol, a commonly used ESI solvent, can react with carbonyl and carboxylic acid functionalities present in organic aerosol constituents. The use of ESI-MS for the quantitative analysis of complex samples can be hampered by severe ionization competition (in the electrospray) between different solutes, especially within matrixes containing both ions and molecules of varying polarity; such ionization suppression effect has recently been shown by Boris et al.[73] to be significant at concentrations of nitrate and sulfate present in cloudwater samples.

2.2.2. High-Resolution Mass Spectrometry (HRMS). Ultrahigh-resolution Fourier-transform ion cyclotron resonance mass spectrometry (FT-ICR) has now been applied several times to the identification of organic compounds present in fog, cloudwater, and aerosol particles collected in the field (see, e.g., Mazzoleni et al.[74] for fog as an example and Schmitt-Kopplin et al.[75] for aerosol particles). This technique can also be applied to the study of laboratory samples, provided access to such an

DOI: 10.1021/cr500447k
Chem. Rev. 2015, 115, 4259−4334

instrument is possible. It should be noted, however, that considerable concern exists that, although HRMS is a very valuable tool for the identification of chemical species, quantification using this technique can become extremely difficult or even impossible. A very valuable general review of the application of high-resolution mass spectrometric techniques has been provided by Nizkorodov et al.,[76] and Laskin et al.[77] have reviewed DESI (desorption electrospray ionization). Here, Laskin et al.[78] have demonstrated extraordinarily low detection limits for limonene SOA dimers using nano-DESI-MS applied to the quantification of carbonyl compounds via derivatization with "Girard's reagent T". This technique shows a huge potential for the determination of such compounds in complex mixtures. In this context, O'Brien et al. have very recently applied nano-DESI-MS for a comparison of SOA generated in chamber experiments to that found in field samples.[79]

Another review[80] focused on advanced MS techniques for studying the physical chemistry of atmospheric heterogeneous processes. This in-depth treatment covers surface methods suitable for deposited particles such as secondary-ion mass spectrometry (SIMS) and laser desorption/ablation, techniques enabling the measurement of depth profiles, and, finally, the MS-based analysis of airborne droplets. Overall, this overview presents a wealth of instrumental possibilities, only some of which have currently been exploited in an atmospheric chemistry context. A broader review of "atmospheric analytical chemistry" addressing a wide variety of different techniques besides HRMS has been published by Hoffmann et al.[81]

Bateman et al. in the group of S. Nizkorodov have applied HRMS to the study of SOA evolution from limonene ozonolysis[82] and to the analysis of samples from a particle-into-liquid sampler (PILS).[83] Other applications of HRMS have been described by Pratt et al.,[84] Mead et al.,[85] Leclair et al.,[86] and Altieri et al.[63] for field measurements (rain and fog) and by Renard et al.[87] for laboratory measurements.

2.2.3. Other MS-Based Studies. Besides the above-mentioned application of ESI-MS, HRMS, and specialized MS for surface, depth profile, and droplet analysis, there have been many additional applications of mass spectrometry documented in a huge number of publications, only some of which can be highlighted here.

Norgaad et al.[88] have recently demonstrated that a wealth of molecular information regarding the products of limonene ozonolysis can be obtained using low-temperature plasma (LTP) ionization quadrupole time-of-flight (QTOF) mass spectrometry. This technique seems to be very promising for product identification, but results are currently very sparse.

Fang et al.[89] have reported a thermal desorption/tunable vacuum-UV TOF photoionization aerosol mass spectrometer for SOA investigations in chamber experiments. These authors have shown this complex technique to be a very powerful tool for detailed compositional analysis of SOA formed from the oxidation of toluene and isoprene. Finally, for a state-of-the-art overview on analytics of interest for atmospheric chemistry, the reader is referred to the *Chemical Reviews* contribution by Nozière et al. in this issue.

2.2.4. NMR. Chalbot and Kavouras[90] have very recently reviewed the use of NMR for the elucidation of organic content in aerosol particles. While that review primarily addresses particle analytics from a field experiment perspective, it also provides a useful overview of NMR techniques for future laboratory experiments. Paglione et al.[91] and Tagliavini et al.[92] also applied NMR for the study of organic aerosols from field measurements.

2.2.5. Droplet Evaporation Techniques. The effects of droplet evaporation on mass transfer, aerosol particle properties, and chemical conversions have been the subject of much research interest. Generally, the goal of droplet evaporation experiments is to mimic the changing concentration regimes that occur when a cloud droplet loses water by evaporation to yield a processed aerosol particle, for example, at a cloud rim. However, an aerosol particle with already a much lower LWC than a cloud droplet might be forced to evaporate the remaining water and also organic constituents, for example, through ramping up temperature, thus mimicking aerosol liquid water reduction in the course of particle drying, which does not involve aerosol−cloud interactions.

There is considerable treatment of droplet evaporation and its implications in physical chemistry, as can be seen from the recent publications of Davies et al.[93−95] Transport properties such as water diffusion coefficients can be deduced from single levitated droplet investigations,[96] and changes in droplet pH can also be measured.[97] Increased knowledge regarding these parameters might be helpful for a better coupling of chemistry and microphysics in models.

A second group of studies has focused on the evaporation characteristics or kinetics of simple particles, including maleic acid aerosol droplets,[98] ammonium sulfate solutions,[99] and acetic acid droplets.[100] Ternary mixtures have also been studied, such as ammonium sulfate/succinic acid/water[101] and NaCl/succinic acid/water.[102]

A third set of studies has investigated the effect of water evaporation on chemical conversions. Lee et al.[50] have applied such an approach in the study of the aqueous-phase OH oxidation of glyoxal, and have then employed aerosol mass spectrometry and complementary offline analysis techniques. By shifting the water concentration from cloud conditions toward ALW conditions, changes in chemical conversions can be identified and compared to model predictions. This approach has the potential to be a very valuable alternative to the high-RH aerosol chamber experiments mentioned previously, and may even prove superior, as it allows for tuning water concentration (corresponding to LWC in the atmosphere) over a very wide range, which cannot be achieved in a single aerosol chamber run. In turn, chamber experiments allow for processing time that might not be achieved in droplet evaporation experiments, so that the chamber runs might allow the more realistic process simulation.[103,104]

The single droplet levitation technique (see refs 105−107 for overviews) has been applied to the study of droplet evaporation. Recently, it has been demonstrated that this technique can also be used to study heterogeneous reactions, for example, the surface oxidation of nitrite by gas-phase ozone.[108]

Overall, experiments including evaporation steps and related investigations on suspended single droplets are very valuable in connecting chemical conversions and microphysics as well as in the study of changes in chemical conversion driven by changing LWC over orders of magnitude.

Droplet evaporation techniques have been used in a number of aqueous-phase atmospheric chemistry studies, and hence they are treated in several subsections of the present contribution. Specifically, these techniques have been applied in studies related to aldol condensation and especially limonene SOA (section 6.2.2), hemiacetal formation (section 6.2.3), and

DOI: 10.1021/cr500447k
Chem. Rev. 2015, 115, 4259−4334

Table 1. Size, Liquid Water Content (LWC), pH, and Ionic Strength (I) of Atmospheric Water-Containing Particles

particle or droplet	radius r [μm]	LWC [cm^3 m^{-3}]	pH	ionic strength I [M]	remarks and refs
			rain		
rain	150−1500	0.1−1	3.5−6.5	(0.67−3.81) × 10^{-5}[a] 8.4 × 10^{-5}	r, LWC, and I after Seinfeld and Pandis,[116] pH after Tost et al.[117]
			clouds		
marine/ polluted clouds	3.5−16.5[b]	<0.6[b]	3.5−6[b]	(0.001−6) × 10^{-2}[b,c,t]	Bower et al.[118]
remote cloud	1−25	0.05−1	4−6	(0.75−7.5) × 10^{-4}	r and LWC after Seinfeld and Pandis,[116] pH and I after Collett and Herckes[119]
continental cloud	1−15[d]	0.2−0.35[d]	3.9−4.6[d]	5 × 10^{-4}[d,e]	Wobrock et al.[120]
	1−8	0.1−0.45	4.0−5.0	5.4 (0.04−16) × 10^{-4}	Brüggemann et al.,[121] r and LWC after Wieprecht et al.[122]
			4.1 (3.3−5.9)	9.7 (2.9−22.6) × 10^{-4}[p]	Guo et al.[123] and refs therein
polluted cloud	1−25	0.05−1	2−5	(0.5−1.0) × 10^{-2}	r and LWC after Seinfeld and Pandis,[116] pH and I after Collett and Herckes[119]
			fogs		
polluted fog	∼1−20	0.02−0.5	2−7	(0.07−4) × 10^{-2}	r and LWC after Seinfeld and Pandis,[116] pH and I after Collett and Herckes[119]
continental fog	∼1−20	0.02−0.5	5.4 (3.8−7.2)	4.5 (0.7−9.5) × 10^{-3}[p]	r and LWC after Seinfeld and Pandis,[116] pH and I after Li et al.[124] and refs therein
remote fog		0.06	4.7 (3.1−7.4)	4.3 (0.2−28) × 10^{-4}	Straub et al.[125]
sea fog	2.3 (<1−10)	0.019 (0.01−0.1)	5.2 (4.8−6.1)	3.8 × 10^{-2}	Yue et al.[126]
			aqueous particles		
marine aerosol	0.005−5	(0.01−1) × 10^{-3}[f]	1−9 accumulation/ coarse mode: −1 to 3/(2−10)[s]	6.1[g]	r after Kim et al.,[127] I after Sander and Crutzen,[128] pH after Keene et al,.[129] size-resolved pH after Fridlind and Jacobson,[130] LWC after von Glasow and Sander[131]
	0.07−1.38[h]	9.5 × 10^{-6}[f,h,i]	−0.2[h]	j	Li et al.[132]
	≤1.25	(0.5−1.8) × 10^{-5}[r]	−0.2 to 0.4[r]		Pathak et al.[133]
urban aerosol	≤10[m]	(2.5−4) × 10^{-5}[f,m,n]	3.4−3.7[m,o]	8.0−18.6[g,m]	Stelson and Seinfeld[134]
	0.07−1.38[h]	7.6 × 10^{-7}[f,h,i]	−1.2[h]	j	Li et al.[132]
	≤0.5	(∼4−20) × 10^{-6}[f,q]	∼3−4	∼7−45	Volkamer et al.[135]
	≤1.25	(1.0−7.7) × 10^{-5}	−0.77 to 0.61		Pathak et al.[136]
	0.09−0.9	(0.4−1.6) × 10^{-5}[r]	−2.0 to 0.0[r]		Cheng et al.[137]
	≤0.5	3 × 10^{-7}[r]	<0 (−2.2)[r]		Yao et al.[138]
	≤1.25	∼1 × 10^{-5}	2−5	∼20	Hennigan et al.[139]
continental aerosols	≤5	(0.1−6) × 10^{-5}[f,r]	0−3	2−17[g]	Scheinhardt et al.[140]
	<1.25		−0.8 to 4.5		Meng et al.[141]
	≤0.675		1−2		Ludwig and Klemm[142]
	≤1.25	(0.9−1.3) × 10^{-5}[r]	0.3−0.4[r]		Pathak et al.[133]
haze	0.1−0.5	10^{-5}−10^{-4}[f]	1−8 (1.5−2.5)[k,l]	∼1[g]	Seinfeld[143]
	0.09−0.9	(0.1−7.0) × 10^{-5}[r]	−2.5 to 1.7[r]		Cheng et al.[137]

[a]Ionic strength in rain droplets in remote areas of the world, 6.7 × 10^{-6} M at Poker Flat, Alaska, and 3.8 × 10^{-5} M at Amsterdam Island, Indian Ocean. [b]Parameters for the given case study, measurement on the island of Tenerife in June−July 1997. [c]Ionic strength calculated for the cloud event that took place between the seventh and eighth of July, 23.00−08.00, polluted case. [d]Clouds strongly influenced by industries and other human activities; parameters for the given case study in 1990 at Kleiner Feldberg, Germany. [e]Calculated ionic strength, considering the median concentration of different components measured in cloudwater during the experiment. [f]The liquid water content (LWC) values for aerosol particulate matter depend on relative humidity. [g]The ionic strength is dependent upon the relative humidity. [h]Parameters for the given case study, measurements in southern California, 1994. [i]Calculated from given pH and H$^+$ concentration. [j]The ionic strength is not specified. [k]In regions of high sulfate content, the haze pH can be even lower than 1. [l]In parentheses, the pH value for haze in Tel Aviv, Israel, for particles in the size range 0.4−0.9 μm, Ganor et al.[144] [m]Parameters for this given case study, measurements in the Los Angeles area in 1973. [n]LWC when x_{Pb} = 0, x_{Ca} = 0, x_{Na} = 0, x_K = 0, and x_{Mg} = 0 in mol/1000 g of H_2O and the sum of electrolyte concentration is between 15 and 25 μg m^{-3}. [o]pH and ionic strength when x_{Pb} = 0, x_{Ca} = 0, x_{Na} = 0, x_K = 0, and x_{Mg} = 0 in mol/1000 g of H_2O. [p]Mean and range of all data presented in the paper. [q]Particle water content, acidity, and ionic strength based on ISORROPIA calculations (San Martini et al.[145]). [r]Particle water content or pH based on E-AIM calculations (extended AIM aerosol thermodynamics model, http://www.aim.env.uea.ac.uk/aim/model3/model3a.php, Clegg et al.[146]). [s]Based on both indirect observations and model calculations for remote marine conditions (free of anthropogenic and natural continental influence). [t]Revised value.[12]

in the context of isoprene multiphase oxidation, especially for MVK oligomers (section 7.2.2), and, finally, in the formation of imidazole compounds (section 7.2.5).

2.2.6. Kinetics. Since our last review, moderate progress has been made in the field of studying the kinetics of aqueous-phase radical reactions. Here, refinements in measurement techniques have been made, such as differential optical absorption measurements in time-resolved kinetic[109] and online dissolved oxygen measurements.[110]

Studies of radical chemistry under controlled oxygen concentrations have been performed by Monod et al.,[111,112] Renard et al.,[87,113] Kameel et al.,[114] and Schaefer et al.[110] In this

DOI: 10.1021/cr500447k
Chem. Rev. 2015, 115, 4259−4334

context, more details of aqueous RO_2 radical chemistry have been elucidated, but much more work needs to be done here because RO_2 radicals are central in aqueous-phase radical-initiated oxidation mechanisms.

It should be noted that for studies in radical aqueous-phase chemistry of interest for atmospheric chemistry, few laboratories are active at the time of writing. Especially in Europe, a number of laboratories with pulse radiolysis installations are no longer active; as a result, the capacity for doing radical kinetics has considerably diminished over the last 15 years. As pulse radiolysis is often complementary to laser flash photolysis, it would be desirable to maintain at least a few of such installations.

Finally, it should be noted that with the advent of the sophisticated MS-techniques as described above, such analysis, when taken from aqueous-phase reactors, either online or offline, opens the way for the time-resolved analysis of concentration profiles. The obtained concentration profiles then can be used for evaluation or reaction kinetics. Under certain conditions (i.e., pseudo-first-order conditions), knowledge of absolute concentrations is not necessary. This can compensate for difficulties in quantification of analytes in complex mixtures, such as those previously mentioned for ESI-MS or HRMS. Certain reactions can be measured by the stopped-flow technique, which is especially useful for oxidations by H_2O_2 and O_3, when optical absorption measurements are possible with low optical pathlengths and the respective absorption spectra of educts and products allow for it.[115]

3. A COMPARISON OF AQUEOUS AEROSOL, FOG, AND CLOUD CHEMISTRY

3.1. Overview of Conditions

For the past 20 years, cloud and fog droplets and deliquescent particles have been collectively referred to as the "tropospheric aqueous phase".[13] The tropospheric aqueous phase is characterized by huge variations in microphysical and chemical parameters, which in turn affect aqueous-phase reaction rates. A brief overview of both microphysical conditions (size, liquid water content) and chemical properties (pH, ionic strength) of different aqueous particle solutions in different environments is presented in Table 1. The data presented in this table reveal that tropospheric aqueous-phase reactions can occur under both low and very high ionic strengths and acidities.

The aqueous-phase volume available for chemical reactions ranges from $\sim 1 \times 10^{-6}$ cm^3 m^{-3} under deliquescent aerosol particle conditions to $\sim 10^{-1}$ cm^3 m^{-3} under cloud/fog conditions. This huge difference implies that both phase transfer processes and chemical reactions proceed differently in these different microphysical aqueous-phase regimes. The ionic strength in aqueous particles varies with liquid water content, and ranges from 10^{-4} M for dilute cloud, fog, and rain droplets to >10 M for deliquescent aerosol particles. As a result of these high ionic strengths, chemical processes in deliquescent particles need to be treated differently from those in dilute electrolytes. While both dilute cloud droplets and concentrated deliquescent particles display a wide range of pH values, from highly acidic to slightly alkaline, extreme pH values are typically only achieved in deliquescent particles.

3.1.1. Occurrence of the Tropospheric Aqueous Phase: RH, ALW, and Clouds on a Global Scale. A thorough understanding of the importance of aqueous-phase processes requires not only an understanding of the microphysical and chemical properties discussed above but also knowledge regarding the tropospheric abundance of aerosol and cloud liquid water.

Very recently, satellite data have been used to provide information about relative humidity distributions in the troposphere (see Ruzmaikin et al.[147] for further details). While it is known that ~70% of the earth on average is covered by clouds,[148,149] large regional differences exist in the cloud cover (see, e.g., http://earthobservatory.nasa.gov/GlobalMaps/view.php?d1=MODAL2_M_CLD_FR, http://isccp.giss.nasa.gov/climanal2.html). In a classic study, Pruppacher and Jaenicke[150] used climatology data to estimate the tropospheric volume fraction of clouds and the residence time of an air parcel inside tropospheric clouds. Their calculations revealed that about 15% of the lower half of the troposphere is filled with clouds and that the weighted global average cloud residence time for an air parcel is ~3 h. In addition, they calculated that the mean time spent by an air parcel between two separate cloud interactions is ~16.6 h. Assuming that an air parcel spends about 15% of its ~5-day lifetime in-cloud, a single tropospheric aerosol particle will thus undergo ~6 cloud cycles and spend ~18 h inside of clouds.

The study of Pruppacher and Jaenicke[150] also suggests that tropospheric aerosols spend 85% of their lifecycle time under noncloud conditions (i.e., RH < 100%). In the absence of clouds, and depending largely on their composition and on the local relative humidity, aerosols can be present as (i) deliquescent, (ii) water-carrying (i.e., not totally dry but below the deliquescence point), and (iii) dry particles. The abundance of ALW, therefore, is highly variable in space and time depending on both meteorological and environmental conditions (see, e.g., Carlton and Turpin[151]). For example, as a result of the decrease in water vapor mixing ratio with increasing altitude, the ALW shows a distinct vertical decrease (see, e.g., Zhang et al.[152]).

Global distributions of the annually averaged ALW content have been presented in several model studies.[152−155] Table 2 summarizes the ALW content values and the total aerosol wet mass obtained from the model simulation of Jacobson[153] for different altitudes and regimes.

Table 2. Annually Averaged Aerosol Liquid Water (ALW) Content and Total Wet Aerosol Mass in Two Different Altitudes (0 and 5 km) Modeled by Jacobson[153] for Different Regimes

	ALW content [cm^3 m^{-3}]		wet aerosol mass [μg m^{-3}]	
parameter	at 0 km	at 5 km	at 0 km	at 5 km
global	8.1×10^{-6}	5.8×10^{-7}	32	0.78
southern hemisphere	7.4×10^{-6}	7.3×10^{-7}	20	0.97
northern hemisphere	8.7×10^{-6}	4.3×10^{-7}	44	0.58
land	4.1×10^{-6}	2.8×10^{-7}	45	0.38
sea	6.9×10^{-6}	6.9×10^{-7}	27	0.93

As shown in Table 2, for all regimes the near-surface ALW content is approximately 1 order of magnitude higher than that at 5 km altitude; furthermore, higher values are present over sea than over land.

The horizontal ALW pattern presented in Adams et al.[154] reveals a wider range of ALW content and opposite results for the ALW content of land and sea aerosols. This model study found the highest ALW mixing ratios in industrialized areas

DOI: 10.1021/cr500447k
Chem. Rev. 2015, 115, 4259−4334

with high sulfate concentrations; by contrast, ALW mixing ratios in remote ocean regions, which showed the lowest sulfate concentrations, were an order of magnitude lower than those obtained in urban regions. The large dependence of the ALW on the ambient sulfate aerosol loading has been also shown for North America in a recent study by Carlton and Turpin.[151] Additionally, the study of Adams et al.[154] revealed that the sulfate loading was not the only key parameter determining the ALW; rather, both relative humidity and aerosol nitrate content influenced the ALW content. The association of ALW content to the abundance appears extremely interesting, and much further work is expected here on how the chemical aerosol particle composition actually steers the abundance of ALW and hence the matrix for aqueous aerosol chemical conversions (see also Hodas et al.[29]).

The vertical and zonal annual distribution of the ALW modeled with different water uptake schemes has been presented in work by Zhang et al.,[152] which also shows a significant decrease in ALW content with increasing scale height: the modeled near-ground ALW values are approximately 2 orders of magnitude higher than those at the 500 hPa level. Similar altitude dependencies were also obtained by Adams et al.[154]

Results obtained by remote sensing (see, e.g., Schuster et al.[156]) have shown that the ALW content and the related hygroscopic growth at different sites correlate relatively well with the fine particle mode concentration but not with the coarse particle mode concentration. Finally, the presented climatology also reveals significant seasonal differences in the hygroscopic growth factor (i.e., the ALW content).

Overall, the troposphere provides an environment with a wide range of microphysical and chemical conditions. Chemical kinetic investigations of aqueous-phase processes, therefore, must be performed under a wide variety of ionic strength and pH conditions. Only by keeping this complexity in mind can a comprehensive treatment and understanding of tropospheric processes be possible.

3.2. Aqueous-Phase Transfer

Generally, the troposphere is an oxidizing environment in which emitted volatile gaseous compounds are oxidized by many gas-phase chemical processes. The products of these reactions are usually less volatile and more polar than the starting species, and thus are more likely to partition into the tropospheric aqueous phase, where they can participate in multiphase chemistry processes. The interaction of the tropospheric aqueous phase with the surrounding atmosphere is important for two related reasons. First, the uptake of trace gases has the potential to change both the composition and thus the chemical and physical properties of tropospheric aqueous aerosols. Second, chemical reactions occurring within aqueous aerosol can change the composition and oxidizing capacity of the surrounding atmosphere via the uptake as well as the production of trace gas species. The nature and consequences of interactions between trace gases and tropospheric aqueous aerosol have been addressed in recent reviews by Abbatt et al.,[57] Ammann et al.,[157] Davidovits et al.,[158] and Kolb et al.[58]

In atmospheric multiphase models, partitioning between the gas and aqueous phases is typically implemented on the basis of Henry's law, which describes the thermodynamic equilibrium between a gas-phase species A_{gas} and its aqueous-phase counterpart A_{aq} in a highly dilute solution such as those present in tropospheric clouds. The ratio of the corresponding equilibrium concentrations in both phases is represented by the Henry's law constant K_H (see eq 1). Equation 1 indicates that the aqueous-phase concentration ($[A_{aq}]$) is directly proportional to the partial pressure (p_{Agas}) of the gas-phase species A_{gas}.

$$A_{gas} \rightleftharpoons A_{aq} \quad \text{(R-1)}$$

$$K_H = \frac{[A_{aq}]}{[A_{gas}]} = \frac{[A_{aq}]}{p_{A_{gas}}} \quad (1)$$

Different definitions of the Henry's law constant are used in the literature; the most commonly used definitions are outlined in a very recent paper by Sander,[159] which is the latest in a series of reviews on this topic. This article also presents a very comprehensive compilation of Henry's law constants of potential relevance for atmospheric chemistry (14 775 Henry's law constants for 3214 inorganic and organic compounds), and also provides details on temperature dependencies of Henry's law constants.

It must be noted that Henry's law is generally only applicable for dilute solutions. For concentrated solutions, such as those present in ALW, dependencies of the Henry's law constants on the chemical composition and ionic strength of the electrolyte must be considered.[160] These dependencies, which are typically referred to as "salting in" and "salting out" effects, are explicitly discussed in section 3.4.

Several methods have been developed for the estimation of unknown Henry's law constants (see, again, Sander[159] and references therein for an overview). One of the most recent estimation methods for Henry's law constants, the GROMHE method (group contribution method for Henry's law estimate), was published by Raventos-Duran et al. in 2010.[161] GROHME, a structure−activity relationship (SAR) based on a group contribution approach, enables the estimation of effective Henry's law constants of atmospherically relevant organic compounds at 298 K. This method includes not only the estimation of intrinsic Henry's law constants but also the possible hydration of carbonyl compounds in the aqueous phase, which can substantially promote the aqueous-phase partitioning of tropospheric aldehydes/ketones. Compernolle and Müller have published two very recent papers in which Henry's law constant data of polyols, diacids, and hydroxyl acids are calculated using water activities, solubilities, and vapor pressures and employing thermodynamic relationships.[162,163] These studies have yielded much higher Henry's law constants for diacids and hydroxy-polyacids than previously estimated, for example, by the often-quoted 1996 review by Saxena and Hildemann.[164] Clearly, these results show that large uncertainties in Henry's law constant data still remain. Overall, given that accurate phase-transfer data represent an essential precondition for obtaining meaningful results from multiphase models, improved laboratory data and estimation methods are crucial.

Finally, it should be noted that this Review does not intend to provide a comprehensive overview of gas−aqueous aerosol interactions or an exhaustive compilation of phase-transfer data. However, it will provide an overview of several topics of current research interest related to gas−aqueous particle interactions, including the uptake of HO_x by clouds and aqueous aerosol (see section 7.1.2), the N_2O_5-mediated production of $ClNO_2$ in aqueous aerosol (see section 7.1.3), and the role of aqueous-

DOI: 10.1021/cr500447k
Chem. Rev. 2015, 115, 4259−4334

phase epoxide chemistry in biogenic SOA formation (see sections 7.2.2 and 7.2.3).

3.3. pH Effects

As previously emphasized in this Review, aqueous-phase chemistry occurring in dilute systems (i.e., cloud droplets, fog, and rain) is not completely different from that occurring in aqueous aerosol. However, the reaction environments provided by these two systems are drastically different, especially with respect to ionic strength and pH. The conversion fluxes of reactions that are sensitive to these parameters, therefore, will be enhanced or reduced in aqueous aerosol relative to more dilute systems. In the following paragraphs, families of these "switching reactions" will be individually discussed.

3.3.1. Acid–Base Equilibria of Acids and Diacids. The most common examples of reactions that will change their chemical turnovers according to changes in pH are simple acid–base equilibria. For example, carboxylic acids and dicarboxylic acids, which are abundant in all aqueous tropospheric systems, will be present in their undissociated forms under acidic conditions. As a consequence, under acidic conditions, the probability of free-radical single electron-transfer reactions with the deprotonated carboxylates will decrease; at the same time, H-abstraction pathways will become more feasible, and phase transfer toward the gas phase will be favored.

This change is of special interest for the radicals NO_3 and SO_4^-, both of which are known to be very effective one-electron oxidants. Changes in OH-mediated reactions will be less significant, as OH is generally not a good one-electron oxidant and instead prefers to react by H-abstraction with both the protonated and the deprotonated forms of a substrate. Further details on the mechanism of OH radical reactions with organic acids are given in a number of previous publications.[35,165,166] In general, the higher the one-electron reduction potential of the radical or radical anion in question is, the more it will be affected by acidification of the aqueous phase, which might occur via evaporation of a cloud droplet and the resultant formation of a residual particle.

3.3.2. Dehydration Reactions of Reaction Intermediates: Alkyl Radical Reformation. Dehydration reactions of organic radicals have been extensively studied in early pulse radiolysis work in aqueous solution. These studies have paid special attention to radicals derived from diols.[167−186] In addition, the dehydration reaction has been studied in organic solvents, for example, benzene and acetonitril.[187−190] As shown in Figure 2, this reaction proceeds via protonation of the diol radical; subsequent elimination of water yields a radical carbocation intermediate, which stabilizes by the elimination of a proton from the remaining alcohol group and the transformation of the carbocation into a carbon-centered radical. In this manner, H-abstraction at a diol compound first leads to an α-carbonyl-alkyl radical, and, subsequently, to an α-carbonyl-alkyl peroxyl radical. Additionally, it should be noted that the alkyl radical can react with a present molecule with a C−C double bond leading to a higher molecular weight alkyl radical.

Because diol-type compounds result from the aqueous-phase hydration of carbonyl compounds, this mechanism is of interest for tropospheric aqueous systems. The reaction sequence presented in Figure 2, for example, could be relevant for the aqueous-phase oxidation of glyoxal (see also Figure 3), methylglyoxal, and other α-dicarbonyl species. In fact, the

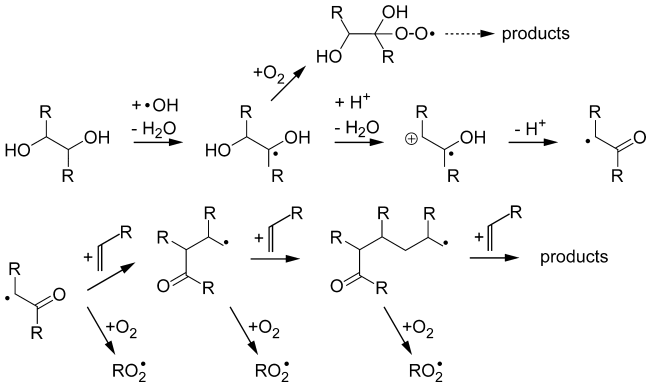

Figure 2. Rearrangement reaction of a diol-type alkyl radical in recent studies based on Schaefer et al.[110]

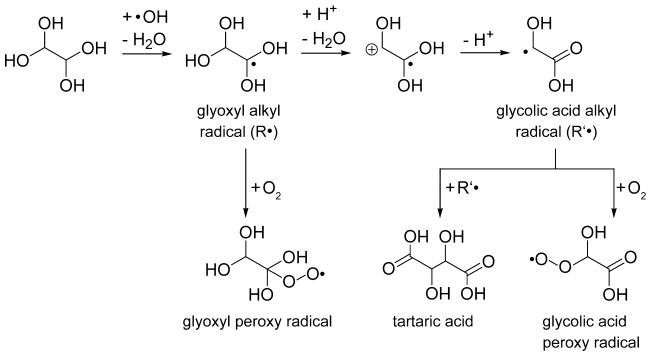

Figure 3. Rearrangement reaction of the glyoxyl alkyl radical to the glycolic acid alkyl radical in the OH-driven oxidation of glyoxal based on recent studies of Schaefer et al.[110]

occurrence of these reactions is supported by product analysis: as discussed in a study by Lim et al.,[31] certain products can be well explained using the protonation–dehydration–deprotonation/isomerization sequence outlined here.

It should be noted that a direct experimental determination of the rate constant for water elimination from the glyoxyl radical itself is not available, and care must be taken in deducing rate constants from similar, but clearly nonidentical, systems, such as for this sequence for the system of ethylene glycol, which has been regarded similar to the glyoxal system.

Although the formation of dehydrated oxygen-containing alkyl radicals provides a pathway to the formation of dimeric products, such as the 2,3-dimethyl tartaric acid identified by Lim et al. in their study of secondary aerosol formation,[31] dimer formation is always in competition with the reaction of the organic radical with oxygen. At times, rate constants for the reactions of alkyl radicals with oxygen of $k = 1 \times 10^6$ M^{-1} s^{-1} [22] contradict a number of existing direct determinations including a very recent redetermination, Schaefer et al.[110] and references therein. Clearly, the mentioned low rate constant for the recombination of an alkyl radical with molecular oxygen is not feasible and must not be further used as it introduces errors in experimental interpretations and into multiphase models. Assuming a saturated oxygen concentration in the atmospheric aqueous phase of 2.6×10^{-4} M and a second-order rate constant in a range of approximately $k_{RO2} = (1–5) \times 10^9$ M^{-1} s^{-1}, one can calculate a first-order rate constant of approximately $k_1 = (0.3–1.3) \times 10^6$ s^{-1}. Comparison of this value with available first-order rate constants for the rearrangement–dehydration reactions discussed above (see Table 3)

DOI: 10.1021/cr500447k
Chem. Rev. 2015, 115, 4259−4334

Table 3. Overview of Rearrangement−Water Elimination Reactions of Organic Radicals[a]

substrate	radical R$^{\bullet}$	dehydration product X$^{\bullet}$	technique	R → X first-order rate constant [s^{-1}]	protonation equilibrium constant K_p [M]	T [K]	refs
ethylene glycol	$^{\bullet}C(OH)-CH(OH)$	$^{\bullet}CH_2-CHO$[b]	PR	8.6×10^5	1.8×10^{-1}		170
			PR	7.5×10^5	4.6×10^{-2}	293 ± 2	171
propane-1,2-diol	$CH_3C^{\bullet}(OH)CH_2(OH)$	$CH_3C(O)CH_2^{\bullet}$	PR	7.1×10^5	5.6×10^{-3}	293 ± 2	171
2-methoxyethanol	$CH_3OCH_2C^{\bullet}H(OH)$	$^{\bullet}CH_2-CHO$[c]	PR	1.0×10^5	4.7×10^{-2}	293 ± 2	171
2-methylpropane-1,2-diol	$(OH)C(CH_3)_2C^{\bullet}H(OH)$	$^{\bullet}C(CH_3)_2CHO$	PR	2.7×10^6	3.7×10^{-3}	293 ± 2	171
butane-1,2-diol	$CH_3CH_2C^{\bullet}(OH)CH_2(OH)$	$CH_3CH_2C(O)CH_2^{\bullet}$	PR	8.5×10^5	5.3×10^{-3}	293 ± 2	171
2-methylbutane-2,3-diol	$(OH)C(CH_3)_2C^{\bullet}(CH_3)(OH)$	$^{\bullet}C(CH_3)_2C(O)CH_3$	PR	1.8×10^6	7.4×10^{-4}	293 ± 2	171
cyclohexane-1,2-diol	α,β-dihydroxycyclohexanyl alkyl radical	cyclohexanonyl alkyl radical	PR	1.8×10^6	1.5×10^{-3}	293 ± 2	171

[a]The listed kinetic data refer to pH values in the range $0 \leq pH \leq 5$. The reference contains information on more systems and additional kinetic and spectroscopic data. PR = pulse radiolysis. [b]$2k = 9 \times 10^8$ M^{-1} s^{-1}. Recombination rate constant of the dehydration product X$^{\bullet}$. [c]Rearrangement by loss of alkoxyl group.

demonstrates that both reaction pathways can be important and competitive under atmospheric conditions.

As can be seen from Table 3, although a reasonable number of kinetic parameters are available for these dehydration reactions, these parameters have been largely determined for systems irrelevant to atmospheric aqueous chemistry. Because nearly all data on this topic come from older pulse radiolysis work and few repeat determinations of rate coefficients exist, further studies on this subject are certainly warranted. Care should be taken when transferring data measured for one system to another one for application.

Dehydration reactions of multihydroxylated organics have the potential to be important reaction steps under aerosol particle chemical conditions, especially when they initiate further reactions. Such reaction sequences can, to some extent, revert the initial hydration of carbonyl compounds, because they reconstitute an unhydrated carbonyl functionality in an intermediate for a given carbonyl compound. This is depicted in Figure 3 for the OH-mediated aqueous-phase oxidation of glyoxal.

The protonation−dehydration−deprotonation/isomerization sequences discussed here lead to the formation of reactive carbon-centered radicals, which can either recombine with each other to form larger units, or react with other organic compounds available in the aqueous atmospheric system in question. For example, the CH_2-CHO radical formed from ethane-1,2-diol can react with the starting diol again via H atom transfer to form acetaldehyde and a new carbon-centered radical. As Buley et al. indicated already in 1966,[167] this pathway serves to initiate a radical chain reaction. The feasibility of such mechanisms in aqueous atmospheric systems deserves exploration.

The low-pH conditions under which these dehydration reactions are thought to occur are typically accompanied by high ionic strength (see Table 1). For this reason, ionic strength-dependent dehydration equilibrium constants and rate constants should be used. Because no such data are presently available, the representation of these reactions in chemical mechanisms must be regarded as preliminary.

The dehydration and isomerization/dehydration reactions discussed here might become especially important if they result in the production of an organic compound that can escape the particle phase. In such a reaction sequence, particle-phase reactions might serve as a source of gas-phase organics. This phenomenon has been demonstrated by Wang and co-workers, who have shown that the acid-catalyzed dehydration of the ring-opening product of isoprene epoxide leads to the production of gas-phase 2-methyl-3-butenal.[191]

In summary, while these reactions should be implemented into tropospheric aqueous-phase mechanisms, care must be taken to properly reflect the influence of the elevated acidity and ionic strength conditions that exist in water-containing aerosol particles. Again, while the throughput of these reactions will be different in aerosols than in fog/clouds, a tropospheric aqueous-phase mechanism should just carry the proper implementation of these reactions. Studies of carbon-centered, oxygen-containing radicals in aqueous solution would be very useful in addressing this issue, as the existing data do not really cover the compounds of highest interest in atmospheric multiphase chemistry at present.

3.3.3. Organic Accretion Reactions. As will be discussed in section 6.2, organic accretion reactions are accelerated under low-pH conditions: for example, aldol condensation starts with the acid-catalyzed enolization of a participating carbonyl compound, and the formation of hemiacetals and acetals is also acid-catalyzed. Accretion reactions are generally believed to be unimportant under dilute cloudwater conditions with pH values in the ranges as depicted in Table 1. Although high-molecular-weight compounds have been identified in cloudwater,[63,84−86,192] it is generally thought that their formation occurs under more acidic ALW particle conditions.

3.4. Ionic Strength Effects and Treatment of Nonideal Solutions

As discussed in the overview of this section, aerosol liquid water constitutes an aqueous electrolyte where high ionic strengths, often greater than 10 M and, at times, up to 20 M, can be reached. The following paragraphs will discuss possible approaches to address ionic strength effects and the use of activity coefficients to describe nonideal solutions.

3.4.1. Radical Reactions. It is very difficult to perform bulk-phase experiments using highly concentrated aqueous salt solutions for several reasons: first, the electrolyte can foster special chemical effects of its own, an electrolyte such as sulfate might be of low reactivity but at very high applied concentrations still be involved in reactions occurring at considerable rates; second, impurities contained in the electrolyte can lead to high concentrations of unwanted species in the system, which hinders defined kinetic and photochemical targeted bulk-phase investigations; and third, current analytical techniques have difficulties with the analysis of organic

DOI: 10.1021/cr500447k
Chem. Rev. 2015, 115, 4259−4334

constituents in concentrated salt solutions, which complicates associated mechanistic investigations.

Nevertheless, a number of radical reactions have been systematically investigated at high electrolyte concentrations as a function of electrolyte concentration, for example, by Herrmann[12] and co-workers; for radical chemistry, here, sodium perchlorate was chosen. The main results of these studies have already been summarized in a previous review by Herrmann[12] and references therein. Some of the effects observed can be attributed to ion-pair formation, where the ion-pair species can react with a rate constant (k_{ip}) different from the non-ion-pair species (k_{nip}), which is referred to as the Olson−Simonson treatment.[193]

$$A^- + C^+ \rightleftharpoons CA \text{ (ion-pair formation equilibrium)} \quad \text{(R-2)}$$

$$A^- + R \xrightarrow{k_{nip}} \text{products (reaction of the non-ion pair)} \quad \text{(R-3)}$$

$$CA + R \xrightarrow{k_{ip}} \text{products (reaction of the ion pair)} \quad \text{(R-4)}$$

This treatment allowed for the quantitative analysis of $NO_{3(aq)}$ reactions with a number of anions as well as the study of reactions of the dichloride radical anion (Cl_2^-) with methanol and hydrated formaldehyde.[12] In these studies, it was emphasized that adjustment of high ionic strengths by adding electrolytes in high concentration must be performed with the knowledge that the electrolyte, even if strong, may not completely dissociate. Since the time of this review[12] in 2003, the authors are not aware of further studies of ionic strength effects in aqueous-phase radical reactions relevant for atmospheric chemistry.

3.4.2. Nonradical Reactions. As was the case for radical chemistry, there have been very few publications on the effects of ionic strength on nonradical aqueous-phase reactions of interest for atmospheric chemistry. Ali et al.[194] have investigated the oxidation of S(IV) by H_2O_2; in this study, empirical expressions describing the H_2O_2 or SO_2 loss rates are given as a function of the concentration of the NaCl electrolyte employed. As a byproduct of this study, NaCl electrolyte ionic strength-dependent H_2O_2 Henry's law constants are available, which might be of interest for marine aerosol chemistry.

In summary, only a few kinetic studies in the past decade have included investigations of aqueous-phase ionic strength effects. Although such studies are important for a better understanding of kinetic salt effects and ion pairing, their applicability for ALW chemistry may be limited, because aerosol particles contain a complex mixture of many inorganic solutes that is impossible to fully mimic in laboratory experiments. Thus, while $NaClO_4$ has largely been used as the background electrolyte in radical chemistry studies because it is quite photochemically inert, the salt effects measured with this background electrolyte might not be directly applicable to ALW conditions. The use of sulfate as an electrolyte is not possible because it would, in many cases, react with photochemically produced radicals to produce sulfate radical anions (SO_4^-).

3.4.3. Salting-in and Salting-out. When a soluble gas is exposed to an electrolyte solution, the amount of gas taken up is a function of the solution-phase electrolyte identity and concentration: while certain electrolytes might lead to enhance uptake of the soluble gas ("salting-in"), other electrolytes are able to suppress the gas uptake below what is expected for pure water uptake ("salting-out"). Salting out is especially known to laboratory chemists as a technique to separate organic solutes from a water phase by adding a salt, and is frequently employed in product isolation following organic synthesis and in the purification of large biomolecules such as proteins.

Quantitatively, salting effects are described by the Setschenow (preferably in English, but also Setchenov or Sechenov) equation.[160]

$$\log\left(\frac{k_H^0}{k_H}\right) = k_S^c \cdot [\text{salt}] \quad (2)$$

Setschenow coefficients are widely available for many combinations of gases and electrolytes.[195,196]

A number of theories exist to describe salting-in and salting-out phenomena on a molecular basis. One such theory, the "scaled-particle" theory, was suggested by Masterton and Lee[197] in the 1970s. Active research in this area is still ongoing: see studies by Millero et al.[198] for the calculation of oxygen solubilities in seawater, and by Graziano and co-workers, who studied a variety of systems with regard to salt effects.[199,200] A short summary of the principles of scaled-particle theory is given by Pitzer.[201] In another theory, fluctuation theory, Ruckenstein and Shulgin[202] showed that the Setschenow equation can be deduced as a special case of the scaled-particle theory.

The theories and the salting-in data available at present are usually restricted to nonpolar gases and dilute electrolyte solutions. In the atmosphere, however, such conditions are often not met: recent research interest has focused more on polar trace gases that can undergo hydration and, in the case of ALW, solutions with extremely high electrolyte concentrations. A significant effect of sulfate on the uptake of glyoxal into aqueous solution was first described by Ip et al.[203] Following this observation, a recent chamber study by Kampf et al.[49] found that particle-phase ammonium sulfate concentration had a very large effect on glyoxal uptake. It is doubtful whether this effect should really be addressed as a salting-in effect, because this term usually refers to the electrolyte-promoted uptake of nonpolar gases to aqueous solution. Because this enhancement may arise via the coordination of glyoxal to sulfate and the formation of a weakly bound adduct (possibly via the substitution of water in the sulfate hydration shell by glyoxal in one of its forms), the uptake might better be considered as a reactive uptake induced by coordination of glyoxal toward sulfate. The question of whether such coordination to sulfate would be reversible or irreversible under ALW conditions is still open, and the potential for dilution-induced glyoxal release to the aqueous-bulk phase upon aerosol particle activation is currently fully unclear. In addition, the aqueous-phase reactivity of sulfate-coordinated glyoxal is currently unknown. Clearly, further experimental and theoretical work is needed here.

3.4.4. Treatment of Nonideality in ALW Chemistry. To assess the importance of chemical and dynamical processes associated with aerosol particles, a variety of complex multiphase chemistry mechanisms have been developed and coupled with atmospheric models (see, e.g., Tilgner and Herrmann[204] and references therein). In the past decade, substantial effort has been expended to characterize the role of chemical aqueous-phase processes in both cloud droplets and deliquescent particles. For example, model studies of Tilgner et al.[205] have suggested that in-situ production of OH radical in deliquescent particles makes these particles a reactive aqueous chemical environment. Other studies by Shen and Anasta-

DOI: 10.1021/cr500447k
Chem. Rev. 2015, 115, 4259−4334

sio[206,207] and later by Arakaki et al.[208] have measured OH formation rates in deliquescent particles. Arakaki and co-workers[208] in particular have shown that OH production rates in highly concentrated aerosols are much higher than those in dilute cloud solutions. Moreover, these authors have shown that numerical models tend to overpredict the aqueous-phase formation rate of OH and significantly underestimate the OH sinks. For example, calculated aqueous in-situ OH formation rates by Tilgner et al.[205] are about an order of magnitude higher than observations.[208]

To date, complex chemistry box models mostly approximate the aqueous particle phase as a dilute electrolyte solution, and thus neglect nonideal solution effects. However, as shown in Table 1, the ionic strengths present in the aqueous phase of deliquescent aerosol particles are typically several orders of magnitude higher than those present in cloud and fog droplets. As a result, aqueous aerosol solutions cannot be considered ideal solutions (i.e., solutions where intermolecular forces between nonsolvent molecules can be neglected). Rather, in the highly concentrated environment presented by deliquescent particles with very low ALW, ions and molecules are much closer to each other; under such conditions, ALW constituents influence each other through electrostatic forces and/or other physical interactions. These intermolecular forces can affect both the phase-transfer behavior of a compound and its propensity to participate in chemical reactions. Consequently, the assumption of ideal solution conditions in complex multiphase chemistry models simulating deliquescent aerosols has to be abandoned, and, in future models, nonideal behavior must be considered in a detailed manner. Hence, activities rather than concentrations must be used in multiphase chemistry models, and appropriate calculation methods have to be applied to compute the required activity coefficients. Moreover, future models should also consider dependencies of the reaction rate constants and phase-transfer data on the nonideality (e.g., ionic strength effects) when those data become available.

To calculate physical aerosol processes, such as particle deliquescence/efflorescence and associated ALW content, chemical aerosol processes, and overall phase-transfer processes under conditions present in multicomponent and multiphase particles, adequate thermodynamic modules are mandatory in complex chemistry models. A number of attempts to realistically estimate the activity coefficients for inorganic, organic, and mixed inorganic−organic solutions have been published.[201,209−219] While interactions between inorganic compounds are relatively well-understood, a full understanding of intermolecular interactions between organic components and organic−electrolyte mixtures has remained elusive, due largely to the complexity and varying properties of organic aerosol constituents. Furthermore, detailed experimental studies characterizing nonideality effects on multiphase chemistry in tropospheric deliquescent particles are still lacking. For this reason, considerable effort has been devoted to the development of kinetic frameworks for modeling processes in multicomponent atmospheric particles that include both detailed descriptions of organic and inorganic multiphase chemistry and detailed thermodynamic studies of nonideal behavior (see Shrivastava et al.[220]).

To this end, recent work at the Leibniz Institute for Tropospheric Research (TROPOS) has focused on the implementation of a combined approach for activity coefficient calculation of mixed solvent electrolyte systems into the Spectral Aerosol Cloud Chemistry Interaction Model (SPACCIM, Wolke et al.[221]). This model was originally developed for the dynamic description of chemical and microphysical cloud processes and has been successfully applied in several multiphase chemistry process studies in combination with the detailed aqueous-phase chemistry mechanism CAPRAM.[204,205,221,222] In its updated version, the SPACCIM model considers nonideality effects, which are treated by means of a modified AIOMFAC activity coefficient model ("Aerosol Inorganic−Organic Mixtures Functional groups Activity Coefficients").[219] The group-contribution concept[219] implemented in this model enables a reliable estimation of activity coefficients for organic−inorganic mixtures composed of various ions and functional groups. In this manner, the updated SPACCIM model permits the computation of both activity coefficients of considered organic−electrolyte mixtures and the multiphase chemistry occurring under both dilute cloud and concentrated deliquescent aerosol conditions.

In the first follow-up studies, the updated SPACCIM model was applied to study the effects of nonideality on aqueous-phase chemistry.[223] First model results have revealed that the activity coefficients of the inorganic ions studied are <1 under deliquescent aerosol conditions and that most organic compounds show activity coefficient values >1. Model runs revealed that the inclusion of nonideality effects has a considerable influence on the multiphase chemical processing of radical oxidants, transition metal ions, and related chemical subsystems. For example, the particle-phase OH turnovers are lowered in model runs that consider nonideality as compared to those in ideal solution model runs. The reduction of the aqueous OH radical reaction flux is mainly caused by its lower in-situ production from the Fenton reaction, which in turn results from low iron activity coefficients. The model runs that considered nonideal solution effects also showed compound-specific effects, largely reductions in aqueous-phase processing, on the multiphase processing of organic compounds.

4. PHOTOCHEMISTRY

The following section gives an overview of aqueous-phase photochemistry and reviews photochemical parameters such as quantum yields of primary photochemical reactions as well as mechanisms, where available. The photochemical reactions of inorganic ions and transition metal ions (TMI) and the resulting radical formation will be described. Subsequently, the photochemistry of organics, including photosensitization, will be discussed. Often only more qualitative information is available, which has been tried to be summarized here as well. As a general remark, we would like to call attention to the photolysis wavelengths used in photochemical experiments and, at best, to perform atmospheric chemistry studies in the actinic region of the solar spectrum, that is, at photolysis wavelengths above λ = 290 nm. When photolysis wavelengths smaller than λ < 290 nm are used in laboratory experiments, this obviously can change the photochemical reaction pathway leading to different products and yields. Moreover, the quantum yield might change and the subsequent chemistry will be affected, due to different chemical species and concentrations of them involved. Finally, in the UV range below the actinic region, even more chemical compounds are able to absorb photons. This could lead to the initiation of additional and unwanted photochemical reactions, which would not proceed under tropospheric actinic conditions.

DOI: 10.1021/cr500447k
Chem. Rev. 2015, 115, 4259−4334

Table 4. Experimental Photochemical Data for Inorganic Compounds in Aqueous Solution Relevant for Atmospheric Chemistry and Related Laboratory Studies

wavelength [nm]	reaction	quantum yield; molar extinction [$M^{-1}cm^{-1}$] values for T = 298 K, if not otherwise stated	remarks	refs
$H_2O_2 + h\nu \rightarrow 2OH$				
313, 334		$\ln\Phi = -\frac{(684 \pm 17)}{T} + (2.27 \pm 0.064)$	T = (239-318K)-dependent data for solution and ice, no dependence observed for pH = 2-7 and ionic strength	226
		$\varepsilon_{313\ nm} = 0.386 \pm 0.016$	I = 0.2-6.2 mM	
240 − 260		$\Phi = 1.02 \pm 0.1$	average values	35
300 − 320		$\Phi = 0.93 \pm 0.09$		
254		$\Phi = 1.03 \pm 0.05$	benzoic acid as OH radical scavenger and determination of hydroxybenzoic acid isomers	227
313		$\Phi = 0.59 \pm 0.01$		
365		$\Phi = 0.009 \pm 0.001$		
$NO_3^- + h\nu \rightarrow$ products				
205	$NO_3^- + H_2O + h\nu \rightarrow NO_2 + OH^- + OH$	$\Phi = 0.129 \pm 0.055$		230
254		$\Phi = 0.037 \pm 0.004$		
254		$\Phi = 0.045$	pH = 6	227
205	$NO_3^- + h\nu \rightarrow ONOO^-$	$\Phi = 0.278 \pm 0.040$		230
254		$\Phi = 0.102 \pm 0.002$		
300		$\Phi < 0.002$		
205	$NO_3^- + h\nu \rightarrow NO_2^- + O(^3P)$	$\Phi = 0.207 \pm 0.011$		230
254		$\Phi = 0.065 \pm 0.002$		
300		$\Phi = 0.0094 \pm 0.0002$		
310		$[NO_3^-] = 0.011 - 14.9$ M in $Ca(NO_3)_2$ solutions:	pH = 4, effect of NO_3^- concentration, OH radical scavenger (formate) and counterion (Na^+ and Ca^{2+})	229
		$\varepsilon_{310\ nm} = 6.4 \pm 0.1$ to 2.5 ± 0.1		
		$\Phi_{[nitrate]\ =\ 0.01\ M} = 0.006$		
		$\Phi_{[nitrate]\ =\ 0.01M} = 0.014 \pm 0.01$ (scavenger formate)		
		$\Phi_{[nitrate]\ =\ 1\ M} = 0.0078 \pm 0.001$		
		$\Phi_{[nitrate]\ =\ 14.9\ M} = 0.00023 \pm 0.0002$		
		$\Phi_{[nitrate]\ =\ 14.9\ M} = 0.0042 \pm 0.0003$ (scavenger formate)		
310	$NO_3^- + h\nu \rightarrow NO_2^- + O(^3P)$	$[NO_3^-] = 0.011 - 6.2$ M in $NaNO_3$ solutions:		229
		$\varepsilon_{310\ nm} = 6.6 \pm 0.2$ to 4.5 ± 0.2		
		$\Phi_{[nitrate]\ =\ 0.01M} = 0.0045$		
		$\Phi_{[nitrate]\ =\ 0.01M} = 0.0079 \pm 0.0008$ (scavenger formate)		
		$\Phi_{[nitrate]\ =\ 1\ M} = 0.0063$		
		$\Phi_{[nitrate]\ =\ 6.2\ M} = 0.0025$		
		$\Phi_{[nitrate]\ =\ 6.2\ M} = 0.013 \pm 0.006$ (scavenger formate)		
$NO_2^- + H_2O + h\nu \rightarrow NO + OH^- + OH$				
302-390		$\Phi = \frac{y_0 + a}{1 + \exp\left(\frac{\lambda - c}{b}\right)} \exp\left(\left(\frac{e\lambda + f}{R}\right)\left(\frac{1}{295} - \frac{1}{T}\right)\right)$	T = (240−295K)- and λ-dependent data for solution and ice	228

Chem. Rev. 2015, 115, 4259−4334 DOI: 10.1021/cr500447k

Table 4. continued

wavelength [nm]	reaction	quantum yield; molar extinction [$M^{-1}cm^{-1}$] values for T = 298 K, if not otherwise stated	remarks	refs
		$y_0 = 0.0204 \pm 0.0010$, $a = 0.0506 \pm 0.0022$, $b = 11.2 \pm 1.2$, $c = 332 \pm 1$, $e = 20.5 \pm 3.2$, $f = 7553 \pm 1204$		
	$HONO + h\nu \rightarrow NO + OH$			
313-366		$\ln\Phi = \frac{(7.14 \pm 0.57) - (2430 \pm 160)}{T}$	T = (274−283K)-dependent data for solution	236
		$\varepsilon_{313\ nm} = 5.01$, $\varepsilon_{366\ nm} = 40.6$; T = 298 K		
	$H_2ONO^+ + h\nu\ (\lambda < 410\ nm) \rightarrow NO + OH + H^+$			
313-366		$\ln\Phi = \frac{(3.16 \pm 0.67) - (1890 \pm 180)}{T}$	T = (255−283K)-dependent data for solution and ice	236
		$\varepsilon_{313\ nm} = 5.59$, $\varepsilon_{366\ nm} = 38.5$; T = 274 K		
	$HOCl + h\nu \rightarrow OH + Cl$			
254		$\Phi = 1.0 \pm 0.1$; ([HOCl] = 3.5 − 70 mg/ L)	concentration dependence of Φ, pH = 5	237
		$\Phi = 1.07 + 0.0025$ [HOCl]; ([HOCl] > 70 mg/ L)		
		$\varepsilon_{254\ nm} = 59 \pm 1$; T = (294 ± 2) K		
	$OCl^- + H_2O + h\nu \rightarrow Cl + OH^- + OH$			
254		$\Phi = 0.9 \pm 0.1$; $\varepsilon_{254\ nm} = 66 \pm 1$; T = (294 ± 2) K	Φ independent of concentration, pH = 10	237
	$HSO_5^- + h\nu \rightarrow OH + SO_4^-$			
254		$\varepsilon_{254\ nm} = 13.8$; $\Phi(SO_4^-) = 0.52 \pm 0.01$; T = 293 K	pH = 7 (pH range 6−12 studied for degradation experiments)	238

DOI: 10.1021/cr500447k
Chem. Rev. 2015, 115, 4259−4334

4.1. Inorganic Bulk Photolysis and Radical Sources

Early studies were concerned with the photochemistry of a manageable number of inorganic ions and neutral molecules such as nitrite, nitrate, or H_2O_2, or, to mention some more exotic representatives, HOCl, peroxodisulfate, and dithionate. These studies usually provided well-characterized photochemical parameters such as molar extinctions and quantum yields as well as mechanisms for aqueous bulk photolysis (see Herrmann[34] and references therein). Some studies over the past years have been concerned with the photochemistry occurring in the thin layer of aqueous solution on top of ice or snow crystals. For comprehensive reviews of photochemistry on snow and in ice, see Bartels-Rausch et al. (2014)[224] and other contributions in that special issue of Atmospheric Chemistry and Physics. Emerging issues in photochemistry, including ice and snow photochemistry, have been treated recently by George et al.[37] This Review will cover contributions where liquid water and ice studies have been performed together, but will not address those focusing on snow and ice exclusively.

4.1.1. Hydrogen Peroxide Photolysis. As shown in Table 4, the quantum yield of H_2O_2 photolysis in solution and ice has been shown to be independent of ionic strength, pH, and wavelength.[35,225,226] These findings are in contradiction to the wavelength dependency of the quantum yield reported by Kwon et al.[227] The quantum yield at T = 298 K observed by Chu et al.[226] is in a good agreement with the averaged values reported in Herrmann et al.[35] In the aforementioned work, the conditions were such that H_2O_2 was present in the quasi liquid layer (QLL) so that the aqueous and ice data both follow the same temperature-dependent relationship.[226]

4.1.2. Nitrite Photolysis. Nitrite photolysis has been investigated in aqueous solution and ice as a function of temperature between 240 and 295 K and wavelength between 302 and 390 nm by Chu and Anastasio,[228] which is represented by an equation shown in Table 4. Additionally, the Supporting Information of the cited study contains molar absorptivities for aqueous nitrite at pH 7 as a function of temperature between 274 and 298 K, but the temperature effect is almost negligible.

Roca et al.[229] studied the minor reaction channel of nitrate photolysis at 310 nm from which nitrite and $O(^3P)$ are produced, and tested the effects of nitrate concentration, counterion (Na^+ vs Ca^{2+}), and the presence of the OH scavenger formate (Table 4). Changes in the electronic structure of nitrate causing an absorption band shift of the $n-\pi^*$ transition in very concentrated calcium nitrate solutions lead to a remarkable decrease in nitrite quantum yields in the presence of OH scavenger formate, which is not the case for sodium nitrate solutions that include formate. The conditions and multicomponent composition applied in the cited study are more representative of the concentrated solutions and high ionic strengths found in deliquescent aerosol particles and ALW. It is shown that deviation from ideal solution behavior in the aerosol phase (in contrast to the more dilute conditions present in cloudwater) can greatly affect not only kinetic constants, as discussed in section 3.4, but also photochemical constants. This should be considered in models.

The mechanism of nitrate photolysis was quite recently reinvestigated by Goldstein and Rabani,[230] due to uncertainties about the primary photoprocesses and subsequent reactions as stated in the literature.[231−234] The Goldstein and Rabani study considers the photoisomerization of nitrate to peroxynitrite ($ONOO^-$) and reports quantum yields for all three possible channels between 205 and 280 nm.[230] The possible channels are formation of: OH + NO_2, $ONOO^-$, and NO_2^- + $O(^3P)$. It should be noted that photoisomerization only occurs at $\lambda < 280$ nm, and hence only OH + NO_2 and NO_2^- + $O(^3P)$ occur in the troposphere. Table 4 lists the reported quantum yields for 205, 254, and 300 nm; for the remaining data set (12 additional wavelengths), the reader is referred to the original publication.

Efforts have been made to model the optical absorption spectrum of nitrate using a combined reflection principle path integral molecular dynamics (RP-PIMD) method, giving special attention to the symmetry-forbidden transition that causes the atmospherically relevant absorption band around 300 nm.[235] On the basis of this calculation, the authors concluded that the weak absorption around 300 nm can be ascribed to A_1'' transitions and that the symmetry breaking is caused by interactions with surrounding water molecules, which leads to the forbidden A_1'' state.

The photolysis of both nitrous acid, HONO (solution), and protonated nitrous acid, H_2ONO^+ (solution and ice), has been investigated between 313 and 366 nm as a function of temperature, with the resulting quantum yields being independent of wavelength (Table 4), in contrast to nitrite and representing the first study of H_2ONO^+ photochemistry to date.[236] UV spectra of HONO and H_2ONO^+ have been reported, in addition to the important finding that the presence of H_2ONO^+ at low pH values such as 1 (indicated by a study of Riordan et al.[239]) has most likely interfered with the determination of the HONO spectrum, and therefore that previous measurements might not have given correct extinction coefficients for HONO in aqueous solution. The light absorption of both HONO and H_2ONO^+ does not differ substantially, but the photolysis efficiency of HONO is ∼6 times higher than that of H_2ONO^+ (Table 4).

The nitrite formation rate from nitrate photolysis has been found to be enhanced in the presence of organic compounds such as methanesulfonate, formate, and formaldehyde.[240] The reason for this is not currently clear.

4.1.3. Photolysis of Chlorine-Containing Species. The photolysis of HOCl and OCl^- has been investigated as a function of concentration for λ = 254 nm at pH 5 and 10, respectively, using pK_a = 7.5 for speciation calculation.[237] A full UV absorption spectrum between 200 and 400 nm is also reported for both HOCl and OCl^-. HOCl shows a concentration dependence for its quantum yield, whereas OCl^- does not (Table 4).

In a study focused on the stable products rather than the primary photochemistry, it was reported that ClO_2^- photolysis at actinic wavelengths is capable of producing perchlorate (ClO_4^-): the fact that irradiation at 300 or 350 nm was 5 times more effective than that at 254 nm[241] highlights its potential to contribute to perchlorate occurrence in natural waters.

4.1.4. Peroxomonosulfate Photolysis. A new experimental determination of the peroxomonosulfate (HSO_5^-) quantum yield was reported for λ = 254 nm with $\Phi(SO_4^-)$ = 0.52 ± 0.01,[238] which is much higher than the only literature values, which were provided by Herrmann[34] ($\Phi(SO_4^-)$ = 0.12 ± 0.02).

$$HSO_5^-/SO_5^{2-} + h\nu \rightarrow SO_4^- + OH \qquad \text{(R-5)}$$

Herrmann[34] obtained the quantum yield by the observation of the SO_4^- radical formed from the direct photolysis at λ = 248 nm of an aqueous solution of 1 mM peroxomonosulfate. The laser pulse energy was determined by using a Gentec energy-

DOI: 10.1021/cr500447k
Chem. Rev. 2015, 115, 4259−4334

meter. Guan et al.[238] used a low-pressure mercury UV-lamp in combination with a cylindrical glass vessel to photolyze a 0.1 mM peroxomonosulfate solution in phosphate/borate buffer in the presence of benzoic acid or nitrobenzene as radical scavenger. The radiation intensity was obtained by using the iodide−iodate actinometer. Concerning the different quantum yields, preference might be given to the lower value because optical detection of the transient absorption of the SO_4^- radical was used for calculation of the quantum yield, which is a direct method. The scavenging by benzoic acid or nitrobenzene and offline detection, involving many steps of complicated secondary reactions, was used in the work by Guan et al.[238] As it was classified as an "apparent" quantum yield by the authors, it is most likely valid only within the experimental conditions applied. Other complications besides secondary reactions when using benzoic acid or nitrobenzene as scavengers for quantum yield determinations might be direct photolytic or photosensitizing effects of the added scavengers, which might have contributed to the much larger measured quantum yield.

4.1.5. Hydrogen Peroxide Formation. Hydrogen peroxide represents a reservoir species for OH production, but can also be an important oxidant itself (see sections 5.1 and 6.1). The formation of H_2O_2 from the OH radical-initiated oxidation of atmospherically relevant organic compounds in the absence and presence of nitrate was reported by Hullar and Anastasio.[242] The OH radical was generated by nitrate photolysis using simulated solar light. The pH- and temperature-dependent H_2O_2 yield observed in these experiments can be explained by the decay of the peroxyl radicals formed during oxidation. These peroxyl radicals can decompose via either the unimolecular decomposition of an α-hydroxyl peroxyl radical, which yields a organic carbonyl compound and hydroperoxyl radical (HO_2), or the recombination of two peroxyl radicals. The HO_2 yield from the decay of the α-hydroxyl peroxyl radical from the OH oxidation of formaldehyde is usually presumed to be 100%. However, a lower H_2O_2 yield from formaldehyde oxidation was observed.[242] The formation rate of OH radical from H_2O_2 and nitrate photolysis was also assessed in irradiation experiments of synthetic and natural cloudwater samples, and the difference between the measured and predicted values was attributed to iron complexes and total organic matter.[243] Hence, organic matter can act as both source and scavenger for generated OH radicals. Similar irradiation experiments at 313 nm were carried out with aqueous extracts of ambient aerosol particles, where OH photoformation rates could be partly attributed to nitrate (but associated with a large error) based on the measured nitrate concentration and were also strongly correlated with iron and dissolved organic carbon (DOC) concentration.[244]

In the present contribution, the photochemistry of iron complexes and total organic matter will be assessed in sections 4.2 and 4.4, respectively.

4.2. Transition Metal Ion (Iron) Complex Photolysis

There is a wide variety of inorganic and organic ligands available for transition metal ion (TMI) complexation in atmospheric waters. Because the photochemistry of inorganic ligand complexes is already relatively well understood, recent research has focused more on the photochemistry of organic ligand complexes, and specifically on that of organic carboxylate anions. In the case of inorganic systems, new quantum yields at 254 nm have been reported only for iron hydroxide complexes.[227] Available photochemical data for Fe-complexes are summarized in Table 5.

Table 5. Experimental Photochemical Data for Iron Complexes in Aqueous Solution Relevant for Atmospheric Chemistry and Related Laboratory Studies

complex/ wavelength [nm]	quantum yield; molar extinction [M^{-1} cm^{-1}] values for T = 298 K, if not otherwise stated	remarks	refs
	$FeOH^{2+} + h\nu \rightarrow Fe^{2+} + OH$		
254	$\Phi_{254nm} = 0.34 \pm 0.03$	pH = 3	227
254	$\Phi_{254nm} = 0.037 \pm 0.001$	pH = 6	227
	$[Fe(III)(C_2O_4)]^+ + h\nu \rightarrow Fe^{2+} + CO_2^- + CO_2$		
296	$\Phi_{296nm} = 0.188$	(molar extinction coefficients are available from 280 to 450 nm for 10 nm increments; see original ref)	259
313	$\Phi_{313nm} = 0.103$		
365	$\Phi_{365nm} = 0.085$		
	$[Fe(III)(OOC-CH(CH_3)-O)]^+ \rightarrow [Fe(II) + OOC-CH(CH_3)-O]^+$		
355	$\Phi_{355nm} = 0.40$ (deoxygenated) $\Phi_{355nm} = 0.22$ (oxygenated)	note that −CHO− contains a deprotonated OH group coordinated to Fe(III)	260

Most work has focused on complexes of iron, the most abundant trace metal; less work has focused on other metals, such as copper and manganese. The general role of iron complexes is the photoreduction of an Fe(III) to an Fe(II) species, which is accompanied by an oxidation of the associated ligands. Production of H_2O_2, HO_2, and OH oxidants is often discussed as relevant, but, as can be seen by comparing atmospheric and surface water investigations or advanced oxidation processes (AOP), different conditions are applied. Moreover, phase transfer plays a role for atmospheric systems. A very recent modeling study showed for the first time[245] that ligand decomposition is relevant for cloud droplets and aerosol particles but not significant as a radical source. Therefore, AOP studies that primarily consider the degradation of contaminants with the help of iron complex photochemistry are briefly mentioned here.[246−251]

Recent advances have been made regarding the experimental photochemistry of atmospherically relevant Fe(III) complexes; these advances have already been the subject of an earlier review, which focused primarily on carboxylate complexes.[37] Two review-like papers by Wang et al.[252,253] give an overview of the latest developments in iron complex photochemistry within the scope of environmental chemistry and advanced oxidation processes and focus on the transformation of low-molecular weight organic matter. Weller et al. reported a large data set of effective overall Fe(II) quantum yields for the photolysis of Fe(III) complexes with oxalate, malonate, malate, succinate, glutarate, tartronate, tartrate, gluconate, lactate, pyruvate, and glyoxalate, and showed that the quantum yields depend on ligand (primary photoreactivity), wavelength (primary photoreactivity), coordination number (primary photoreactivity), dissolved O_2 (secondary reactions), excitation energy (secondary reactions), and concentration of the initial Fe(III) complex (secondary reactions).[254,255] The observed dependence on these factors is either connected to the primary photoreactivity of the complexes or due to secondary reactions of fragments generated in the primary photoreaction step. The observed concentration dependence of the ferrioxalate quantum yield is especially striking.[254] From 6×10^{-3} M to approximately 5×10^{-4} M, and also at higher concentrations, the overall

DOI: 10.1021/cr500447k
Chem. Rev. 2015, 115, 4259−4334

quantum yield of iron oxalate complexes was independent of the initial Fe^{3+} concentration; this result is in agreement with other studies.[256−258] At millimolar and larger concentrations, the Fe−oxalate system is reliably used as a chemical actinometer; at concentrations below 5×10^{-4} M, by contrast, there is a marked concentration dependence of the overall Fe^{2+} quantum yield showing smaller values with decreasing initial Fe^{3+} concentration. This can be explained as follows: two CO_2^- radicals per photon can be produced; one instantly reacts with Fe(III) species, yielding one Fe^{2+}, and the other can subsequently react either with another Fe(III) species (secondary thermal reduction), yielding more Fe^{2+}, or with itself by recombination or with traces of oxygen in the solution. Lowering the concentration of Fe(III) species could make the first reaction path less effective and thus lead to a decrease in quantum yield.

A very interesting approach to the investigation of ferrioxalate chemistry was taken by Long et al.,[259] who performed continuous polychromatic irradiation experiments of synthetic cloudwater solutions with different initial pH values and concentrations of carboxylic acids such as oxalic, formic, acetic, succinic, and malonic acid. The focus of this study was on the effect of oxalate complexes, and these authors attempted to evaluate their experimental findings with a cloud chemistry model mechanism. The authors found large discrepancies between measured and simulated concentrations of H_2O_2, Fe(II), and oxalate, although the oxalate degradation was reproduced in general. The conditions of this study favored monooxalatoiron ($FeC_2O_4^+$) as the main Fe(III) species. These authors suggest that the photolysis of monooxalatoiron ($FeC_2O_4^+$) should be considered in models to correctly reproduce oxalate degradation in cloudwater and further report molar extinction and quantum yield values, which are the first such values available for this complex.

Long et al.[259] suggested the need for models to include a complex of formic acid and Fe(III) because they observed the formation of a stable coordination compound and the model implementation of its photochemistry could help to resolve discrepancies. Finally, concerning the iron/H_xO_y-oxidant cycle, with H_xO_y-oxidants being HO_2, H_2O_2, and OH, differences still remain between experiments and models, which shows the need for additional work. Weller et al.[245] concluded on the basis of coupled gas phase, cloud, and aerosol chemistry modeling implementing the photochemistry of a series of relevant iron complexes that this complex photochemistry is not an important source of H_xO_y-oxidants because it cannot compete with HO_2 uptake from the gas phase and other aqueous radical sources. More work concerning this issue needs to be performed in the future.

Following an earlier line of research, two newer studies employed laser flash photolysis using short time scale transient spectroscopy to investigate the photolysis of Fe(III) tartrate, Fe(III) citrate, and Fe(III) lactate complexes.[260,261] In both studies, the formation of long-lived Fe(II) radical complexes was observed, which confirms previous findings.[262] Time-resolved intermediate absorbance spectra could be assigned to a superposition of internal conversion to the ground state and the formation of such long-lived Fe(II) radical complexes whereby a competition between both processes determines the effective quantum yield of Fe(III) carboxylate complex photolysis.[261] Quantum yields for oxygenated and deoxygenated solutions were given for the photolysis of Fe(III) lactate complexes.[260]

In atmospheric particles, iron can be present not only in the liquid bulk state but also in colloidal mineral phases. For this reason, Borer and Hug[263] tested the photoreactivity of oxalate, tartronate, malate, malonate, and succinate adsorbed on the Fe(III) hydroxide surfaces of lepidocrocite, goethite, maghemite, and hematite during irradiation experiments at 365 nm. The degradation of oxalate, tartronate, and malate proceeded very rapidly, whereas that of malonate and succinate occurred at slower rates. The authors excluded efficient generation of OH radicals, as this would have led to an efficient degradation of all investigated compounds. Instead, ligand-to-metal charge transfer or oxidizing valence band holes must have been responsible for the efficient decomposition of oxalate, tartronate, and malate. Other work with potential relevance for atmospheric aerosol particle chemistry involving heterogeneous processes investigated gallic acid and catechol as a proxies for humic-like substances (HULIS) and used $FeCl_3$ as a photoactive substance.[264−266]

Light-absorbing dissolved organic matter was shown to complex Cu(II) in ambient rainwater samples irradiated in a solar simulator.[267] It was found that the photolabile ligands were also the stronger ligands, and that ligands adsorbed on particles were more efficiently degraded than dissolved ones. The simultaneous photodecomposition and photoformation of ligands was also observed in this study.

An interesting study involving photochemistry of mixtures including Fe^{3+} or Cu^{2+} ions, propionic acid, and halide ions was published by Carraher et al.[268] Although this work was published in the context of chemical synthesis, the chemistry could also be relevant under environmental conditions. Photolysis of these solutions in the presence of oxygen generated Fe^{2+} and converted alkyl radicals to intermediate species (peroxyl and alkoxyl radicals and hydroperoxides) that efficiently reoxidized part of the photoreduced Fe^{2+}. Feasible pathways of Fe^{2+} reoxidation are very important for the redox cycling of this and other transition metal ions in environmental systems, which often enables a catalytic action of these metals, and different aspects and possible mechanisms are frequently discussed.[254,269] Furthermore, hydrocarbons such as ethane, ethylene, and butane were formed in both oxygenated and in deoxygenated solutions. In the presence of chloride or bromide, ethyl halides were formed via halogen atom abstraction by ethyl radicals from iron-halide species. Rate constants for ethyl radical reactions with $FeCl^{2+}$ and $FeBr^{2+}$ were given as $k = (4.0 \pm 0.5) \times 10^6$ and $k = (3.0 \pm 0.5) \times 10^7$ M^{-1} s^{-1}, respectively. Using Cu^{2+} instead of Fe^{3+} produced ethylene and Cu^+. As can be seen from this example, chemistry involving transition metal ions might even lead to new and unexpected routes of product formation in the atmospheric aqueous phase.

4.3. Organic Bulk Photochemical Reactions

The photolysis of organic compounds in aqueous atmospheric systems has received increasing attention in recent years. It is now well-documented that aqueous-phase chemistry, especially aqueous particle chemistry, can lead to the formation of higher molecular weight compounds (cf., sections 6.2 and 7.2). However, photochemical degradation might counteract the formation of such higher molecular weight compounds and might lead to a "selection" of observable photochemically stable products. The very recent studies by Epstein and Nizkorodov[270] (see below) and Epstein et al.[271] have led the way to screen for compounds that might be subject to direct photochemical degradation. These authors found that only

DOI: 10.1021/cr500447k
Chem. Rev. 2015, 115, 4259−4334

Table 6. Photochemical Data of Organic Compounds in Aqueous Solution Relevant for Atmospheric Chemistry[a]

(A) experimental quantum yields

compound/wavelength [nm]	reaction	quantum yield; molar extinction [M^{-1} cm^{-1}] values for T = 298 K, if not otherwise stated	remarks	refs
		carboxylic acids		
pyruvic acid (PA)	PA + $h\nu$ → products			
320 nm	photoinduced oligomerization			22
	formation of acetoin, lactic acid, acetic acid, and oligomers with four or six carbon atoms			25
			comment on doubted acteoin formation	273
			reply to the above comment	274
Xe lamp output		n/a	only J-values available: J = (8.08 ± 0.09) × 10^{-5} s^{-1} for lowest PA	275
1125 ≤ λ ≤ 1440 nm	PA + $h\nu$ → CO_2 + other products	Φ = (3.5 ± 1.0) × 10^{-4}	PA overtone excitation	276
		terpenoic acids		
cis-pinonic acid (*c*PA) 280 ≤ λ ≤ 400 nm	cPA + $h\nu$ → products	Φ = 0.5 ± 0.3	mean of different measurements and models	277
		aromatics		
2-nitrobenzaldehyde (2-NB)	2-NBA + $h\nu$ → products	Φ = 0.41 ± 0.02	valid for liquid water and ice	278
2,4-dinitrophenol 300 ≤ λ ≤ 500 nm	2,4-DNP + $h\nu$ → products	Φ = (8.1 ± 0.4) × 10^{-5}		279
2,4-dinitrophenol 290 nm	2,4-DNP + $h\nu$ → products	Φ = (3.6−4.4) × 10^{-6} in H_2O; T = 293 K; Φ = (1.6−2.0) × 10^{-6} in octanol	$\Phi(H_2O) \ll \Phi$(octanol)	280
2-bromophenol	BP + $h\nu$ → products	Φ = 1.2 × 10^{-4}	low pressure mercury lamp, HBO 200 W	281
3-bromophenol		Φ = 5.3 × 10^{-5}		
4-bromophenol		Φ = 1.2 × 10^{-4}		
4-hydroxy-3,5-dimethoxybenzoic acid (syringic acid) λ = 300 nm	SyA + $h\nu$ → CH_3OH + products	Φ = 0.01	Rayonet RPR 100 photochemical reactor with 300 nm lamps	282
3,4,5-trimethoxybenzoic acid λ = 300 nm	3,4,5-TMB + $h\nu$ → CH_3OH + Products	Φ = 0.006		282
		peroxides		
methylhydroperoxide λ > 275 nm	CH_3OOH + $h\nu$ → CH_3O + OH	$\ln \Phi = \frac{(2175 \pm 448)}{T} + \left(7.66 \pm 1.56\right)$	same QY in liquid and frozen water	270

(B) findings on photochemistry

system	main findings	remarks/techniques	refs
	phenols		
phenol	formation of highly oxidized compounds via hydroxylation of the aromatic ring; in the absence of H_2O_2 no SOA was formed; formation of oxalate and other small organic acids (<10%) of SOA mass	HR-AMS	283
guaiacol (2-methoxyphenol)	formation of phenolic dimers and higher oligomers; SOA was formed in the presence and absence of H_2O_2; formation of oxalate and other small organic acids (<10%) of SOA mass		283
syringol (2,6-dimethoxyphenol)			283
phenol	formation of phenolic dimers and higher oligomers; triplet excited states of aromatic carbonyl-mediated SOA; formation faster than OH-mediated reaction; oxygen-to-carbon ratio from phenol similar to low-volatility oxygenated organic aerosol (LV-OOA)	HR-AMS, nano-DESI MS, IC	284
guaiacol (2-methoxyphenol)			284
syringol (2,6-dimethoxyphenol)			284
phenol	formation of phenolic dimers and higher oligomers; triplet excited states of aromatic carbonyl-mediated SOA; formation faster than OH-mediated reaction; rate constants for the reaction with triplet state molecule (see section 4.4, Table 8)	Xe-lamp, RPR-200 photoreactor, HPLC-UV	285
guaiacol (2-methoxyphenol)			285
syringol (2,6-dimethoxyphenol)			285
2-nitrophenol	conversion efficiency in the aqueous phase: OH > NO_3 > direct photolysis > nitration	photolysis at 300 ≤ λ ≤ 500 nm, HPLC-DAD, laser flash experiment	286
4-nitrophenol			286
2,4-nitrophenol	conversion efficiency in the aqueous phase: at pH < 4, OH > direct photolysis > NO_3; at pH > 4, OH ≈ direct photolysis > NO_3	photolysis at 300 ≤ λ ≤ 500 nm, HPLC-MS	279
2,4-nitrophenol	conversion efficiency in surface water: direct photolysis > OH > ^{3}CDOM ≈ $^1O_2$; OH formation and consumption in lake water	photolysis at 315 ≤ λ ≤ 380 nm, HPLC-DAD, TOC analysis	279
2,4-nitrophenol	$\Phi(H_2O) \ll \Phi$(octanol)	Xe-lamp, optical measurment	280
methoxy phenol	formation of phenolic dimers in the absence of H_2O_2; formation of small organic acids and aldehydes in the presence of H_2O_2	photolysis in the presence of ammonium sulfate, HPLC-DAD, HR-AMS, UPLC-ESI-ToF-MS, GC-MS, HTDMA, CCN counter	280
vanillin (4-hydroxy-3-methoxybenzaldehyde)			287

DOI: 10.1021/cr500447k
Chem. Rev. 2015, 115, 4259−4334

Table 6. continued

(B) findings on photochemistry			
system	main findings	remarks/techniques	refs
	phenols		
2-bromophenol	main product: pyrocatechol; photodegradation rate: 0.041 min^{-1}	reported kinetic isotope effect of the photolysis Hg-lamp, GC-MS, HPLC-UV, GC-C-IRMS	281
3-bromophenol	main product: resorcinol; photodegradation rate: 0.011 min^{-1}		281
4-bromophenol	main product: benzoquinone; photodegradation rate: 0.0049 min^{-1}		281
	other aromatics		
2-nitrobenzaldehyde (2-NB)	main product: nitrosobenzoic acid; temperature- and wavelength-independent quantum yield	used as field actinometer	278
4-hydroxy-3,5-dimethoxybenzoic acid (syringic acid)	formation of CH_3OH via C−O bond cleavage; presence of chloride yields CH_3Cl	NMR, ESI-MS, MIMS	282
3,4,5-trimethoxybenzoic acid			282
methyl-benzoquinone (mBQ)	main product: hydroxylated quinones; presence of DMSO suppress the formation of hydroxylated quinone and yields methyl radicals; triplet quenching rate constants with mBQ, Cl^-, NO_3^-, formate, and salicylic acid	Xe-lamp monochromator combination, λ = 300 ± 10 nm, EPR	288
	terpenoic acids		
cis-pinonic acid (*c*PA)	yields limononic acid by Norrish type II reaction	GC-CIMS, LC-ESI-MS, NMR, PTR-ToF-MS	277

[a]Remarks: HR-AMS, high-resolution aerosol mass spectrometry; nano-DESI MS, nanospray desorption electrospray ionization mass spectrometry; IC, ion-exchange chromatography; HPLC-UV, high-performance liquid chromatography-UV detection; HPLC-MS, high-performance liquid chromatography-mass spectrometry; HPLC-DAD, high-performance liquid chromatography-diode array detector; TOC, total organic carbon; UPLC-ESI-ToF-MS, ultra-performance liquid chromatography-electrospray ionization-time of flight-mass spectrometry; GC-MS, gas chromatography-mass spectrometry; HTDMA, hygroscopic tandem differential mobility analyzer; CCN counter, cloud condensation nuclei counter; GC-C-IRMS, gas chromatography-combustion-isotope-ratio mass spectrometry; MIMS, membrane-introduction mass spectrometry; EPR, 62 electron paramagnetic resonance; GC-CIMS, gas chromatography-chemical ionization mass spectrometry; LC-ESI-MS, liquid chromatography-electrospray ionization-mass spectrometry; NMR, nuclear magnetic resonance spectroscopy; PTR-ToF-MS, proton transfer reaction-time of flight-mass spectrometry.

some carbonyls were photochemically degradable in aerosol particles, clouds, and fog to a significant extent.

In the following subsections, systems where direct photolysis can represent a significant sink of substrates or source of products in atmospheric aqueous bulk systems will be discussed, cf., Table 6A.

4.3.1. Carbonyl Compounds. Carbonyl compounds, including keto-substituted compounds, represent an important class of atmospherically relevant species because they efficiently partition between the gas and the aqueous phase and are photoreactive in both phases at wavelengths around 280 nm via forbidden n → π^* transitions. The significance of aqueous-phase photolysis of carbonyl compounds has been evaluated in comparison to gas-phase photolysis.[270,271] Because carbonyl compounds can fully or partially hydrate in aqueous solution to form nonphotoactive geminal diols, a correct assessment of their photochemistry must involve a good characterization of their hydration behavior, for example, by predictions such as those described by Raventos-Duran et al.[161] For pyruvate, the effect of a water limitation (for example at low relative humidities) on the hydration equilibrium has been studied and is of atmospheric importance.[272] However, Epstein and Nizkorodov considered 27 carbonyls in a theoretical study and concluded that only glyceraldehyde and pyruvic acid may undergo aqueous photolysis as a significant sink reaction.[270] A follow-up study showed that aqueous quantum yields are highly molecule-specific and should therefore not be extrapolated from measurements of structurally similar compounds, and in addition that out of 92 screened carbonyls, only acetoacetic acid and again pyruvic acid had aqueous photolysis rates that exceeded the rates of OH radical reaction.[271]

4.3.2. Pyruvic Acid (PA). Results obtained to date suggest that the photochemistry of pyruvic acid may play a significant role in atmospheric aqueous chemistry.

In the pioneering study on this subject, Guzman et al. showed that pyruvic acid photolysis leads not only to its photodegradation but also to the photoformation of oligomer compounds,[22] although the mechanism of this reaction is still the topic of much discussion. The rate constant for the alkyl radical reaction with molecular oxygen provided by Guzman et al.[22] appears to the authors to be much too small, and should not have been extrapolated to other aqueous-phase $R^\bullet + O_2$ reactions. Following the above study, new research on pyruvic acid photochemistry reported the production of acetoin (partly lost to the gas phase), lactic acid, acetic acid, and oligomers with four or six carbon atoms.[25] Concerted hydrogen atom transfer and decarboxylation, which leads to the formation of dimethyltataric acid or lactic and acetic acid or the formation of acetoin, was proposed to explain these observations. This is in contrast to Guzman et al.,[22] who proposed long-range electron transfer between carbonyl groups. Furthermore, an additional dimer previously undetected was reported, but no structural and mechanistic information was given. Although the formation of the minor product acetoin was questioned in a comment by Eugene et al.,[273] Griffith et al. seem to present the stronger arguments in favor of their mechanism with their original paper[25] and the reply to this comment[274] because acetoin was detected by NMR in the aqueous solution and via its characteristic odor in the gas phase. The scheme given in Figure 4 summarizes the different suggested mechanisms for pyruvic acid photochemistry.

In the most recent contribution by Reed Harris et al.,[275] aqueous first-order photochemical decay rate constants were reported to be sensitive to pyruvic acid concentration and oxygen concentration[275] because, as to be expected, at lower concentrations the organic radicals are scavenged by oxygen. At aerobic conditions and the lowest pyruvic acid concentration of 0.02 M, the aqueous first-order photochemical decay rate

DOI: 10.1021/cr500447k
Chem. Rev. 2015, 115, 4259−4334

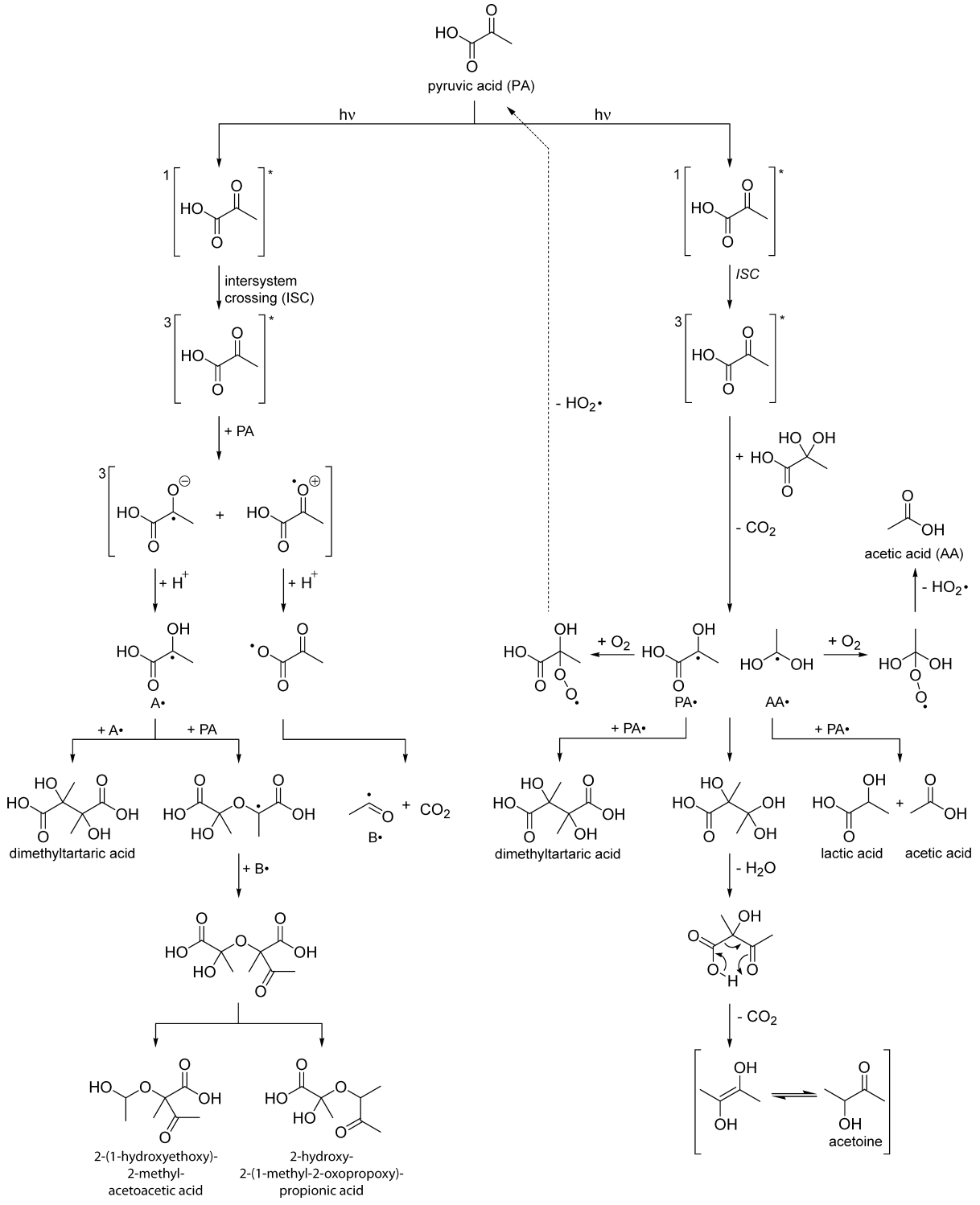

Figure 4. Schematic depiction of photoinduced pyruvic acid oxidation in the aqueous phase according to recent studies by Guzman et al. (printed on the left),[22] Griffith et al.,[25] and Reed-Harris et al.[275] (both on the right-hand side).

constant was $J = (8.08 \pm 0.09) \times 10^{-5}$ s^{-1}. Unfortunately, in that contribution, no absolute effective photochemical quantum yields were reported, which might complicate the further use of its results. The hydration of pyruvic acid has necessarily also been studied, and time- and concentration-dependent hydration constants have been reported. More details on the hydration are given earlier in Maron et al.[272] Very recently, the influence of real cloudwater components on pyruvic acid photochemistry has been studied.[73]

Finally, for the photolysis of pyruvic acid in aqueous solution, the possible contribution of near-infrared excitation of the OH vibrational overtone band followed by decarboxylation has been studied. The quantum yield of the resulting CO_2 formation was calculated to be $\Phi = (3.5 \pm 1.0) \times 10^{-4}$, which is too low to represent a significant sink reaction.[276]

In general, the photochemistry of pyruvic acid is currently a field of intense research, and it would be helpful for future

DOI: 10.1021/cr500447k
Chem. Rev. 2015, 115, 4259−4334

studies in this area to provide quantum yields, because these will enable the further numerical modeling of the system.

As a general remark regarding the aqueous photochemistry of carbonyl compounds, it should be noted that a relative scaling of aqueous-phase photolysis rates using gas-phase rates is not possible, as suggested earlier,[271] because different reaction pathways will occur in these two phases.[275]

4.3.3. Aqueous Photochemistry of Phenolic Compounds. The aqueous-phase chemistry of phenols has been studied very widely in the context of environmental and water treatment chemistry. Here, only recent studies of interest for atmospheric aqueous-phase chemistry will be discussed; quantitative results are summarized in Table 6.

In summary, direct photolysis should be studied as a potentially competitive conversion pathway to the radical-driven one for phenols in atmospheric aqueous systems. In this context, Rayne et al.[289] provide an overview of the mechanism of the direct photolytic degradation of phenol and halogenated phenols.

Sun et al.[283] and Yu et al.[284] report contributions of the direct photolysis of phenol, guaiacol, and syringol to SOA formation. Unfortunately, in this AMS-based study, no absolute quantum yields were reported. In addition, Smith et al.[285] reported the formation of secondary organic aerosol via the reaction of triplet excited-state phenols.

Vione et al.[286] have studied the effectiveness of different degradation and conversion pathways for 2- and 4-nitrophenol and Albinet et al.[279] for 2,4-dinitrophenol. In a companion paper, the same authors discuss the phototransformation of 2,4-dinitrophenol in surface waters.[279] In addition, Lignell et al.[280] investigated the photochemistry of 2,4-dinitrophenol and reported an increased quantum yield by changing the solvent from water to octanol or secondary organic material (SOM). These authors also studied matrix effects on the photolysis of 2,4-dinitrophenol.

The photodegradation of vanillin (4-hydroxy-3-methoxybenzaldehyde) has been investigated by Li et al.[287] Because of its methoxy group, vanillin has been regarded as a valid proxy compound for biomass burning aerosol particle constituents, which have been shown to often contain methoxyphenols. Photolysis led to large amounts of SOA, which was identified by AMS measurements.

Bromine and carbon isotope effects have been investigated for the photolysis of the three isomeric bromophenols.[281]

4.3.4. Other Aromatic Compounds. The direct photolysis of 2-nitrobenzaldehyde (2-NB) has been investigated in the context of its application as an actinometer[278] in the field; this work might also be of interest for the photochemical conversion of this compound in atmospheric aqueous systems.

A very interesting photochemistry has been revealed in the aqueous-phase photolysis of syringic acid, which in the presence of chloride leads to the formation of methyl chloride (CH_3Cl) via a photosubstitution reaction.[282]

Gan et al.[288] studied the direct photolysis of methylbenzoquinone in aqueous solution.

4.3.5. Terpenoic Acids: *cis*-Pinonic Acid. Lignell et al.[277] investigated the photochemistry of *cis*-pinonic acid (cPA) in aqueous solution. cPA can decompose via Norrish type I and type II pathways or via direct ring opening.

4.3.6. Amine Photochemistry. The tropospheric multiphase chemistry of amines has received increased interest recently, largely due to the fact that carbon capture and storage (CCS) might apply amine-based CO_2 capture technologies, which could, potentially, lead to the release of amines into the atmosphere (see Nielsen et al.[290] for further discussion of this topic). Kwon et al.[291] have investigated the direct UV photolysis of NDMA (*N*-nitrosodimethylamine) and observed the formation of nitrate and nitrite as well as a reactive intermediate, which has been identified as peroxynitrite (^-OONO). Apparently, the observed intermediate can either react similarly to OH or release OH. OH might be formed from the decomposition of peroxynitrous acid. The authors have determined a rate constant for the reaction of the intermediate with NDMA that is identical to the known OH rate constant.

4.3.7. Hydroperoxyl Species in Aqueous Solution. This section reviews available material on the chemistry of organic hydroperoxyl species in aqueous solution, including hydroxyhydroperoxides, hydroperoxyenals, and hydroperoxides.

4.3.7.1. α-Hydroxyhydroperoxides (α-HHPs). It has been known for some time that organic hydroperoxides might constitute a considerable fraction of SOA, especially that from biogenic sources (see, e.g., Bonn et al.[292]). Following Zhao et al.,[59,60] several formation pathways are discussed.

As can be seen from the scheme presented in Figure 5, α-HHPs can be formed by the reaction of stabilized carbonyl oxides (Criegee intermediates) with water, or by nucleophilic attack of hydrogen peroxide on the central carbon atom of aldehydes or ketones. These latter formation pathways are very interesting, as they have the potential to convert significant fractions of aqueous-phase carbonyls into α-HHPs, which makes these compounds accessible to direct photolysis as well as radical attack, then, however, leading to different products as compared to those from radical reactions with the substrate carbonyl compounds.

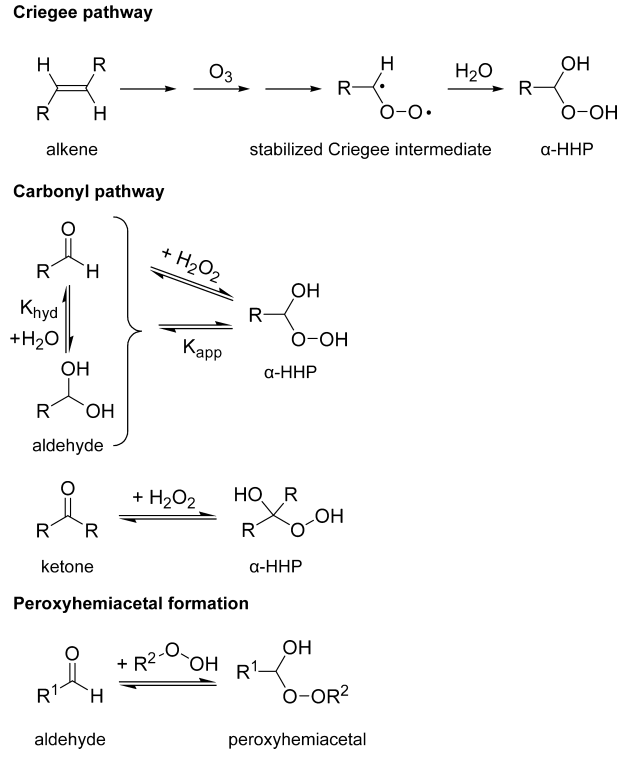

Figure 5. Possible formation pathways of α-hydroxyhydroperoxides (α-HHP) in the aqueous phase modified after Zhao et al.[60]

DOI: 10.1021/cr500447k
Chem. Rev. 2015, 115, 4259−4334

The definition of the hydration equilibrium constant (K_{hyd}) is given in eq 3, whereas eq 4 represents the apparent equilibrium constant for α-HHP formation (K_{app}).

$$K_{hyd} = \frac{[\text{hydrated-carbonyl compound}]}{[\text{nonhydrated-carbonyl compound}]} \quad (3)$$

$$K_{app} = \frac{[\text{entire } \alpha\text{-hydroxyhydroperoxide}]}{[\text{hydrogen peroxide}] \times [\text{entire carbonyl compounds}]} \quad (4)$$

Hydration equilibrium constants (K_{hyd}) resulting from the studies of Zhao and other authors and the α-HHP formation equilibrium constants (K_{app}) of Zhao are compiled in Table 7.

Table 7. Summary of Hydration Equilibrium Constants K_{hyd} and of the Apparent Equilibrium Constant of α-HHP Formation K_{app} at T = 298 K Taken from Zhao et al.[60]

reactant	K_{hyd}	K_{app} [M^{-1}]	refs
formaldehyde	>18[a]	164 ± 31[b] (NMR)	60
	2300		293
		126	294
		150	295
		94	296
acetaldehyde	1.43 ± 0.04	94.8 ± 12.5 (NMR) 132 ± 15 (PTR)	60
	1.43		293
		48	296
propionaldehyde	1.26 ± 0.13	51.1 ± 8 (NMR) 84 ± 12 (PTR)	60
	0.7		297
glycolaldehyde	16 ± 1.3	43.3 ± 3.9 (NMR)	60
	10		298
	17.5[c]		299
methacrolein	5×10^{-3}[a]	0.8 ± 0.7 (NMR)	60
glyoxal	40−200		59
	2.2×10^{5}		300
methylglyoxal	57 ± 155[a]	25 ± 4[d] (NMR)	60
	2.3×10^{3}		300
	40−200		59
glyoxylic acid	>18		60
	3×10^{3}	440 ± 270[d] (NMR)	301
acetone	2×10^{-2}[a]	8×10^{-3}[a]	60
	2×10^{-3}		302
methylethyl ketone	5×10^{-3}[a]	2×10^{-2}[a]	60

[a]Calculated using the detection limit of the method. [b]Including the formation of bis-hydroxymethyl hydroperoxide (BHMP). [c]In D_2O. [d]Formic acid was detected. The K_{app} value was determined with the consideration of the formation of formic acid.

With the kinetic data from Table 7, first-order reaction rates were estimated to assess the importance of α-HHP formation in the tropospheric aqueous phase. To do this, for the backward reaction of the equilibrium K_{app}, the rate constants of the hydration equilibrium of small carbonyls (HCHO) with k_{back} = 5×10^{-3} M^{-1} s^{-1} were used. Oxidant concentrations of 1×10^{-6} M for H_2O_2 and 1×10^{-14} M for the OH radicals, respectively, then were applied. Next, $k = 1 \times 10^{9}$ M^{-1} s^{-1} was used as the OH radical rate constant. The comparison of the estimated first-order rate constants indicates that the α-HHP formation might be important under cloudwater conditions. The flux into α-HHPs can reach about 10% of the OH degradation rate.

Interestingly, α-HHP formation will influence phase partitioning of carbonyl compounds and enhance their cloudwater and aerosol liquid water (ALW) fractions considerably. It should be noted, however, that even for the very soluble smallest aldehydes, partitioning fractions are much higher for cloud conditions than for ALW even when α-HHP formation is considered. In conclusion, α-HHP formation and degradation are strong candidates for inclusion into complex tropospheric aqueous-phase models.

4.3.7.2. Hydroperoxyenals or Unsaturated Hydroperoxyaldehydes (HPALDs). Hydroperoxyenals have received much recent attention because of their role in isoprene oxidation. Because of their polarity, they would be expected to partition effectively into aqueous particles and cloud droplets; however, this partitioning has not yet been quantified. As a result, currently available attempts to model multiphase chemistry in the context of isoprene oxidation have to be regarded as, at best, incomplete.

4.3.7.3. Methylhydroperoxide (or "Methylperoxide", CH_3OOH). Monod et al.[112] reported the photooxidation of methylhydroperoxide and ethylhydroperoxide in the aqueous phase at T = 279 K. Corresponding aldehydes, acids, and hydroxyhydroperoxides were determined as primary reaction products.[112] Epstein et al.[270] have studied the photolysis of methylhydroperoxide. For temperatures above 301 K, the measured overall quantum yields exceed unity, as they have not been corrected for subsequent reactions. The gas-phase photochemical loss of CH_3OOH dominates, but for higher zenith angles and lower temperatures, aqueous-phase photolysis might become more competitive and could contribute, at maximum, up to 20% of the overall photolytic loss of this compound in the tropospheric multiphase system.[270]

4.3.8. Photochemistry of SOA. As previously discussed in this section, many investigations dealing with the aqueous-phase photochemistry of organic compounds are motivated by the possible contribution to organic particle mass of the reaction products formed in these processes. In addition to these studies, it is also legitimate to undertake photochemical studies with SOA that has previously been generated under defined conditions, and to investigate how photochemical processes contribute to the formation of organic mass or to changes in its composition via photolysis and subsequent reactions. Evidence exists to suggest that many SOA constituents, as studied by Nguyen et al.[51] for SOA formed from isoprene under NO_x-rich conditions, are prone to undergo photochemical conversion. For this reason, SOA particle chemistry has to be regarded incomplete when photochemical reactions in the particle bulk phase are neglected. As has been shown by Bateman et al.,[23] photochemical conversion might also take place under cloudwater conditions when SOA dissolves from cloud condensation nuclei (CCN). Direct photochemical conversion might considerably change SOA composition; care has to be taken, however, to discern whether this photochemistry does really occur in the aqueous medium (i.e., in aerosol liquid water) or, alternatively, in the particle organic phase. Interestingly, Lee et al.[303] have very recently shown that exposure of biogenic SOA constituents to reduced nitrogen species such as NH_3 results in the production of fluorescent SOA. Fluorescence is known to be a well-established detection technique for biological particles such as viruses, bacteria, spores, pollen, and others.[304] Given

DOI: 10.1021/cr500447k
Chem. Rev. 2015, 115, 4259−4334

the above work, care must be taken in assigning fluorescence signals to such intact bioparticles.

4.3.9. Humic Substances and Humic-Like Substances: Links to Surface Water Photochemistry. Humic-like substances, often addressed as HULIS in atmospheric research, have been suggested to play a role in aqueous aerosol and cloud chemistry.[305,306] Currently, however, it appears unclear if these substances really represent an important aerosol constituent class, because humic material might be exported from the Earth's surface by mobilization of crustal material during erosion or, in the other extreme, HULIS could just be a group of individual SOA constituents that are not individually identifiable. It might be that the truth is between these two extremes: both organic material from solids and organics, which are being formed and transformed through atmospheric processing, might contribute to HULIS. In this manner, HULIS could partly be of primary and partly of secondary origin. Clearly, more work is needed here to elucidate primary and secondary contributions to this compound class.

The sheer amount of organic compounds in tropospheric particles constitutes an important sink for reactive species, and hence it is important in modeling to mimic the overall organic content of tropospheric particles by proxies, which often rely on total carbon measurements or the determination of humic-like substances.

The photochemistry of humic substances (HS) is important because these compounds can act as photosensitizers. These photochemically active species might change the molecular composition of humic substances itself. Hence, studies of humics photochemistry are of strong interest for atmospheric aqueous-phase chemistry. Sharpless et al.[307] have investigated how important properties of humic substances change upon photochemical processes with regard to both of the two aspects mentioned above. These authors primarily address surface water chemistry, but much of the information presented is relevant for atmospheric aqueous-phase chemistry as well. Key findings show that for humic substances containing many phenolic groups, the apparent quantum yields of the formation of H_2O_2, OH radicals, and triplet HS decreased with photooxidation, as a result of the destruction of HS photosensitizing chromophores. By contrast, the apparent quantum yield of singlet oxygen ($^1O_2$) increased, either by photochemically stable sensitizers or a decrease in the singlet oxygen quenching rate. Bulk aqueous-phase photosensitization studies of interest for atmospheric chemistry have been performed by a variety of authors and are reviewed in the subsequent section in more detail.

A recent methodological study by Sun et al.,[308] which also addresses surface water photo- and radical chemistry, might also be of interest for atmospheric aqueous-phase chemistry. The authors show that OH degradation rates might become incorrect when photochemical experiments are run for lengthy (>2 h) irradiation times.

4.3.10. Direct Photochemistry Summary. The contributions reviewed here show that particle bulk-phase organic photochemistry can considerably contribute to the formation of SOA and/or change the composition of existing SOA. The exploration of this organic photochemistry is currently only in a preliminary stage, and many findings are very interesting but not yet quantitative enough to be included into models. The same care as has been applied to gas-phase atmospheric photochemistry over the past decades should now also be applied to studies of aqueous aerosol and cloud organic chemistry: a system can only be regarded as understood when absorption coefficients, photolysis quantum yields, and the most important photolysis products have been identified over the range of actinic wavelengths. Many studies available now either lack these data or report them in an "assembled" format; more clarity seems to be needed here. If more complete photochemical data become available, implementation into multiphase models will allow a quantitative assessment of the extent to which organic photochemistry is competitive not only with radical oxidation but also with other competing photolysis processes only possible in the atmospheric aqueous phase, such as the photolysis of TMI−organic complexes for a given organic compound.

4.4. Photosensitized Reactions in the Bulk Aqueous Phase

The formation of light-absorbing species has the potential to induce new photochemical processes within tropospheric aerosol water and in cloud droplets. A significant body of literature exists on photoinduced charge or energy transfer in organic molecules (biochemistry and water waste treatment).[309] A photosensitizer is a light-absorbing molecule that in its excited state is able to react with another molecule. Both with regard to its rate constants and its mechanism, the following reaction of the photosensitizer depends on the redox properties of the medium and the reaction partners involved. Two possible reaction pathways then can occur: (i) a one-electron charge transfer reaction (photosensitization type I) to produce a radical or a radical ion in both the reaction partner and the photosensitizer, or (ii) an energy transfer reaction (photosensitization type II) to transfer the excess energy of the excited photosensitizer to the reaction partner to produce a ground-state photosensitizer and an excited-state reaction partner. While aquatic photochemistry has recognized that several of these processes accelerate the degradation of dissolved organic matter,[309−311] little is known regarding such processes in/on atmospheric particles.[312] Because many photosensitizers are amphiphilic, it might be argued that photosensitized reactions might be more prevalent at interfaces as compared to the bulk. However, because many studies exist on bulk aqueous-phase photosensizitation, the authors believe that this chemistry should be treated within the present contribution.

The study of photosensitized reactions in the context of atmospheric chemistry and especially secondary organic aerosol (SOA) is an emerging field with enormous potential but many remaining uncertainties,[37] especially regarding the role of atmospheric HULIS as potential photosensitizer, among other compounds. HULIS is generally ill-defined, has a variable composition, no suitable standards are existing but only proxy-compounds, and the adequacy can be debated; due to this the connected processes are hard to quantify both experimentally and in simulations. As was already stated above, an adequate representation of this topic in models will represent one of the major challenges in atmospheric multiphase chemistry studies.

Publications such as the early Canonica et al.[313] study of phenol degradation have led the scientific interest toward photosensitization reactions in surface waters. In this study, several aromatic ketones were applied as photosensitizers, mechanisms were elucidated through the determination of kinetic isotope effects, and surface water concentrations of excited reactive species in Lake Greifensee in Switzerland were derived. A wide variety of photosensitized reactions have been investigated not only in the context of surface water chemistry

DOI: 10.1021/cr500447k
Chem. Rev. 2015, 115, 4259−4334

Table 8. Experimental Data for Bulk Aqueous-Phase Photosensitized Reactions Involving Organic Compounds in Aqueous Solution Relevant for Atmospheric Chemistry[a]

compound/wavelength [nm]	photo excitation reaction	quenching reactant	quenching rate constant [M^{-1} s^{-1}]	remarks	refs
imidazole-2-carboxaldehyde (IC), 266 nm	IC + $h\nu \rightarrow {}^3$IC*	iodide (I^-)	$(5.33 \pm 0.25) \times 10^9$	absolute measurement from Stern–Volmer analysis	323
		bromide (Br^-)	$(6.27 \pm 0.53) \times 10^6$	absolute measurement from Stern–Volmer analysis	323
		chloride (Cl^-)	$(1.31 \pm 0.16) \times 10^5$	absolute measurement from Stern–Volmer analysis	323
3,4-dimethoxy-benzaldehyde (DMB), simulated sunlight	DMB + $h\nu \rightarrow {}^3$DMB*; ^{3}DMB* + $H^+ \rightleftharpoons$ [^{3}DMB*H^+]	phenol (C_6H_5OH)	HT, $(3.4 \pm 1.2) \times 10^9$; T, $(1.3 \pm 0.9) \times 10^8$	analysis of reactant depletion	285
		guaiacol (2-methoxyphenol, $CH_3OC_6H_4OH$)	HT, $(5.3 \pm 1.9) \times 10^9$; T, $(4.2 \pm 3.0) \times 10^9$	analysis of reactant depletion	285
		syringol (2,5-dimethoxyphenol, $(CH_3O)_2C_6H_3OH$)	HT, $(1.1 \pm 0.3) \times 10^{10}$; T, $(5.8 \pm 4.1) \times 10^9$	analysis of reactant depletion	285
1-nitronaphtalene (1-NN)	1-NN + $h\nu \rightarrow {}^3$1-NN*	bromide (Br^-)	$(7.5 \pm 0.2) \times 10^8$		6,324
		nitrite (NO_2^-)	$(3.36 \pm 0.28) \times 10^9$		325
2-acetonaphtone (2-AN)	2-AN + $h\nu \rightarrow {}^3$2-AN*	2,4,6-trimethylphenol (TMP)	$(6.2 \pm 0.2) \times 10^8$		326
			$(7.2 \pm 0.1) \times 10^8$		309
		fulvic and humic acid isolates	$(1.30–3.85) \times 10^7$	different substrates, see ref for single data	326

[a]T, triplet species; HT, protonated triplet species.

but also in the context of atmospheric aqueous-phase chemistry.[314−318]

It should be noted that photosensitized reactions might occur at both the interfaces of particles as well as in their bulk and that this class of reactions is well-known in other areas of environmental photochemistry. Interfacial photochemistry involving photosensitization will be discussed by the contribution of George and co-workers in this volume of *Chemical Reviews* (key references include, but are not limited to, Monge et al.,[319] and, more recently, Aregahegn et al.[320] and Rossignol et al.[321]). These cited papers elucidate particle growth due to both interfacial and bulk-phase photosensitized chemistry. A recent feature article gives a further overview on photosensitization, including the heterogeneous and multiphase reactions involved and the occurrence of such processes not only in the environment but also indoors.[322]

In the following sections, important findings for photosensitized bulk photochemistry will be discussed; available process parameters are summarized in Table 8.

4.4.1. Glyoxal and Imidazole Photosensitized Chemistry. Tinel et al.[323] have recently investigated the aqueous-phase chemistry of imidazole-2-carboxaldehyde (IC) acting as a photosensitizer and characterizing the reactions of its excited triplet state with halides after its formation via irradiation at λ = 266 nm. Stern–Volmer kinetic analysis was performed, from which a set of absolute quenching rate constants for this photosensitizer was determined. These kinetic data listed in Table 8 might be very useful in forthcoming descriptions not only of aerosol liquid water chemistry, fog, and cloud chemistry but also of sunlit surface water chemistry. This approach clearly leads the way for further quantitative descriptions of atmospheric aqueous-phase photochemistry studies involving photosensitization.

Rossignol et al.[321] have recently shown in flow-tube and bulk chemistry studies with direct (±)ESI-HRMS and UPLC-(±)ESI-HRMS product studies that IC, when irradiated, reacts with limonene, which leads to a variety of recombination products and oxygen-containing species, which in turn leads to significant aerosol particle growth directly observed in the flow tube experiments. It is interesting to note that in these experiments no gas-phase oxidant was present; particle-phase chemistry alone led to the observed growth. Such chemistry should be further elucidated not only for photosensitized chemistry but also for other particle-phase oxidation reactions and could help to establish benchmarking experiments when comparing particle growth rates differentiating between different particle chemistry pathways.

4.4.2. Photosensitized HULIS Formation. It has been discussed by De Laurentiis et al.[327] whether humic-like substances (HULIS) can be formed by photosensitized chemical reactions, for example, from the reaction of the photosensitizer 1-nitronaphthalene with phenols. This subject deserves further exploration. Actually, because the definition of HULIS is not very clear, although the production of any particle-phase organic compounds might be seen as a contribution to atmospheric particle HULIS, it would better be referred to simply as a contribution to particle organics. Because this study focused on the reactions of phenols, its results might be of interest in atmospheric biomass burning studies (see the subsequent section).

Vione et al.[328] present another contribution on this topic as a mini-review. In this context, it might be worthwhile to mention that the same group found a negligible photoactivity of DOM (dissolved organic matter) in rainwater samples collected at a polluted site in Turin.[329]

4.4.3. Photosensitization Reactions and SOA Related to Phenols and Biomass Burning. A number of publications on this issue are available, which are referenced in a recent contribution by Smith et al.[285] Equally as shown in the above-mentioned contributions from the group of C. George for interfacial photosensitized reactions, here the potential for photosensitized reactions in bulk atmospheric aqueous chemistry is demonstrated. Besides radical and nonradical oxidation reactions and direct photochemistry, photosensitized reactions can potentially be important to correctly describe the oxidation of organics within aqueous atmospheric particles.

DOI: 10.1021/cr500447k
Chem. Rev. 2015, 115, 4259−4334

Specifically, the contribution by Smith et al.[285] from the group of Cort Anastasio investigated the reactions of 3,4-dimethoxybenzaldehyde (DMB), which is excited into its triplet state and then reacts with three different phenols: phenol itself, guaiacol, and syringol. Absolute rate constants for the reactions of ^{3}DMB* with these phenols are derived, which are included in Table 8. The reactions are found to be very fast, with all three rate constants above 10^9 M^{-1} s^{-1}. Interestingly, the excited ^{3}DMB* can be protonated, and the resulting protonated species appears to be even more reactive than the unprotonated species. A pK_A value for the excited species is derived. All of the triplet species together can be regarded as a pool of the nonprotonated and the protonated species linked by their specific pK_A values.

4.4.4. Nitrite and Bromide Oxidation. Maddigapu et al.[325] have investigated 1-nitronaphthalene as photosensitizer and have shown that this compound is able to oxidize bromide to bromine atom and nitrite to NO_2. The actual concentrations of 1-nitronaphthalene in ALW, fogs, and clouds need to be clearly addressed to be able to judge if such oxidations might lead to considerable turnovers in the real atmosphere. The experimentally determined rate constants for these reactions have been included in Table 8.

4.4.5. Surface Water Chemistry. Vione and coauthors have very recently summarized the photoproduction of reactive transient species in surface waters.[328] The reader is referred to this overview if interested in a current account of surface water chemistry, which, in many ways, might also be of interest for atmospheric aqueous-phase chemistry, with, however, at times largely differing concentrations of soluble material. Similarly, another recent review accounts for the degradation of pesticides by indirect photochemistry in surface waters.[330]

The role of humic and fulvic acids in the degradation of phenols in seawater has been treated by Calza et al.[331] Clark et al.[332] studied the production of hydrogen peroxide from chromophoric dissolved organic matter (CDOM) in seawater.

4.4.6. Other Systems. The aqueous photochemistry of methyl-benzoquinone has been studied in detail by Gan et al.[288] Like other quinone-type compounds, this molecule might act as a photosensitizer in atmospheric aqueous systems.

Liu et al.[333] have recently studied an approach to use the photosensitization chemistry of diketones for the removal of dyes from aqueous solutions. Liang et al. have studied the role of nitrate and natural organic matter (NOM) as photosensitizers in the photolysis of phenol.[334]

Photosensitization has been very successfully considered as a possible pathway for the oxidation of organic compounds in surface waters since the mid-1990s.[313] Such studies, with much improved experimental laboratory effort, continue until today[326] and have recently demonstrated that dissolved natural organic matter present in environmental waters can also quench excited triplet states of organic molecules. Similar sensitizers and quenchers might, of course, also be expected to be present in atmospheric waters, and hence care needs to be taken to not overestimate the importance of chemical conversions driven by triplet state excited organic molecules. Selected quenching rate constants from this work are included in Table 8. It has to be mentioned that these quenching rate constants are of the same order of magnitude as the corresponding OH radical rate constants (section 5.2). Under conditions where the OH radical concentration in aqueous solution is limited,[335] the photosensitization reaction might be the major pathway in the aqueous phase.[113] Humic and fulvic acids from different sources have been shown to quench the excited triplet state formed from model photosensitizers such as 2-acetonaphthone, with rate constants of the order of 10^7 M^{-1} s^{-1}.[326]

4.5. Summary of Section 4

In conclusion, remarkable progress in our understanding of aqueous-phase photochemistry has been achieved in the last 5 years: new photolysis process data are available in all three areas discussed in this section. First, new data regarding the photolysis of inorganic constituents have improved our knowledge of these systems, which are special for the aqueous phase and which are known to be important in atmospheric aqueous-phase chemistry. Second, in the case of the photochemistry of complexes of transition-metal ions (TMI) with organics, some progress has been made after many years during which our knowledge was essentially restricted to the photolysis of iron−oxalato complexes (which, as it has been mentioned at several occasions throughout this text, must not be neglected in any "aqSOA" formation prediction). Third, it is now clear that the aqueous photochemistry of organics plays an important role in aerosol chemistry.

Photosensitized reactions are another topic of current interest, but their potential to significantly change organic constituents' molecular identities and hence the overall organic composition of the aerosol phase must still be better explored. Specifically, more quantitative data are needed, including absolute quenching rate constants for photosensitized systems and experiment-based photolysis frequencies for the photolysis processes in question, based on wavelength-dependent absorption coefficients and quantum yields.

Overall, the appearance of a high number of pioneering studies for photochemistry related to atmospheric aqueous-phase elements is remarkable; this is a section of rising importance in atmospheric aqueous-phase chemistry, and one that clearly must be further explored.

5. RADICAL REACTIONS

5.1. Nonphotolytic Radical Sources

In addition to photolytic radical sources, some nonlight-induced reactions have the potential to act as radical sources in the tropospheric aqueous phase. In the following section, a short overview of important tropospheric nonphotolytic radical sources is given. One of the best known and most important reactions for atmospheric chemistry is the Fenton reaction.[336−349] The Fenton (Fe(II)/H_2O_2), or Fenton-like (Fe(III)/H_2O_2), reactions involve the production of OH radicals by the decomposition of H_2O_2 catalyzed by low-valence transition metals such as Fe(II), Fe(III), Cu(I), Mn(III), or Mn(IV).[33,207] Organic hydroperoxides are also able to act as OH radical sources through photolysis or Fenton-type reactions.[350] See et al.[351] and the references therein reported the presence of reactive oxygen species (ROS) in the water-soluble fraction of fine particles of combustion origin, which contained the transition metals Ag, Cd, Co, Cu, Fe, Mn, Ni, Ti, V, and Zn. The metal-catalyzed oxidation of S(IV), such as sulfurous acid, leads to S(VI) species, which involves the formation of SO_4^- and SO_5^- radicals.[6,33] In addition, the pH-dependent decomposition of ozone in the aqueous phase can act as an OH radical source.[352−359] The reaction of ozone with unsaturated organic compounds leads to the formation of reactive Criegee intermediates, which decompose in water to yield organic α-hydroxyhydroperoxides (α-HHPs)[352,360] (see

DOI: 10.1021/cr500447k
Chem. Rev. 2015, 115, 4259−4334

section 4.3). This class of organic hydroperoxides is also able to act as an OH radical source via photolysis or Fenton-type reactions.

5.2. Kinetics

The importance of the radicals OH, NO_3, and SO_4^- for tropospheric multiphase chemical conversion processes has long been known.[12,35] In the tropospheric aqueous system, radicals can react by three different mechanisms: (i) by H atom abstraction from saturated compounds, (ii) by electrophilic addition to carbon−carbon double bonds present in unsaturated compounds and aromatic systems, and (iii) by electron transfer. The efficiency of the third pathway strongly depends on the properties of the reactant (e.g., its structure and reduction potential). In contrast to other atmospheric free radicals, OH radicals are both highly reactive and nonselective. An overview on atmospheric aqueous-phase radical reactions is given in Herrmann[12] and Herrmann et al.[35] The radical concentrations in clouds and deliquescent particles estimated by the multiphase mechanism CAPRAM 3.0i are $[OH] = 1.4 \times 10^{-16}$ to 8.0×10^{-12} M; $[NO_3] = 1.6 \times 10^{-16}$ to 2.7×10^{-13} M; and $[SO_4^-] = 5.5 \times 10^{-17}$ to 9.1×10^{-13} M.[35]

5.2.1. OH Radical Kinetics. In the 5 years since the publication of Herrmann et al.,[35] a number of new rate constants for the reaction of OH with different compound classes have been obtained from laboratory studies (Table 9). Only a few new rate constants are available for oxygenated organic compounds. The values of the rate constants for acetone, methylglyoxal, and glyoxal are in good agreement with the literature values.[35,166] In addition, the rate constants of the crown ethers are within the expected range for this compound class.[361]

New rate constants for unsaturated compounds include a first determination of the rate of OH radical addition to isoprene, with $k_{283K} = (1.4 \pm 0.4) \times 10^{10}$ M^{-1} s^{-1}.[362] These authors also investigated the OH reactivity of the first-generation isoprene oxidation products methacrolein and methyl vinyl ketone (see section 7.2.2). The measured values for these compounds are close to the diffusion limit of OH radicals in the aqueous phase and, when compared to those obtained by Schöne et al.,[363] appear slightly too high. By contrast, the value at $T = 279$ K for the OH oxidation of methacrolein reported by Liu et al.[47] is in good agreement with the rate constant obtained by Schöne et al.[363] In the case of methyl vinyl ketone, Zhang et al.[364] obtained a modeled value of $k_{283K} = 8 \times 10^8$ M^{-1} s^{-1}, which seems to be too low for this reaction type. Within this compound class, new temperature dependencies are only available from Schöne et al.[363] and Richards-Henderson et al.[365] Sets of rate constants for carboxylic acids and halogenated carboxylic acids are available from Schaefer et al.[109] and Minakata et al.[366] The measured temperature-dependent rate constants for pyruvic acid and pyruvate are slightly higher than the values reported by Ervens et al.[367] The values reported by Minakata et al.[366] clearly show the influence of the different halogen substituents on the measured rate constants. These authors also reported rate constants for tribromoacetic acid ($k_{296K} = (1.7 \pm 0.1) \times 10^8$ M^{-1} s^{-1}) and trichloroacetic acid ($k_{296K} = (6.2 \pm 0.1) \times 10^7$ M^{-1} s^{-1}). In these cases, OH radicals can react only by an electron transfer reaction with the carboxyl group.

In a study of the aqueous-phase reaction of OH radicals with a number of nitramines, Mezyk et al.[371] showed that the rate constant increased from $k = 5.4 \times 10^8$ M^{-1} s^{-1} to $k = 4.4 \times 10^9$ M^{-1} s^{-1} with increasing carbon chain length, and suggested that the oxidation primarily occurs by hydrogen atom abstraction from the alkyl chain.

A number of new OH rate constants are available for aromatic compounds. Wen et al.[375] investigated the oxidation of a series of substituted phthalates, including dimethyl phthalate, in a continuous flow system (CFS). Their results, which were obtained using the completion kinetics method with *p*-chlorobenzoic acid as reference compound, agree well with direct measurements at $\lambda = 260$ nm and $\lambda = 320$ nm by An et al.[374] and Wu et al.[373] Solar et al.[381] and Venu et al.[378] have measured the rate constants of the aromatic compounds 2-aminobenzoic acid, 4-aminobenzoic acid, and thymol with OH and its deprotonated form, O^- ($pK_a = 11.9$[166]). These authors showed that the rate constant for the O^- radical anion reaction is smaller than that measured for the OH radical reaction. The reason for this is that in its reaction with organic molecules, the OH radical behaves as an electrophile, whereas the O^- radical behaves as a nucleophile: OH radicals readily add to unsaturated bonds, but O^- radicals do not. The radical anion, by contrast, is known to react by one-electron oxidation.[35,165,166] Both forms of the radical are able to abstract H-atoms from C−H bonds.[166] Albinet et al.[279] and Biswal et al.[382] measured the difference between the OH rate constants for 2,4-dinitrophenol/2,4-dinitrophenolate and 4-nitrophenol/4-nitrophenolate, and found that the deprotonated phenolates react faster with the OH radicals than their corresponding protonated forms. It should be mentioned that a number of OH radical rate constants are also available for trace pollutants such as pesticides, insecticides, and pharmaceuticals. These compounds are often substituted aromatic compounds with heteroatoms such as nitrogen, phosphorus, or sulfur. The treatment of these compounds has become a high-priority task for the drinking and wastewater industries as they can influence the quality, taste, or odor of drinking water. A brief overview of this topic has been given in some recent studies.[327,383−394] In general, the rate constants for this compound class are in the typical range ($k \approx 10^9$−10^{10} M^{-1} s^{-1}).

In addition to these species-specific rate constants, several studies of overall OH radical loss via reaction with dissolved organic carbon (DOC) present in atmospheric or surface water samples are available. For example, OH sinks have been investigated in rainwater from Italy,[279] cloud and fogwater from the U.S.,[340,395] and aerosol extracts from Japan.[208] The OH sinks in surface water from different lakes in Italy,[396] the U.S.,[397] Switzerland,[398] and Norway[399] and from rivers in the U.S.[397] have also been investigated. In these studies, the OH scavenging rate constant was found to range from $k_{DOC} = 3.0 \times 10^7$ M^{-1} s^{-1} to $k_{DOC} = 2.4 \times 10^9$ M^{-1} s^{-1}. Arakaki et al.[208] compared the mean scavenging rate constant for the rain, cloud, and fogwater samples with their results obtained for aerosol extracts and obtained a general value for the OH sink in atmospheric water of $k_{DOC} = (3.8 \pm 1.9) \times 10^9$ M^{-1} s^{-1}. To avoid overestimations of free radical concentrations in both ALW and cloudwater, OH scavenging by DOC should be implemented in models.

5.2.2. NO_3 Radical Kinetics. In contrast to other free radicals, which are largely photochemically produced, the nitrate radical (NO_3) undergoes efficient daytime photolysis and is thus an important night-time oxidant in the troposphere. As shown in Table 10, the number of available rate constants for NO_3 is much smaller than that for the OH radical. Summaries of nitrate radical kinetics in aqueous solution have

DOI: 10.1021/cr500447k
Chem. Rev. 2015, 115, 4259−4334

Table 9. Overview of OH Radical Kinetic Data in the Aqueous Phase since 2010[a]

reactant	technique	pH	k_{second} [M^{-1} s^{-1}]	temperature [K]	A [M^{-1} s^{-1}]	E_A [kJ mol^{-1}]	measurement technique	k_{ref} [M^{-1} s^{-1}]	refs
				oxygenated compounds					
acetone	LFP/H_2O_2	6	1.3×10^8	298			model fit		109
crown ether 12-crown-4	PR		$(7.2 \pm 0.2) \times 10^9$	298			C.K./SCN^-		361
crown ether 15-crown-5	PR		$(8.2 \pm 0.2) \times 10^9$	298			C.K./SCN^-		361
glyoxal	LFP/H_2O_2	6	$(9.2 \pm 0.5) \times 10^8$	298	$(5.8 \pm 0.1) \times 10^{10}$	10 ± 1	C.K./SCN^-	1.19×10^{10}	110
levoglucosan	SPR	3	$(7.9 \pm 0.1) \times 10^8$	293		12 ± 10	C.K./BA		368
	SPR	5.5	$(2.4 \pm 0.3) \times 10^9$	293		2 ± 5	C.K./BA		368
	SPR	8	$(1.6 \pm 0.1) \times 10^9$	293		27 ± 10	C.K./BA		368
methyl glyoxal	LFP/H_2O_2	6	$(6.1 \pm 0.2) \times 10^8$	298	$(7.8 \pm 0.2) \times 10^9$	12 ± 2	C.K./SCN^-	1.24×10^{10}	109
				unsaturated compounds					
acrylic acid	LFP/H_2O_2	1	$(5.1 \pm 0.8) \times 10^9$	298	$(9.4 \pm 0.1) \times 10^{10}$	7 ± 1	C.K./SCN^-	1.24×10^{10}	363
acrylate	LFP/H_2O_2	8	$(5.9 \pm 0.9) \times 10^9$	298	$(1.8 \pm 0.1) \times 10^{10}$	3 ± 1	C.K./SCN^-	1.24×10^{10}	363
isoprene	SPR	4/7	$(1.4 \pm 0.4) \times 10^{10}$	283			C.K./SA	1.6×10^{10}	362
methacrolein	SPR	4/7	$(1.3 \pm 0.2) \times 10^{10}$	283			C.K./SA	1.6×10^{10}	362
	LFP/H_2O_2	6	$(9.4 \pm 0.5) \times 10^9$	298	$(5.6 \pm 0.6) \times 10^{11}$	10 ± 7	C.K./SCN^-	1.24×10^{10}	363
	SPR	6	$(5.8 \pm 0.9) \times 10^9$	279			C.K./1-propanol	2.7×10^9	47
methacrylic acid	LFP/H_2O_2	1	$(1.1 \pm 0.1) \times 10^{10}$	298	$(1.0 \pm 0.1) \times 10^{12}$	11 ± 3	C.K./SCN^-	1.24×10^{10}	363
methacrylate	LFP/H_2O_2	8	$(1.1 \pm 0.1) \times 10^{10}$	298	$(8.0 \pm 0.5) \times 10^{10}$	16 ± 6	C.K./SCN^-	1.24×10^{10}	363
methyl vinyl ketone	SPR	4	8×10^8	283			model fit		364
	SPR	4/7	$(1.2 \pm 0.1) \times 10^{10}$	283			C.K./SA	1.6×10^{10}	362
	LFP/H_2O_2	6	$(7.3 \pm 0.5) \times 10^9$	298	$(9.0 \pm 0.4) \times 10^{11}$	12 ± 3	C.K./SCN^-	1.24×10^{10}	363
			7.4×10^9	298					87
2-methyl-3-buten-1-ol	SPR	3.1	$(7.5 \pm 1.4) \times 10^9$	298			C.K./BA	6.2×10^9	365
	SPR	5.4	$(8.0 \pm 0.6) \times 10^9$	298	$(3.7 \pm 0.8) \times 10^{11}$	10 ± 1	C.K./BA	6.2×10^9	365
	SPR	6.9	$(7.3 \pm 0.7) \times 10^9$	298			C.K./BA	6.2×10^9	365
cis-3-hexen-1-ol	SPR	3.1	$(5.1 \pm 0.8) \times 10^9$	298			C.K./BA	6.2×10^9	365
	SPR	5.4	$(5.3 \pm 0.3) \times 10^9$	298	$(1.7 \pm 0.6) \times 10^{11}$	9 ± 1	C.K./BA	6.2×10^9	365
	SPR	6.9	$(5.3 \pm 0.2) \times 10^9$	298			C.K./BA	6.2×10^9	365
cis-3-hexenyl acetate	SPR	3.1	$(8.7 \pm 1.1) \times 10^9$	298			C.K./BA	6.2×10^9	365
	SPR	5.4	$(8.6 \pm 0.5) \times 10^9$	298	$(4.5 \pm 0.7) \times 10^{11}$	10 ± 2	C.K./BA	6.2×10^9	365
	SPR	6.9	$(8.3 \pm 0.6) \times 10^9$	298			C.K./BA	6.2×10^9	365
methyl jasmonate	SPR	3.1	$(6.8 \pm 0.8) \times 10^9$	298			C.K./BA	6.2×10^9	365
	SPR	5.4	$(6.7 \pm 0.3) \times 10^9$	298	$(4.0 \pm 0.3) \times 10^{11}$	9 ± 2	C.K./BA	6.2×10^9	365
	SPR	6.9	$(6.8 \pm 0.5) \times 10^9$	298			C.K./BA	6.2×10^9	365
				carboxylic acids					
pyruvic acid	LFP/H_2O_2	0	$(3.2 \pm 0.6) \times 10^8$	298	$(1.1 \pm 0.1) \times 10^{11}$	15 ± 5	C.K./SCN^-	1.24×10^{10}	109
pyruvate	LFP/H_2O_2	6	$(7.1 \pm 1.8) \times 10^8$	298	$(1.5 \pm 0.4) \times 10^{13}$	25 ± 19	C.K./SCN^-	1.24×10^{10}	109
				halogenated carboxylic acids					
$Br_2CHC(O)O^-$	PR	7	$(2.1 \pm 0.1) \times 10^8$	296	$(2.2 \pm 0.1) \times 10^{12}$	23 ± 1	C.K./SCN^-	1.05×10^{10}	366
$Br_3CC(O)O^-$	PR	7	$(1.7 \pm 0.1) \times 10^8$	296	$(2.0 \pm 0.2) \times 10^{12}$	23 ± 1	C.K./SCN^-	1.05×10^{10}	366
$ClCH_2C(O)O^-$	PR	7	$(1.8 \pm 0.1) \times 10^8$	296	$(4.3 \pm 1.1) \times 10^{10}$	14 ± 4	C.K./SCN^-	1.05×10^{10}	366
$Cl_2CHC(O)O^-$	PR	7	$(1.5 \pm 0.1) \times 10^8$	295.5	$(6.0 \pm 0.3) \times 10^{11}$	20 ± 1	C.K./SCN^-	1.05×10^{10}	366
$Cl_3CC(O)O^-$	PR	7	$(6.2 \pm 0.1) \times 10^7$	295.5	$(5.9 \pm 1.7) \times 10^{13}$	34 ± 1	C.K./SCN^-	1.05×10^{10}	366

Chem. Rev. 2015, 115, 4259−4334
DOI: 10.1021/cr500447k

Table 9. continued

reactant	technique	pH	k_{second} [M^{-1} s^{-1}]	temperature [K]	A [M^{-1} s^{-1}]	E_A [kJ mol^{-1}]	measurement technique	k_{ref} [M^{-1} s^{-1}]	refs
				halogenated carboxylic acids					
$F_2CHC(O)O^-$	PR	7	$(6.0 \pm 1.0) \times 10^7$	296	$(4.7 \pm 4.6) \times 10^{12}$	28 ± 3	C.K./SCN^-	1.05×10^{10}	366
$ICH_2C(O)O^-$	PR	7	$(4.7 \pm 0.2) \times 10^9$	295.5	$(4.1 \pm 1.6) \times 10^{14}$	28 ± 1	C.K./SCN^-	1.05×10^{10}	366
				sulfur-containing compounds					
methylisothiocyanat	PR	7	$(5.7 \pm 0.6) \times 10^8$	295.3	$(1.1 \pm 0.4) \times 10^{11}$	13 ± 1	C.K./SCN^-	1.05×10^{10}	369
2-thiouracil	PR	6.5	9.6×10^9	298			C.K./2-propanol$^-$	1.9×10^9	370
				amines					
N-nitrodimethylamine	PR	7	$(5.4 \pm 0.2) \times 10^8$	293			C.K./SCN^-	1.1×10^{10}	371
N-nitromethylethylamine	PR	7	$(7.6 \pm 0.4) \times 10^8$	293			C.K./SCN^-	1.1×10^{10}	371
N-nitrodiethylamine	PR	7	$(8.7 \pm 0.5) \times 10^8$	293			C.K./SCN^-	1.1×10^{10}	371
N-nitrodipropylamine	PR	7	$(2.3 \pm 0.1) \times 10^9$	293			C.K./SCN^-	1.1×10^{10}	371
N-nitrobutylethylamine	PR	7	$(3.1 \pm 0.2) \times 10^9$	293			C.K./SCN^-	1.1×10^{10}	371
N-nitropyrrolidine	PR	7	$(1.9 \pm 0.2) \times 10^9$	293			C.K./SCN^-	1.1×10^{10}	371
N-nitromorpholine	PR	7	$(2.3 \pm 0.2) \times 10^8$	293			C.K./SCN^-	1.1×10^{10}	371
N-nitropiperidine	PR	7	$(2.8 \pm 0.2) \times 10^9$	293			C.K./SCN^-	1.1×10^{10}	371
N-nitrodibutylamine	PR	7	$(3.8 \pm 0.1) \times 10^9$	293			C.K./SCN^-	1.1×10^{10}	371
N-nitrohexamethylenimine	PR	7	$(4.4 \pm 0.3) \times 10^9$	293			C.K./SCN^-	1.1×10^{10}	371
cyclotrimethylenetrinitramine	PR	7	$(7.5 \pm 0.8) \times 10^9$	293			C.K./SCN^-	1.1×10^{10}	371
cyclotrimethylenetrinitramine	PR	7	$(7.5 \pm 0.8) \times 10^9$	293			C.K./SCN^-	1.1×10^{10}	371
				aromatic compounds					
bisphenol A	SPR	6.8	$(1.7 \pm 0.2) \times 10^{10}$				C.K./atrazine	1.8×10^{10}	372
dimethyl phthalate	PR	6	3.4×10^9	RT			PBK/320 nm		373
dimethyl phthalate	PR	7	$(3.2 \pm 0.1) \times 10^9$	298			PBK/260 nm		374
dimethyl phthalate	CFS	10	$(2.7 \pm 0.3) \times 10^9$	298			C.K./pCBA	5×10^9	375
diethyl phthalate	CFS	10	$(4.0 \pm 0.2) \times 10^9$	298			C.K./pCBA	5×10^9	375
dipropyl phthalate	CFS	10	$(4.5 \pm 0.4) \times 10^9$	298			C.K./pCBA	5×10^9	375
dibutyl phthalate	CFS	10	$(4.6 \pm 0.4) \times 10^9$	298			C.K./pCBA	5×10^9	375
benzoic acid	PR	7	$(5.9 \pm 0.5) \times 10^9$	298					376
salicylic acid	PR	7	$(1.1 \pm 0.1) \times 10^{10}$	298					376
2-methylsalicylic acid	SPR	3.1	$(7.8 \pm 0.5) \times 10^9$	298			C.K./BA	6.2×10^9	365
	SPR	5.4	$(8.4 \pm 0.6) \times 10^9$	298	$(2.2 \pm 0.8) \times 10^{11}$	8 ± 1	C.K./BA	6.2×10^9	365
	SPR	6.9	$(8.1 \pm 0.6) \times 10^9$	298			C.K./BA	6.2×10^9	365
3-methylsalicylic acid	PR	7	$(7.5 \pm 0.2) \times 10^9$	298					376
4-methylsalicylic acid	PR	7	$(7.3 \pm 0.3) \times 10^9$	298					376
5-methylsalicylic acid	PR	7	$(5.5 \pm 0.3) \times 10^9$	298					376
6-methylsalicylic acid	PR	7	$(6.9 \pm 0.1) \times 10^9$	298					376
2,4,5-trichloro-phenoxyacetic acid	PR	8.5–9.5	$(6.4 \pm 0.5) \times 10^9$	298			PBK/320 nm		377
4-chloro-2-methyl-phenoxyacetic acid	PR	8.5–9.5	$(8.5 \pm 0.8) \times 10^9$	298			PBK/305 nm		377
thymol	PR	5.8	8.1×10^9	298			PBK/340 nm		378
thymol	PR	>13.5	1.1×10^9	298			PBK/340 nm		378
terephthalic acid	SPR	6.0	$(4.0 \pm 0.1) \times 10^9$	293			C.K./2-propanol	1.9×10^9	379
mesotrione	SPR	6.0	$(1.7 \pm 0.2) \times 10^{10}$	293			C.K./terephthalic acid	4×10^9	243
sodium *p*-cumenesulfonate	PR	9.2	8.7×10^9	RT			PBK/330 nm		380

DOI: 10.1021/cr500447k
Chem. Rev. 2015, 115, 4259−4334

Table 9. continued

reactant	technique	pH	k_{second} [M^{-1} s^{-1}]	temperature [K]	A [M^{-1} s^{-1}]	E_A [kJ mol^{-1}]	measurement technique	k_{ref} [M^{-1} s^{-1}]	refs
				aromatic compounds					
2-aminobenzoic acid	PR	10	$(5.5 \pm 0.6) \times 10^9$	RT			PBK/400 nm		381
2-aminobenzoic acid	PR	14	$(1.1 \pm 0.2) \times 10^9$	RT			PBK/400 nm		381
4-aminobenzoic acid	PR	9.5	$(8.0 \pm 1.0) \times 10^9$	RT			PBK/405 nm		381
4-aminobenzoic acid	PR	14	$(2.4 \pm 0.4) \times 10^9$	RT			PBK/405 nm		381
4-nitrophenol	PR	5.2	4.1×10^9	298			PBK/290 nm		382
4-nitrophenolate	PR	9.2	8.7×10^9	298			PBK/300 nm		382
2,4-dinitrophenol	SPR	2.5	$(1.8 \pm 0.1) \times 10^9$	RT			C.K./methanol	9.7×10^8	279
2,4-dinitrophenolate	SPR	8.7	$(2.3 \pm 0.1) \times 10^9$	RT			C.K./methanol	9.7×10^8	279

[a]PR = pulse radiolysis; LFP = laser flash photolysis; CFS = continuous flow system; SPR = static photoreactor; TWG = Teflon waveguide; PBK = product build-up kinetics; C.K. = competition kinetics; C.K./BA = benzoic acid; SA = salicylic acid; pCAB = *para*-chloro benzoic acid; RT = room temperature, T = 293−296 K.

been provided in Neta et al.,[400] Herrmann and Zellner,[32] the NIST Solution Kinetics Database 3.0 (NIST),[401] Herrmann,[12] and Herrmann et al.[35] Since the last data compilation from Herrmann et al.,[35] only a few atmospherically relevant NO_3 rate constants with oxygenated, unsaturated, and nitrogen-containing compounds in aqueous solution have been published.

Wan et al.[361] published rate constants of the NO_3 radical reaction with crown ethers obtained using the pulse radiolysis method at T = 298 K. These authors report that the rate constant increased linearly as a function of the number of H atoms in the crown ethers. In addition, they investigated the influence of the different precursor cation on the NO_3 radical rate constant, and showed that the reactivity of the crown ethers changed as a result of their complexation with either sodium or ammonium. There is no clear trend for these rate constants.

An investigation of the temperature-dependent aqueous-phase reactivity of the main isoprene oxidation products methacrolein and methyl vinyl ketone and their oxidation products acrylic acid and methacrylic acid (in both protonated and deprotonated form) toward the NO_3 radical was performed by Schöne et al.[363] Surprisingly, in the case of methacrylic acid, no significant temperature influence on the measured rate constant was observed over the range (278 K ≤ T ≤ 318 K). The rate constants obtained in this study (k = 10^6−10^8 M^{-1} s^{-1}) are in the typical range for NO_3 radical reaction with unsaturated compounds.

A set of new NO_3 radical rate constants for amines and nitrosoamines has been reported by Weller and Herrmann.[402] In recent years, the research topic of the atmospheric processing of amines has become more important as a result of their possible usage in carbon capture and storage (CCS) technology within CO_2 scrubbers. The oxidation of amines might lead to carcinogenic nitrosoamines. The NO_3 radical undergoes an H atom abstraction reaction with these reactants in aqueous solution.[402] These authors obtained rate constants for the oxidation of amines ranging from k = 10^5−10^6 M^{-1} s^{-1}. In the case of the nitrosoamines, the rate constants were up to 3 orders of magnitude higher.

The reaction between the NO_3 radical and nitro-substituted toluenes has been investigated by Elias et al.[403] The measured rate constants decrease from k = $(1.7 \pm 0.1) \times 10^9$ M^{-1} s^{-1} for toluene to k = $(3.1 \pm 1.5) \times 10^5$ M^{-1} s^{-1} for 2,4-dinitrotoluene as a result of the deactivating influence of the nitro substituent. The presence of the nitro group reduces the electron density of the aromatic ring by resonance and induction effects and leads to a decrease in reactivity of approximately 2 orders of magnitude for each nitro group.

5.2.3. SO_4^- Radical Kinetics. The number of new sulfate radical rate constants available from the literature is even smaller than that for the nitrate radical. Since Herrmann et al.,[35] the reactivity of the sulfate radical with water-soluble organic reactants such as crown ethers, ketones, unsaturated compounds, and aromatics has been measured. These new rate constants are summarized in Table 11. Wan et al.[361] measured the reactivity of crown ethers with sulfate radicals by using the pulse radiolysis and the laser flash photolysis of peroxodisulfate. Their results show that the rate constant is proportional to the number of hydrogen atoms in the crown ethers. The cation (K^+ or Na^+) of the peroxodisulfate salt had no influence on the measured rate constant. It should be mentioned that the rate constants obtained using pulse radiolysis are systematically higher than those measured using laser flash photolysis, but no

DOI: 10.1021/cr500447k
Chem. Rev. 2015, 115, 4259−4334

Table 10. Overview of NO_3 Radical Kinetic Data in the Aqueous Phase since 2010[a]

reactant	technique	pH	k_{298K} [M^{-1} s^{-1}]	A [M^{-1} s^{-1}]	E_A [kJ mol^{-1}]	measurement technique	refs
			oxygenated compounds				
crown ether 12-crown-4	PR/$NaNO_3$		$(2.4 \pm 0.1) \times 10^7$			direct/NO_3/630 nm	361
crown ether 12-crown-4	PR/NH_4NO_3		$(2.3 \pm 0.1) \times 10^7$			direct/NO_3/630 nm	361
crown ether 15-crown-5	PR/$NaNO_3$		$(5.1 \pm 0.1) \times 10^6$			direct/NO_3/630 nm	361
crown ether 15-crown-5	PR/NH_4NO_3		$(1.6 \pm 0.1) \times 10^7$			direct/NO_3/630 nm	361
crown ether 18-crown-6	PR/$NaNO_3$		$(1.1 \pm 0.1) \times 10^7$			direct/NO_3/630 nm	361
crown ether 18-crown-6	PR/NH_4NO_3		$(6.7 \pm 0.1) \times 10^6$			direct/NO_3/630 nm	361
1,4-dioxane	PR/$NaNO_3$		$(3.7 \pm 0.1) \times 10^6$			direct/NO_3/630 nm	361
1,4-dioxane	PR/NH_4NO_3		$(2.3 \pm 0.1) \times 10^6$			direct/NO_3/630 nm	361
glyoxal	LFP/$S_2O_8^{2-}$/NO_3^-		$(4.5 \pm 0.3) \times 10^6$	$(6.2 \pm 0.8) \times 10^{12}$	35 ± 10	direct/NO_3/630 nm	110
			unsaturated compounds				
methyl vinyl ketone	LFP/$S_2O_8^{2-}$/NO_3^-		$(9.7 \pm 3.4) \times 10^6$	$(6.2 \pm 1.1) \times 10^8$	10 ± 8	direct/NO_3/635 nm	363
methacrolein	LFP/$S_2O_8^{2-}$/NO_3^-		$(4.0 \pm 1.0) \times 10^7$	$(5.8 \pm 0.5) \times 10^8$	7 ± 4	direct/NO_3/635 nm	363
acrylic acid	LFP/$S_2O_8^{2-}$/NO_3^-	1	$(6.9 \pm 1.0) \times 10^6$	$(2.2 \pm 0.3) \times 10^{13}$	37 ± 12	direct/NO_3/635 nm	363
acrylate	LFP/$S_2O_8^{2-}$/NO_3^-	8	$(4.4 \pm 0.6) \times 10^7$	$(2.2 \pm 0.2) \times 10^9$	10 ± 5	direct/NO_3/635 nm	363
methacrylic acid	LFP/$S_2O_8^{2-}$/NO_3^-	1	$(9.2 \pm 1.6) \times 10^7$			direct/NO_3/635 nm	363
methacrylate	LFP/$S_2O_8^{2-}$/NO_3^-	8	$(1.7 \pm 1.2) \times 10^8$			direct/NO_3/635 nm	363
			amines				
dimethylamine	LFP/$S_2O_8^{2-}$/NO_3^-	4	$(3.7 \pm 0.8) \times 10^5$			direct/NO_3/635 nm	402
diethanolamine	LFP/$S_2O_8^{2-}$/NO_3^-	4	$(8.2 \pm 6.8) \times 10^5$			direct/NO_3/635 nm	402
pyrrolidine	LFP/$S_2O_8^{2-}$/NO_3^-	4	$(8.7 \pm 6.5) \times 10^5$			direct/NO_3/635 nm	402
nitroso-dimethylamine	LFP/$S_2O_8^{2-}$/NO_3^-	4	$(1.2 \pm 0.2) \times 10^8$	$(2.7 \pm 0.3) \times 10^{10}$	13 ± 6	direct/NO_3/635 nm	402
nitroso-diethanolamine	LFP/$S_2O_8^{2-}$/NO_3^-	4	$(2.3 \pm 0.6) \times 10^8$	$(7.0 \pm 0.9) \times 10^9$	9 ± 7	direct/NO_3/635 nm	402
nitroso-pyrrolidine	LFP/$S_2O_8^{2-}$/NO_3^-	4	$(2.4 \pm 0.3) \times 10^8$	$(4.4 \pm 0.4) \times 10^9$	7 ± 5	direct/NO_3/635 nm	402
			aromatic compounds				
toluene	PR/HNO_3	0	$(1.7 \pm 0.1) \times 10^9$			direct/NO_3/640 nm	403
3-nitrotoluene	PR/HNO_3	0	$(2.8 \pm 0.1) \times 10^7$			direct/NO_3/640 nm	403
2,4-dinitrotoluene	PR/HNO_3	0	$(3.1 \pm 1.5) \times 10^5$			direct/NO_3/640 nm	403
3,4-dinitrotoluene	PR/HNO_3	0	$(9.6 \pm 1.4) \times 10^5$			direct/NO_3/640 nm	403
benzene	PR/HNO_3	0	$<1 \times 10^6$			direct/NO_3/640 nm	403

[a]PR = pulse radiolysis; LFP = laser flash photolysis.

possible reasons for this discrepancy are given. In addition, Schaefer et al.[110] measured the rate constant for the reaction of glyoxal with sulfate radicals as a function of pH and temperature. The rate constants are in the typical range for H atom abstraction reactions of the sulfate radical, with $k = 10^7-10^8$ M^{-1} s^{-1}.

A recent study by Schöne et al.[363] reported sulfate radical rate constants for six unsaturated isoprene oxidation products. In this study, the sulfate radical was formed via the photolysis of peroxodisulfate. Rate constants were determined for each isoprene oxidation product by direct observation of the absorption−time profile of the sulfate radical at $\lambda = 407$ nm. Generally, the measured rate constants for sulfate radical reactions did not display a strong temperature dependence. Arrhenius parameters were obtained only for methacrylic acid, methacrylate, and acrylic acid. For methacrolein, methyl vinyl ketone, and acrylate, no change in rate constant with increasing temperature was observed. The values of the measured rate constants are $\sim 10^8$ M^{-1} s^{-1}.

For the reaction of atmospherically relevant aromatic compounds with the sulfate radical, only one new rate constant has been published in the last 5 years. In a study by Sanchez-Polo et al.,[372] the reactivity of bisphenol A was investigated using a photoreactor and the competition kinetics method with atrazine as reference reactant. The rate constant obtained, $k = (1.4 \pm 0.2) \times 10^9$ M^{-1} s^{-1}, is in good agreement with reported values from the literature for this compound.[12,35,401]

5.3. Summary of Section 5

In the last 5 years, only a few new rate constants for reactions of the OH, SO_4^-, and NO_3 radicals have been measured. The general trend in aqueous-phase reactivity for these species is as follows: OH > SO_4^- ≫ NO_3. In recent years, a number of studies have investigated the aqueous-phase reactivity of unsaturated and aromatic compounds with radicals. Although these compound classes typically have low Henry's law constants and poor water solubilities, recent studies have indicated that such species arising from biogenic emissions might play an important role in tropospheric aqueous chemistry. In addition to radical reactions, nonradical reactions might play an important role in the atmospheric multiphase system. Consequently, these reactions are the topic of the following section.

6. NONRADICAL REACTIONS

Aqueous-phase nonradical reactions (e.g., H_2O_2 oxidation, esterification, and condensation reactions) have been the subject of significant interest in the scientific community in recent years (see, e.g., refs 1,31,55,404−408 and references therein). In addition to radical reactions, these reactions represent a potential pathway contributing to the formation and processing of SOA, the magnitude of which is often underestimated in current tropospheric models. Another motivation for the increasing interest in these processes in recent years is related to their ability to form products with higher carbon numbers, thus leading to an increased

DOI: 10.1021/cr500447k
Chem. Rev. 2015, 115, 4259−4334

Table 11. Overview of SO_4^- Radical Kinetic Data in the Aqueous Phase since 2010[a]

reactant	technique	pH	k_{298K} [M^{-1} s^{-1}]	A [M^{-1} s^{-1}]	E_A [kJ mol^{-1}]	measurement technique	refs
			oxygenated compounds				
crown ether 12-crown-4	PR/Na_2SO_4		$(2.3 \pm 0.1) \times 10^8$			direct/SO_4^-/460 nm	361
crown ether 12-crown-4	LFP/$K_2S_2O_8$		$(1.7 \pm 0.1) \times 10^8$			direct/SO_4^-/460 nm	361
crown ether 12-crown-4	LFP/$Na_2S_2O_8$		$(1.7 \pm 0.1) \times 10^8$			direct/SO_4^-/460 nm	361
crown ether 15-crown-5	PR/Na_2SO_4		$(2.7 \pm 0.1) \times 10^8$			direct/SO_4^-/460 nm	361
crown ether 15-crown-5	LFP/$K_2S_2O_8$		$(2.2 \pm 0.1) \times 10^8$			direct/SO_4^-/460 nm	361
crown ether 15-crown-5	LFP/$Na_2S_2O_8$		$(2.0 \pm 0.1) \times 10^8$			direct/SO_4^-/460 nm	361
crown ether 18-crown-6	PR/Na_2SO_4		$(4.2 \pm 0.1) \times 10^8$			direct/SO_4^-/460 nm	361
crown ether 18-crown-6	LFP/$K_2S_2O_8$		$(2.5 \pm 0.1) \times 10^8$			direct/SO_4^-/460 nm	361
crown ether 18-crown-6	LFP/$Na_2S_2O_8$		$(2.4 \pm 0.1) \times 10^8$			direct/SO_4^-/460 nm	361
1,4-dioxane	PR/Na_2SO_4		$(6.6 \pm 0.1) \times 10^7$			direct/SO_4^-/460 nm	361
1,4-dioxane	LFP/$K_2S_2O_8$		$(4.2 \pm 0.2) \times 10^7$			direct/SO_4^-/460 nm	361
1,4-dioxane	LFP/$Na_2S_2O_8$		$(4.0 \pm 0.1) \times 10^7$			direct/SO_4^-/460 nm	361
glyoxal	LFP/$K_2S_2O_8$	6	$(2.4 \pm 0.2) \times 10^7$	$(5.4 \pm 0.1) \times 10^9$	13 ± 1	direct/SO_4^-/407 nm	110
glyoxal	LFP/$K_2S_2O_8$	2	$(2.2 \pm 0.2) \times 10^7$			direct/SO_4^-/407 nm	110
glyoxal	LFP/$K_2S_2O_8$	9	$(2.6 \pm 0.2) \times 10^7$			direct/SO_4^-/407 nm	110
			unsaturated compounds				
methyl vinyl ketone	LFP/$K_2S_2O_8$		$(1.0 \pm 0.2) \times 10^8$			direct/SO_4^-/407 nm	363
methacrolein	LFP/$K_2S_2O_8$		$(9.9 \pm 4.9) \times 10^7$			direct/SO_4^-/407 nm	363
acrylic acid	LFP/$K_2S_2O_8$	1	$(9.5 \pm 0.8) \times 10^7$	$(2.0 \pm 0.2) \times 10^8$	2 ± 4	direct/SO_4^-/407 nm	363
acrylate	LFP/$K_2S_2O_8$	8	$(9.9 \pm 2.0) \times 10^7$			direct/SO_4^-/407 nm	363
methacrylic acid	LFP/$K_2S_2O_8$	1	$(2.5 \pm 1.2) \times 10^8$	$(1.2 \pm 0.4) \times 10^{10}$	11 ± 19	direct/SO_4^-/407 nm	363
methacrylate	LFP/$K_2S_2O_8$	8	$(3.5 \pm 1.1) \times 10^8$	$(3.5 \pm 1.1) \times 10^9$	6 ± 17	direct/SO_4^-/407 nm	363
			aromatic compounds				
bisphenol A	SPR	6.8	$(1.4 \pm 0.2) \times 10^9$			C.K./atrazine	372

[a]PR = pulse radiolysis; LFP = laser flash photolysis; SPR = static photoreactor.

Table 12. Kinetic Data for Hydrogen Peroxide (H_2O_2) Reactions in Aqueous Solution

reactant	formula	k_{298K} [M^{-1} s^{-1}]	pH/remarks	refs
		aldehyde compounds		
formaldehyde	$HCHO/CH_2(OH)_2$	1.4×10^{-3}		417
	HCHO	0.11		416
	$HCHO/CH_2(OH)_2$	1.33×10^{-3}	pH = 5, $k = 1.33 \times 10^{-3} \times (1-53 \times [H^+])$ M^{-1} s^{-1}	
	HCHO	0.05	recalculated by Satterfield and Case[416] based on Dunicz et al.[415]	416
acetaldehyde	CH_3CHO	0.61	E_A = 5.9 kJ mol^{-1}	416
		0.012		59
propionaldehyde	CH_3CH_2CHO	0.75	T = 283 K	416
gycolaldehyde	$CH_2(OH)CHO$	0.04	pH = 5	115
glyoxal	$(CHO)_2$	1.67×10^{-4}	pH = 5	115
		1		419
		0.06		59
methylglyoxal	$CH_3C(O)CHO$	0.04		59
methacrolein	$CH_2{=}C(CH_3)CHO$	0.08	pH = 2	115
		0.13	upper limit estimate	420
		carboxylic acids		
formic acid	HCOOH	0.2		419
		0.13		420
glyoxylic acid	$HC(OH)_2COOH$	3.96×10^{-3}	pH = 1	115
	HC(O)COOH	0.9	unhydrated	419
	$HC(O)COOH/HC(O)COO^-$	0.3		423
glyoxylate	$HC(OH)_2COO^-$	0.11	pH = 7	115
	$HC(O)COO^-$	16.5		423
pyruvic acid	$CH_3C(O)COOH$	0.12	pH = 1	115
pyruvate	$CH_3C(O)COO^-$	0.75	pH = 7	115
		0.11	pH not exactly specified	422
		sulfur-containing organic compounds		
dimethyl sulfoxide (DMSO)	CH_3SOCH_3	2.75×10^{-6}		424
methane sulphinic acid anion ($MSIA^-$)	$CH_3SO_2^-$	1.20×10^{-2}		425

DOI: 10.1021/cr500447k
Chem. Rev. 2015, 115, 4259−4334

partitioning to the condensed phase. Accretion reactions can also explain the formation of higher molecular weight compounds observed in ambient particles.

Most existing studies of aqueous-phase nonradical reactions only report the identities of the products formed in these reactions, and provide only little of the mechanistic and kinetic information necessary for implementation into multiphase mechanisms. A number of open questions still exist with regard to the importance of nonradical condensed-phase reactions relative to well-known radical chemical reactions.

In general, organic nonradical reactions can be divided into nonradical oxidation reactions (i.e., reactions of organics with nonradical oxidants such as hydrogen peroxide, organic hydroperoxides, and ozone) and organic accretion reactions. These reaction classes are discussed individually in the following two subsections.

6.1. Nonradical Oxidation Reactions

6.1.1. Hydrogen Peroxide (H_2O_2). H_2O_2, a known important oxidant, is present in the atmospheric aqueous phase in concentrations up to 100 μM.[409] The main sources of aqueous H_2O_2 are transfer from the gas phase and in-situ photochemical production.[205,242,410−412] Aqueous H_2O_2 is known to be one of the major oxidants for the S(IV) to S(VI) conversion in the atmosphere[205] and a key species in TMI redox cycling.[33] Besides its importance for inorganic chemistry (see the NIST database[401] and references therein), H_2O_2 can also contribute to the aqueous-phase oxidation of organic compounds (see Schumb et al.[413]), such as the substituted carboxylic acids pyruvic acid[414] and glyoxylic acid.[66] It has long been known that H_2O_2 reacts with unsaturated organic compounds, converting double bonds into diol functionalities, and with aldehydes, forming carboxylic acids. However, the kinetics of the reactions of H_2O_2 with water-soluble organics have not yet been systematically investigated. The NIST database[401] contains 107 reactions of H_2O_2 in water, mainly transition metal/metal complexes and reaction with inorganic and organic radicals, but contains no reactions with stable organic compounds. Given this lack of data, a comprehensive overview of the kinetics of organic oxidation reactions initiated by H_2O_2 cannot be given. Table 12 summarizes the available kinetic data for H_2O_2 reactions with atmospherically relevant organic constituents.

It is well-known from previous laboratory studies that hydrogen peroxide reacts with aldehyde compounds.[415−417] However, aldehydes react very slowly with H_2O_2. The second-order reaction rate constants available in the literature are in the range of 10^{-3} M^{-1} s^{-1} for formaldehyde and ~1 M^{-1} s^{-1} for propionaldehyde. The very low reactivity of formaldehyde toward H_2O_2 in acid solution has been intensively investigated, for example, by Dunicz et al.[415] and Satterfield and Case,[416] and later by Patai and Zabicki.[417] Dunicz et al.[415] have presented a reaction rate constant that depends linearly on $[H^+]$. It should be noted that the reaction with H_2O_2 depends on the identity of the carbonyl group functionality.[416] Thus, the formation of hydrated aldehydes reduces the turnover of the H_2O_2 reaction. Taking this issue into account, Satterfield and Case[416] corrected the value of Dunicz et al.[415] and recalculated a rate constant value of 5×10^{-2} M^{-1} s^{-1} for the reaction of unhydrated formaldehyde with H_2O_2. Additionally, it should be noted that while the reaction between H_2O_2 and formaldehyde has been reported to proceed very rapidly in alkaline solution,[418] to the authors' knowledge, no kinetic data are presently available for these reaction conditions. For other unsubstituted aldehydes, Satterfield and Case[416] reported higher reaction rate constants of 0.61 and 0.75 M^{-1} s^{-1} for acetaldehyde and propionaldehyde, respectively. More recent atmospherically relevant studies[59,115,419] focused on the H_2O_2 reactivity of important substituted aldehydes and dialdehydes (e.g., glyoxal, glycolaldehyde, and methylglyoxal) formed in the gas-phase oxidation of isoprene. For glycolaldehyde, Schöne and Herrmann[115] measured a reaction rate constant of 4×10^{-2} M^{-1} s^{-1}. In the case of glyoxal, three quite different reaction rate constants are presently available in the literature. Carlton et al.[419] proposed a rate constant of 1 M^{-1} s^{-1} and the formation of two formic acid molecules from the reaction of glyoxal with H_2O_2. This proposed rate constant was not measured but rather derived from their model studies. As shown in Table 12, the measured value of Schöne and Herrmann[115] is approximately 4 orders of magnitude smaller. The third value estimated by Zhao et al.,[59] 6×10^{-2} M^{-1} s^{-1}, is between the two others. Recently, Zhao et al.[59] observed the formation of small amounts of formic acid and reported the first direct detection of hydroxyhydroperoxides (α-HHPs) in the reaction of glyoxal/methylglyoxal with hydrogen peroxide. The formation of α-HHPs was also found for the reaction of H_2O_2 with other aldehydes and glyoxalic acid (see Zhao et al.[60]). The formation of such species had already been proposed in earlier studies, for example, by Satterfield and Case.[416] For the equilibrium constants and further details regarding this reversible process, the reader is referred to section 4.3, Table 7, and the references therein.

As mentioned previously, H_2O_2 also reacts with unsaturated compounds such as methacrolein.[115] The determined rate constant of 7.56×10^{-2} M^{-1} s^{-1} is in the same range as those of the aldehydes discussed previously. The upper-limit estimate of Zhang et al.[420] for this reaction is about a factor of 2 larger. In 2004, Claeys et al.[421] proposed an acid-catalyzed pathway for the H_2O_2 oxidation of methacrolein, which leads to the formation of 2,3-dihydroxymethacrylic acid. However, the more recent study of Zhao et al.[60] did not report the formation of this specific product.

Table 12 also presents kinetic data for the reactions of several carboxylic acids with H_2O_2. The second-order rate constants for these reactions vary between 0.11 and 16.5 M^{-1} s^{-1}. In 1999, Stefan and Bolton[422] proposed a mechanism for the reaction of pyruvate with H_2O_2. In their study, a rate constant of 0.11 M^{-1} s^{-1} was reported, which is somewhat smaller than the measured rate constant of Schöne and Herrmann[115] (0.75 M^{-1} s^{-1}).

Further investigations of Schöne and Herrmann[115] have shown that the reactivity of glyoxalic acid toward H_2O_2 is about 1−2 orders of magnitude smaller than that of its deprotonated form, glyoxalate (see Table 12). Proposed reaction schemes for both pyruvate and glyoxalate are presented in Schöne and Herrmann.[115] The two oxidation mechanism pathways are analogous and lead to the formation of acetate and formate for pyruvate and glyoxalate oxidation, respectively. Several other studies[60,67,115] have also reported the production of formate during the reaction of glyoxalate. Additionally, Zhao et al.[60] proposed the formation of α-HHPs to explain the fact that the quantity of formic acid produced was smaller than the quantity of glyoxalate lost in these experiments. In addition to these laboratory studies, Schöne and Herrmann[115] and Tilgner and Herrmann[204] have compared potential chemical turnovers of H_2O_2 reactions with those of inorganic radicals (OH, NO_3). Both studies found that H_2O_2 reactions show chemical

DOI: 10.1021/cr500447k
Chem. Rev. 2015, 115, 4259−4334

Table 13. Kinetic Data for Ozone (O_3) Reactions in Aqueous Solution

reactant	k_{298K} [M^{-1} s^{-1}]	formula	remarks	refs
		saturated organic compounds		
gycolaldehyde	0.52	$H_2C(OH)CHO$	pH = 5	115
glyoxal	0.9	$(CH(OH)_2)_2$	pH = 5	115
methylglyoxal	2.89	$CH_3C(O)CH(OH)_2$	pH = 5	115
glycolic acid	0.055	$CH_2(OH)COOH$	pH = 1	115
glycolate	0.71	$CH_2(OH)COO^-$	pH = 7	115
glyoxylic acid	0.14	$HC(OH)_2COOH$	pH = 1	115
glyoxylate	2.3	$HC(OH)_2COO^-$	pH = 7	115
pyruvic acid	0.13	$CH_3C(O)COOH$	pH = 1	115
pyruvate	0.98	$CH_3C(O)COO^-$	pH = 7	115
diethylene glycol	20	$HOCH_2CH_2OCH_2CH_2OH$	pH = 4	430
cyclopentanone	9.6×10^{-1}	C_4H_8CO	T = 303 K	431
			E_A = 75 kJ mol^{-1}	
cyclohexanone	2.7×10^{-2}	$C_5H_{10}CO$	T = 303 K	432
			E_A = 65 kJ mol^{-1}	
methylbutylketone	9.9×10^{-1}	$H_3CCOC_4H_9$	T = 303 K	431
			E_A = 68 kJ mol^{-1}	
		amines and nitro-compounds		
dimethylamine (DMA)	$<3 \times 10^{-3}$	$HN(CH_3)_2$	(upper limit estimate) pH = 2	402
diethanolamine (DEA)	<0.6	$HN(CH_2CH_2OH)_2$	(upper limit estimate) pH = 2	402
pyrrolidine (PYL)	$<3 \times 10^{-3}$	$HN(CH_2)_4$	(upper limit estimate) pH = 2	402
nitroso-dimethylamine (NDMA)	<0.2, 0.052	$O{=}NN(CH_3)_2$	(upper limit estimate) pH = 2	402
nitroso-diethanolamine (NDEA)	27	$O{=}NN(CH_2CH_2OH)_2$	(upper limit estimate) pH = 2	433
nitroso-pyrrolidine (NPYL)	0.4	$O{=}NN(CH_2)_4$	(upper limit estimate) pH = 2	
trimethylamine	5.1×10^6	$N(CH_3)_2$	pH = 4–9	428
triethylamine	4.1×10^6	$N(CH_2CH_3)_2$	pH = 4–9	428
diethylamine	9.1×10^5	$HN(CH_2CH_3)_2$	pH = 4–9	428
ethylamine	2.4×10^5	$H_2NCH_2CH_3$	pH = 4–9	428
glycine	2.1×10^5	H_2NCH_2COOH	pH = 4–9	428
alanine	2.8×10^5	$H_2NCH(CH_3)COOH$	pH = 4–9	428
		unsaturated aliphatic organic compounds		
methacrolein (MACR)	2.3×10^4	$CH_2{=}C(CH_3)CHO$	pH = 2	115
	2.4×10^4		pH = 2	434
			E_A = 24 kJ mol^{-1}	
methyl vinyl ketone (MVK)	7.1×10^4	$CH_2{=}CHC(CH_3){=}O$	pH = 2	115
	4.4×10^4		pH = 2	434
			E_A = 18 kJ mol^{-1}	
acrylic acid	2.8×10^4	$CH_2{=}CHCOOH$	pH = 2	435
acrylate	1.6×10^5	$CH_2{=}CHCOO^-$	pH = 7	435
methacrylic acid	1.5×10^5	$CH_2{=}C(CH_3)COOH$	pH = 2	435
methacrylate	3.7×10^6	$CH_2{=}C(CH_3)COO^-$	pH = 7	435
maleic acid	1.4×10^3	$HOOCCH{=}CHCOOH$		435
maleic acid monoanion	4.2×10^3	$HOOCCH{=}CHCOO^-$		435
maleic acid dianion	$\sim 7.0 \times 10^3$	$^-OOCCH{=}CHCOO^-$		435
fumaric acid	8.5×10^3	$HOOCCH{=}CHCOOH$		435
fumaric acid dianion	$\sim 6.5 \times 10^4$	$^-OOCCH{=}CHCOO^-$	pH = 10	435
	2.7×10^5			436
cis,*cis*-muconic acid monoanion	4×10^4	$HOOC(CH{=}CH)_2COO^-$	pH = 3.1	437
	2.65×10^4			435
cis,*trans*-muconic acid	1.4×10^4	$HOOC(CH{=}CH)_2COOH$	pH = 3	438
	2.5×10^5		pH = 7	438
trans,*trans*-muconic acid	1.6×10^4	$HOOC(CH{=}CH)_2COO^-$	pH = 3	439
	1.5×10^4			
trans,*trans*-muconic acid dianion	1.4×10^5	$HOOC(CH{=}CH)_2COO^-$	pH = 7	439
vinyl acetate	1.6×10^5	$H_2CCHOCOCH_3$		440
vinylene carbonate	2.6×10^4	$C_3H_2O_3$		440
		unsaturated chlorinated organic compounds		
vinyl chloride	1.4×10^4	$H_2C{=}CHCl$	pH ≤ 7	441
vinyl bromide	1×10^4	$H_2C{=}CHBr$		440
1,1-dichloroethene	110	$Cl_2C{=}CH_2$	pH ≤ 7	441

DOI: 10.1021/cr500447k
Chem. Rev. 2015, 115, 4259–4334

Table 13. continued

reactant	k_{298K} [M^{-1} s^{-1}]	formula	remarks	refs
		saturated organic compounds		
		unsaturated chlorinated organic compounds		
cis-1,2-dichloroethene	540	HClC═CClH	pH ≤ 7	441
trans-1,2-dichloroethene	6.5×10^3	HClC═CHCl	pH ≤ 7	441
trichloroethene	14	Cl_2C═CHCl	pH ≤ 7	441
	6.3		pH = 5.4	442
1,1-dichloropropene	2.6×10^3	Cl_2C═$CHCH_3$	pH ≤ 7	441
dichloromaleic acid	10	HOOCCClCClCOOH		435
		unsaturated organic compounds with heteroatoms		
vinyl phosphonic acid	1.4×10^4	H_2C═$CHOPO(OH)_2$		440
vinyl phosphonic acid monoanion	2.7×10^4	H_2C═$CHOPOHO_2^-$	pH ≈ 7	440
vinyl phosphonic acid dianion	1×10^5	H_2C═$CHOPO_3^{2-}$	pH = 10.2	440
vinyl sulfonate	8×10^3	H_2C═$CHSO_3^-$		440
		aromatic organic compounds		
phenol	8.67×10^2	C_6H_5OH	pH = 2	443
	1.17×10^3		pH = 7	443
catechol	5.2×10^5	$C_6H_4(OH)_2$	pH = 7	437
1,4-benzoquinone	2.5×10^3	$C_6H_4O_2$		437
1,4-dimethoxybenzene	1.3×10^5	$C_6H_4(OCH_3)_2$		444
1,3,5-trimethoxybenzene	9.4×10^5	$C_6H_3(OCH_3)_3$		444
benzaldehyde	120	C_6H_5CHO	pH = 2.3	445
	10^4		pH = 6	445
benzoic acid anion	3.5×10^5	$C_6H_5COO^-$	pH = 8.6	436
p-hydroxybenzoic acid	200	$HOOCC_6H_4OH$	pH = 2	446
	1.8×10^5		pH = 6.3	446
	6.4×10^7		pH = 9	446
gallic acid	9.7×10^4	$C_6H_2(OH)_3COOH$	pH = 2	446
	4.7×10^5		pH = 6.3	446
tyrosol	3×10^3	$HOC_6H_4CH_2CH_2OH$	pH = 2	446
	2.0×10^5		pH = 6.3	446
	6.8×10^7		pH = 9	446
1-phenoxy-2-propanol	320	$C_6H_5OCH_2CHOHCH_3$		447
cinnamic acid	1.0×10^5	$C_6H_5CHCHCOOH$		448
cinnamic acid monoanion	1.2×10^6	$C_6H_5CHCHCOO^-$		448
	3.8×10^5			423
4-methoxycinnamic acid	1.3×10^5	$CH_3OC_6H_4CH$═$CHCOOH$		423
4-methoxycinnamic acid monoanion	6.8×10^5	$CH_3OC_6H_4CH$═$CHCOO^-$		423
4-nitrocinnamatic acid monoanion	1.2×10^5	$O_2NC_6H_4CH$═$CHCOO^-$		423
3-methoxy-4-hydroxy cinnamic acid	1.1×10^6	$HOC_6H_3(OCH_3)CH$═$CHCOOH$		448
3-methoxy-4-hydroxy cinnamic acid monoanion	7.9×10^6	$HOC_6H_3(OCH_3)CH$═$CHCOO^-$		448
3,4-dihydroxy cinnamic acid	2.0×10^6	$(HO)_2C_6H_3CHCHCOOH$		448
3,4-dihydroxy cinnamic acid monoanion	1.2×10^7	$(HO)_2C_6H_3CHCHCOO^-$		448
2,6-di-*t*-butyl-4-methylphenol (BHT)	7.4×10^4	$C_6H_2CH_3(C_4H_9)_2OH$	pH = 7	449
4-octylphenol	4.3×10^4	$H_3C(CH_2)_7C_6H_4OH$		450
octylphenol ethoxylate	1.3×10^2	$H_3C(CH_2)_7C_6H_4O(CH_2CH_2O)_nH$	pH = 3−6	451
4-*n*-nonylphenol	3.8×10^4	$H_3C(CH_2)_8C_6H_4OH$		452
	3.9×10^4			450
4-*n*-nonylphenol anion	6.8×10^9	$H_3C(CH_2)_8C_6H_4O^-$		452
nonylphenol ethoxylate	3.6×10^2	$H_3C(CH_2)_8C_6H_4O(CH_2CH_2O)_nH$	pH = 3−6	451
(+)-catechin	5.3×10^5	$C_{15}H_{14}O_6$	pH = 2	446
	1.1×10^6		pH = 6.3	446
		aromatic organic compounds with heteroatoms		
nitrobenzene	1.6	$C_6H_5NO_2$		453
	2.2			454
p-chloronitrobenzol	6.4×10^{-2}	$C_6H_4ClNO_2$	pH = 2	455
	1.1			453
m-chloronitrobenzol	3.9×10^{-2}	$C_6H_4ClNO_2$	pH = 2	455
o-chloronitrobenzol	6.4×10^{-3}	$C_6H_4ClNO_2$	pH = 2	455
2,4-dinitrotoluene	<14	$C_6H_3CH_3(NO_2)_2$		360
2,6-dinitrotoluene	<14	$C_6H_3CH_3(NO_2)_2$		360

DOI: 10.1021/cr500447k
Chem. Rev. 2015, 115, 4259−4334

Table 13. continued

reactant	k_{298K} [M^{-1} s^{-1}]	formula	remarks	refs
		saturated organic compounds		
		aromatic organic compounds with heteroatoms		
2,6-dinitrotoluene	5.7	$C_6H_3CH_3(NO_2)_2$		454
p-nitrophenol	2.0×10^6	$HOC_6H_4NO_2$		456
2,3-dichloronitrophenol	6.5×10^3	$HOC_6H_4Cl_2$	pH = 2	457
	6.12×10^6		pH = 5	457
2,4-dichloronitrophenol	4.4×10^3	$HOC_6H_4Cl_2$	pH = 2.1	457
	1.04×10^7		pH = 6	457
2,5-dichloronitrophenol	6.85×10^4	$HOC_6H_4Cl_2$	pH = 2.1	457
	7.75×10^6		pH = 5	457
4-chlorophenol	6.55×10^2	HOC_6H_4Cl	pH = 2	458
	2.44×10^3		pH = 3	458
2,4-cichlorophenol	1.89×10^3	$HOC_6H_3Cl_2$	pH = 2	458
	9.16×10^3		pH = 3	458
2,4,6-trichlorophenol	9.49×10^3	$HOC_6H_2Cl_3$	pH = 2	458
	4.75×10^4		pH = 3	458
2,3,4,6-tetrachlorophenol	1.50×10^4	HOC_6HCl_4	pH = 2	458
	8.10×10^4		pH = 3	458
pentachlorophenol anion	1.2×10^6	$C_6Cl_5O^-$		437
2,4,6-triiodophenol anion	6.8×10^6	$C_6H_2I_3O^-$		437
tetrachlorocatechol	2.57×10^4	$C_6Cl_4(OH)_2$	pH = 2	458
	5.41×10^4		pH = 3	458
4-chloroguiacol	3.92×10^4	$HOC_6H_3ClOCH_3$	pH = 2	458
	1.38×10^5		pH = 3	458
phenyl vinylsulfonate	~200	$C_6H_5OSO_2CH{=}CH_2$		440

turnovers similar to those of the radicals. For example, calculations by Schöne and Herrmann[115] demonstrated that H_2O_2 reactions with organic compounds such as pyruvic acid/pyruvate and glyoxalate can compete with OH radical conversions under polluted environmental conditions when H_2O_2 is not used up by the S(IV) conversion. Using a simple calculation that considers typical urban ambient aqueous-phase concentrations of H_2O_2 (~1×10^{-4} M) and OH (~1×10^{-14} M),[115] it can be shown that typical differences of ~10 orders of magnitude in the reaction rate constants of these oxidants can be compensated for, leading to comparable chemical conversion rates. These results suggest that oxidation reactions of H_2O_2 with organic compounds should be more comprehensively considered in multiphase mechanisms and accompanying models. The importance of H_2O_2 processes also arises from the high water solubility of H_2O_2 and the fact that it is present under both day- and night-time conditions. However, comprehensive conclusions regarding the importance of H_2O_2 reactions for aqSOA formation and the overall aqueous-phase processing of organic aerosol constituents cannot yet be drawn based on the sparse kinetic data currently available. Further kinetic and mechanistic laboratory investigations as well as subsequent modeling are needed in the future.

6.1.2. Ozone. Nonradical oxidations in the tropospheric aqueous phase can also proceed via reactions with ozone (O_3), an important atmospheric oxidant. The most important source of aqueous O_3 is its transfer from the gas phase. The aqueous-phase reaction of O_3 with S(IV) has long been known as an important S(IV) to S(VI) conversion pathway. However, the importance of ozone reactions for the degradation of organic compounds in aqueous tropospheric aerosols has received much less investigation than the corresponding radical reactions. As compared to radical oxidants such as the OH radical, ozone is also a reactive electrophilic but very selective oxidant, which is less stable in water due to its reactivity toward the water matrix. The decay of ozone in water strongly depends on the acidity of the aqueous solution.[353,358,426,427] Previous laboratory studies have shown that ozone is quite selective for double bonds and thus reacts predominantly with unsaturated aliphatic compounds and aromatic compounds as well as deprotonated amines.[428]

The NDRL/NIST Solution Kinetics Database 3.0[401] contains several hundred reactions of organic compounds with ozone in aqueous solution. In addition, numerous studies have focused on the kinetics and mechanisms of aqueous-phase ozone reactions of organic compounds (see von Gunten et al.,[352] the recent monograph by von Sonntag and von Gunten,[429] and references therein as an overview). Since the 1998 finalization of the NDRL/NIST Solution Kinetics Database 3.0,[401] several new kinetic studies of ozone reactions with organic compounds in aqueous solution have been reported in the literature. Rate constants for atmospherically relevant ozone reactions measured since that time are summarized in Table 13. As can be seen from the data presented in this table, kinetic data have recently been obtained for the reactions of ozone with aliphatic carbonyls, substituted organic acids, unsaturated aliphatic organic compounds, halogenated compounds, and aromatic organic compounds.

Using these kinetic data in combination with typical atmospheric oxidant concentrations, chemical conversions can be roughly estimated and compared. Considering typical urban in-cloud concentrations of about 2×10^{-9} M for O_3 and 1×10^{-14} M for OH radicals (see Schöne and Herrmann[115] for details) as well as typical OH reaction rates with organic compounds of 10^8–10^{10} M^{-1} s^{-1},[12,35] it can be estimated that O_3 reaction rate constants have to be on the order of about 10^3–10^5 M^{-1} s^{-1} to be competitive with chemical conversions initiated by OH radicals. From Table 13, it can be seen that the

DOI: 10.1021/cr500447k
Chem. Rev. 2015, 115, 4259–4334

O_3 reaction rates of unsaturated aliphatic organic compounds, aromatic organic compounds, and amines are in this range; for these compounds, O_3 reaction might compete with OH radical oxidation. This degradation pathway should therefore be considered in future aqueous-phase mechanisms.

6.1.3. Saturated Nonaromatic Organic Compounds. Ozone reactions of saturated organic compounds are generally slow.[459] Recently, rate constants for the aqueous-phase reaction of ozone with a set of saturated aliphatic carbonyls and substituted organic acids formed from the oxidation of isoprene and other atmospheric precursors have been measured by Schöne and Herrmann.[115] The rate constants obtained in this study, which are mainly in the range of 0.1−1 M^{-1} s^{-1}, are substantially smaller than those measured for unsaturated organic compounds. Schöne and Herrmann[115] have provided the first kinetic measurements at 298 K of the ozone reactions of glyoxal, glycolaldehyde, and methylglyoxal. These authors have also proposed a possible oxidation mechanism for glyoxal. However, because of missing product studies, reaction mechanisms for glycolaldehyde and methylglyoxal were not given in this study.

Zimin et al.[431,432] have investigated the ozone reactions of cyclopentanone, cyclohexanone, and methylbutylketone and the corresponding keto−enol equilibria. Low reactivities were found for the keto forms (see Table 13). This finding is consistent with previous studies, which have also revealed low reactivities of ketones toward ozone. From their studies and the obtained keto−enol equilibria data, Zimin et al.[431,432] concluded that both the keto and the enol tautomers of ketones react with ozone in the presence of an acid and that the importance of the enol reaction increases with increasing acid concentration. At higher acidities, the keto−enol equilibrium shifts toward the enol tautomer. Moreover, as a result of its double bond and electron-donating OH group, the enol form is expected to react much faster than the keto form.

6.1.4. Amines. The atmospheric multiphase chemistry of amines is currently the subject of much research interest as a result of their abundance in marine environments, their importance for new particle formation, and their use in amine-based carbon capture and storage (CCS) techniques. Weller and Herrmann[402] have investigated the reactivity of different amines and their potential atmospheric oxidation products, nitrosamines, toward ozone under acidic conditions (pH = 2). Specifically, these authors have studied the aqueous reactivity of dimethylamine (DMA), diethanolamine (DEA), and pyrrolidine (PYL) and their corresponding nitrosamines, nitroso-dimethylamine (NDMA), nitroso-diethanolamine (NDEA), and nitroso-pyrrolidine (NPYL). As shown in Table 13, the reactivity of ozone toward these amines and nitrosamines was found to be very low under these acidic conditions. Muñoz and von Sonntag[428] have investigated the ozone reactions of several amines and two amino acids. This study clearly shows that the rate constant of the ozone reaction with amines strongly depends on the pH conditions, which reflects the fact that only the free unprotonated amine reacts with ozone. This is probably also the reason why the second-order rate constants of Muñoz and von Sonntag[428] are substantially larger than those of Weller and Herrmann.[402] Finally, Sharma and Graham[460] have published a review on the oxidation of amino acids, peptides, and proteins by ozone. Some further data of interest regarding the atmospheric chemistry of amines are presented in section 7.2.6.

6.1.5. Unsaturated Aliphatic Organic Compounds. Several new rate constants for the reaction of ozone with olefins and unsaturated mono- and dicarboxylic acids have been reported in the literature.[115,420,434−441,449] The reaction of ozone with olefins such as ethene, propene, isoprene, and α-pinene proceeds via the reaction of ozone with the double bond in the molecules, which leads to reaction rates ∼5 orders of magnitude higher than those observed for the saturated compounds discussed before. An exception is represented by α-pinene, whose ozone reaction rate constant of $1-3 \times 10^7$ M^{-1} s^{-1} at pH = 7 (see King et al.[436]) is nearly 2 orders of magnitude higher than the kinetic constants of the other olefins (e.g., isoprene) presented in Table 13. Rate constants of the important isoprene oxidation products methacrolein (MACR) and methyl vinyl ketone (MVK) have been determined by Schöne and Herrmann[115] and Pedersen and Sehested.[434] Both studies reported almost the same rate constant for MACR. However, the rate constant for MVK measured by Pedersen and Sehested[434] is about 40% smaller than that measured by Schöne and Herrmann.[115] On this topic, Chen et al.[360] have published reaction mechanisms for the reaction of ozone with MACR and MVK in aqueous solution. The proposed mechanisms include ozone addition, which leads to the subsequent formation of the ozonide, that rapidly decomposes to formaldehyde and methylglyoxal as well as several Criegee intermediates, which further react to yield formaldehyde, methylglyoxal, pyruvic acid, and H_2O_2. Therefore, the aqueous ozonation of unsaturated organic compounds provides a pathway for the production of organic carbonyl compounds, substituted carboxylic acids, and H_2O_2.

Table 13 also reports a set of reaction rate constants for mono- and dicarboxylic acids.[435−440] The reported second-order rate constants are generally similar or slightly smaller than those of the olefins. The available kinetic data show mostly higher values for the deprotonated acids as compared to the protonated forms. For example, Leitzke and von Sonntag[435] have measured an ozonation rate constant of 1.5×10^5 and 3.7×10^6 M^{-1} s^{-1} for methacrylic acid and methacrylate, respectively. This behavior could be caused by the stronger electron-withdrawing properties of the deprotonated carboxylate group.

Dowideit and von Sonntag[441] have studied the reaction of O_3 with a number of halogenated alkenes in water. The measured kinetic data show that the reactivity toward ozone decreases with increasing number of halogen substituents.

6.1.6. Aromatic Organic Compounds. Since the 1998 publication of the NDRL/NIST Solution Kinetics Database 3.0,[401] several new rate constants have been reported for aromatic compounds (see Table 13). Most of the new kinetic data are for oxygenated aromatic compounds. Poznyak and Vivero[443] have determined the ozonation rate constant for phenol at pH = 2 and pH = 7, and found quite similar rate constants at these two pH values. The rate constant of 1.17×10^3 M^{-1} s^{-1} obtained at pH = 7 is in good agreement with the one reported by Hoigné and Bader ($k = 1.3 \times 10^3$ M^{-1} s^{-1}).[461] Ramseier and von Gunten[438] published details in 2009 on the chemical mechanism of phenol ozonation, including the primary and secondary products formed. Bin et al.[445] investigated the ozonation of benzaldehyde in aqueous solution at two different pH values (pH = 2.3 and pH = 6). The value measured at pH = 2.3 ($k = 1.2 \times 10^2$ M^{-1} s^{-1}) is substantially smaller than the value measured at pH = 6 ($k = 10^4$ M^{-1} s^{-1}). Beltrán et al.[446] studied the ozonation kinetics of two phenolic

DOI: 10.1021/cr500447k
Chem. Rev. 2015, 115, 4259−4334

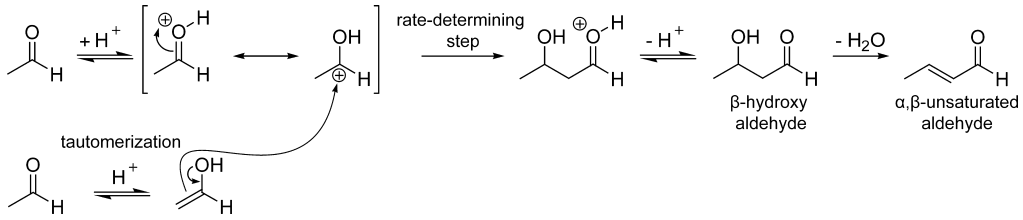

Figure 6. Schematic mechanism of the acid-catalyzed aldol condensation.

acids, *p*-hydroxybenzoic acid and gallic acid, at three different pH conditions (pH = 2, pH = 6.3, and pH = 9). The reaction rate constants for *p*-hydroxybenzoic acid displayed a strong pH dependency. While the reaction rate constant for the ozonation of *p*-hydroxybenzoic acid at pH = 2 is only $k = 2 \times 10^2$ M^{-1} s^{-1}, the corresponding rate constant at pH = 9 is $k = 6.4 \times 10^7$ M^{-1} s^{-1}, that is, about 5 orders of magnitude higher. Table 13 also includes numerous new kinetic data for the ozonation reactions of heteroatom-containing aromatic compounds. The kinetic rate constants of this group cover a huge span, ranging from $k = 6.4 \times 10^{-3}$ M^{-1} s^{-1} (*o*-chloronitrobenzene) to $k = 1.0 \times 10^7$ M^{-1} s^{-1} (2,4-dichloronitrophenol).

As in some other area subjects of this Review, it needs to be noted that quantitative structure activity relationships (QSARs) have been established by Lee and von Gunten[462] in 2012 based on the existing kinetic data set. In their publication, QSAR equations are reported for the reactivity of ozone in aqueous solution with nondissociated and dissociated phenols, benzene derivatives, anilines, olefins, amines, and their derivatives. Comparisons of the modeled and predicted reactions rate constants have shown a reasonably good agreement.

Finally, it should be mentioned that ozone reactions are also important in the context of advanced oxidation processes (AOPs). Because of the focus of this Review on atmospherically relevant processes, AOPs are not discussed here, but overviews of this topic can be found in a number of available other publications.[375,420,449,462−470]

6.2. Organic Accretion Reactions

6.2.1. Overview. Recently, not only radical reactions have been discussed because of their potential importance for tropospheric aqueous-phase chemistry, but also nonradical reactions. On the one hand, these reactions can be oxidative (usually driven by H_2O_2 and ozone); those reactions have been treated in section 6.1. On the other hand, there is growing interest in nonoxidative reactions where molecules are aggregated from smaller units to form larger product molecules. These reactions, which are usually referred to as aggregation or accretion reactions, will be discussed in the subsequent subsections. To some extent, these reactions have already been summarized in the 2009 review by Hallquist et al.[38] A subsequent summary of aqSOA chemistry focused primarily on reactions of glyoxal and methylglyoxal.[1]

Generally, tropospheric aqueous-phase chemistry is not limited at all to only one or two compounds of interest. Despite significant progress in the last two decades, at the time of writing, the authors regard most of the potential of aqueous-phase conversions in the troposphere as yet unexplored. As for the special case of SOA, aqueous-phase conversion will surely contribute, but a huge multitude of atmospheric systems will do the same; SOA is a complex product mixture from a very wide variety of compounds and conversions in different media, including the gas phase. The organic chemistry of particle constituents, however, has the potential not only to lead to products that contribute to organic particle mass but also to influence a variety of other properties in the tropospheric multiphase system: the systems' oxidative capacity will be influenced by organics, certain chemical pathways are very sensitive to the presence of organic compounds (e.g., aqueous-phase sulfur oxidation), and some systems will not work at all without organic compounds being present (e.g., photolysis of metal−organic complexes). Finally, various health effects of particles are associated with organics of certain compound classes, either alone or in combination with other particle constituents such as the transition metal ions. Of course, particle organics might also influence light absorption and have some influence on CCN and IN ability, thus linking particle chemistry with radiative properties and, by extension, climate.

6.2.2. Aldol Condensation Reactions. As shown in Figure 6, the aldol reaction in its classic form is a carbon−carbon bond-forming reaction between the nucleophilic enol and electrophilic keto form of a single aldehyde.[471] The product of this reaction, a *β*-hydroxy aldehyde (i.e., an aldehyde alcohol), can subsequently undergo dehydration to form an *α*,*β*-unsaturated aldehyde.[471] More generally, the aldol reaction can occur between any two carbonyl compounds, provided that at least one is enolizable.

Although the aldol reaction was discovered in 1872,[472] its study in a tropospheric context dates to a relatively recent set of influential chamber and flow tube studies performed by Jang and co-workers, in which enhanced organic aerosol yields from gas-phase carbonyls observed in the presence of acidic seed aerosol were attributed to the presence of acid-catalyzed reactions, including the aldol condensation reaction, in the particle phase.[473,474] Since that time, researchers have examined plausible catalytic mechanisms, measured reaction rates, and assessed the atmospheric consequences of the aldol reaction. The following paragraphs aim to summarize the current state of knowledge in this field.

6.2.2.1. Sulfuric Acid-Catalyzed Aldol Condensation Reactions. The work of Jang and colleagues[473,474] provided indirect evidence that the acid-catalyzed aldol reactions of carbonyls could contribute to SOA formation via the production of lower-volatility condensation products. Further evidence for the contribution of this pathway to SOA mass was provided by mass spectral evidence of aldol condensation products in SOA produced from both *α*-pinene[475,476] and 1-methylcyclopentene ozonolysis.[477] The significance of this pathway, however, was drawn into question by experiments performed by Kroll and co-workers, who found no difference in particle volume when a wide variety of carbonyls were introduced to a chamber containing acidic seed aerosol.[478]

In an effort to determine the significance of this reactive pathway, a large number of studies have examined both the uptake kinetics of carbonyls to sulfuric acid solutions[479−482] and the bulk liquid-phase reactivity of carbonyls in sulfuric acid

DOI: 10.1021/cr500447k
Chem. Rev. 2015, 115, 4259−4334

Table 14. Summary of Available Kinetic Parameters for Aldol Condensation Reactions in Aqueous Solution

reagent	catalyst	rate constant	remarks	refs
acetaldehyde	H_2SO_4 (47.8−88.2 wt %)	$(2.01 \times 10^{-5}$−$3.06 \times 10^{-3})$ M^{-1} s^{-1}	conversion of acetaldehyde to its aldol product and its subsequent dehydration were measured using UV/vis spectroscopy; complete dehydration of the aldol product was observed at H_2SO_4 > 64%	493
acetone	H_2SO_4	0.23 M^{-1} s^{-1} (75 wt %; 201 K) 0.27 M^{-1} s^{-1} (85 wt %; 221 K)	experiments were performed by exposing thin H_2SO_4 films to gas-phase acetone, and rate constants were determined by fitting irreversible uptake curves using a two-step kinetic model	479
acetone	H_2SO_4	4×10^{-5} M^{-1} s^{-1} (76 wt %; 250 K) 8×10^{-5} M^{-1} s^{-1} (79 wt %; 270 K)	experiments were performed in a wetted-wall flow reactor, and the liquid-phase reaction rate was calculated from gas-phase uptake coefficients	480
acetone	H_2SO_4 (80.8 wt %; reactive uptake observed only at >74 wt %)	2.3×10^{-4} s^{-1}	experiments were performed in a rotating wetted-wall reactor, and liquid-phase reaction rates were calculated from gas-phase uptake coefficients; second-order rate constants are presented graphically as a function of H_2SO_4 concentration	481
2-butanone	H_2SO_4 (80.8 wt %; reactive uptake observed only at >70 wt %)	2.0×10^{-4} s^{-1}		
2,4-pentanedione	H_2SO_4 (80.8 wt %; reactive uptake observed only at >64 wt %)	1.9×10^{-3} s^{-1}		
acetaldehyde	H_2SO_4 (85 wt %; reactive uptake observed only at >85 wt %)	5.2×10^{-5} s^{-1}		
methyl vinyl ketone	H_2SO_4 (80 wt %; reactive uptake observed only at >80 wt %)	~3 M^{-1} s^{-1}	experiments were performed in a rotating wetted-wall reactor, and the liquid-phase reaction rate was estimated from the gas-phase uptake coefficient	482
acetaldehyde	H_2SO_4 (60−85 wt %); results from 80 wt % summarized here	~0.005 M^{-1} s^{-1}	kinetics of formation of the dehydrated aldol product were measured in solution using UV/vis spectroscopy; second-order rate constants are presented graphically as a function of aldehyde identity, H_2SO_4 concentration, and temperature	483
propanal		~0.15 M^{-1} s^{-1}		
butanal		~0.17 M^{-1} s^{-1}		
pentanal		~0.065 M^{-1} s^{-1}		
hexanal		~0.035 M^{-1} s^{-1}		
heptanal		~0.025 M^{-1} s^{-1} (85 wt %)		
octanal		~0.005 M^{-1} s^{-1} (75 wt %)		
acetaldehyde	H_2SO_4	$(2.5 \pm 1.4) \times 10^{-7}$ s^{-1} (75 wt %) $(1.2 \times 2/2) \times 10^{-4}$ s^{-1} (96 wt %)	first-order rate constant for product formation was determined by measuring increase in solution absorption with time	484
acetaldehyde	glycine	$(10.9 \pm 2.1) \times 10^{-6}$ s^{-1} × [glycine (M)]	the first-order rate constant for reaction was determined by measuring the kinetics of aldol product formation; the reaction was second-order in amino acid concentration at elevated amino acid concentrations; additional rate constants are presented for reaction in NaCl solution	490
	alanine	$(3.9 \pm 1.1) \times 10^{-6}$ s^{-1} × [alanine (M)]		
	serine	$(3.8 \pm 1.0) \times 10^{-6}$ s^{-1} × [serine (M)]		
	arginine	$(4.5 \pm 1.1) \times 10^{-5}$ s^{-1} × [arginine (M)]		
	proline	$(8.5 \pm 2.1) \times 10^{-6}$ s^{-1} × [proline (M)]		
acetaldehyde	$(NH_4)_2SO_4$	2.5×10^{-7} s^{-1} (20 wt %) 6.7×10^{-7} s^{-1} (40 wt %)	in the case of acetaldehyde, the first-order rate coefficients for reaction were determined by measuring the kinetics of aldol product formation; first-order reaction rates were also determined for additional ammonium salts	489
acetone		~4.5×10^{-6} s^{-1} (40 wt %; 308 K)		
methylglyoxal	$(NH_4)_2SO_4$	5×10^{-6} M^{-1} min^{-1} (NH_4^+ catalysis) $\leq 1 \times 10^{-3}$ M^{-1} min^{-1} (H_3O^+ catalysis)	the second-order rate coefficients for hydronium- and ammonium-catalyzed aldol condensation were derived from UV−vis absorption data of the reaction products; reactions were performed at pH 2	53
methylglyoxal	arginine	$\log k = 0.422$ (pH) − 4.09 M^{-1} s^{-1}	methylglyoxal reaction in the presence of ammonium sulfate primarily results in methylimidazole formation (i.e., rather than aldol product formation)	492
	glycine	$\log k = 0.262$ (pH) − 3.40 M^{-1} s^{-1}		
	serine	$\log k = 0.421$ (pH) − 3.91 M^{-1} s^{-1}		
	methylamine	$\log k = 0.334$ (pH) − 3.22 M^{-1} s^{-1}		

DOI: 10.1021/cr500447k
Chem. Rev. 2015, 115, 4259−4334

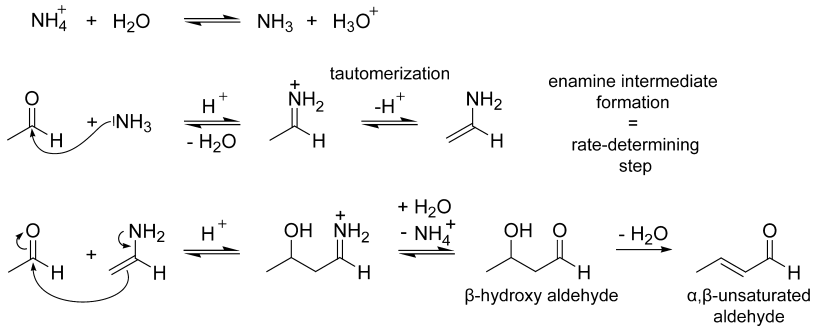

Figure 7. Schematic mechanism of the ammonium-catalyzed aldol condensation based on investigations of Nozière et al.[489]

solutions.[483,484] The kinetic parameters obtained in these studies are summarized in Table 14.

Together, these studies suggest that sulfuric acid-catalyzed aldol reactions are too slow to result in significant transfer of organic material to the bulk phase. In their study of the uptake kinetics of small carbonyl compounds to sulfuric acid solutions, for example, Esteve and Nozière[481] estimated that the aldol-mediated uptake of acetone to acidic aerosol (50 wt % H_2SO_4) would result in the transfer of only $\sim 10^{-21}$ g cm^{-3} h^{-1} to the particle phase, which is a factor of 10^{10} smaller than the typical seed aerosol mass concentrations used in chamber experiments.

In addition, as noted by Casale and co-workers,[483] because the sulfuric acid-catalyzed aldol condensation is second-order in aldehyde concentration (i.e., the rate-limiting step is the formation of the hydrated aldol product), its rate displays a quadratic dependence on aerosol-phase aldehyde content and is therefore largely limited by aldehyde solubility. Direct evidence for this limitation has been provided by two studies of octanal uptake by sulfuric acid droplets, both of which showed that substantial uptake only occurred at high gas-phase octanal concentrations (20−200 ppm).[485,486]

Finally, a number of laboratory studies have shown that the formation of condensed-phase aldol products is significant only at sulfuric acid concentrations much higher than those typically seen in tropospheric aerosol.[481,482,485,487] For example, in their study of hexanal uptake to sulfuric acid aerosols, Garland and co-workers found that the aldol condensation product 2-butyl-2-octenal was formed only at initial aqueous sulfuric acid concentrations of >75 wt %.[488]

Even if these reactions are too slow to result in significant contributions to SOA formation, they may still change the optical properties of the SOA itself: Nozière and Esteve, for example, found that sulfuric acid solutions (25−50 wt %) exposed to a gas-phase mixture of nine atmospherically relevant carbonyls displayed absorbance in the actinic region.[484] The impact of aldol condensation reactions on aerosol optical properties has since emerged as a major topic of research, and will be discussed in more detail below.

6.2.2.2. Ammonium- and Amine-Catalyzed Aldol Condensation Reactions. Work by Nozière and colleagues has shown that both inorganic ammonium salts and amino acids efficiently catalyze the bulk solution-phase aldol condensation of carbonyl compounds, including acetaldehyde and acetone.[489−491] More recently, Sedehi et al. have shown that methylamine can also catalyze the aldol condensation reaction of methylglyoxal.[492] The kinetic parameters obtained in these studies are summarized in Table 14.

The mechanism of the amino acid-catalyzed aldol condensation of acetaldehyde was studied in detail by Nozière and Córdova.[490] Analogous to the mechanism shown in Figure 7, the reaction proceeds via the rate-limiting formation of an enamine intermediate, which subsequently adds to the keto form of acetaldehyde; the resultant β-hydroxy imine undergoes hydrolysis to yield the usual β-hydroxy aldehyde. At high amino acid concentrations, this reaction is believed to occur via a Mannich-type pathway, in which the enamine intermediate described above attacks the iminium product of reaction between the amino acid and the initial aldehyde (not shown; see reference for further details regarding this mechanism).

Unlike the acid-catalyzed aldol condensation, which requires high acidities to proceed efficiently, the ammonium-catalyzed aldol reaction proceeds at pH values more typical of tropospheric aerosol. In addition, as shown in Table 14, this reaction pathway is rapid: the rate constant for reaction of acetaldehyde in the presence of tropospherically relevant quantities of amino acids (~10 mM),[494] for example, is comparable to that observed in concentrated sulfuric acid.[490] Moreover, since work by Casale et al.[483] has shown that the reactivity of acetaldehyde toward sulfuric acid-catalyzed aldol condensation is significantly lower than that observed for larger aldehydes, this reaction pathway may be even more atmospherically significant.

It should be noted here that the existence of bulk-phase reactivity is a necessary but insufficient condition for SOA formation via condensed-phase processes: despite the efficiency of ammonium- and amino acid-catalyzed condensation reactions in bulk aqueous media, Kroll and co-workers did not observe carbonyl uptake to aqueous ammonium sulfate seed particles,[478] and Chan and co-workers did not observe oligomeric products upon extended exposure of ammonium sulfate particles alone to gas-phase methyl vinyl ketone (MVK);[495] only the addition of sulfuric acid led to observable oligomer formation from MVK. This apparent discrepancy may arise from the limited partitioning of gas-phase aldehydes to the aqueous phase in the absence of pre-existing organic material or, alternatively, strong acidity. In the following paragraphs, a number of nonreactive and reactive mechanisms by which pre-existing organic species facilitate the uptake of gas-phase carbonyls will be discussed.

6.2.2.3. Aldol Reactions in Complex Matrices. As discussed above, the majority of studies of the aldol condensation reaction have been performed in simple, two-component reaction systems (i.e., aqueous solutions of a single carbonyl and a single catalyst). A smaller number of studies have explicitly considered multicomponent aldol reactions (i.e., cross-condensations): Schwier and co-workers, for example, found mass spectral evidence of cross-condensation products from glyoxal and methylglyoxal in ammonium sulfate

DOI: 10.1021/cr500447k
Chem. Rev. 2015, 115, 4259−4334

solution,[55] and Nozière and Esteve found UV/vis spectral evidence for the production of cross-condensation products from a variety of small carbonyl compounds in sulfuric acid solution.[484]

In ambient aqueous aerosol, however, carbonyl species are not present in isolation (or as binary mixtures) but rather as minor components of a highly complex mixture, which may itself influence the rate and extent of aldol-type reactions. For example, the uptake of both octanal and nonanal by sulfuric acid droplets has been shown to increase over time as a result of the accumulation of condensed-phase reaction products,[485,496] and the nonreactive uptake of acetaldehyde by sulfuric acid solutions has been shown to be enhanced by the presence of ethanol or acetone.[497] Very recent work by Drozd and McNeill suggests that the aqueous aerosol matrix may also hinder aldol-type reactivity: these authors found that the presence of glycerol and other polyols depressed the formation of light-absorbing products from methylglyoxal via the competitive formation of unreactive hemiacetals/acetals.[498]

6.2.2.4. Aldol Reactions in Evaporating Droplets. Recent studies have shown that the production of oligomeric[499] and light-absorbing[500] species in SOA is enhanced at low relative humidities. Given these results, it is perhaps unsurprising that studies have shown that the production of aldol condensation products is accelerated in evaporating droplets. For example, De Haan and co-workers showed that methylglyoxal undergoes efficient aldol condensation in evaporating droplets, presumably catalyzed by trace (~2%) quantities of pyruvic acid impurities formed by methylglyoxal disproportionation.[501] In addition, Nguyen et al. showed that the evaporation of limonene-O_3 SOA in the presence of added sulfuric acid led to the production of light-absorbing organosulfate derivatives of aldol condensation products.[502]

6.2.2.5. The Influence of Aldol Reactions upon Aqueous Aerosol Properties. Aldol condensation reactions in sulfuric acid solution have been shown to lead to the slow formation of light-absorbing products: the acid-catalyzed aldol condensation of acetaldehyde has been estimated to lead to a 4-orders-of-magnitude increase in the absorption index of sulfuric acid over a 2-year time period (i.e., the typical lifetime of stratospheric sulfuric acid aerosol).[503] The ammonium-, amino acid-, and amine-catalyzed aldol condensations of a variety of small carbonyl compounds have also been shown to yield light-absorbing products.[53,491,504] Interestingly, the contribution of these light-absorbing species to aerosol optical properties may be limited by their own photochemical degradation: in a recent study, Sareen and co-workers showed that light-absorbing SOA formed from the reaction of methylglyoxal in ammonium sulfate undergoes rapid photolysis.[54]

In recent years, a number of studies have focused on the mechanisms underlying the formation of light-absorbing species in biogenic SOA.[500,502,505] In these complex cases, an assessment of the role that aldol reactions play in enhancing the optical absorption properties of aqueous aerosol is often complicated by the production of light-absorbing products via different reactive pathways: for example, the reaction of limonene–O_3 SOA with ammonium ions and amino acids in aqueous solution has been shown to result in the production of not only light-absorbing aldol condensation products but also nitrogen-containing chromophores.[502,506] Insight into the relative importance of these pathways can be provided by spectral analysis of product mixtures: by comparing the absorption spectra of the products of reaction of methylglyoxal with aqueous-phase ammonium sulfate, glycine, and methylamine, Powelson and colleagues were able to show that these species acted as catalysts rather than reagents.[504] In real aerosol samples, however, the situation can be much more complex: as very recently noted by Phillips and Smith, aerosol light absorption may arise not only from individual chromophores but also from charge-transfer complexes formed between alcohol and carbonyl functionalities.[507]

Evidence exists to suggest that the formation of light-absorbing products may not be the only pathway by which aldol reactions influence aqueous aerosol properties. Studies have shown, for example, that the reaction of acetaldehyde, methylglyoxal, and acetaldehyde–methylglyoxal mixtures leads to a reduction in surface tension via the production of surface-active products.[53,56] In addition, the reaction of methylglyoxal with methylamine under conditions designed to mimic an evaporating cloud droplet has very recently been shown to result in the production of semisolid particles, which has implications for particle aging via the further uptake of gas-phase organics and oxidants and for the ice nucleation properties of the particles.[508,509] It should be noted, however, that in these studies the specific role of the aldol condensation reaction in these transformations has not been estimated.

6.2.2.6. Thermodynamic Analyses. In two studies designed to investigate the thermodynamics of formation of aldol condensation products, Barsanti and Pankow reported that whereas the aldol condensation reactions of methyl glyoxal, 1,6-dihexanal, and larger dialdehydes can be expected to contribute to the formation of atmospheric organic particulate matter, its formation via the aldol condensation reactions of 1,4-butanedial, 2,3-butanedione, 2,5-hexanedione, and a number of straight-chain aldehydes is not thermodynamically favorable.[510,511] In a later study, Tong and coworkers used quantum mechanical calculations of physical properties of carbonyls and their condensation products to estimate the solution-phase equilibrium constants for the aldol reactions of acetaldehyde, acetone, butanal, and hexanal.[512]

Krizner et al. used density functional theory calculations to show aldol condensation to be the most thermodynamically favored oligomerization reaction for methylglyoxal.[513] This theoretical result agrees with experimental results obtained by Yasmeen and colleagues, who found that the reaction of methylglyoxal in aqueous ammonium sulfate led to the formation of aldol condensation products.[408]

Finally, in a recent computational study of the thermodynamics of dimer formation from early-generation oxidation products of α-pinene, DePalma and co-workers showed that the aqueous-phase aldol condensation of pinonaldehyde and pinonic acid is thermodynamically favorable.[514] Indeed, the hydrated aldol product of this reaction has been observed by Hall and Johnston in a high-performance mass spectrometric study of the condensed-phase products of α-pinene ozonolysis.[515] This computational result also provides support for the work of Liggio and Li, who found evidence for high-molecular-weight products upon uptake of pinonaldehyde by acidic aerosols.[516]

6.2.2.7. Summary. In summary, available evidence suggests that aldol condensation reactions have the potential to contribute to organic aerosol mass and also to result in the formation of light-absorbing products, thereby changing the optical properties of organic aerosol. The influence of aldol condensation pathways upon other aerosol properties,

DOI: 10.1021/cr500447k
Chem. Rev. 2015, 115, 4259–4334

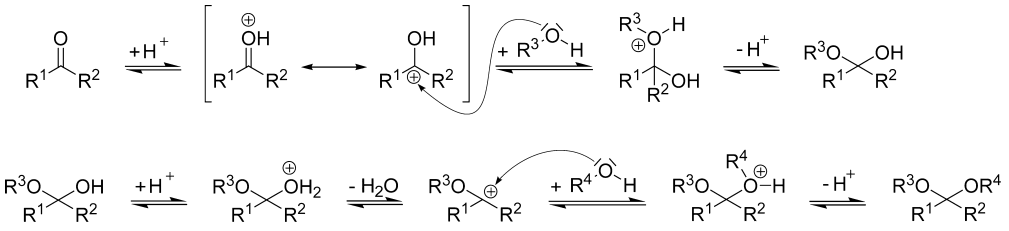

Figure 8. Schematic depiction of hemiacetal and acetal formation in the aqueous phase.

including surface tension, phase, and ice nucleation ability, is currently less clear and deserves further study.

6.2.3. Acetal and Hemiacetal Formation. The principle of acetal formation is shown in Figure 8. First, a carbonyl compound is protonated, which leads to the formation of a carbocation bound to a hydroxyl group. This carbocation can then be subject to nucleophilic attack by an alcohol, which results in the formation of an ether-type C−O−C bond after deprotonation. In this way, a hemiacetal $R_1R_2C(OH)OR_3$ is formed. As shown in the lower half of Figure 8, the hemiacetal can further react to the full acetal, again promoted by acidity, which is needed to protonate the alcohol group of the hemiacetal, eliminate water, and produce a carbocation again. For the special case that, in aqueous solution chemistry, a geminal diol (an α-diol) is involved, as is the case for hydrated carbonyl compounds, acetal formation corresponds to the formation of oxygen-containing ring structures with two internal C−O−C ether-type groups (i.e., molecules of the 1,4-dioxane type). If a hydroperoxide is involved in hemiacetal formation, a peroxy hemiacetal will result.

Hemiacetal and acetal formation received great attention in SOA studies conducted by Paul Ziemann and co-workers as early as 2003.[517] It is interesting to note that hemiacetals can also be strongly linked to gas-phase chemistry: when 1,4-hydroxycarbonyl compounds are formed via isomerization of alkoxy radicals in the gas phase, they are expected to readily undergo phase transfer into aqueous particles, where they can form a cyclic hemiacetal (a hydroxy-furan), which can subsequently eliminate water to yield a dihydrofuran. Details for this sequence are discussed in a review by Ziemann and Atkinson[518] and in another study by Lim and Ziemann.[519] This latter study focuses on organic particles and shows that increasing relative humidity slows the process of dihydrofuran formation and its possible back-release to the gas phase as a result of the dilution of HNO_3 acidity. Another study by the same group[520] showed the formation of hemiacetals during the aging of aerosol particles formed in the oxidation of *n*-pentadecane by OH. The potential of these processes to occur, at least to some extent, in aerosol liquid water and other aqueous systems still needs to be explored. Acetal formation has been described by Liggio et al.[404] in 2005 for acetals from glyoxal.

Recent studies relating to hemiacetal and acetal formation are discussed in the following subsections. Only publications that have appeared since 2009 or key papers will be discussed here. For earlier work or work more specifically focused on glyoxal and methylglyoxal chemistry, the reader is referred to other available overviews.[1,2,31]

6.2.3.1. Glyoxal and Methylglyoxal. As will be detailed in section 7.2.1, acetal formation is involved in the oligomeriziation reactions that occur when glyoxal is present in aqueous solution in concentrations greater than 1 mM; here, the formation of acetal oligomers is expected.[492] Schwier et al.[55] have studied cross-reactions between glyoxal and methylglyoxal. While their contribution contains a wealth of information on identified products, no kinetic parameters are presented for the aqueous-phase formation of the observed compounds; instead, an aggregated kinetic model is used to describe the observed light absorption at λ = 280 nm. Hemiacetal and acetal compounds at m/z of 260.8, 289.5, and 293.1 have been measured with CIMS ionization by iodide.

Methylglyoxal oligomers formed in the absence of light have been investigated by Yasmeen et al.[408] to understand SOA formation by cloud processing during nighttime. The oligomers identified are suggested to arise via hydration of methylglyoxal, followed by acetal formation and, finally, oligomerization. Again, kinetic information is not presented in this study.

Jia and Xu[521] have photo-oxidized benzene and ethylbenzene under varying relative humidity and ozone concentration conditions. Glyoxal hydrates, acids, hemiacetal, and acetal species were identified as reaction products in the resulting SOA particles. In the case of benzene oxidation, both aqueous-phase radical reactions and hemiacetal formation were observed after evaporation; in the case of ethylbenzene oxidation, glyoxal/ethylglyoxal cross-reactions were found to occur.

6.2.3.2. Glycolaldehyde Oligomer Formation. Kua et al.[522] studied the formation of oligomers via hemiacetal formation by means of a computational protocol and compared this to experimental NMR measurements in water.

6.2.3.3. N-Containing Hemiacetal Oligomers from Isoprene. Recently, Nguyen et al.[523] observed nitrogen-containing SOA oligomers following isoprene photooxidation. The formation of hemiacetal oligomers from units of 2-methylglyceraldehyde ($HO{-}CH_2C(CH_3)(OH)CHO{=}C_4H_8O_3$) was observed; however, the hemiacetal from these units was not among the most abundant oligomers identified.

6.2.3.4. Hemiacetal Oligomers from Limonene Ozonolysis. Kundu et al.[524] have identified high-molecular-weight SOA compounds from limonene ozonolysis. In this work, complex reaction patterns for the formation of SOA components have been elucidated, and, as the authors state, hemiacetal formation appears to dominate, followed by products from hydroperoxide and Criegee reaction channels.

6.2.3.5. Matrix Effects. As mentioned in section 6.2.2, Drozd and McNeill[498] have very recently presented a highly innovative study in which they showed that carbonyl compounds in the particle phase might undergo (hemi)acetal formation with organic matrix constituents, which could reduce the rate of formation of imidazoles (see section 7.2.5) as well as oligomer species. The authors have employed highly concentrated sugars, sugar alcohols, and glycerol, which are similar to proxies that have been used by other authors. The study highlights a problem that always needs to be considered when organic particle chemistry is treated in laboratory experiments: laboratory studies are in some cases conducted in environments that are too simplistic as compared to real-world systems, and

DOI: 10.1021/cr500447k
Chem. Rev. 2015, 115, 4259−4334

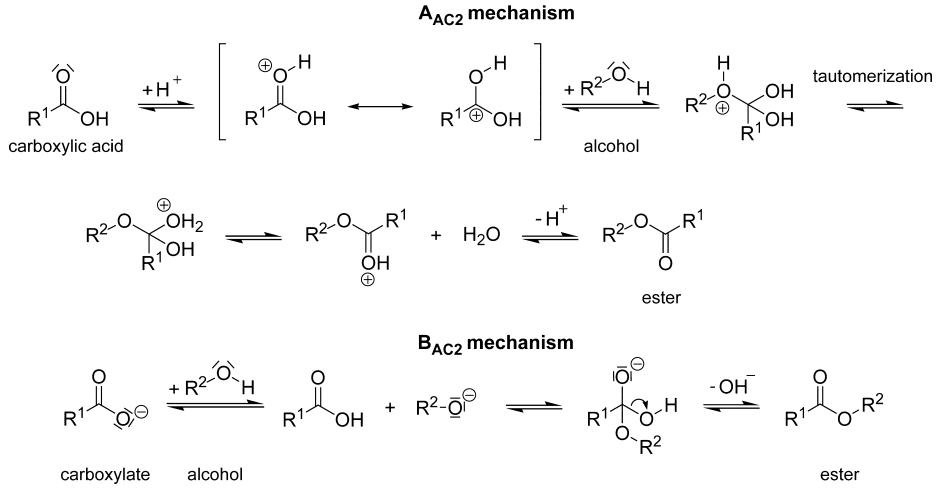

Figure 9. Schematic depiction of the two most common acid-catalyzed (A) and base-catalyzed (B) esterification/hydrolysis pathways (A_{AC2}/B_{AC2}) of carboxylic esters in aqueous solution.

therefore results from these studies might not easily be transferable to real-world aqueous aerosol particles, fogs, and clouds.

6.2.3.6. Droplet Evaporation. Ortiz-Montalvo et al.[525] studied the formation of SOA from glycolaldehyde in aqueous bulk solution with an additional step of water evaporation. Hemiacetal oligomeric products from glycolaldehyde were suggested to contribute to the measured SOA mass increase.

Although a number of experimental findings have confirmed the formation and existence of both cyclic and acyclic hemiacetals, acetals, and peroxy hemiacetals, to the best of the authors' knowledge, nearly no kinetic data exist that would allow for the formation of these important products to be modeled. In fact, there is an early study by Guthrie on hemiacetal−acetal equilibrium constants for carbonyl compounds,[526] and some related references are mentioned in the review by Ziemann and Atkinson.[518] Rather, qualitative identification prevails at the time of writing, and there is the urgent need to investigate these processes better and in a more quantitative way by establishing valid kinetic data for the reactions involved, preferably at the level of individual elementary reactions. For more information on droplet evaporation techniques, see section 2.

6.2.3.7. Thermochemistry of Hemiacetal and Acetal Formation. Interestingly, the thermodynamics of hemiacetal and acetal formation has recently been studied.[527] These thermochemical findings are especially important as they may lay the foundation for a better understanding of hemiacetal and acetal formation. The study of Azofra et al.[528] uses DFT calculations to study the model reaction between formaldehyde and methanol to form a hemiacetal.

6.2.4. Esterification and Hydrolysis of Organic Esters. Another accretion process leading to higher molecular weight compounds and thus contributing to SOA mass is esterification.[529] This section focuses solely on the formation (esterification) and degradation (hydrolysis) of organic carboxylic acid esters. Other inorganic ester reactions, such as the formation of sulfate esters, are not discussed here but rather in section 7.2.

Carboxylic acid esters ($R_1C(=O)OR_2$) are common organic compounds, which can be formed through a reversible acid/base-catalyzed condensation reaction between carboxylic acids and hydroxyl-containing organic compounds such as alcohols or phenols, that leads to an aliphatic or aromatic ester, respectively. Several mechanisms for the formation and degradation of esters have been proposed in the literature.[518,530,531] The two most common equilibrium mechanisms[532] according to the classification of Ingold[530] are the A_{AC2} (acid-catalyzed, acyl-oxygen cleavage, bimolecular reaction) and the B_{AC2} (base-catalyzed, acyl-oxygen bond cleavage, bimolecular reaction) mechanisms. The reverse A_{AC2} reaction of this equilibrium mechanism is known as the Fischer esterification. Esters can also be formed through acid-catalyzed decomposition, for example, of peroxyhemiacetals (see Ziemann and Atkinson[518] and references therein). However, the present description will be limited to the A_{AC2}/B_{AC2} reaction mechanisms, which are depicted in Figure 9. The Fischer esterification represents a nucleophilic acyl substitution, which is based on the increased electrophilicity of the polarized carbonyl carbon and the nucleophilicity of an alcohol. In detail, the Fischer esterification includes several reaction steps. Initially, the carbonyl group is protonated by an acid catalyst. The polarized carbonyl group is characterized by an increased electrophilicity, which makes it more prone to the nucleophilic attack of the alcohol. The activated tetrahedral complex formed after nucleophilic attack of the alcohol subsequently collapses, with the concurrent elimination of water and numerous accompanying protonation/deprotonation steps, to yield the ester.

By means of a general theoretical approach using methods of equilibrium thermodynamics, Barsanti and Pankow[533] have investigated the thermodynamic feasibility of organic accretion reactions, including esterifications, under atmospheric conditions. These authors concluded that ester formation is thermodynamically favored and, if kinetically favorable, likely to contribute significantly to SOA formation under atmospheric conditions. More recent studies by DePalma et al.[514] have used multistep quantum chemical structure optimizations together with continuum solvation modeling to examine the formation potential for various postulated dimerization mechanisms, including acid-catalyzed esterification. This study indicated, by contrast, that ester formation in both the gas and the condensed phases (solvent: water, methanol, acetonitrile) is not favored.

It should be noted that the majority of esters are metastable and hydrolyze in the presence of water. Moreover, under

DOI: 10.1021/cr500447k
Chem. Rev. 2015, 115, 4259−4334

Table 15. Hydrolysis of Different Aliphatic Esters at Different pH Values (T = 298 K, Data Taken from Mabey and Mill[535])[a]

R_1	R_2	pH	$k_A[H^+]$ [s^{-1}]	$k_B[OH^-]$ [s^{-1}]	overall	$t_{1/2}$
Me	Et	7	1.1×10^{-11}	1.1×10^{-8}	1.1×10^{-8}	2.0 y
		5	1.1×10^{-9}	1.1×10^{-10}	1.2×10^{-9}	18.2 y
		3	1.1×10^{-7}	1.1×10^{-12}	1.1×10^{-7}	0.2 y
		1	1.1×10^{-5}	1.1×10^{-14}	1.1×10^{-5}	17.5 h
		−1	1.1×10^{-3}	1.1×10^{-16}	1.1×10^{-3}	0.17 h
Me	*i*-Pr	7	6.0×10^{-12}	2.6×10^{-9}	2.6×10^{-9}	8.4 y
		5	6.0×10^{-10}	2.6×10^{-11}	6.2×10^{-10}	35.1 y
		3	6.0×10^{-8}	2.6×10^{-13}	6.0×10^{-8}	0.37 y
		1	6.0×10^{-6}	2.6×10^{-15}	6.0×10^{-6}	32.1 h
		−1	6.0×10^{-4}	2.6×10^{-17}	6.0×10^{-4}	0.32 h
Me	*t*-Bu	7	1.3×10^{-11}	1.5×10^{-10}	1.6×10^{-10}	134.8 y
		5	1.3×10^{-9}	1.5×10^{-12}	1.3×10^{-9}	16.9 y
		3	1.3×10^{-7}	1.5×10^{-14}	1.3×10^{-7}	0.17 y
		1	1.3×10^{-5}	1.5×10^{-16}	1.3×10^{-5}	14.8 h
		−1	1.3×10^{-3}	1.5×10^{-18}	1.3×10^{-3}	0.15 h
Me	$C_6H_5CH_2$	7	1.1×10^{-11}	2.0×10^{-8}	2.0×10^{-8}	1.1 y
		5	1.1×10^{-9}	2.0×10^{-10}	1.3×10^{-9}	16.9 y
		3	1.1×10^{-7}	2.0×10^{-12}	1.1×10^{-7}	0.2 y
		1	1.1×10^{-5}	2.0×10^{-14}	1.1×10^{-5}	17.5 h
		−1	1.1×10^{-3}	2.0×10^{-16}	1.1×10^{-3}	0.17 h

[a]The sixth column represents the calculated overall hydrolysis rate (k_{hydro} in s^{-1}) according to both acid- and base-catalyzed mechanism. $t_{1/2} = 0.693/k_{hydro}$; Me, CH_3; Et, CH_3CH_2; *i*-Pr, $CH_3(CH_3)CH$; *t*-Bu, $CH_3(CH_3)_2CH$.

neutral or mildly acidic aerosol conditions, carboxylic acids are also present in their deprotonated anion form, which makes them unreactive as electrophiles. Thus, esterifications under ambient conditions are restricted to very acidic (e.g., catalysis by H^+) and very low ALW conditions, because water is a product of the esterification. Measured esterification equilibrium constants (K_E) given in the literature for water-containing solutions (see, e.g., Lee et al.[534]) show values of ∼10 for a series of alkyl acetates, which indicates a slight preference for the products at high water concentrations.

$$K_E = \frac{[H_2O][R_1C(=O)OR_2]}{[R_2OH][R_1C(=O)O]} \quad (5)$$

Additionally, investigations of Lee et al.[534] revealed that the K_E values are very sensitive to electronic effects; that is, larger K_E values are measured with increasing electron-donation ability of the alkyl group. Beside the K_E values, the kinetics of the different hydrolysis processes of esters (A_{AC2}/B_{AC2}) have been investigated in the past (see Hilal[531] and references therein), and recently mathematical methods have been developed to estimate hydrolysis rate constants of carboxylic acid esters.[531] Available kinetic values (see compiled data of Hilal[531]) for the base-catalyzed hydrolysis (B_{AC2}) of aliphatic esters (without halogen substituents) are generally on the order of 10^{-1}–10^{1} M^{-1} s^{-1}. In contrast, the rate constants for the acid-catalyzed hydrolysis (A_{AC2}) of aliphatic esters are generally in the range of 10^{-4}–10^{-5} M^{-1} s^{-1}. Therefore, B_{AC2} will be the main pathway in less acidic aqueous solutions, and the A_{AC2} pathway will be dominant in acidic cloudwater and ALW (pH < 4, cf., Table 15). Additionally, the hydrolysis is affected by both electronic and steric effects: for example, the addition of halogen substituents to the R_1 group of the ester leads to a substantial increase in B_{AC2} reaction rate constants.[535] Thus, halogenated esters hydrolyze much faster than esters without halogen substitutions. On the basis of the kinetic hydrolysis data and the available K_E values, it can be concluded that both the formation and the hydrolysis of esters are relatively slow processes at typical acidity conditions present in tropospheric ALW, with fairly long times to establish equilibrium. However, under highly acidic conditions, the lifetime of an ester via the A_{AC2} pathway is substantially reduced. Table 15 shows the calculated first-order hydrolysis rate constants and lifetimes of selected aliphatic esters (data based on Mabey and Mill[535]).

Over the past 10 years, the formation and occurrence of organic esters resulting from VOC oxidation have been observed under near-atmospheric conditions in environmental chamber and other laboratory studies.[24,536−543] Chamber studies focusing on the photo-oxidation of isoprene[499,536,538,539,541] have identified esters formed from reactions of 2-methylglyceric acid under conditions of low ALW (i.e., low RH) and high NO_x. Esters have been also identified in chamber studies investigating the photooxidation of 3-methylfuran[540] and α-pinene.[543]

Nguyen et al.[499] have found a significant reduction (∼60%) in the total signal from oligomeric esters of 2-methylglyceric acid under humid conditions. The lowered ester formation under increased RH conditions is related to the increased ALW and thus to the shift in the reaction equilibrium toward the esterification educts, and to the lowered acid catalysis. Recently, Birdsall et al.[541] have proposed that the Fischer esterification mechanism might not be efficient enough to explain the observed production rates of the 2-methylglyceric acid oligoesters under realistic aerosol acidities. The study suggested that another esterification mechanism is needed to explain the presence of 2-methylglyceric acid oligoesters observed in chamber and ambient aerosols.

Organic ester compounds have also been measured in ambient aerosols.[543−545] However, the contribution of the measured ester compounds to the total organic aerosol mass has been shown to be rather small. Kristensen et al.[543] compared two different sampling periods characterized by different RH conditions. These authors found higher ester concentrations during the low RH condition period than during the period with about 2 times higher RH conditions. This

DOI: 10.1021/cr500447k
Chem. Rev. 2015, 115, 4259−4334

finding is in good agreement with the results of chamber sensitivity studies,[499,539] suggesting an enhanced particle-phase esterification and SOA contribution under low RH conditions.

6.2.5. Other Oligomerizations and Polymerizations. In an oligomerization only a few molecules of a monomer react with each other, in contrast to polymerization, which, at least in principle, involves the reaction of a nearly unlimited number of monomers. The products of oligomerization reactions are termed dimers, trimers, tetramers, and oligomers, according to the number of molecules from which they are formed. A molecule with less than 30 repeating monomer units is defined as an oligomer. According to the IUPAC definition, addition or subtraction of a single monomer unit from an oligomer will change its chemical and physical properties, while it will not for a polymer. Oligomer formation can occur by aldol condensation (section 6.2.2), acetal or hemiacetal formation (section 6.2.3), esterification (section 6.2.4), and polymerization.

In principle, polymerization reactions involve three steps: (i) initiation, (ii) propagation, and (iii) termination. Under atmospheric conditions, where the number of the same available monomer molecule is limited, oligomer formation is much more likely than polymer formation. This is especially true for deliquescent particles, where polymer propagation is inhibited by the large number of different inorganic and organic compounds present in the ALW. There are three main types of polymerization: (i) anionic polymerization,[546] (ii) cationic polymerization, and (iii) free radical polymerization.[87]

Anionic polymerization is a repetitive conjugate addition reaction with an anionic intermediate (Figure 10). This anion is

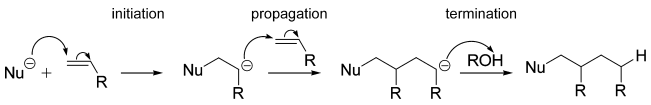

Figure 10. Mechanism scheme for anionic polymerization.

itself nucleophilic and can attack another monomer. The monomer molecule must have a double bond with an electron-withdrawing substituent (e.g., an ester or cyano group or a group with double bonds or aromatic rings) that can stabilize by resonance the negative charge that is developed in the transition state for the monomer addition (propagation) step.

Covalent or ionic alkali metal alkoxides, hydroxides, or amines as nucleophiles can initiate the polymerization reaction. Termination of the polymerization reaction occurs via proton transfer from water or alcohol molecules. The anionic polymerization of α-carbonyl acids in water under high basic conditions has been reported by Kimura et al.[546] This type of polymerization reaction is rather unlikely under atmospheric conditions, which are typically acidic or neutral.

Cationic polymerization is a repetitive alkylation reaction of monomer molecules, which require an electron-donating group (e.g., alkyl, alkoxy, or phenyl groups) to stabilize the carbocation transition state by resonance (Figure 11). The resulting cation intermediate must be stable; otherwise, the reaction can be terminated by loss of a proton.

The initiator for the polymerization can be a protic acid with an unreactive counterion (e.g., H_2SO_4) or a Lewis acid with a proton source (e.g., H_2O). The termination reaction randomly occurs by chain transfer, ejection reaction, or the loss of a proton. Because of the large number of different compounds available to terminate the polymerization reaction, this type of

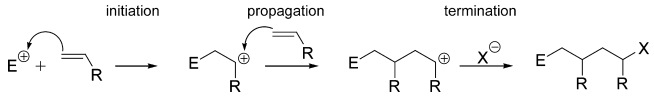

Figure 11. Mechanism scheme for cationic polymerization.

polymerization would only be expected to form small oligomeric compounds under atmospheric conditions.

6.3. Summary of Section 6

In summary, enormous progress has been made in the area of aqueous-phase nonradical reactions since 2010. According to the large number of publications in this area, accretion chemistry became an important part of atmospheric aqueous-phase chemistry studies. However, much of this work has still to undergo its "litmus test": when kinetic parameters are available, the reactions must be implemented into tropospheric aqueous-phase chemical mechanism frameworks and their effects have to be characterized and tested. How much SOA formation from aqueous-phase chemistry can really be observed? Are the time scales of solution kinetics and the microphysics fitting, and do they allow the formation of compounds identified in laboratory experiments? Some aqueous-phase processes, the kinetics of which have recently been thoroughly studied, appear to be too slow to lead to significant turnovers in a typical aerosol particle lifetime, which is not much beyond a week for particle sizes with the longest atmospheric lifetimes.[547]

Extensive mechanism testing has to be done here, and it seems that important pathways have so far been identified from IEPOX uptake and organosulfate formation by McNeill et al.[548] Many other pathways discussed in this Review still need to be implemented and their main characteristics assessed.

Besides this more theoretical evaluation in models, a link to real-world particle, fog, and cloudwater composition should also be established: which product molecules observed in the laboratory can really be identified in field or chamber studies under realistic conditions? The development of the study of organosulfates, which will be outlined in more detail in the subsequent section, clearly shows how such a link might work out, and also shows how first there was mainly analytical identification in field samples and a later in laboratory studies, including chamber studies. It then took some time until only in the recent past have aqueous-phase rate constants been determined, which only now allow the proper modeling of the formation of these important compounds. The authors believe that a similar way of establishing field evidence after evidence from the laboratory and then pursuing kinetic formation studies is also the approach of choice for a deeper understanding of the formation of the compounds discussed in section 6 of this contribution.

7. MAIN SYSTEMS OF CURRENT INTEREST

7.1. Inorganic Systems

In this section, three key areas where aqueous-phase and multiphase chemistry is of importance for inorganic atmospheric constituents will be discussed: sulfur oxidation, HO_x uptake, and $ClNO_2$ release.

7.1.1. Sulfur Oxidation. Multiphase sulfur oxidation remains a topic of global importance in the 21st century. According to one recent study, global sulfur emissions reached a maximum in 2006 and are currently decreasing.[549] Since then, reduction technologies in many areas of the world, including

DOI: 10.1021/cr500447k
Chem. Rev. 2015, 115, 4259−4334

Europe and China, have resulted in a decrease in SO_2 emissions, whereas they are still strongly growing in India. India and eastern China are the regions with the strongest growth in SO_2 emissions between 2005 and 2010.

As in previous decades, sulfur oxidation is an important component of global atmospheric chemistry, and there is a wealth of literature treating it in textbooks,[20,116] on its aqueous solution chemistry in reviews,[6] or, recently, by Gupta.[550] As documented in recent publications, which will be discussed in the following paragraphs, recent measurements, especially in China, have reignited research interest in multiphase S(IV) oxidation.

7.1.1.1. Role of Transition Metals: Relation to Mineral Dust. Recent hill-cap-cloud experiments have indicated that the transition metal-catalyzed oxidation of S(IV) by molecular oxygen in clouds might be much more important than previously thought.[9,551,552] The leaching of mineral dust to release transition metal ions should be considered in models, and the best available parametrizations for TMI-catalyzed reactions should be applied. Unfortunately, even with the tremendous work that has been performed to date, this is an area in atmospheric multiphase chemistry modeling where reaction-condition-dependent empirical rate laws, rather than condition-independent elementary reactions, must still be employed. Especially to improve our understanding of PM sulfate levels in China, further developments are urgently needed in this area. Transition metal-catalyzed S(IV) oxidation has been previously studied by Alexander et al.,[8] and this study clearly indicates the global importance of this process.

7.1.1.2. Criegee Radicals. Sawar et al.[553] have updated the carbon-bond mechanism to include gas-phase sulfur oxidation by stabilized Criegee radicals (sCI). A fairly recent account of implementations of cloud processing of gases and aerosols is given in Gong et al.[554]

7.1.1.3. Aqueous-Phase Studies. Recent specialized aqueous-phase studies in this area include investigations of the effect of light on the Fe-catalyzed reaction;[555] the influence of dicarboxylic acids;[556] and the inhibition of S(IV) oxidation by NH_3 and NH_4^+,[557] hydroxylated VOCs (i.e., alcohols[558]), and other organic inhibitors,[559] with this latter study referring to rainwater. Finally, the mechanism of aqueous S(IV) oxidation by ozone has been investigated.[560]

7.1.1.4. A Note on Organosulfates. Studies have shown that organosulfates comprise considerable fractions of particle sulfur and can contribute significantly to overall particulate organic mass (see the Hallquist et al.[38] review for an early overview of this topic, and a recent contribution by Schindelka et al.[45] and references therein). A summary of our current understanding of this compound class is presented in section 7.2.4.

7.1.2. Uptake of HO_2 by Clouds and Aqueous Aerosol Particles. The oxidizing capacity of the atmosphere is largely determined by the concentration of HO_x radicals (OH + HO_2), because OH reacts rapidly with trace species in cycles that result in the production of tropospheric ozone[561] and a continuous recycling from HO_2 to OH takes place. Results from both field[562,563] and modeling[205,564,565] studies have suggested that the heterogeneous uptake of HO_2 can have a substantial impact on gas-phase HO_x concentrations; the HO_2 concentration is directly diminished and OH is expected to follow because of a reduced HO_2-to-OH conversion. As a consequence, the atmospheric gas-phase oxidation capacity will decrease.

In the only large-scale modeling study that has specifically investigated the impact of HO_2 uptake upon atmospheric composition, Stavrakou et al. reported that the inclusion of efficient heterogeneous HO_2 loss in a global chemistry-transport model results in an increase of up to 50% in NO_2 columns in areas with high aerosol loadings.[566] In this section, the current state of knowledge regarding the mechanism and impacts of HO_2 uptake to aqueous aerosol will be discussed.

7.1.2.1. Laboratory Studies of HO_2 Uptake to Aqueous Aerosols. The first study of HO_2 uptake by aqueous surfaces was performed by Mozurkewich et al. in 1987, who found very little uptake to NH_4HSO_4 droplets in the absence of aqueous-phase catalysts.[567] A number of subsequent studies have provided support for these findings:[568−570] the most recent such study, by George et al.,[570] found uptake coefficients (γ) ranging from 0.003 to 0.016 for aqueous salt aerosols. In a set of laboratory experiments performed at atmospherically relevant HO_2 concentrations, by contrast, Taketani et al. observed significant uptake of HO_2 to both synthetic (γ = 0.07−0.19) and natural (γ = 0.1) salt-containing aqueous aerosol.[571,572] Although no conclusive reason for these discrepancies has yet been found, George and co-workers have recently provided evidence that HO_2 uptake decreases with increasing HO_2 concentration and gas−aerosol interaction time.[570] These results suggest that the low HO_2 concentrations and short reaction times employed in the Taketani experiments[571,572] may have contributed to the high observed uptake coefficients.

A comprehensive summary of HO_2 loss pathways in aqueous aerosol, including a parametrization of HO_2 uptake, has been provided by Thornton and co-workers.[573] The uptake of HO_2 by aqueous solutions is generally believed to result in the production of H_2O_2 via the following set of reactions:[569,573]

$$HO_{2(aq)} \rightleftharpoons H^+_{(aq)} + O_2^-{}_{(aq)} \quad \text{(R-6)}$$

$$HO_{2(aq)} + HO_{2(aq)} \rightarrow H_2O_{2(aq)} + O_{2(aq)} \quad \text{(R-7)}$$

$$HO_{2(aq)} + O_2^-{}_{(aq)} + H_2O_{(l)} \rightarrow H_2O_{2(aq)} + OH^-_{(aq)} + O_{2(aq)} \quad \text{(R-8)}$$

Uncertainties regarding this mechanism still exist, however: although it implies second-order HO_2 uptake kinetics, most studies have observed first-order kinetics for HO_2 uptake;[570,572] in addition, only one study has directly measured H_2O_2 production from HO_2 uptake, and this study was performed not on aqueous aerosol but rather on solid salt films.[574]

The uptake of HO_2 has long been known to be enhanced in the presence of aqueous-phase transition metal ions (TMI), including Cu, which catalyzes the conversion of HO_2 to H_2O_2 via the following set of reactions:[567,575,576]

$$HO_{2(aq)} + Cu^{2+}_{(aq)} \rightarrow H^+_{(aq)} + O_{2(aq)} + Cu^+_{(aq)} \quad \text{(R-9)}$$

$$HO_{2(aq)} + Cu^+_{(aq)} + H_2O_{(l)} \rightarrow H_2O_{2(aq)} + OH^-_{(aq)} + Cu^{2+}_{(aq)} \quad \text{(R-10)}$$

Note that copper cations abundant in the tropospheric aqueous phase will continuously switch their oxidation state between Cu(I) and Cu(II) while in each step destroying solution-phase HO_2. Experimental evidence for the importance of TMI-catalyzed HO_2 loss has recently been provided by Taketani and

DOI: 10.1021/cr500447k
Chem. Rev. 2015, 115, 4259−4334

co-workers, who found HO_2 uptake coefficients ranging from 0.09 to 0.4 for atomized aqueous extracts of ambient aerosol particles obtained at Chinese sites influenced by local and regional pollution.[577] While inclusion of TMI-catalyzed HO_2 loss in models has been shown to result in better predictions of ambient HO_2 levels, it has also been shown to lead to overpredictions of H_2O_2.[578−580] Recently, Mao et al.[581] have provided evidence for a coupled Cu−Fe catalytic cycle, which does not produce H_2O_2 but rather results in the net conversion of HO_2 to H_2O:

$$HO_{2(aq)} + Cu^{2+}{}_{(aq)} \rightarrow H^{+}{}_{(aq)} + O_{2(aq)} + Cu^{+}{}_{(aq)} \quad \text{(R-9)}$$

$$Cu^{+}{}_{(aq)} + Fe^{3+}{}_{(aq)} \rightarrow Cu^{2+}{}_{(aq)} + Fe^{2+}{}_{(aq)} \quad \text{(R-11)}$$

$$Fe^{2+}{}_{(aq)} + OH_{(aq)} \rightarrow Fe^{3+}{}_{(aq)} + OH^{-}{}_{(aq)} \quad \text{(R-12)}$$

According to the simplified set of reactions shown here, this mechanism yields no H_2O_2. However, $Fe^{2+}{}_{(aq)}$ would also be expected to react with HO_2 and H_2O_2, with the former leading to H_2O_2 and the latter leading to H_2O. As discussed by Mao et al., the yield of H_2O_2 via this catalytic pathway depends on aerosol pH and Cu/Fe ratio.[581]

7.1.2.2. HO_2 Uptake to Aqueous Aerosols: Measurements and Models. Evidence, both direct and indirect, of the importance of heterogeneous HO_2 chemistry has been provided by a large number of field and modeling studies. Direct observational evidence for heterogeneous loss of HO_x has been provided by aircraft studies:[562,582] in the most recent such study, Commane and co-workers measured significant (~20 ppt) reductions in HO_2 in the vicinity of liquid clouds.[563] The most comprehensive study to date of the impact of liquid clouds on HO_2 concentration was performed as part of the Hill Cap Cloud Thuringia experiment (HCCT-2010), in which HO_x concentrations at the summit of Mt. Schmücke, Germany, were found to be significantly (~90%) reduced in the presence of warm clouds.[583,584] This observational evidence is supported by a number of modeling studies.[205,564,585] Work by Tilgner et al., for example, has shown that gas-phase HO_2 concentrations are often reduced by more than an order of magnitude under simulated cloud conditions.[205] In modeling work conducted as part of the HCCT-2010 campaign, Whalley et al. showed that current multiphase models and associated chemical mechanisms of HO_2 uptake are able to reproduce the reduced gas-phase HO_2 concentrations observed in warm clouds during the campaign.[584] Global model simulations conducted as part of this study showed that the uptake of HO_2 by liquid cloud droplets has the potential to influence the overall oxidizing capacity of the troposphere, with the magnitude of influence displaying a strong dependence on the identity of the aqueous-phase reaction products (i.e., H_2O_2 vs H_2O).

The bulk of field evidence for heterogeneous HO_2 chemistry is indirect: standard gas-phase chemistry models often overestimate measured HO_2 concentrations, which suggests the existence of an additional, heterogeneous loss pathway.[579,586−588] Comprehensive overviews of field campaigns in which accurate predictions of HO_2 concentrations required inclusion of heterogeneous processes have been provided by Stone et al.[589] and Mao et al.[581]

The heterogeneous chemistry of HO_2 has been implemented into models using a number of strategies, with varying degrees of complexity. Kanaya and co-workers, for example, showed that inclusion of efficient heterogeneous HO_2 uptake ($\gamma = 1$) led to a halving of the disparity between observed and calculated HO_2 concentrations at a Japanese coastal site.[586] More recently, in their study of HO_x chemistry, Mao et al. incorporated values of $\gamma(HO_2)$ calculated from the HO_2 uptake parametrization of Thornton and co-workers,[573] and found that this approach resulted in a substantial reduction in the ~100% overprediction of HO_2 found in the absence of heterogeneous chemistry.[579] Finally, in their study of HO_x and peroxide concentrations in Beijing, Liang et al.[580] did not incorporate a single uptake coefficient for HO_2 but rather included the specific set of Cu−Fe-mediated HO_x-depleting reactions proposed by Mao et al.[581] In this case, inclusion of this catalytic mechanism led to better agreement between observed and measured H_2O_2 concentrations during haze days.

One area deserving of future research is the role that aqueous-phase organic species may play in influencing the uptake of HO_2. Although work by Taketani et al.[590] has shown that HO_2 exhibits significant uptake to aqueous dicarboxylic acid particles ($\gamma = 0.06−0.18$), the aqueous-phase production of HO_2 by atmospheric organics has not been considered. As noted by Tilgner et al., this in-situ production has the potential to result in reduced uptake of HO_x from the gas phase.[205] It might be speculated that HO_2 production might even fully compensate its uptake and, under certain circumstances, result in HO_2 transfer from particles into the gas phase.

7.1.3. Cloud- and Aqueous Aerosol-Mediated $ClNO_2$ Production. The heterogeneous hydrolysis of dinitrogen pentoxide (N_2O_5) results in the conversion of reactive nitrogen (NO_x) to particulate nitrate, which can subsequently undergo wet deposition, and thus represents a significant nighttime NO_x loss pathway.[591] In the presence of aqueous-phase chloride, however, N_2O_5 uptake also leads to the production of gas-phase $ClNO_2$ via a nitronium ion intermediate (see R-13−R-18 in the mechanism presented below).[592−595] This latter pathway is of interest for two main reasons: first, it has the potential to reduce the rate of nocturnal NO_x removal; in addition, because $ClNO_2$ photolyzes efficiently to yield NO_2 and Cl, the latter of which is a strong atmospheric oxidant, it also has the potential to change the local atmospheric oxidative capacity. Until recently, however, an assessment of the atmospheric importance of this reactive pathway was hampered by a lack of $ClNO_2$ field measurements.

The first ambient observations of $ClNO_2$ were reported in 2008 by Osthoff et al., who measured concentrations that occasionally exceeded 1 ppb in the vicinity of Houston, TX.[596] Since this time, a large number of laboratory and field studies have explored the factors influencing $ClNO_2$ production; further field and modeling studies have aimed to gain a better understanding of the atmospheric consequences of its production. The following paragraphs aim to summarize the current state of knowledge in this area.

7.1.3.1. Laboratory Studies of Aqueous-Phase $ClNO_2$ Production. The chemistry of N_2O_5 in chloride-containing solutions is believed to proceed via the following set of reactions:[595,597]

$$N_2O_{5(g)} \rightleftharpoons N_2O_{5(aq)} \quad \text{(R-13)}$$

$$N_2O_{5(aq)} \rightleftharpoons NO_2^{+}{}_{(aq)} + NO_3^{-}{}_{(aq)} \quad \text{(R-14)}$$

$$NO_2^{+}{}_{(aq)} + H_2O \rightleftharpoons 2H^{+}{}_{(aq)} + NO_3^{-}{}_{(aq)} \quad \text{(R-15)}$$

DOI: 10.1021/cr500447k
Chem. Rev. 2015, 115, 4259−4334

$$NO_2^+{}_{(aq)} + Cl^- \rightleftharpoons ClNO_{2(aq)} \quad \text{(R-16)}$$

$$ClNO_{2(aq)} \rightleftharpoons ClNO_{2(g)} \quad \text{(R-17)}$$

$$ClNO_{2(g)} + h\nu \rightarrow Cl + NO_2 \quad \text{(R-18)}$$

In this mechanism, aqueous-phase N_2O_5 undergoes reversible hydrolysis to yield the nitronium ion (NO_2^+), which can subsequently react with either water or chloride. The yield of $ClNO_2$ production from N_2O_5 uptake thus depends on the relative importance of these two pathways, which in turn depends on the chloride concentration.[595,597,598] Work by Roberts et al., for example, found $ClNO_2$ yields ranging from 0.2 to 0.8 for aqueous-phase chloride concentrations ranging from 0.02 to 0.5 M.[598] Interestingly, these authors also observed production of gas-phase Cl_2 from uptake of N_2O_5 to acidic (pH < 2) NaCl solutions.[598,599] However, field evidence for this pathway is limited at present.[600,601]

As noted by Riedel et al.,[602] the absolute quantity of $ClNO_2$ formed via this mechanism depends not only upon this branching ratio but also upon the aerosol surface area, the concentration of N_2O_5, and the uptake coefficient of N_2O_5. While a discussion of these parameters is beyond the scope of this Review, we briefly note here that the N_2O_5 uptake coefficient has been shown to depend upon both the bulk[597] and the surficial[603,604] composition of aqueous aerosol.

The nitronium ion is strongly electrophilic and thus would be expected to react with other aqueous-phase nucleophiles. Schweitzer and co-workers, for example, have shown that the uptake of N_2O_5 by aqueous NaBr solutions leads to the production of $BrNO_2$, Br_2, and HONO, while its uptake by aqueous NaI solutions leads to the production of I_2.[605] In addition, Heal et al. have shown that exposure of aqueous phenol solutions to gas-phase $ClNO_2$ results in the formation of 2-nitrophenol, 4-nitrophenol, and 4-nitrosophenol.[606]

7.1.3.2. Field Observations of $ClNO_2$. Since its first detection by Osthoff et al. in Houston, TX, $ClNO_2$ has been observed in a wide variety of environments, with average mixing ratios of one to several hundred ppt.[596,600−602,607−614] Studies performed in continental environments (i.e., those not influenced directly by sea-salt chloride) have shown that the production of $ClNO_2$ does not require the presence of high levels of particulate chloride: in Boulder, CO, for example, Thornton et al. measured $ClNO_2$ mixing ratios of 100−450 ppt, which were well in excess of those expected given measured particulate chloride levels.[607] These authors suggested that this apparent contradiction could be resolved by the replenishment of aerosol chloride via the condensation of gas-phase HCl; this pathway has been subsequently modeled by Simon and co-workers.[615] In a study performed as part of the Nitrogen, Aerosol Composition, and Halogens on a Tall Tower (NACHTT) campaign, Young and co-workers used simultaneous measurements of HCl and particulate chloride to show that HCl condensation was sufficient to prevent chloride depletion induced via $ClNO_2$ production, and by extension that $ClNO_2$ production was not limited by Cl availability.[612]

While $ClNO_2$ concentrations have generally been observed to be well-correlated with N_2O_5, the ratio of these two species (i.e., a proxy for the $ClNO_2$ yield) often changes substantially with changes in particulate chloride, water content, and organic content.[607,608,611] A number of methods exist for deriving $ClNO_2$ yields from field measurements.[600,602,607] For example, Riedel and co-workers used the ratio of measured changes in $ClNO_2$ and total nitrate to derive an average $ClNO_2$ yield of 0.05 ± 0.15 for the duration of the NACHTT study.[602] In another study, Riedel et al. used an entrained aerosol flow reactor to directly investigate the conversion of N_2O_5 to $ClNO_2$ on ambient particles.[616] In these experiments, these authors used simultaneous measurements of N_2O_5 loss and $ClNO_2$ production to calculate a $ClNO_2$ yield of ∼10%.

Two studies have investigated the nocturnal vertical distribution of $ClNO_2$, with differing results: while Riedel et al.[602] observed elevated mixing ratios of $ClNO_2$ near ground level, Young et al.[610] observed no trend in $ClNO_2$ mixing ratio with height. In the former case, the authors suggested that ground-level $ClNO_2$ arose from N_2O_5 uptake to the surface and/or water-rich near-surface aerosols; in the latter case, the authors speculated that the lack of surface $ClNO_2$ enhancement might have arisen from suppression of N_2O_5 production via competitive reaction of NO_3 with reactive VOCs and/or NO near the surface.

Very recently, Kim et al. have used measurements of the vertical flux of both N_2O_5 and $ClNO_2$ above the ocean surface to show that $ClNO_2$ undergoes net deposition to the ocean surface. These authors attributed this surprising observation to reduced $ClNO_2$ production via competitive reactions of the nitronium ion in the organic-rich surface microlayer and/or to aqueous-phase loss of produced $ClNO_2$.[613]

7.1.3.3. Consequences of $ClNO_2$ Production: Results from Laboratory and Modeling Studies. The production and subsequent photolysis of $ClNO_2$ has the potential to influence tropospheric ozone both directly via NO_2 production and indirectly via Cl-induced oxidation of VOCs. For this reason, a number of modeling studies have investigated the impact of $ClNO_2$ production upon air quality.[617−620] In some cases, these studies predict substantial $ClNO_2$-mediated enhancements in O_3 concentration (7−12 ppb).[619,620] By contrast, in a model study of $ClNO_2$-mediated O_3 formation in Houston, Simon and co-workers predicted large enhancements in reactive chlorine but only modest enhancements in O_3 concentration.[617] These authors attributed this seeming discrepancy to the specific VOC mixture in the Houston area, which they showed using an incremental reactivity-based technique to be particularly insensitive to addition of chlorine. Perhaps unsurprisingly, modeling studies have also suggested that heterogeneous $ClNO_2$ formation results in substantial (∼10−25%) reductions in particle-phase nitrate.[618,620]

Very recent modeling work by Riedel and co-workers has suggested that Cl-mediated VOC oxidation in the presence of elevated levels of $ClNO_2$ should lead to the production of detectable quantities of chlorinated VOCs, including chloroacetaldehyde and formyl chloride.[619] Indeed, the chlorinated products of Cl addition to unsaturated VOCs have previously been used as tracers of Cl-mediated oxidation: studies by Riemer et al.[621] and Tanaka et al.,[622] for example, have used the chlorinated carbonyls chloromethylbutenal and chloromethylbutenone as tracers of isoprene−chlorine chemistry. The formation of chlorinated organics is not the only potential result of interactions between VOCs and Cl atoms: several laboratory studies have shown that exposure of both biogenic[623,624] and anthropogenic[625] VOCs to Cl can also lead to new particle formation.

7.2. Organic Systems

7.2.1. Glyoxal-Related Systems. Glyoxal, the simplest α-dicarbonyl, has been studied extensively in recent years due to

DOI: 10.1021/cr500447k
Chem. Rev. 2015, 115, 4259−4334

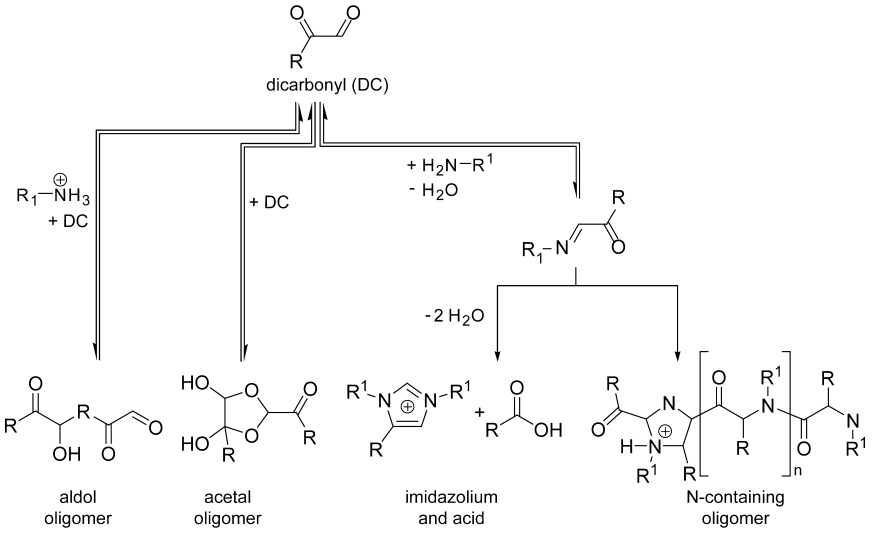

Figure 12. Nonoxidative accretion reactions of α-dicarbonyl compounds modified after Sedehi et al.[492]

the fact that it is an ubiquitous organic compound formed from a wide variety of VOC oxidation processes (e.g., tropospheric isoprene oxidation),[626] emitted from primary sources,[627,628] and, possibly, formed by ocean surface layer chemistry,[629,630] and shows a very high water solubility.[159] Since Aumont et al.[631] and Blando and Turpin[632] very early suggested glyoxal and related compounds as possible aqueous-phase SOA precursors, many studies of glyoxal processing have been performed, and glyoxal has been used as a model compound to understand the formation of SOA.

Glyoxal can undergo both radical and nonradical reactions in the tropospheric aqueous phase. In the dilute aqueous phase of cloud/fog/rain, glyoxal uptake leads to the production of glyoxylic acid and, finally, oxalic acid formation by OH radical reactions.[12,633] In the presence of hydrogen peroxide or ozone, glyoxal can undergo dark oxidation to glyoxylic acid (see section 6.1).[115] Lim et al.[31] investigated the photochemically induced oxidation of glyoxal by OH radicals in the bulk phase, and provided an overview of its nonradical aqueous-phase chemistry. As summarized in modeling studies by Lim et al.,[31] Ervens and Volkamer,[1] and Ervens et al.,[2] many experiments have demonstrated that the self-oligomerization of both glyoxal and methylglyoxal can occur at elevated solution-phase concentrations. The mentioned authors provided overviews of the current knowledge regarding aqueous organic reactions that form SOA in deliquescent aerosol particles, with special emphasis paid to glyoxal and methylglyoxal. Tan et al.[68] investigated oligomer and SOA formation from the photo-oxidation of methylglyoxal and acetic acid in a bulk-phase experiment. Kirkland et al.[64] studied glyoxal oxidation in the presence of nitrate and ammonium, demonstrating in a bulk-phase experiment that for dilute systems (cloud or fog) the concentrations of inorganic nitrogen species have only a minor effect on the glyoxal oxidation by OH radicals. These authors found no evidence for the formation of organic nitrate species from the reaction of glyoxal with NO_3 radicals, because the required C═C double bond, which can be provided by the enol form of glyoxal, is rather unlikely to be formed because of the hydration of glyoxal. It should be mentioned here that the assumed rate constant for the nitrate radical reaction of $k = 1 \times 10^4$ M^{-1} s^{-1} is 2 orders of magnitude lower than available literature values.[32,110,400] Furthermore, no evidence of the imidazole formation reported by Galloway et al.[542] was found. Lim et al.[65] provide an oxidation mechanism for the photochemically induced OH radical reactions of glyoxal, methylglyoxal, and acetic acid in the aqueous bulk phase, including peroxyl radical chemistry, to provide SOA yields. However, in this study, an oxygen addition rate constant of the peroxyl radical formation $k(R + O_2) \approx 10^6$ M^{-1} s^{-1} was used, based on a photochemistry study of pyruvic acid by Guzman et al.[22] (see section 4.3). This value is 3 orders of magnitude lower than the one determined earlier by Buxton et al.[634] and just recently reinvestigated by Schaefer et al.[110] Reaction rates of $k(R + O_2) \approx 10^9$ M^{-1} s^{-1} have been observed for numerous compounds similar to glyoxal.[635,636] Only for aromatic radicals and noncarbon centered radicals, such as nitrogen centered radicals, have somewhat smaller rate constants been observed, with $k(R + O_2) \approx 5 \times 10^6$ to 5×10^8 M^{-1} s^{-1};[636,637] see also section 4.3 of this Review.

Interestingly, glyoxal and methylglyoxal oligomerization in the presence of amines or ammonium can proceed via many of the different pathways discussed in section 6.2: (i) aldol and (ii) acetal oligomers can be formed by the self-condensation of glyoxal, (iii) imidazole and an acid can be formed, and, finally, N-containing oligomers can be formed (see Figure 12).

Temperature- and pH-dependent rate constants for the reaction of glyoxal and methylglyoxal with ammonium sulfate and amines have been measured by Sedehi et al.[492] (see section 7.2.4). Rate constants for a number of these processes have now been provided, and a comparison of the efficiencies of these nonradical condensation pathways to OH oxidation pathways shows that the latter radical pathway prevails under acidic and daytime conditions.

Hawkins et al.[508] studied the hygroscopic growth of particles containing oligomer species formed from the reaction of small amines with different precursor compounds, including glyoxal, methylglyoxal, glycolaldehyde, and hydroxyacetone. Particles that contained oligomers from glyoxal or glycine as precursor were the most hygroscopic, with a hygroscopic growth between 1.16 and 1.2 at 80% RH. This study also provided evidence that the hygroscopic growth of aldehyde−methylamine aqSOA is dependent on the humidification time: after <1 h drying under ambient conditions, the aerosol particles were still liquid, but after 20 h drying, the particles were semisolid. The presence of

DOI: 10.1021/cr500447k
Chem. Rev. 2015, 115, 4259−4334

ammonium, therefore, can not only promote nonradical reactions but also change the volatility behavior of aqueous solutions. Ortiz-Montalvo et al.[638] showed that ammonium addition, coupled with a change in pH from acidic to neutral conditions, decreases the effective vapor pressure of a glyoxal reaction mixture subject to OH oxidation under cloud-relevant conditions. These authors conclude that such an evaporation step will enhance the yield of SOA formation during cloud processing, when residual aerosol particles are formed. Other glyoxal-related studies have been addressed in the preceding subsections of section 6.

7.2.2. Multiphase Isoprene Oxidation. Biogenic volatile organic compounds (BVOCs) are emitted to the atmosphere in large quantities. Isoprene alone contributes approximately 40% of BVOC emissions, with an estimated source strength of 500 ± 100 Tg C a^{-1}.[639] In the group of nonmethane hydrocarbons (NMHC), isoprene is the largest single source of atmospheric organic carbon.[640] Because of this isoprene source strength, isoprene oxidation products are thought to have a significant impact on both regional ozone,[641,642] and secondary organic aerosol (SOA) formation.[43,536,643−650]

The reaction of isoprene with ozone and the resultant SOA formation via the partitioning of low-molecular-weight compounds into the particle phase was investigated by Nguyen et al.,[651] in comparison to the SOA formation from the photooxidation of isoprene by Liu et al.[652] These authors stated that SOA produced from this reaction is a mixture of highly oxygenated organic compounds of low molecular weight and oligomers, only a few of which have been identified (e.g., pyruvic acid, glycolic acid, and methylglyoxal). Liu et al.[652] studied the aqueous-phase processing of SOA particles and reported an increase of small organic acids during the aging process. Isoprene itself will react exclusively in the gas phase by OH or NO_3 radical addition[626,653,654] and by the reaction of ozone[655] because of its small Henry's law constant (H = 0.029 M atm^{-1}).[656] The kinetics and mechanism of the aqueous-phase isoprene oxidation by ozone and OH radicals have been the subject of a number of studies.[362,657,658] However, given its low water solubility, the direct oxidation of isoprene in the bulk aqueous phase is probably a process of minor relevance, while its interfacial heterogeneous oxidation might warrant further study. Gäb et al.[657] reported the formation of H_2O_2 (~0.1% yield), hydroxymethanehydroperoxide (HMHP) (11.1 ± 0.9%), and organoperoxides (13.1 ± 0.8%) from ozone-driven isoprene oxidation in the aqueous phase. Wang et al.[658] studied the oxidation of isoprene by ozone in a mixture of water and acetonitrile at different pH's (3−7) and temperatures (277−298 K). The reported molar yields of the products were independent of the investigated pH's and temperatures. The molar yields based on the isoprene consumption have been given, with 42.8 ± 2.5% for MACR, 57.7 ± 3.4% for MVK, 15.1 ± 3.1% for HMHP, 56.7 ± 3.7% for HCHO, 53.4 ± 4.1% for H_2O_2, and a total carbon yield of 94.8 ± 4.1%. Huang et al.[362] determined the OH radical rate constants of isoprene in a mixture of water and acetonitrile and its first oxidation products methacrolein (MACR) and methyl vinyl ketone (MVK) in aqueous solution, and found the typical order of magnitude 10^{10} M^{-1} s^{-1} for unsaturated compounds (see section 5.2). Furthermore, these authors analyzed the product distribution, including carbonyl compounds and organic acids under in-cloud conditions. The molar yields based on the isoprene consumption have been given, with 10.9 ± 1.1% for MACR, 24.1 ± 0.8% for MVK, 11.4 ± 0.3% for methylglyoxal, and 3.8 ± 0.1% for glyoxal. After isoprene was consumed completely, the observed yield for oxalic acid was found to be 26.2 ± 0.8%. The reported carbon balance accounted for ~50% of the consumed isoprene. These authors suggested that high-molecular-weight compounds may have contributed significantly to the missing carbon. Kameel et al.[114] investigated the heterogeneous reaction of isoprene in the gas phase toward OH radicals in the aqueous phase. These authors reported the formation of $C_{10}H_{15}OH$ species as the primary product by radical polymerization. A minimum of seven isomers have been found, but no oxidized compounds like MACR, MVK, or tetrols. Because the Henry's law constants of the first-generation oxidation products of isoprene, that is, MACR and MVK, are quite small (H_{MACR} = 6.5 M atm^{-1} at T = 298 K, H_{MVK} = 41 M atm^{-1} at T = 298 K[659]), it has been suggested that these compounds are too volatile to be taken up and undergo reaction in the tropospheric aqueous phase.[633] However, a recent field study reports much higher aqueous-phase concentrations than would be expected from the Henry's law constants for some carbonyl compounds, including MACR and MVK.[660] Therefore, MACR and MVK may also appear from reactive uptake or other sources in enhanced concentrations in the aqueous phase; this important point, however, needs more systematic investigation.

For the oxidation reaction of methacrolein by ozone[115,360,434,661] (section 6.1), H_2O_2[115] (section 6.1), NO_3 radical,[363,662] and OH radicals[47,362,363,663] (section 5.2), several kinetic data sets are now available. The photooxidation of methacrolein in aqueous solution has been studied by Liu et al.,[47] Zhang et al.,[364] and Schöne et al.[363]

It has been proposed by Liu et al.[47] that the OH radical reaction of methacrolein primarily leads to low-molecular-weight compounds such as methylglyoxal, hydroxyacetone, formaldehyde, acetic acid, 2,3-dihydroxy-2-methylpropanal, 2-hydroxy-2-methylmalonaldehyde, and peroxymethacrylic acid. A similar product distribution was found by Schöne et al.,[363] with the exception of the C_4 polyfunctional compound 2-hydroxy-2-methylmalonaldehyde. Zhang et al.[364] observed carbonyl compounds and organic acids. The yields of methylglyoxal were given as 9.9 ± 2%,[363] 6−9.1%,[47] and 7.5%,[364] for hydroxyacetone 16.2 ± 0.8%[363] and 9.8−15%,[47] and for glycolaldehyde 5.1 ± 0.4%.[363] In addition, oligomer and SOA formation from methacrolein oxidation and its properties have been studied.[46,48,364,664] El Haddad et al.[46] and Liu et al.[664] estimated a contribution to the SOA yield of 2−12%.

The oxidation of methyl vinyl ketone (MVK) has been investigated by a number of authors.[87,363,364,664,665] In contrast to methacrolein, only a few kinetic data for the reactions of methyl vinyl ketone with ozone,[115,360] H_2O_2,[115] OH radicals,[87,362,363] and the radicals NO_3 and SO_4^-[363,662] are available. The aldol condensation of MVK in sulfuric acid was investigated by Nozière et al.[482](see section 6.2.1). The photooxidation leads, as was the case for methacrolein oxidation, primarily to low-molecular-weight compounds but also to high-molecular-weight compounds.[364] Product yields of low-molecular-weight compounds have been reported for methylglyoxal as 5.2 ± 1%,[363] 4.5%,[364] and for glycolaldehyde as 11.1 ± 0.4%.[47] Liu et al.[664] studied the contribution of the high-molecular-weight compounds and the SOA formation potential, which was estimated to have a yield of 4−10%. The OH radical-induced radical oligomerization of MVK and the influence of dissolved molecular oxygen were studied by Renard et al.[87] These authors estimated the ratios of

DOI: 10.1021/cr500447k
Chem. Rev. 2015, 115, 4259−4334

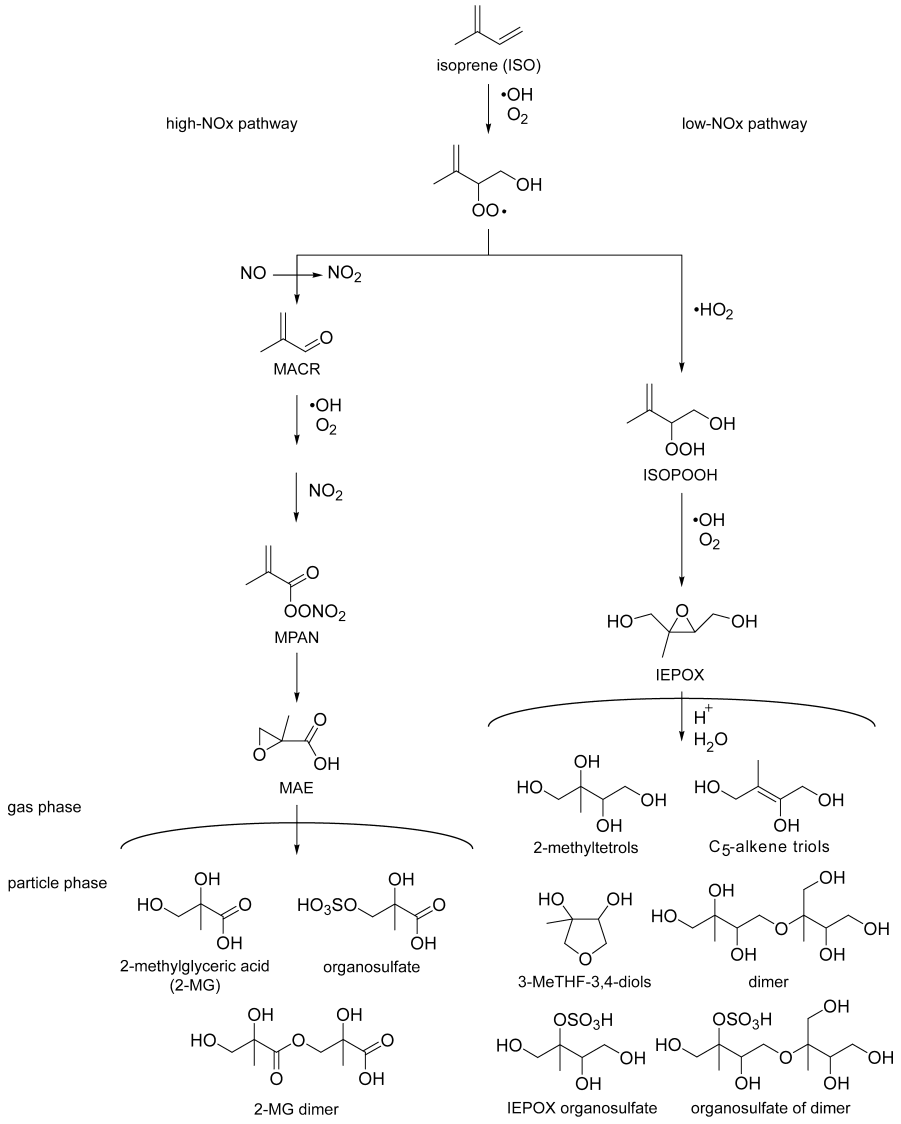

Figure 13. Epoxide formation pathways from isoprene adapted from Lin et al.[681]

unsaturated dissolved organic carbon concentration to oxygen concentration in atmospheric waters (rain, cloud, fog, and wet aerosols) and proposed that the radical-induced oligomerization would occur mainly in wet aerosols and partly in fog, with a value of the above ratio of ∼160. The occurrence of this reaction pathway would decrease the atmospheric lifetime of MVK by 13−79% when it is assumed that 10 times more soluble unsaturated compounds will be present in ALW according to Renard et al.[87] In a recent publication, Renard et al. reported the aging of MVK oligomers formed by aqueous-phase photooxidation and formation of secondary aerosol (SOA) upon water evaporation.[665]

7.2.3. Uptake and Aqueous-Phase Reactions of Biogenic Epoxides. In 2009, Paulot and co-workers showed that the OH-mediated oxidation of hydroxyhydroperoxides (ISOPOOH) produced during the low-NO_x oxidation of isoprene results in the efficient (>75% yield) production of dihydroxyepoxides (IEPOX).[666] These species, in turn, partition effectively to the aerosol aqueous phase, where they can undergo ring-opening reactions with water, inorganic sulfate, or previously produced ring-opening products to yield 2-methyl tetrols, sulfate esters, dimers, C_5-alkene triols, and 3-methyltetrahydrofuran-3,4-diols, and thus participate in SOA formation.[667,668] This series of reactions is depicted in Figure 13.

More recently, Lin et al. provided evidence that a gas-phase epoxide is also involved in the formation of SOA from the photooxidation of isoprene under high-NO_x conditions.[669] As shown in Figure 13, these authors suggest that SOA formation from isoprene under these conditions occurs via the acid-catalyzed uptake of methacrylic acid epoxide (MAE), which is itself formed from the rearrangement of the transient product formed from OH addition to methylacryloylperoxynitrate (MPAN), a previously recognized intermediate in isoprene oxidation in the presence of NO_x.[667]

The epoxide-mediated pathways described above contribute significantly to SOA mass: Froyd et al., for example, have shown that the IEPOX sulfate ester alone contributes ∼0.4% to tropospheric aerosol mass in the remote tropics and up to 20% in regions with substantial isoprene emissions.[670] In the following paragraphs, the current state of knowledge regarding atmospheric aqueous-phase epoxide chemistry will be discussed.

DOI: 10.1021/cr500447k
Chem. Rev. 2015, 115, 4259−4334

Table 16. Summary of Available Kinetic Parameters for Acid-Catalyzed Ring-Opening Reactions of Epoxides

epoxide	rate constant/uptake coefficient	remarks	refs
1,2-epoxybutane	0.074 M^{-1} s^{-1}	reaction kinetics followed using NMR spectroscopy in deuterated solution (D_2O/D_2SO_4)	406
trans-2,3-epoxybutane	0.20 M^{-1} s^{-1}		
2-methyl-1,2-epoxypropane	8.7 M^{-1} s^{-1}		
2-methyl-2,3-epoxybutane	9.0 M^{-1} s^{-1}		
2,3-dimethyl-2,3-epoxybutane	15 M^{-1} s^{-1}		
1,2-epoxyisoprene	56 000 M^{-1} s^{-1}	reaction kinetics followed using NMR spectroscopy in deuterated solution (D_2O/D_2SO_4)	671
3,4-epoxyisoprene	5.6 M^{-1} s^{-1}		
3,4-epoxy-1-butene	3.1 M^{-1} s^{-1}		
1,2−3,4-diepoxybutane	0.0013 M^{-1} s^{-1}		
1,2-epoxy-3,4-dihydroxybutane	0.0012 M^{-1} s^{-1}		
3-methyl-3,4-epoxy-1,2-butanediol	0.0079 M^{-1} s^{-1}	reaction kinetics followed using NMR spectroscopy in deuterated solution (D_2O/D_2SO_4)	672
2-methyl-2,3-epoxy-1,4-butanediol	0.036 M^{-1} s^{-1}		
2-methyl-1,2,3,4-diepoxybutane	0.035 M^{-1} s^{-1} (for the 1,2 epoxide ring)		
2-methyl-3,4-epoxy-1,2-butanediol	0.0015 M^{-1} s^{-1}		
2,3-epoxy-1,4-butanediol	0.0014 M^{-1} s^{-1}		
3-methyl-2,3-epoxy-1-butanol	0.48 M^{-1} s^{-1}		
3-methyl-3,4-epoxy-1-butanol	0.37 M^{-1} s^{-1}		
3,4-epoxy-1-butanol	0.015 M^{-1} s^{-1}		
3,4-epoxy-2-butanol	0.0043 M^{-1} s^{-1}		
cis-2,3-epoxybutane-1,4-diol	$(1.3 \pm 0.1) \times 10^{-3}$ M^{-1} s^{-1}	reaction kinetics followed using NMR spectroscopy with water suppression in 10% D_2O/90% H_2O	673
3,4-epoxybutane-1,2-diol	$(2.2 \pm 0.2) \times 10^{-3}$ M^{-1} s^{-1}		
3-methyl-2,3-epoxybutan-1-ol	0.3 ± 0.05 M^{-1} s^{-1}		
3-methyl-3,4-epoxybutan-1-ol	0.2 ± 0.05 M^{-1} s^{-1}		
isoprene epoxide	$\gamma = (1.7 \pm 0.1) \times 10^{-2}$	uptake coefficients determined on 90 wt % H_2SO_4 in a low-pressure laminar flow reactor	674
α-pinene oxide	$\gamma = (4.6 \pm 0.3) \times 10^{-2}$		
isoprene epoxide	$\gamma = (0.189 \pm 0.006) \times 10^{-4}$ (pH = 3)	uptake coefficients determined as a function of H_2SO_4 concentration in a rotating wetted-wall flow reactor; production of gas-phase 2-methyl-3-butanal was observed upon uptake of 1,2-epoxyisoprene	191
	$\gamma = (2.78 \pm 0.08) \times 10^{-4}$ (1 wt %)		
	$\gamma = (26.7 \pm 1.1) \times 10^{-4}$ (20 wt %)		
butadiene epoxide	$\gamma = (0.224 \pm 0.019) \times 10^{-4}$ (1 wt %)		
	$\gamma = (7.96 \pm 0.03) \times 10^{-4}$ (20 wt %)		
butadiene diepoxide	$\gamma = (1.12 \pm 0.09) \times 10^{-4}$ (pH = 3)		
	$\gamma = (1.70 \pm 0.03) \times 10^{-4}$ (1 wt %)		
	$\gamma = (24.1 \pm 1.2) \times 10^{-4}$ (20 wt %)		
limonene oxide	$\gamma = (7.10 \pm 0.02) \times 10^{-5}$ (30 wt %)	uptake coefficients determined as a function of H_2SO_4 concentration in a rotating wetted-wall flow reactor	675
α-pinene oxide	$\tau < 5$ min in neutral D_2O	formation kinetics of α-pinene oxide products presented; product distribution determined as a function of solution acidity	676

7.2.3.1. Reactions of IEPOX and Other Biogenic Epoxides in the Tropospheric Aqueous Phase: Kinetics and Products. A number of studies have investigated the kinetics of the acid-catalyzed ring-opening reaction of epoxides in an atmospheric context.[191,406,671−676] The kinetic parameters obtained in these studies are summarized in Table 16. As shown in this table, the hydrolysis of IEPOX-type epoxides (i.e., those containing neighboring hydroxyl groups) occurs significantly more slowly than that of the analogous unsubstituted epoxides. The effect of neighboring hydroxyl groups on epoxide ring-opening rate constants has been parametrized by Cole-Filipiak and co-workers.[672]

The acid-catalyzed ring-opening reactions of epoxides largely proceed via nucleophilic attack by water on the epoxide ring, which ultimately yields diol functionalities. However, as shown in Figure 14, the participation of other solution-phase nucleophiles, including inorganic sulfate, is also possible. The first laboratory evidence for organosulfate production via sulfate-mediated ring-opening reactions of epoxides was provided by Minerath and Elrod[406] in a study performed prior to the identification of the IEPOX pathway: these authors found that reaction of a set of epoxybutanes in deuterated sulfuric acid solution led to the production of a variety of

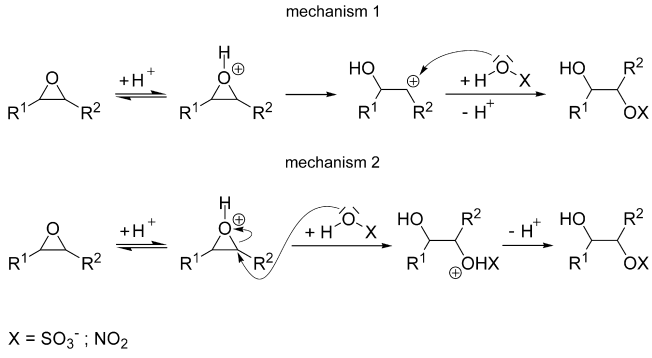

Figure 14. Organosulfate and organonitrate formation mechanisms produced after Eddingsaas et al.[673]

organosulfate products in moderate yields (7−14%). These authors also observed the formation of organosulfates from a set of isoprene-derived epoxides.[671] Additional laboratory studies of organosulfate formation have been performed by Lal et al.[674] and Eddingsaas et al.[673] A compilation of organosulfate yields from epoxide ring-opening reactions is

DOI: 10.1021/cr500447k
Chem. Rev. 2015, 115, 4259−4334

provided in Table 17, and a more in-depth discussion of organosulfates is presented in section 7.2.4.

Although nitrate might also be expected to participate in ring-opening reactions of epoxides, the expected organonitrate products of this reaction have been less commonly detected in ambient particles than their organosulfate analogues. An explanation for this observation has been provided by Darer et al.[677] and Hu et al.,[678] who showed that tertiary organonitrates are highly susceptible to hydrolysis and to nucleophilic attack by sulfate, with the former pathway leading to the formation of polyols and the latter pathway leading to the formation, again, of organosulfates.

7.2.3.2. Influence of Particle-Phase Acidity on IEPOX-Mediated SOA Production. Results obtained in chamber studies have largely suggested that the reactive uptake of IEPOX and the production of condensed-phase ring-opening products (e.g., the 2-methyl tetrols) are both enhanced in the presence of acidic seed aerosol.[667,668] By contrast, field evidence for the influence of particle-phase acidity on IEPOX-mediated SOA formation (and on SOA formation in general) is mixed.[670,679−681] For example, Lin et al. found that while the contribution of particle-phase IEPOX products to total organic matter was enhanced in the presence of elevated SO_2, the correlation between the mass of these products and calculated aerosol acidity was weak.[681] In addition, in their recent study of SOA composition in downtown Atlanta, Budisulistiorini and co-workers found that IEPOX-derived SOA (i.e., the IEPOX-OA factor extracted from the SOA organic mass spectra) was weakly correlated (r^2 = 0.3) with aerosol acidity; it should be noted, however, that elevated values for this factor were often observed even under low-acidity conditions.[680]

Insight into the source of this discrepancy has been recently provided by Nguyen et al., who investigated the uptake of IEPOX to neutral ammonium sulfate aerosols under dry and humid conditions.[682] Under dry conditions, these authors observed no IEPOX uptake. This result is in agreement with the previous chamber studies described above, both of which were performed under dry conditions.[667,668] Under humid conditions, by contrast, these authors observed not only substantial organic growth but also production of the IEPOX sulfate ester. Interestingly, Nguyen et al. did not observe IEPOX uptake to Na_2SO_4 aerosols, even under humid conditions, which implies that ammonium-catalyzed ring opening may have played a role in the observed chemistry.[682] In summary, these experiments provide evidence that IEPOX-mediated SOA formation can proceed efficiently in neutral aerosol, and suggest a need for further study of aqueous epoxide chemistry.

7.2.3.3. Competitive Gas-Phase Reactive Loss of IEPOX. Recent work by Jacobs et al.[683] has suggested that OH-mediated oxidation of IEPOX has the potential to compete with aqueous-phase uptake: using a relative rate technique, these authors determined an OH rate constant of $k = (3.60 \pm 0.76) \times 10^{-11}$ cm^3 molecule^{-1} s^{-1} for *trans*-β-IEPOX, which corresponds to a gas-phase lifetime of ∼8 h at an OH concentration of 1×10^6 molecules cm^{-3}. In a more recent study, by contrast, Bates et al.[684] reported an OH rate constant of only $k = (0.98 \pm 0.05) \times 10^{-11}$ cm^3 molecule^{-1} s^{-1}. Despite this disagreement, these studies both imply that IEPOX also has the potential to contribute to isoprene-derived SOA indirectly via its OH-mediated gas-phase production of glyoxal, methylglyoxal, and other SOA precursors.[683,684]

7.2.3.4. The Impact of IEPOX-Mediated SOA Production: Measurements and Model Results. IEPOX and its aqueous-phase reaction products have been observed in a large number of field campaigns.[680,681,685−687] In some cases, these species are collectively a dominant component of tropospheric aerosol: IEPOX-derived SOA has been shown to represent 33 ± 10% of the total organic aerosol mass fraction in summertime Atlanta[680] and 12−19% of total organic matter in $PM_{2.5}$ samples obtained in rural Georgia.[681]

Several modeling studies have attempted to quantify the relative contribution of IEPOX-mediated SOA formation pathways.[548,688,689] Under some modeling conditions, the global SOA burden from IEPOX has been shown to exceed those from the gas-to-particle partitioning of semivolatile organics, the aerosol-phase production of oligomers, and the uptake of soluble dicarbonyls (glyoxal and methylglyoxal).[688] Similarly, work by McNeill et al. has suggested that IEPOX pathways can contribute as much as 70−100% of aqueous SOA formation under low-NO_x conditions.[548]

In a recent study, Pye et al. included the formation of condensed-phase IEPOX products (2-methyltetrols and IEPOX-derived organosulfates/organonitrates) in the Community Multiscale Air Quality (CMAQ) model.[690] Using this modified model, these authors were able to accurately reproduce the measured concentrations of these species in a variety of urban and rural locations. However, very recent work by Karambelas and co-workers has shown that this model in its current state significantly underestimates IEPOX-derived SOA mass as compared to ambient measurements.[691] These authors suggest that this discrepancy may arise from contributions from IEPOX-derived products not considered in the model and/or from model underestimation of the IEPOX uptake coefficient.

7.2.3.5. Reactions of Other Epoxides. The O_3- and OH-mediated oxidation of α-pinene has been shown to result in the formation of the epoxide α-pinene oxide as a minor product.[692,693] In a chamber study, Iinuma and co-workers showed that introduction of this epoxide to a chamber containing acidic seed aerosol led to a substantial increase in particle volume and to the formation of condensed-phase organosulfate species.[694]

Work by Lal and colleagues provided evidence that the acid-catalyzed reaction of α-pinene oxide in aqueous solution results in products similar to those observed for IEPOX (i.e., diols and sulfate esters).[674] However, in a more recent bulk-phase study, Bleier and Elrod[676] found that the ring-opening reaction of this epoxide in aqueous solution did not result in the formation of the organosulfates observed in the chamber experiments of Iinuma et al.[694] Instead, these authors observed a complex range of products, some of which would be expected to partition back into the gas phase.[676] One such product, campholenic aldehyde, has been implicated in the production of further SOA via its gas-phase oxidation.[695] These differences likely arise from the fact that these experiments were conducted under less extreme conditions than those attained in acidic sulfate aerosol particles in chamber experiments.

It is a standing task to further adjust bulk chemical conditions to mimic those present in aerosol particles (i.e., high acidity and low water content), because otherwise the kinetic results derived from these experiments cannot be regarded as representative of those occurring in real atmospheric particles, and their use in models might therefore be misleading. Recent evidence for the value of chamber work has been provided by Drozd et al., who showed that the reactive uptake of α-pinene

DOI: 10.1021/cr500447k
Chem. Rev. 2015, 115, 4259−4334

oxide to acidic sulfate aerosol occurs only under highly acidic conditions (pH < 0) and results in the formation of an organic surface coating, which limits further uptake.[696]

Finally, a very recent study by Zhang and co-workers has provided evidence that SOA formation from the biogenic VOC 2-methyl-3-buten-2-ol (MBO) also proceeds via a reactive epoxide intermediate.[697] Together, these results imply that epoxide-mediated chemistry may contribute to SOA formation even in areas where isoprene emissions are low.

7.2.4. Organosulfates. Early laboratory evidence for the existence of aerosol-phase organosulfates (OS) was provided by Liggio et al.,[404] who reported the formation of sulfate esters upon uptake of glyoxal by sulfate-containing seed aerosol, and Nozière et al.,[482] who observed steady-state (i.e., reactive) uptake of the biogenic VOC 2-methyl-3-butene-2-ol (MBO) by sulfuric acid solutions but did not, at the time, attribute this observation to OS formation. These laboratory studies were complemented by a number of field studies, which showed OS to be present in atmospheric particulate matter samples obtained from a variety of North American and European locations.[43,698−700] For a summary of the early OS work, see the review by Hallquist et al.[38]

The following paragraphs aim to summarize our current understanding of the formation pathways, kinetics of formation, and atmospheric abundance of aerosol-phase organosulfates, and to complement recent discussions of the topic by McNeill et al.,[548] Ye. et al.,[701] and Szmigielski.[702] While key field studies will be discussed, this section does not aim to provide a comprehensive overview of OS-related field work.

7.2.4.1. Mechanisms and Kinetics of Organosulfate Formation from Epoxides. Several early studies of aerosol-phase organosulfates postulated that these species arose under acidic conditions via the SN_1 reaction of alcohols with hydrogen sulfate as nucleophile (see, e.g., work by Surratt et al.[43]). The atmospheric significance of this acid-catalyzed pathway was called into question, however, by Minerath and Elrod,[703] who showed that the direct reaction of alcohols with sulfuric acid is kinetically insignificant under acidity conditions typical of lower tropospheric SOA. An alternative, more efficient, mechanism for OS production, which was first proposed by Iinuma et al. in 2007 for the reaction of β-pinene with ozone in the presence of acidic sulfate seed particles, involves the reactive uptake of gas-phase epoxides.[698] Since the pioneering work of Paulot and co-workers,[666] which showed that the OH-mediated oxidation of isoprene under low-NO_x conditions results in the formation of dihydroxyepoxides (IEPOX; see section 7.2.3), this mechanism has received much research attention. The following paragraphs describe in more detail our current understanding of this organosulfate formation pathway.

Although the chamber work described above provided qualitative evidence for epoxide-mediated organosulfate formation, quantitative evidence for the importance of this pathway was still missing. This information was provided in 2010 by Eddingsaas et al., who conducted a comprehensive bulk-phase kinetic and mechanistic investigation of organosulfate formation from the acid-catalyzed ring-opening reactions of four hydroxy-substituted epoxy butanes.[673] The value of quantitative organosulfate formation data has recently been shown by McNeill et al.,[548] who used the kinetic parameters obtained in this study to model the formation of organosulfates from IEPOX. Our current knowledge regarding the kinetics of organosulfate formation from epoxides in the aqueous phase is summarized in Table 17.

The acid-catalyzed ring-opening reactions of epoxides can occur via an A-1 mechanism, in which the nucleophile HOX (here, X = H, SO_3^-, or NO_2) adds to a carbocation intermediate formed after breakage of one of the C−O epoxide bonds, or via an A-2 mechanism, in which nucleophilic attack and C−O bond breakage occur in a concerted fashion.[673] The relative importance of these two mechanisms depends on the epoxide identity.[673]

The products of epoxide ring-opening reactions depend on the identity of the nucleophile: nucleophilic attack by water results in the formation of diol functionalities, whereas nucleophilic attack by nitrate and sulfate results in the competitive formation of organonitrates and organosulfates, respectively. Studies have shown that the organosulfate yield increases with increasing sulfate concentration and displays a strong dependence on epoxide identity.[406,671,673] Although organosulfates are kinetically stable against hydrolysis on SOA time scales, some organonitrates are not: work by Darer et al.[677] and Hu et al.[678] has shown that a variety of tertiary organonitrates are susceptible to nucleophilic attack by both water and sulfate, the latter of which represents an additional pathway for organosulfate formation.

Despite the significant progress made to date in this area, a comprehensive understanding of the formation of organosulfates from epoxides other than dihydroxyepoxides (i.e., IEPOX and its analogues) is still missing. For example, no quantitative information regarding the kinetics and yields of organosulfate formation from methacrylic acid epoxide (MAE), which is formed from the photooxidation of isoprene under high-NO_x conditions,[669] and MBO epoxide, which is formed during the low-NO_x photooxidation of the biogenic SOA precursor 2-methyl-3-buten-2-ol (MBO),[697,704,705] is currently available. Even in the case of α-pinene oxide, which has been the subject of several studies, uncertainties remain: as outlined in section 7.2.3, while Lal and co-workers[674] observed the production of typical ring-opening organosulfate products upon its uptake to acidic solution, Bleier and Elrod[676] observed breakage of the α-pinene bicyclic backbone and production of a complex range of products, which included only a single organosulfate, *trans*-sobrerol sulfate, which hydrolyzed quickly to yield *trans*-sobrerol.

7.2.4.2. Sulfate Radical-Mediated Organosulfate Production. In 2009, Rudzinski et al.[706] showed that the interaction of aqueous-phase isoprene with sulfate radical anions led to the production of a variety of organosulfate products. Although the direct applicability of this study is limited by the fact that isoprene does not partition appreciably into aqueous aerosols or cloud droplets, OS formation via sulfate radical-initiated pathways has been explored in a number of further studies. For example, Perri et al.[70] observed OS formation in the aqueous OH radical oxidation of glycolaldehyde in the presence of sulfuric acid, and attributed this observation to a reaction between organic radicals and either sulfuric acid or hydrogen sulfate radicals. It should be noted that this reaction would be most effective at low concentrations of dissolved oxygen, where the reaction of organic radicals with molecular oxygen to yield peroxyl radicals would be less competitive. In addition, in a set of bulk-phase aqueous experiments, Nozière et al.[707] showed that OS can also be formed from reactions of the sulfate radical anion with isoprene, α-pinene, and the isoprene oxidation products methacrolein (MACR) and methyl vinyl ketone

DOI: 10.1021/cr500447k
Chem. Rev. 2015, 115, 4259−4334

(MVK). More recently, Schindelka et al.[45] conducted a set of chamber experiments investigating sulfate radical-initiated OS formation from MACR and MVK. These authors found that the illumination of sulfuric acid seed particles containing the sulfate radical precursor $K_2S_2O_8$ in the presence of MACR and MVK led to particle mass growth and to the formation of organosulfates.

7.2.4.3. Field Measurements of Organosulfates. Field studies have shown that a significant fraction of particulate sulfur is often present as OS, and that OS in turn often represents a significant fraction of particulate organic mass. In one early study, for example, Surratt and co-workers used the difference between total particulate sulfur, measured using particle-induced X-ray emission spectrometry (PIXE), and inorganic sulfate, measured using ion chromatography, at the Hungarian forest site K-puszta to estimate a maximum OS contribution of 30% to PM_{10} organic mass.[699] In 2012, Tolocka and Turpin employed a similar strategy, although on a larger scale: using the National Park Service IMPROVE $PM_{2.5}$ database, which consists of over 150 000 measurements, these authors estimated an upper bound of 5−10% contribution by OS to particulate organic mass.[708] More specifically, the contribution of the sulfate ester of the second-generation isoprene oxidation product IEPOX (see section 7.2.3) alone to total particle mass in the summertime southeastern United States has been found to reach ∼3% downwind of isoprene emission sources and in the presence of acidic aerosol.[670]

Although early measurements of organosulfates were conducted in North American and European locations, the geographic scope of organosulfate field work has since expanded: in the past several years, for example, organosulfates have been measured in locations ranging from the remote Arctic[709,710] to urban locations in China[711−714] and Pakistan.[715,716] These studies have revealed the presence of a wide range of organosulfates, including nitrooxy-organosulfates,[712,713] aromatic organosulfates,[714−716] and long-chain aliphatic organosulfates.[711]

As shown by He and co-workers, the abundance of traditional (i.e., IEPOX-derived) biogenic organosulfates can be quite low in polluted, high-NO_x environments.[712] Moreover, the organosulfates observed in these environments may form via mechanisms different from those proposed for the biogenic organosulfates studied to date. For example, Staudt et al. have very recently shown that the photooxidation of toluene in the presence of NO_x and acidic sulfate aerosol (i.e., under conditions that promote the formation of biogenic organosulfates) does not result in the formation of aromatic organosulfates.[716] In addition, work by He and co-workers has suggested that the formation of pinene-derived nitrooxy-organosulfates observed in the Pearl River Delta (PRD) region of China proceeds via the sulfate esterification of a hydroxynitrate intermediate formed from the oxidation of α-pinene by NO_3 or OH; although sulfate esterification has been shown to be slow under typical tropospheric aerosol acidities,[703] these authors suggest that it is promoted by the high aerosol acidities present in the PRD.[712] The mechanisms and kinetics of organosulfate formation in these polluted regions deserve further study. Time-resolved field measurements, such as those performed by Hatch et al. in Atlanta, GA, have the potential to aid in our understanding of organosulfate formation processes.[717]

To date, quantification of individual organosulfates in field samples has been limited by the lack of commercially available

Table 17. Overview of Organosulfate-Related Kinetic Data

epoxide	hydrolysis rate constant [M^{-1} s^{-1}]	total organosulfate yield [%]	remarks	refs
1,2-epoxybutane	0.074	27	reaction kinetics followed using NMR spectroscopy in deuterated solution (D_2O/D_2SO_4); product yields determined in 1 M Na_2SO_4/0.02 M D_2SO_4/D_2O solutions	406
trans-2,3-epoxybutane	0.20	11		
2-methyl-1,2-epoxypropane	8.7	14		
2-methyl-2,3-epoxybutane	9.0	11		
2,3-dimethyl-2,3-epoxybutane	15	7		
1,2-epoxyisoprene	56 000	<1	reaction kinetics followed using NMR spectroscopy in deuterated solution (D_2O/D_2SO_4); product yields determined in 1 M Na_2SO_4/0.2 M D_2SO_4/D_2O solutions; for 1,2−3,4-diepoxybutane, the quoted organosulfate yield is for the first epoxide ring-opening reaction	671
3,4-epoxyisoprene	5.6	15		
3,4-epoxy-1-butene	3.1	13		
1,2−3,4-diepoxybutane	0.0013	38		
1,2-epoxy-3,4-dihydroxybutane	0.0012	43		
cis-2,3-epoxybutane-1,4-diol	(1.3 ± 0.1) × 10^{-3}	29	reaction kinetics followed using NMR spectroscopy with water suppression in 10% D_2O/90% H_2O; product yields determined in 1 M Na_2SO_4/0.1 M H_2SO_4; product yields are also available for *cis*-2,3-epoxybutane-1,4-diol as a function of sulfate concentration	673
3,4-epoxybutane-1,2-diol	(2.2 ± 0.2) × 10^{-3}	32		
3-methyl-2,3-epoxybutan-1-ol	0.3 ± 0.05	10		
3-methyl-3,4-epoxybutan-1-ol	0.2 ± 0.05			

DOI: 10.1021/cr500447k
Chem. Rev. 2015, 115, 4259−4334

standards for this compound class. Progress has been made in this area, however: for example, Olson et al.[718] synthesized and quantified glycolic and lactic acid sulfate in ambient aerosol sampled in several urban locations, and two recent studies have reported the synthesis and quantification of a variety of aromatic organosulfates in aerosol samples obtained from cities including Lahore, Pakistan.[712,716]

7.2.5. Imidazoles. A number of recent studies have focused on the formation and effects of imidazoles in tropospheric particulate matter.[303,320,321,323,407,492,498,504,718−722] The first evidence for the presence of imidazoles in atmospheric particles was found by Laskin et al.[723] in laboratory-generated biomass burning aerosols, where mass fragments could be assigned to methylimidazole. However, Galloway et al.[542] were the first to identify an imidazole, 1*H*-imidazole-2-carboxaldehyde, by using a commercial available standard in ammonium sulfate seed aerosol during glyoxal uptake experiments. A real in-situ field measurement of imidazole compounds in aerosol particles is, at the time of writing, and according to the knowledge of the authors, not available.

Imidazoles have been suggested to form in the atmosphere via a Debus mechanism, in which a dialdehyde (e.g., glyoxal or methylglyoxal) reacts with ammonia or with a primary or secondary amine to form imines. Those imines can further react to form imidazoles (see Figure 12). The formation of imidazoles during the reaction of glyoxal with ammonia has been known since the 19th century.[724] The reaction observed by Debus was accompanied by browning of the solution. Similar findings were reported in other laboratory studies, which suggests that imidazoles may contribute to brown carbon in the atmosphere.[407,718,719,725] Furthermore, it has been shown that, even if these compounds might be present only in small quantities, imidazoles can affect aerosol optical properties[722] and act as photosensitizers[320,321] (see section 4.4).This latter effect, the in-situ atmospheric production of a class of molecules able to act as photosensitizers, is a very interesting new topic in aerosol photochemistry, which will be covered in much more detail in the contribution by George et al. in this issue.

Sedehi et al.[492] provided estimated rate constants for imidazole formation under aqueous-aerosol conditions at pH = 5.5 (Table 18). Under the conditions applied, the OH radical reaction of the organic carbonyl compound (glyoxal and methylglyoxal) is the dominant pathway, followed by the ammonium sulfate reaction.[492] The rates for the glyoxal or methylglyoxal reactions, respectively, with amino acids or other amines are 1 order (marine conditions) to 2 orders of magnitude (continental conditions) smaller than the OH radical reaction rate.[492]

In a computational study, Kua et al.[527] investigated the thermochemistry and kinetics of imidazole formation reactions from glyoxal, methylamine, and formaldehyde.

Available kinetic data for reactions leading to imidazole production are summarized in Table 18. Yu et al.[718] observed extremely low reaction rate constants, on the order of 10^{-11}–10^{-12} M^{-1} s^{-1}, for the production of imidazoles during bulk solution experiments with glyoxal and ammonium sulfate, which suggests that imidazoles do not contribute significantly to ambient SOA mass. However, de Haan et al.[407,719] found much faster reaction rates of glyoxal with amino acids and primary amines under droplet drying conditions and for aerosols, which demonstrates that extrapolation of reaction rates determined in bulk solution experiments to aerosol conditions should be done with care. Apparently, certain accretion reactions currently discussed appear to require (droplet) drying conditions, that is, a strong increase in reactant concentrations, to yield products on atmospherically relevant time scales.

7.2.6. Amines. Postcombustion carbon capture and storage (CCS), which may employ amine gas washers, is of current interest as a method for decreasing the CO_2 emissions from power plants.[729,730] In this context, the tropospheric multiphase processing of amines has become more relevant, because these species may be released into the atmosphere, along with NO_x emissions, in the flue gas stream. A recent review by Nielsen et al.[290] summarizes the current knowledge regarding the atmospheric chemistry of amines; since this contribution, only a few new amine-related studies have been reported. The aqueous-phase UV photolysis of NDMA (*N*-nitrosodimethylamine) was reported by Kwon et al.[291] (see section 4.3). These authors reported the formation of an unknown reactive species, which has a reactivity similar to that of OH radicals toward NDMA. This result was obtained by performing a competition reaction using *p*-nitrosodimethylaniline (PNDA) as the reference substance to probe the reactivity of the unknown reactive species, and a second-order rate constant of $k = 5.13 \times 10^8$ M^{-1} s^{-1} was obtained for the reaction of the unknown intermediate with NDMA.

Sedehi et al.[492] investigated imidazole formation from α-dicarbonyl compounds (cf., sections 7.2.1 and 7.2.5), amines, and ammonium sulfate. Qui et al.[731] summarized the multiphase chemistry of atmospheric amines, with a special focus on their heterogeneous reactions, which can play an important role in the formation and transformation of aerosols. Wang et al.[732] reported measurements of amines in fog in Norway: the amine concentration was in the nanomolar range, and very low concentrations of *N*-nitrosodimethylamine were observed.

A compilation of amine and amine-related compounds in surface water was provided by Poste et al.[733] These authors summarized the concentrations, sources, fate, and toxicity of amines in surface waters, rivers, lakes, reservoirs, wetlands, and seawater. It was reported that the amine concentration in surface water was often below the detection limit and rarely exceeded 10 μg L^{-1}.

Finally, results obtained in a recent kinetic study of the aqueous-phase reactions of NO_3 and ozone with nitrosamines and amines suggest that, rather than enhancing the formation of harmful compounds such as nitrosamines, aqueous-phase chemistry generally seems to lead to the degradation of these species.[402]

8. MICROBIOLOGY

Aerosols are often only considered as suspensions of liquid, solid, or multiphase matter, consisting of various organic and organic species, in the surrounding gas phase. However, it is long-standing knowledge that atmospheric organic aerosols and cloud droplets also contain microbial content (see Morris et al.[734] and references therein). Biological aerosols, or bioaerosols (i.e., particles originating from biological organisms), can be spores, pollen, bacteria, and viruses.[735] Further details on the different characteristic types of bioaerosols and methods presently used for their measurement/analysis are given in a review by Després et al.[735] Biological aerosols are ubiquitously present in the atmosphere[736,737] and can represent a substantial fraction of the aerosol mass. For example, Jaenicke[738] estimated

DOI: 10.1021/cr500447k
Chem. Rev. 2015, 115, 4259−4334

Table 18. Kinetic Data for the Imidazole Formation in the Aqueous Solution[a]

organic reactant		reactants/solutes	rate constant k	products	rel. contrib., marine aerosol	rel. contrib., terrestrial aerosol	refs
glyoxal	1 M	1 M glycine	0.12 ± 0.04 M^{-1} s^{-1}	imidazoles[c]			407
	1 M	0.48 M serine	0.09 ± 0.01 M^{-1} s^{-1}				
	1 M	0.86 M arginine	$(4.5 \pm 0.6) \times 10^{-4}$ M^{-1} s^{-1}				
	8.8 mM	0.35–9.3 mM methylamine	1.8 ± 0.4 M^{-1} s^{-1}	imidazoles[c]			719
	0.1 M	0.5–4 M ammonium salts	$(2 \pm 1) \times 10^{-10}$ $\exp^{(1.5\pm0.8)a_{NH_4^+}}$ $\exp^{(2.5\pm0.2)pH}$ M^{-1} s^{-1}	glyoxal oligomers[d]			405
	2.21 M	3.1 M AS	$k < 4.8 \times 10^{-4}$ M^{-1} min^{-1}	2,2′-bi-imidazole[b,d]			726
	0.33–0.5 M	0.67–1 M AS	$10^{(1.05\times(pH)-7.45)}$ M^{-1} s^{-1}	imidazole, aldol oligomers, N-containing oligomers[c]	0.08	0.02	492
	0.46–1.5 M	0.46–1 M glycine	$10^{(0.741\times(pH)-6.84)}$ M^{-1} s^{-1}		0.001	0.00007	
	0.33–1 M	0.33–0.5 M serine	$10^{(0.998\times(pH)-7.59)}$ M^{-1} s^{-1}		0.005	0.0004	
	0.44–1 M	0.25–0.86 M arginine	$10^{(0.994\times(pH)-7.69)}$ M^{-1} s^{-1}		0.0007	0.00005	
	0.5 M	0.5 M methylamine	$10^{(0.972\times(pH)-8.33)}$ M^{-1} s^{-1}		0.00003	0.00002	
		other amino acids	(70 ± 60) M^{-1} s^{-1} $f_{Ald}[Glx]_{tot}f_{Am}$, $[AM]_{tot}$	imidazole, aldol oligomers, N-containing oligomers[c]	0.035	0.0014	
		other primary amines	(70 ± 60) M^{-1} s^{-1} $f_{Ald}[Glx]_{tot}f_{Am,}[AM]_{tot}$		0.001	0.0003	
	1–1.5 M	1–1.6 M AS	$(1.23 \pm 0.25) \times 10^{-11}$ M^{-2} s^{-1}	imidazole + 1N-glyoxal substituted imidazole[c,d]			727
	1–1.5 M	1–1.6 M AS	$(2.01 \pm 0.40) \times 10^{-12}$ M^{-2} s^{-1}	imidazole-2-carboxalde-hyde[c,d]			
methyl-glyoxal	2 M	3.1 M AS	5×10^{-6} M^{-1} min^{-1}	aldol condensation products[d]			53
	0.5 M	0.5 M AS	$10^{(0.834\times(pH)-5.91)}$ M^{-1} s^{-1}	methylimida-zole, aldol oligomers, N-containing oligomers[c]	0.31	0.12	492
	0.5 M	0.5 M glycine	$10^{(0.262\times(pH)-3.40)}$ M^{-1} s^{-1}		0.013	0.001	
	0.33–0.5 M	0.25–0.33 M serine	$10^{(0.421\times(pH)-3.91)}$ M^{-1} s^{-1}		0.03	0.003	
	0.2–0.5 M	0.2–0.43 M arginine	$10^{(0.422\times(pH)-4.09)}$ M^{-1} s^{-1}		0.003	0.0004	
		other amino acids	$10^{((0.36\pm0.06)\times pH-(3.6\pm0.3))}$ M^{-1} s^{-1} $f_{Ald}[MG]_{tot}[AM]_{tot}$		0.08	0.005	
	0.5 M	0.5 M methylamine	$10^{(0.334\times(pH)-3.22)}$ M^{-1} s^{-1}		0.002	0.002	
		other primary amines	$10^{((0.36\pm0.06)\times pH-(3.6\pm0.3))}$ M^{-1} s^{-1} $f_{Ald}[MG]_{tot}$ $[AM]_{tot}$		0.005	0.001	
2-methyl-glyceric acid			$(3.1–19.7) \times 10^5$ M^{-1} s^{-1}	oligoesters[c]			541

[a] f_{Ald}, fraction of aldehyde with a dehydrated aldehyde functional group. f_{Am}, fraction of amine or ammonia that is deprotonated at a given pH. $[Glx]_{tot}$, concentration of hydrated and unhydrated glyoxal. $[AM]_{tot}$,[728] concentration of protonated and unprotonated amines/amino acids/ammonia. $[MG]_{tot}$, concentration of hydrated and unhydrated methylglyoxal. $a_{NH_4^+}$, ammonium ion activity. AS, ammonium sulfate. [b] Identified by ref 721. [c] Rate constants are derived from NMR data. [d] Rate constants are derived from UV–vis data.

that up to 25% of aerosol mass can be cellular and proteinaceous material. Biological aerosols are known to be constantly transported through the atmosphere.[735,739] Burrows et al.[739] estimated atmospheric residence times ranging from 2.2 days (simulation including CCN activity and ice-phase scavenging) to 188 days (simulation without CCN activity and ice-phase scavenging).

Biological aerosols may contribute to several atmospheric issues, including health, weather, and climate (Morris et al.[734]), via their role as cloud condensation nuclei and/or ice nuclei (CCN/IN)[735,740−742] and their effects on ALW content (see Després et al.[735] and references therein), and, finally, the local radiation budget. Bioaerosols can also influence atmospheric chemical processes: for example, as a result of their metabolic activity, living microorganisms such as bacteria and fungal spores can process chemical compounds in atmospheric solutions and both consume as well as produce organic constituents of the tropospheric aqueous-phase particles and cloud droplets, which will be treated below in detail.

Because of their ability to act as CCN/IN, microorganisms are present in cloud, fog, and rainwater as well as in ice particles.[737,743−749] Moreover, under cloud conditions, different types of microorganisms, such as bacteria and viruses, can partition between the cloud and interstitial aerosol phases according to their different sizes and resulting CCN/IN abilities.[735] Investigations by Sattler et al.[743] have shown that the metabolic activity of microorganisms is not zero below the freezing point of water, as typically found in warm tropospheric clouds. Amato et al.[745] have observed that cloud droplets represent an environment in which bacteria can develop significantly, and Sattler et al.[743] have argued that cloudwater needs to be considered as a microbial habitat.

DOI: 10.1021/cr500447k
Chem. Rev. 2015, 115, 4259−4334

Cloudwater and ALW solutes might be reduced in concentration when compounds are consumed by microorganisms or enhanced in concentration when they are produced. Such biological sources and sinks of atmospheric aqueous-phase constituents can potentially have turnovers similar to those associated with pure chemical, that is, abiotic production and loss; the following paragraphs aim to summarize the results obtained in a number of recent studies focusing on the influence of microorganisms (bioaerosols) on aqueous atmospheric chemistry.[744−753]

The first study on the biodegradation of organic compounds in rainwater was published in 1987 by Herlihy and co-workers, who focused on the consumption of formic and acetic acid by bacteria.[750] Later, Ariya et al.[751] provided evidence that biodegradation could be an important chemical transformation pathway for organic compounds in the troposphere. Specifically, these authors concluded that dicarboxylic acids (DCAs) can be effectively degraded by existing microbes (i.e., bacteria and fungi). Evidence from isotopic studies performed using ^{13}C NMR indicated that these microbes used DCAs as a nutrient source. Associated product studies showed the production by microbes not only of non- or slightly toxic compounds, such as acetamine, acetoacetic, butanoic, and propionic acid, but also of some highly toxic and carcinogenic compounds, such as kojic acid and aflatoxin B1. Furthermore, these authors observed the formation of a variety of volatile compounds, including aromatic and heterocyclic compounds with different substituents; from this finding, they concluded that DCA are recycled back to the gas phase via microbiological processing. Finally, these authors investigated the kinetics of reaction between microorganisms and several dicarboxylic acids, and compared the lifetime of these dicarboxylic acids against microbiological degradation to that expected against degradation by tropospheric radicals. This comparison revealed that biodegradation is very efficient for this compound class, with in-cloud lifetimes on the order of several days (i.e., comparable to calculated lifetimes against OH radical reactions). It should be noted, however, that these authors also showed that fungi growth is restricted to conditions with pH values larger than 2. Therefore, acidic ALW in deliquescent aerosol particles does not seem to be an adequate medium for biodegradation processes.

Work by Amato et al.[744] has further established that pH is the key factor controlling the structure of the microorganism community in cloud waters. In a further publication, Amato et al.[745] confirmed previous findings that microbiological activity can act as a sink not only for organic acids, such as formic acid, acetic acid, and succinic acid, but also for methanol and formaldehyde. In addition, these authors showed that biological in-cloud processing might also be a source of organic compounds, such as pyruvic acid formed from lactic acid. In their paper, they also showed metabolic pathways that could give rise to the different organic compounds measured.

In a more recent study, Vaïtilingom et al.[746] concluded that the degradation of organic compounds should be dominated by OH radical chemistry during the day but by biological activity at night. In further investigations, Vaïtilingom et al.[754] reported biological degradation rate constants of 17 strains of microflora toward acetate, formate, and succinate. By comparing these data to OH radical turnovers, these authors concluded that, as compared to photochemical degradation, biodegradation processes are unimportant for oxalate, of minor importance for formate, and the main atmospheric degradation pathway for acetate and succinate.

In 2011, Kourtev et al.[749] published a paper on the diversity of the bacterial community in atmospheric cloudwater. Unlike other studies, which largely collected water samples in near-ground orographic clouds,[743−745,747,750,751,753] these researchers employed an aircraft to obtain samples from higher-altitude clouds. Their measurements confirm the presence of a diverse bacterial community, which is mainly dominated by members of cyanobacteria, proteobacteria, actinobacteria, and firmicutes. More recently, DeLeon-Rodriguez and co-workers reported aircraft measurements of the composition and prevalence of microorganisms in the middle-to-upper troposphere under cloud and noncloud conditions above the oceans before, during, and after two tropical hurricanes.[755] Results obtained in this study suggest that hurricanes are able to aerosolize a large number of new bacterial cells. Because Methylobacteriaceae and Oxalobacteraceae, which were detected as two of the core families in this study, are able to metabolize oxalic acid, which is ubiquitous in tropospheric aerosols, these authors concluded that these bacterial communities could remain metabolically active in clouds. Overall, these authors suggested, based on their findings, that airborne microbes may have significant impacts on the hydrological cycle, clouds, and climate.[755]

In 2012, Vaïtilingom et al.[747] reported long-term features of the cloud microbiology present at the Puy de Dôme mountain in France. From the long-term data set, it was reported that a small number of microbiological genera largely dominate the pool of microorganisms in clouds. For example, the two bacteria *Pseudomonas* and *Sphingomonas* were observed in more than 40% of the cloud samples, and the yeasts Dioszegia and Udeniomyces were detected in more than 60% of the field samples.

Studies by Husárová et al.[753] examined the kinetics of the biodegradation of methanol and formaldehyde by four bacterial strains (*Pseudomonas graminis*, *Pseudomonas syringae*, *Bacillus sp.*, and *Frigoribacterium sp.*). Interestingly, the analysis of the metabolic intermediates showed the formation of the C_3 compounds glycerol and 1,2- and 1,3-propanediol. These authors proposed that a complex metabolism, involving numerous enzymes, might be able to lead to (i) the functionalization of the molecule and (ii) the condensation to larger molecules (C_3) starting from a C_1 compound such as formaldehyde.

More recent investigations by Vaïtilingom et al.[748] suggested that microorganisms might play a double role in atmospheric chemistry: first, microorganisms might be able to metabolize organic compounds; second, they might reduce potential radical sources via the biodegradation of H_2O_2 by catalase-type enzymes. This finding is stated to have major implications for atmospheric chemistry. However, it should be noted that many model studies have revealed that the main source of OH radicals in clouds is its direct transfer from the gas phase.[33,205] H_2O_2 as a direct source of OH radicals is mostly only of minor importance under cloud conditions. Furthermore, it has been shown in several studies that chemical cloud processes are able to produce H_2O_2, depending on the transition metal ion concentration.[33,205] Therefore, the microbiological effect on H_2O_2 may be only of minor importance. Nevertheless, microbially mediated H_2O_2 consumption should be considered in a process model to test the magnitude of its effect on the cloud oxidation capacity.

In summary, studies have revealed that microbiological processes have the potential to influence atmospheric chemistry or, at least, to influence the lifetime and abundance of some

DOI: 10.1021/cr500447k
Chem. Rev. 2015, 115, 4259−4334

specific compounds. Despite recent progress, our knowledge of microbiological processes is still rather restricted; in particular, an understanding of the complex dependencies of these processes on atmospheric condition parameters such as temperature, pressure, humidity, radiation, pH, and different nutrients is still lacking. Therefore, further investigations combining laboratory, field, and model studies will be needed to better characterize the chemical effects of microbiological processes in the different atmospheric phases and to estimate their global importance, for example, for atmospheric chemistry and the climate. Similar to the consideration of radical sinks established by organic compounds, it might be helpful to consider sink and source terms for the biological consumption and production of atmospheric aqueous-phase inorganic and organic solutes, including dissolved oxygen[752] and product species such as dicarboxylic acids, in the further development of tropospheric multiphase models.

9. THE ATMOSPHERIC AQUEOUS PHASE AND A CHANGING ATMOSPHERE

Earth and its atmospheric and climate systems are undergoing significant change. According to the much-manifested knowledge of leading atmospheric researchers, climate change is happening and will lead to a variety of changes, which are expected to also affect atmospheric aqueous-phase processes and their coupling to the gas phase. In the following paragraphs, a number of areas where changes might be expected to occur are discussed.

9.1. Temperature Change: The Atmosphere and the Oceans

Earth's temperature is rising: according to the IPCC AR5,[756] an increase of about 0.85 °C has been observed over the period 1880−2012. Although this increase will change the rate constants of all of the chemical reactions involved in atmospheric multiphase chemistry, it is expected that the resulting increases in rate constants will be small and therefore will not have significant direct effects.

Temperature change is affecting the oceans; the near-surface (75 m) layer has warmed by 0.11 °C per decade from 1971 to 2010. Hence, surface ocean biology and chemistry might change: changes in ocean biology productivity could affect the bulk surface ocean and the surface organic microlayer, which then in turn could influence how the oceans export organic material to marine aerosol or how the oceans' emissions of trace gases, some of which are climate-relevant, might be influenced. As a result of these related processes, marine aerosol and, eventually, cloud chemistry could be affected by ocean temperature change. These possible changes are presently the subject of study in the ocean sciences, sometimes linked to corresponding atmospheric studies;[757,758] collaborative studies should be much enhanced in this area in the future.

9.2. Humidity, ALW, ALW Acidity, Clouds, and Cloudwater

In principle, increased temperatures will lead to an overall increase in the humidity of the atmosphere. The AR5 gives a more detailed statement, however: "It is very likely that near-surface and tropospheric air specific humidity have increased since the 1970s. However, during recent years the near-surface moistening trend over land has abated (medium confidence). As a result, fairly widespread decreases in relative humidity near the surface are observed over the land in recent years." As of the AR5, the change in tropospheric water vapor was + 3.5% over the last 40 years, which is consistent with the observed temperature change, while relative humidity (RH) stayed approximately constant.[756] In addition, with the presently available data, a trend in cloud cover has low confidence.

It might be expected, however, that because of increasing temperature, tropospheric water content will increase and that this will lead to a generally moister and warmer atmosphere.

In fact, the annual mean hydrological cycle changes for 2081−2100 as compared to 1986−2005 Representative Concentration Pathways (RCP8.5)[759] indicate that RH will reduce over the continents and increase over the oceans. In the same scenario run, cloud cover will reduce significantly over the continents, with maximum reductions in regions of South and Eastern Europe, Asia, South Africa, Amazonia, and southern North America. Over the oceans, again, cloud cover is expected to increase.

As a result of these changes, tropospheric aqueous-phase cloud chemistry might become enhanced over the oceans but reduced for continental clouds. Hence, specific marine multiphase chemistry questions might become the subject of growing interest in the future.

Although the AR5 does not address aerosol liquid water (ALW), it can be speculated that trends in its abundance would track those of clouds; that is, ALW might decrease over the continents and increase over the oceans. If this is indeed the case, the conclusion would be that ALW marine chemistry might increase in global importance, while ALW chemistry over the continents might change somewhat. If continental ALW becomes more water-restricted, deliquescent particles might become more acidic, which would have consequences for the many aqueous-phase reactions discussed in the present contribution. To the best of our knowledge, the authors are not aware of studies that have attempted to predict changes in ALW arising from future climate change; such studies would be very useful, and would fill a gap in the scientific interaction between atmospheric chemistry and climate science.

9.3. Atmospheric CO_2 Concentration Change: The Atmosphere and the Ocean

Clearly, the CO_2 level in Earth's atmosphere will rise, which will, again, not affect atmospheric chemistry directly, because CO_2 is an end point of rather than a participant in oxidation reactions. Aqueous environments will be affected, however, because rising CO_2 will lead to the acidification of aqueous systems in contact with the gas phase; this effect obviously affects the oceans with their finely adjusted marine chemistry and biology and is therefore a subject of intense study.[760−763] Again, changes in ocean chemistry and biology occurring as a result of enhanced CO_2 levels could alter the emission characteristics of the ocean with regard to both primary marine aerosol composition and trace gas release.

As ALW is usually quite strongly acidified, a change in CO_2 will not have any significant effect on aerosol chemistry; the impact of particle pH on the actual occurrence of organic accretion reactions remains a conundrum at present where more field evidence is needed.[764] By contrast, rising CO_2 might be expected to have a small effect on cloudwater pH for clouds in the unperturbed atmosphere, such as those located in areas over the oceans with little continental influence. However, even in these isolated locations, it should be noted that ship emissions influence the marine aerosol pattern and hence cloud pH. Cloudwater pHs ranging from 2.9 to 7.2 were recently found for clouds over the Pacific between 71−85° W and 18−30° S.[765] Marine clouds with pH values at the upper end of this

DOI: 10.1021/cr500447k
Chem. Rev. 2015, 115, 4259−4334

range might be affected somewhat by increased atmospheric CO_2 level, but, again, as soon as other anthropogenic influences come into play (e.g., S(IV) oxidation), acidification will be governed by these latter processes.

9.4. Continental Environments: Biogenic Plant Emission Changes

On the microscale, biogenic plant emissions are controlled by radiation and, more importantly, temperature. However, because BVOC emission is known to depend on CO_2 levels and be influenced by changes in landcover/land use, these factors must also be considered in assessments of global trends in BVOC emissions. This has been outlined by Navarro et al.[766] very recently in their consideration of BVOC emission changes over the last millennium.

Increases in global BVOC emissions arising from changes in land cover, CO_2 level, and temperature will have consequences for the tropospheric gas-phase oxidative capacity and, by extension, for the formation of oxidized VOC and SOA. Therefore, as outlined on many occasions in the present contribution, aqueous-phase chemistry will also be affected, for example, by increased gas-phase levels of glyoxal or other OVOCs.

9.5. Anthropogenic Emission Changes

As previously mentioned, since 2006, global SO_2 emissions have exhibited a decreasing trend.[549] Therefore, if this trend can be maintained as China is expected to undergo more environmental protection efforts and maybe India could be motivated to work on its emissions as well, a global trend toward decreasing atmospheric sulfur oxidation and sulfate formation, which mainly occurs in cloud droplets,[767] is to be expected. In a way, inorganic aqueous-phase chemistry might then become less important than was previously the case, while the conversion of organics might become even more important because of increased BVOC emissions and the globally much more important amount of BVOC over anthropogenic VOC.

GOME and SCIAMACHY satellite-based measurements over the period 1996 to 2011 show NO_x reductions over the U.S., Europe, and Japan and increases over China, the Middle East, and India.[756] According to the AR5, anthropogenic global emissions of NO_x show a trend, which is somewhat different from that of SO_2: in the near future, NO_x is expected to be more or less constant, and reductions are only expected to be seen from 2030 until the end of the prognostic time frame, that is, up to the year 2100. This means that for the next several decades, NO_x will continue to play an important role in atmospheric chemistry, as will its coupling to aqueous particles, which ultimately results in the formation of nitrate. All of the aqueous-phase chemistry related to NO_x, including nitrate photochemistry, N_2O_5 chemistry, and its coupling to particulate chloride, and finally chlorine release, will therefore remain of high importance.

9.6. Anthropogenic Emission Changes Caused by Mitigation Technologies

Carbon capture and storage has the potential to act as a technology to enable further energy production via fossil fuel combustion without the serious drawback of CO_2 emission. Different technologies for the removal of CO_2 from flue gas are available, and some of them are based on the application of amine washer solutions. Depending on technology, this might lead to the release of amines, which could then be involved in a variety of gas-phase and multiphase chemistry processes. This topic has recently been reviewed by Nielsen et al.,[290] and is discussed briefly in section 7.2.6 of this Review.

9.7. Air Pollution and the Natural Atmosphere

Air pollution prevention and climate change mitigation may go together when non-CO_2 climate-relevant gases are concerned as well as aerosol particles of both primary and secondary origin. In a sense, a better analysis will be needed in the future regarding the relative contributions of anthropogenic and biogenic/natural emissions to aqueous-phase SOA formation. This perspective is currently missing from the "aqSOA" discussion; because much glyoxal is formed from isoprene, it may be that much of glyoxal-related aqueous-phase chemistry actually arises via the chemistry of the natural atmosphere. Such an analysis would be very helpful in the future: is aqueous-phase SOA formation mainly attributable to the chemistry of the unperturbed atmosphere, and what is the contribution of anthropogenic precursor emissions?

9.8. Air Pollution and Climate Change

The abatement of the emission of climate-active gases and particles should be accompanied by reductions in air pollution.[768−772] In the case of NO_x (≡NO + NO_2), this would be very desirable, as reduced NO_x emissions will lead to a less pronounced N_2O_5 chemistry and nitrate and acidity production together with its associated aqueous chemistry leading to NO_x/NO_y (≡sum of the reactive nitrogen: NO_x + NO_3 + 2 × N_2O_5 + HNO_2 + HNO_3 + HNO_4 + $ClONO_2$ + PAN (peroxyacetylnitrate) + other organic nitrates),[773] which could establish a partial recycling of NO_x/NO_y via nitrate photolysis and the coupling to chlorine chemistry. Reducing NO_x emissions could drive this chemistry in the direction of a natural level. However, the IPCC scenario calculations do not predict a decrease in global NO_x emissions until 30 years from now; in addition, the radiative forcing associated with NO_x is negative; that is, it has a cooling effect.

According to the AR5, the overall radiative forcing of aerosol, including that from mineral dust, sulfate, nitrate, OC, and BC, is expected to be more negative than positive. As discussed previously, aqueous-phase chemistry is strongly involved in the formation of particle sulfate; in addition, nitrate multiphase chemistry might change when NO_x changes. According to research discussed in this contribution, a fraction of the particle organic carbon (OC) is formed via aqueous-phase reactions, including radical and nonradical oxidation reactions and organic accretion reactions. In this context, the authors would like to remark that the analytical quantification of the carbonaceous fractions of aerosol particles in field experiments is a demanding future task and should be accompanied by proper process elucidation by laboratory studies and the respective modeling. As anthropogenic emissions contribute an important fraction of the compounds of interest here, aqueous-phase chemistry involved in the formation of SOA might become reduced when anthropogenic precursor emissions reduce to adhere to better air pollution standards as well as to reduced emissions of climate-relevant atmospheric constituents. However, as in the case of nitrate, particle OC has a negative radiative forcing. An analysis of how much aqSOA relates arises from natural versus anthropogenic emissions would be very helpful; at present, the authors are not aware of such an analysis.

Although it is clearly very difficult to predict how the relative importance of aqueous-phase bulk chemistry will change in the context of a changing atmosphere, the authors intended to introduce some ideas regarding the ways in which atmospheric

DOI: 10.1021/cr500447k
Chem. Rev. 2015, 115, 4259−4334

aqueous-phase chemistry may respond to the changing conditions predicted by the AR5 scenario calculations.

10. SUMMARY AND OUTLOOK: THE PERSPECTIVE OF THE FIELD

Over the past 25 years, a wide range of atmospheric aqueous-phase chemistry laboratory studies have been performed by groups investigating nonradical processes as well as groups more specialized in radical chemistry. Early efforts in Europe were very much due to the work of Peter Warneck and associated scientists such as H. Elias, L. Elding, W. Pasiuk-Bronikowska, and R. van Eldik. Much of the progress toward our current understanding of S(IV) goes back to the work of these colleagues. For summaries of this topic, the reader is referred to selected literature such as Warneck,[774] Borell and Borell,[775] and chapters in Zellner.[21]

It should be noted that even 25 years ago, researchers in the field of tropospheric aqueous-phase chemistry were already well aware that there are different regimes: a high-electrolyte concentration regime, encountered in ALW, and an about 4 orders of magnitude more dilute concentration regime, present in cloud droplets, and, in addition and when applicable, an intermediate fog regime. One key feature of past collaborations in Europe was the involvement of inorganic chemists in the quantitative study of systems related to S(IV) oxidation. Correspondingly, it might be worthwhile now to collaborate much more with organic chemists, because the focus of aqueous-phase chemistry has much changed into the study of organic systems, as can be seen from the content of this Review. This is true not only for radical reactions but also for reactions of organics with nonradical oxidants and, of even more interest at present, the study of reactions just between organic reactants, which lead to larger organic molecules and are addressed as "accretion reactions". There has been an enormous wealth of results on organic accretion and related reactions in the aqueous phase, which the authors have attempted to reflect in this Review. A second subarea where atmospheric chemists might fruitfully interact with colleagues from the other chemical sciences is, naturally, analytical chemistry. Many of the studies discussed in this Review have reported the analytical identification of new products, and here really pioneering work took place. Hence, to proceed further with understanding and being able to model the organic content of ambient aerosol particles, much more advanced analytical techniques both in the laboratory as well as in field measurements have to be developed and deployed. Third, the authors of this contribution would like to call for an increased focus on kinetic studies. Some of the recent studies have already begun to provide kinetic data, and the authors believe that this is an important topic of research over the next years: without kinetic studies, the community will be lost in speculation in adjusting aqueous-phase models to the new findings, which are, very luckily, now available. A slight call for care should also be presented here: not each "potentially important" accretion reaction observed in the laboratory will really be important in the real aerosol particles found in the environment. There should be more cross-talk between laboratory and field experimentalists to compare which accretion products can actually be found in real-world particles. It is recommended to use idealized conditions in the laboratory to elucidate undisturbed process kinetics but then screen the effects of the studied processes at least in a small box model with realistic conditions for atmospheric aqueous particle chemistry, or even in a more complex mixture mimicking atmospheric aqueous solutions, or, even still better, apply original aerosol, cloud, or fog solutions. The laboratory atmospheric chemist carries responsibility for a reasonable screening of the processes studied also under realistic and not just idealized conditions. This can apply to using the actinic region of the solar spectrum for photochemical experiments and not lower wavelengths, which could lead to unwanted effects as discussed before. Moreover, care should be taken that processes in the laboratory also have the potential to really be important under environmental conditions and not be suppressed by natural constituents or under natural conditions.

Can aqSOA fully resolve the open question of missing SOA sources? Most likely not, but it might, depending on conditions, contribute part of the missing sources and help in closing the budget. Currently, however, knowledge on multiphase chemistry is regarded as far from complete, and even if some compounds have a huge effective Henry's law constant, this does necessarily mean that they must lead to the most significant SOA contributions in real world particles, because aqSOA compounds, once formed, can readily be destroyed again by radicals or photochemistry. Certain pathways may, at times, currently gain much importance because other pathways are not yet correctly treated in models and hence are much underestimated. The current picture might not be a complete one; there is enormous uncertainty in the production of acids, that is, monocarboxylic acids (MCAs) and dicarboxylic acids (DCAs) together with their functionalized derivatives, for example. The possible SOA contribution from this huge compound group is not well assessed in multiphase models because of problems with (i) missing acid formation pathways, (ii) neglecting DCA degradation pathways, (iii) over- or underestimation of radical oxidant levels, (iv) uncertainty of freely available Fe(II) and Fe(III) and its feedback on DCA degradation and OH formation, and (v) uncertainty on HULIS/DOM levels and their role in complexing iron or triggering chemical conversion by themselves, for example, by photosensitization. Besides these uncertainties, aqueous-phase chemistry cannot be seen as restricted to small organic compounds; rather, the potential of higher organics, at least those that partition into aqueous solutions, must be explored.

It should not be forgotten that another candidate for resolving the SOA conundrum is, quite surprisingly, pure gas-phase chemistry, which leads to the production of highly oxidized products that can effectively partition into tropospheric particles.[776] It might be anticipated that our scientific understanding of SOA might be strongly improved by the combination of different SOA sources, then, of course, including the aqueous-phase SOA formation. It will be very interesting to assess the relative contributions of gas phase, bulk aqueous phase, and heterogeneous processes to the budget of important particle constituents with the demand for predictive modeling and, not at least, with the background of a changing planet and its changing atmosphere.

Newly identified aqueous-phase chemistry, such as found in the field of organic accretion reaction as treated in section 6.2, should not be considered alone in multiphase chemical mechanisms but rather coupled to known and also new radical chemistry, considering only one part will probably lead to an incomplete picture. Radical chemistry needs to be extended in multiphase chemical mechanisms to complete C_3 and C_4 chemistry and should then be further developed to deal with higher organics; this work is in progress.

DOI: 10.1021/cr500447k
Chem. Rev. 2015, 115, 4259−4334

A chemical aqueous-phase mechanism for aqueous-phase chemistry should be able to produce valid results by means of a scheme of elementary reactions, but, of course, reaction conditions will change when going from one system to the other. Differences in aqueous-phase conditions, but, additionally, in physical and chemical state, will influence how chemistry occurs and what throughput it produces both qualitatively and quantitatively. Some reaction paths will become more important and others less important upon changing from one set of conditions to another, but the basic full mechanistic scheme will be the same provided it has been designed in such a way that key reactions that are sensitive to the changing parameters of ionic strength, pH, and, last, but not least, temperature, follow these changes in a correct physicochemical manner. There is no need for extra aqueous aerosol mechanisms or separate cloud chemistry schemes; as the throughput in the mechanistic scheme will only change at some points, it is important to implement these "switching points" correctly. So, great care should be taken to formulate a mechanism or a parametrization that is solely suitable for ALW chemistry: What will happen if such particle is diluted as a result of activation to a cloud droplet; will the model switch off that part of chemistry? At such stage, any condition-dependent parametrization valid for ALW will lose its validity; hence, mechanisms must be created that are not condition-dependent. Parameterizations, when needed due to limited computing resources, should be carefully compared to at least box model runs of higher complexity. Overall, newly developed multiphase models need to be applied simulating advanced multiphase chamber experiments to validate the chemical model mechanism and future field experiments to support their data interpretations.

In the future, the principle of formulating mechanisms through elementary reactions should be followed, proper high-end analytical and kinetic studies should be performed, and the last remaining empirical rate laws (i.e., as seen in S(IV) oxidation, see above) should be removed from mechanistic schemes; this can only be done with a correct process understanding, however. In addition, care should be taken in creating new parametrizations just because our insights in organic chemistry mechanisms and especially kinetics are limited. When parametrizations are necessary due to computational restrictions, they should be based on comparisons to mechanisms that are as explicit as possible. In the long run, the elementary-step-based or, at least, "near-explicit" mechanism is the best choice. This has been proven correct in the past in combustion chemistry modeling as well as in gas-phase atmospheric chemistry, where the near-explicit MCM is now one of the cornerstones of model development.

AUTHOR INFORMATION

Corresponding Author

*Phone: ++49341 2717 7024. Fax: ++ 49341 2717 99 7024. E-mail: herrmann@tropos.de.

Notes

The authors declare no competing financial interest.

Biographies

Dr. Hartmut Herrmann, Professor of Atmospheric Chemistry, is the head of the Atmospheric Chemistry Department (ACD) of the Leibniz Institute for Tropospheric Research (TROPOS) in Leipzig (see http://www.tropos.de) and a member of both the Faculties of Physics and Chemistry at the University of Leipzig. He finished his Habilitation with Reinhard Zellner in 1998 and then moved from Essen to Leipzig. Previously, he was a scientific assistant at the Institute of Physical Chemistry of the University of Essen (1992−1998), a postdoc with Michael Hoffmann at Caltech (1992−1993), and, before, at Hannover (1991−1992) and Göttingen (1990) where he obtained both his Diploma (1987) and his Ph.D. (1990) at the Institute of Physical Chemistry. In 2011 he was a Visiting Professor in Lyon with Christian George. He is the Deputy Director of TROPOS since 2011. He is an Adjunct Professor at Fudan University (FDU), Shanghai, and a Visiting Professor at Shandong University (SDU, Jinan). His research aims at a better understanding of tropospheric multiphase chemistry. To this end, his group is engaged in field measurements on aerosols and clouds, laboratory studies of phase transfer, gas-, aqueous-phase, and heterogeneous reactions, and, finally, multiphase model development (CAPRAM).

Dr. Thomas Schaefer is a postdoc at the Leibniz Institute for Tropospheric Research (TROPOS) in Leipzig. He studied chemistry at the University of Leipzig and received his Diploma in 2007. Afterward, he did his Ph.D. (2012) at TROPOS. He is currently working on atmospheric aqueous-phase reactions.

DOI: 10.1021/cr500447k
Chem. Rev. 2015, 115, 4259−4334

Dr. Andreas Tilgner studied meteorology at the Faculty of Physics and Earth Sciences of the University of Leipzig, Germany. Since 2003, he is working at the chemistry department of Leibniz Institute for Tropospheric Research (TROPOS) in Leipzig, Germany, in the field of tropospheric multiphase chemistry. There, he received his diploma in 2004, worked as a Ph.D. student with support of the DBU (German Federal Environmental Foundation, 2005−2007), received his Ph.D. in April 2009, and is presently working as a research scientist. His research interests and expertise lie mainly in the field of tropospheric chemistry modeling with special emphasis on the development of complex multiphase chemical mechanisms and their application in sophisticated tropospheric models.

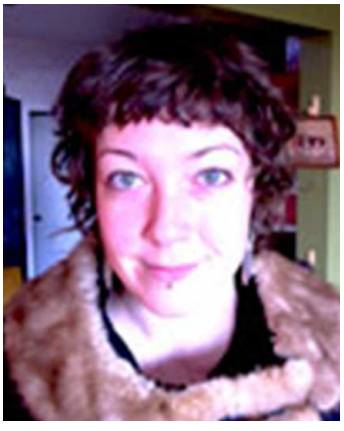

Dr. Sarah A. Styler received her Ph.D. from the University of Toronto in 2013 under the supervision of Dr. D. James Donaldson. Her doctoral work focused on the nature and consequences of photochemical interactions between mineral dust and gas-phase pollutants in urban environments. As a postdoctoral researcher at the Leibniz Institute for Tropospheric Research (TROPOS) in the laboratory of Dr. Hartmut Herrmann, she is currently working to characterize the photochemical reactive environment provided by "urban film", the complex chemical mixture that coats buildings, windows, and other surfaces in urban environments. In Autumn 2015, she will begin a position as an Assistant Professor of Environmental Chemistry at the University of Alberta.

Dr. Christian Weller studied geoecology at the TU Bergakademie Freiberg, Germany. At the Leibniz Institute for Tropospheric Research (TROPOS), he obtained his diploma in 2006 and started his Ph.D. on iron complex photochemistry, which he completed in 2011. He worked as a postdoc on multiphase amine chemistry, and he is interested in atmospheric aqueous-phase reactions, photochemistry, and analytics of organic trace compounds. Since July of 2014, Dr. Weller is with Thermo Scientific, Germany.

Monique Teich studied chemistry at the University of Leipzig, where she obtained her Master of Science degree in 2011. Since 2012, she is a Ph.D. student in the atmospheric chemistry department of the Leibniz Institute for Tropospheric Research (TROPOS). She is currently working on the analysis of single organic species in field samples and their relation to aerosol light absorption.

Tobias Otto studied chemistry at the Friedrich Schiller University in Jena and received his Diploma in 2013. He has been a Ph.D. student in the department of atmospheric chemistry of the Leibniz Institute for Tropospheric Research (TROPOS) since 2014. His research focus lies in the field of atmospheric aqueous-phase chemistry.

DOI: 10.1021/cr500447k
Chem. Rev. 2015, 115, 4259−4334

ACKNOWLEDGMENTS

We would like to thank Konstanze Kunze for her assistance with this manuscript. Our own, more recent aqueous-phase studies have been supported by DFG (ACETOX, MISOX, MISOX II) under FK HE 3086/8-1, HE 3086/13-1, and HE 3086/13-3. Other laboratory experiments were funded through the EU FW 7 project PEGASOS (FP7-265148). CAPRAM has been supported by DFG within FK HE 3086/15-1 in the HCCT-2010 project. Amine studies were supported by contractual work by TELTEK, Gasnova, and TCM via the contracts 2211030-AQ05, 257430116, 257430117, and 257430118.

REFERENCES

(1) Ervens, B.; Volkamer, R. *Atmos. Chem. Phys.* **2010**, *10*, 8219.
(2) Ervens, B.; Turpin, B. J.; Weber, R. J. *Atmos. Chem. Phys.* **2011**, *11*, 11069.
(3) Graedel, T. E.; Weschler, C. J. *Rev. Geophys. Space Phys.* **1981**, *19*, 505.
(4) Calvert, J. G.; Lazrus, A.; Kok, G. L.; Heikes, B. G.; Walega, J. G.; Lind, J.; Cantrell, C. A. *Nature* **1985**, *317*, 27.
(5) Goliff, W. S.; Stockwell, W. R.; Lawson, C. V. *Atmos. Environ.* **2013**, *68*, 174.
(6) Brandt, C.; van Eldik, R. *Chem. Rev.* **1995**, *95*, 119.
(7) He, H.; Li, C.; Loughner, C. P.; Li, Z.; Krotkov, N. A.; Yang, K.; Wang, L.; Zheng, Y.; Bao, X.; Zhao, G.; Dickerson, R. R. *J. Geophys. Res.: Atmos.* **2012**, *117*, D00K37.
(8) Alexander, B.; Park, R. J.; Jacob, D. J.; Gong, S. *J. Geophys. Res.: Atmos.* **2009**, *114*, D02309.
(9) Harris, E.; Sinha, B.; van Pinxteren, D.; Tilgner, A.; Fomba, K. W.; Schneider, J.; Roth, A.; Gnauk, T.; Fahlbusch, B.; Mertes, S.; Lee, T.; Collett, J. L., Jr.; Foley, S.; Borrmann, S.; Hoppe, P.; Herrmann, H. *Science* **2013**, *340*, 727.
(10) Jacob, D. J.; Waldman, J. M.; Munger, J. W.; Hoffmann, M. R. *Environ. Sci. Technol.* **1985**, *19*, 730.
(11) Jacob, D. J. *J. Geophys. Res.: Atmos.* **1986**, *91*, 9807.
(12) Herrmann, H. *Chem. Rev.* **2003**, *103*, 4691.
(13) Zellner, R.; Herrmann, H. *Adv. Environ. Sci.* **1995**, *24*, 381.
(14) Huie, R. E. Free Radical Chemistry of the Atmospheric Aqueous Phase. In *Progress and Problems in Atmospheric Chemistry*; Barker, J. R., Ed.; World Scientific: Singapore, 1995.
(15) Chebbi, A.; Carlier, P. *Atmos. Environ.* **1996**, *30*, 4233.
(16) Ravishankara, A. R. *Science* **1997**, *276*, 1058.
(17) Chameides, W. L.; Davis, D. D. *J. Geophys. Res.* **1982**, *87*, 4863.
(18) Chameides, W. L.; Davis, D. D. *Nature* **1983**, *304*, 427.
(19) Warneck, P. *Phys. Chem. Chem. Phys.* **1999**, *1*, 5471.
(20) Finlayson-Pitts, B. J.; Pitts, J. N., Jr. *Chemistry of the Upper and Lower Atmosphere: Theory, Experiments, and Applications*; Academic Press: San Diego, CA, 1999.
(21) Zellner, R. *Global Aspects of Atmospheric Chemistry*; Springer Science & Business Media: Berlin, 1999.
(22) Guzmán, M. I.; Colussi, A. J.; Hoffmann, M. R. *J. Phys. Chem. A* **2006**, *110*, 3619.
(23) Bateman, A. P.; Nizkorodov, S. A.; Laskin, J.; Laskin, A. *Phys. Chem. Chem. Phys.* **2011**, *13*, 12199.
(24) Altieri, K. E.; Seitzinger, S. P.; Carlton, A. G.; Turpin, B. J.; Klein, G. C.; Marshall, A. G. *Atmos. Environ.* **2008**, *42*, 1476.
(25) Griffith, E. C.; Carpenter, B. K.; Shoemaker, R. K.; Vaida, V. *Proc. Natl. Acad. Sci. U.S.A.* **2013**, *110*, 11714.
(26) Herckes, P.; Valsaraj, K. T.; Collett, J. L., Jr. *Atmos. Res.* **2013**, *132*, 434.
(27) Herrmann, H.; Wolke, R.; Müller, K.; Brüggemann, E.; Gnauk, T.; Barzaghi, P.; Mertes, S.; Lehmann, K.; Massling, A.; Birmili, W.; Wiedensohler, A.; Wieprecht, W.; Acker, K.; Jaeschke, W.; Kramberger, H.; Svrcina, B.; Bächmann, K.; Collett, J. L., Jr.; Galgon, D.; Schwirn, K.; Nowak, A.; van Pinxteren, D.; Plewka, A.; Chemnitzer, R.; Rüd, C.; Hofmann, D.; Tilgner, A.; Diehl, K.; Heinold, B.; Hinneburg, D.; Knoth, O.; Sehili, A. M.; Simmel, M.; Wurzler, S.; Majdik, Z.; Mauersberger, G.; Müller, F. *Atmos. Environ.* **2005**, *39*, 4169.
(28) Herckes, P.; Marcotte, A. R.; Wang, Y.; Collett, J. L., Jr. *Atmos. Res.* **2015**, *151*, 20.
(29) Hodas, N.; Sullivan, A. P.; Skog, K.; Keutsch, F. N.; Collett, J. L., Jr.; Decesari, S.; Facchini, M. C.; Carlton, A. G.; Laaksonen, A.; Turpin, B. J. *Environ. Sci. Technol.* **2014**, *48*, 11127.
(30) Wang, X. F.; Chen, J. M.; Sun, J. F.; Li, W. J.; Yang, L. X.; Wen, L.; Wang, W. X.; Wang, X. M.; Collett, J. L.; Shi, Y.; Zhang, Q. Z.; Hu, J. T.; Yao, L.; Zhu, Y. H.; Sui, X.; Sun, X. M.; Mellouki, A. *Sci. Total Environ.* **2014**, *493*, 133.
(31) Lim, Y. B.; Tan, Y.; Perri, M. J.; Seitzinger, S. P.; Turpin, B. J. *Atmos. Chem. Phys.* **2010**, *10*, 10521.
(32) Herrmann, H.; Zellner, R. Reactions of NO_3-Radicals in Aqueous Solution. In *N-Centered Radicals*; Alfassi, Z. B., Ed.; Wiley: Chichester, 1998.
(33) Deguillaume, L.; Leriche, M.; Desboeufs, K.; Mailhot, G.; George, C.; Chaumerliac, N. *Chem. Rev.* **2005**, *105*, 3388.
(34) Herrmann, H. *Phys. Chem. Chem. Phys.* **2007**, *9*, 3935.
(35) Herrmann, H.; Hoffmann, D.; Schaefer, T.; Bräuer, P.; Tilgner, A. *ChemPhysChem* **2010**, *11*, 3796.
(36) Potter, T. D.; Colman, B. R. *Handbook of Weather, Climate, and Water: Atmospheric Chemistry, Hydrology, and Societal Impacts*; Wiley-Interscience: Hoboken, NJ, 2003.
(37) George, C.; D'Anna, B.; Herrmann, H.; Weller, C.; Vaida, V.; Donaldson, D. J.; Bartels-Rausch, T.; Ammann, M. *Top. Curr. Chem.* **2014**, *339*, 1.
(38) Hallquist, M.; Wenger, J. C.; Baltensperger, U.; Rudich, Y.; Simpson, D.; Claeys, M.; Dommen, J.; Donahue, N. M.; George, C.; Goldstein, A. H.; Hamilton, J. F.; Herrmann, H.; Hoffmann, T.; Iinuma, Y.; Jang, M.; Jenkin, M. E.; Jimenez, J. L.; Kiendler-Scharr, A.; Maenhaut, W.; McFiggans, G.; Mentel, T. F.; Monod, A.; Prévôt, A. S. H.; Seinfeld, J. H.; Surratt, J. D.; Szmigielski, R.; Wildt, J. *Atmos. Chem. Phys.* **2009**, *9*, 5155.
(39) Wang, J.; Doussin, J. F.; Perrier, S.; Perraudin, E.; Katrib, Y.; Pangui, E.; Picquet-Varrault, B. *Atmos. Meas. Technol.* **2011**, *4*, 2465.
(40) Benz, S.; Megahed, K.; Möhler, O.; Saathoff, H.; Wagner, R.; Schurath, U. *J. Photochem. Photobiol., A* **2005**, *176*, 208.
(41) Tajiri, T.; Yamashita, K.; Murakami, M.; Saito, A.; Kusunoki, K.; Orikasa, N.; Lilie, L. *J. Meteorol. Soc. Jpn.* **2013**, *91*, 687.
(42) Schnitzhofer, R.; Metzger, A.; Breitenlechner, M.; Jud, W.; Heinritzi, M.; De Menezes, L.-P.; Duplissy, J.; Guida, R.; Haider, S.; Kirkby, J.; Mathot, S.; Minginette, P.; Onnela, A.; Walther, H.; Wasem, A.; Hansel, A.; CLOUD Team. *Atmos. Meas. Technol.* **2014**, *7*, 2159.
(43) Surratt, J. D.; Kroll, J. H.; Kleindienst, T. E.; Edney, E. O.; Claeys, M.; Sorooshian, A.; Ng, N. L.; Offenberg, J. H.; Lewandowski, M.; Jaoui, M.; Flagan, R. C.; Seinfeld, J. H. *Environ. Sci. Technol.* **2007**, *41*, 517.
(44) Iinuma, Y.; Müller, C.; Böge, O.; Gnauk, T.; Herrmann, H. *Atmos. Environ.* **2007**, *41*, 5571.
(45) Schindelka, J.; Iinuma, Y.; Hoffmann, D.; Herrmann, H. *Faraday Discuss.* **2013**, *165*, 237.
(46) El Haddad, I.; Liu, Y.; Nieto-Gligorovski, L.; Michaud, V.; Temime-Roussel, B.; Quivet, E.; Marchand, N.; Sellegri, K.; Monod, A. *Atmos. Chem. Phys.* **2009**, *9*, 5107.
(47) Liu, Y.; El Haddad, I.; Scarfogliero, M.; Nieto-Gligorovski, L.; Temime-Roussel, B.; Quivet, E.; Marchand, N.; Picquet-Varrault, B.; Monod, A. *Atmos. Chem. Phys.* **2009**, *9*, 5093.
(48) Michaud, V.; El Haddad, I.; Liu, Y.; Sellegri, K.; Laj, P.; Villani, P.; Picard, D.; Marchand, N.; Monod, A. *Atmos. Chem. Phys.* **2009**, *9*, 5119.
(49) Kampf, C. J.; Waxman, E. M.; Slowik, J. G.; Dommen, J.; Pfaffenberger, L.; Praplan, A. P.; Prévôt, A. S. H.; Baltensperger, U.; Hoffmann, T.; Volkamer, R. *Environ. Sci. Technol.* **2013**, *47*, 4236.
(50) Lee, A. K. Y.; Zhao, R.; Gao, S. S.; Abbatt, J. P. D. *J. Phys. Chem. A* **2011**, *115*, 10517.
(51) Nguyen, T. B.; Laskin, A.; Laskin, J.; Nizkorodov, S. A. *Phys. Chem. Chem. Phys.* **2012**, *14*, 9702.

DOI: 10.1021/cr500447k
Chem. Rev. 2015, 115, 4259−4334

(52) Daumit, K. E.; Carrasquillo, A. J.; Hunter, J. F.; Kroll, J. H. *Atmos. Chem. Phys.* **2014**, *14*, 10773.
(53) Sareen, N.; Schwier, A. N.; Shapiro, E. L.; Mitroo, D.; McNeill, V. F. *Atmos. Chem. Phys.* **2010**, *10*, 997.
(54) Sareen, N.; Moussa, S. G.; McNeill, V. F. *J. Phys. Chem. A* **2013**, *117*, 2987.
(55) Schwier, A. N.; Sareen, N.; Mitroo, D.; Shapiro, E. L.; McNeill, V. F. *Environ. Sci. Technol.* **2010**, *44*, 6174.
(56) Li, Z.; Schwier, A. N.; Sareen, N.; McNeill, V. F. *Atmos. Chem. Phys.* **2011**, *11*, 11617.
(57) Abbatt, J. P. D.; Lee, A. K. Y.; Thornton, J. A. *Chem. Soc. Rev.* **2012**, *41*, 6555.
(58) Kolb, C. E.; Cox, R. A.; Abbatt, J. P. D.; Ammann, M.; Davis, E. J.; Donaldson, D. J.; Garrett, B. C.; George, C.; Griffiths, P. T.; Hanson, D. R.; Kulmala, M.; McFiggans, G.; Poeschl, U.; Riipinen, I.; Rossi, M. J.; Rudich, Y.; Wagner, P. E.; Winkler, P. M.; Worsnop, D. R.; O' Dowd, C. D. *Atmos. Chem. Phys.* **2010**, *10*, 10561.
(59) Zhao, R.; Lee, A. K. Y.; Abbatt, J. P. D. *J. Phys. Chem. A* **2012**, *116*, 6253.
(60) Zhao, R.; Lee, A. K. Y.; Soong, R.; Simpson, A. J.; Abbatt, J. P. D. *Atmos. Chem. Phys.* **2013**, *13*, 5857.
(61) Vogel, A. L.; Äijälä, M.; Brüggemann, M.; Ehn, M.; Junninen, H.; Petäjä, T.; Worsnop, D. R.; Kulmala, M.; Williams, J.; Hoffmann, T. *Atmos. Meas. Technol.* **2013**, *6*, 431.
(62) Poulain, L.; Monod, A.; Wortham, H. *J. Photochem. Photobiol., A* **2007**, *187*, 10.
(63) Altieri, K. E.; Turpin, B. J.; Seitzinger, S. P. *Atmos. Chem. Phys.* **2009**, *9*, 2533.
(64) Kirkland, J. R.; Lim, Y. B.; Tan, Y.; Altieri, K. E.; Turpin, B. J. *Environ. Chem.* **2013**, *10*, 158.
(65) Lim, Y. B.; Tan, Y.; Turpin, B. J. *Atmos. Chem. Phys.* **2013**, *13*, 8651.
(66) Tan, Y.; Perri, M. J.; Seitzinger, S. P.; Turpin, B. J. *Environ. Sci. Technol.* **2009**, *43*, 8105.
(67) Tan, Y.; Carlton, A. G.; Seitzinger, S. P.; Turpin, B. J. *Atmos. Environ.* **2010**, *44*, 5218.
(68) Tan, Y.; Lim, Y. B.; Altieri, K. E.; Seitzinger, S. P.; Turpin, B. J. *Atmos. Chem. Phys.* **2012**, *12*, 801.
(69) Perri, M. J.; Seitzinger, S.; Turpin, B. J. *Atmos. Environ.* **2009**, *43*, 1487.
(70) Perri, M. J.; Lim, Y. B.; Seitzinger, S. P.; Turpin, B. J. *Atmos. Environ.* **2010**, *44*, 2658.
(71) Reinhardt, A.; Emmenegger, C.; Gerrits, B.; Panse, C.; Dommen, J.; Baltensperger, U.; Zenobi, R.; Kalberer, M. *Anal. Chem.* **2007**, *79*, 4074.
(72) Bateman, A. P.; Walser, M. L.; Desyaterik, Y.; Laskin, J.; Laskin, A.; Nizkorodov, S. A. *Environ. Sci. Technol.* **2008**, *42*, 7341.
(73) Boris, A. J.; Desyaterik, Y.; Collett, J. L., Jr. *Atmos. Res.* **2014**, *143*, 95.
(74) Mazzoleni, L. R.; Ehrmann, B. M.; Shen, X. H.; Marshall, A. G.; Collett, J. L., Jr. *Environ. Sci. Technol.* **2010**, *44*, 3690.
(75) Schmitt-Kopplin, P.; Gelencser, A.; Dabek-Zlotorzynska, E.; Kiss, G.; Hertkorn, N.; Harir, M.; Hong, Y.; Gebefügi, I. *Anal. Chem.* **2010**, *82*, 8017.
(76) Nizkorodov, S. A.; Laskin, J.; Laskin, A. *Phys. Chem. Chem. Phys.* **2011**, *13*, 3612.
(77) Laskin, J.; Laskin, A.; Roach, P. J.; Slysz, G. W.; Anderson, G. A.; Nizkorodov, S. A.; Bones, D. L.; Nguyen, L. Q. *Anal. Chem.* **2010**, *82*, 2048.
(78) Laskin, J.; Eckert, P. A.; Roach, P. J.; Heath, B. S.; Nizkorodov, S. A.; Laskin, A. *Anal. Chem.* **2012**, *84*, 7179.
(79) O'Brien, R. E.; Nguyen, T. B.; Laskin, A.; Laskin, J.; Hayes, P. L.; Liu, S.; Jimenez, J. L.; Russell, L. M.; Nizkorodov, S. A.; Goldstein, A. H. *J. Geophys. Res.: Atmos.* **2013**, *118*, 1042.
(80) Laskin, J.; Laskin, A.; Nizkorodov, S. A. *Int. Rev. Phys. Chem.* **2013**, *32*, 128.
(81) Hoffmann, T.; Huang, R.-J.; Kalberer, M. *Anal. Chem.* **2011**, *83*, 4649.
(82) Bateman, A. P.; Nizkorodov, S. A.; Laskin, J.; Laskin, A. *Phys. Chem. Chem. Phys.* **2009**, *11*, 7931.
(83) Bateman, A. P.; Nizkorodov, S. A.; Laskin, J.; Laskin, A. *Anal. Chem.* **2010**, *82*, 8010.
(84) Pratt, K. A.; Fiddler, M. N.; Shepson, P. B.; Carlton, A. G.; Surratt, J. D. *Atmos. Environ.* **2013**, *77*, 231.
(85) Mead, R. N.; Mullaugh, K. M.; Brooks Avery, G.; Kieber, R. J.; Willey, J. D.; Podgorski, D. C. *Atmos. Chem. Phys.* **2013**, *13*, 4829.
(86) LeClair, J. P.; Collett, J. L.; Mazzoleni, L. R. *Environ. Sci. Technol.* **2012**, *46*, 4312.
(87) Renard, P.; Siekmann, F.; Gandolfo, A.; Socorro, J.; Salque, G.; Ravier, S.; Quivet, E.; Clément, J.-L.; Traikia, M.; Delort, A.-M.; Voisin, D.; Vuitton, V.; Thissen, R.; Monod, A. *Atmos. Chem. Phys.* **2013**, *13*, 6473.
(88) Nørgaard, A. W.; Vibenholt, A.; Benassi, M.; Clausen, P. A.; Wolkoff, P. *J. Am. Soc. Mass Spectrom.* **2013**, *24*, 1090.
(89) Fang, W.; Gong, L.; Shan, X.; Liu, F.; Wang, Z.; Sheng, L. *Anal. Chem.* **2011**, *83*, 9024.
(90) Chalbot, M.-C. G.; Kavouras, I. G. *Environ. Pollut.* **2014**, *191*, 232.
(91) Paglione, M.; Saarikoski, S.; Carbone, S.; Hillamo, R.; Facchini, M. C.; Finessi, E.; Giulianelli, L.; Carbone, C.; Fuzzi, S.; Moretti, F.; Tagliavini, E.; Swietlicki, E.; Stenstrom, K. E.; Prévót, A. S. H.; Massoli, P.; Canaragatna, M.; Worsnop, D.; Decesari, S. *Atmos. Chem. Phys.* **2014**, *14*, 5089.
(92) Tagliavini, E.; Moretti, F.; Decesari, S.; Facchini, M. C.; Fuzzi, S.; Maenhaut, W. *Atmos. Chem. Phys.* **2006**, *6*, 1003.
(93) Davies, J. F.; Haddrell, A. E.; Miles, R. E. H.; Bull, C. R.; Reid, J. P. *J. Phys. Chem. A* **2012**, *116*, 10987.
(94) Davies, J. F.; Haddrell, A. E.; Rickards, A. M. J.; Reid, J. P. *Anal. Chem.* **2013**, *85*, 5819.
(95) Davies, J. F.; Miles, R. E. H.; Haddrell, A. E.; Reid, J. P. *Proc. Natl. Acad. Sci. U.S.A.* **2013**, *110*, 8807.
(96) Lienhard, D. M.; Huisman, A. J.; Bones, D. L.; Te, Y. F.; Luo, B. P.; Krieger, U. K.; Reid, J. P. *Phys. Chem. Chem. Phys.* **2014**, *16*, 16677.
(97) Malevanets, A.; Consta, S. *J. Chem. Phys.* **2013**, *138*, 9.
(98) Dennis-Smither, B. J.; Marshall, F. H.; Miles, R. E. H.; Preston, T. C.; Reid, J. P. *J. Phys. Chem. A* **2014**, *118*, 5680.
(99) Drisdell, W. S.; Saykally, R. J.; Cohen, R. C. *Proc. Natl. Acad. Sci. U.S.A.* **2009**, *106*, 18897.
(100) Duffey, K. C.; Shih, O.; Wong, N. L.; Drisdell, W. S.; Saykally, R. J.; Cohen, R. C. *Phys. Chem. Chem. Phys.* **2013**, *15*, 11634.
(101) Yli-Juuti, T.; Zardini, A. A.; Eriksson, A. C.; Hansen, A. M. K.; Pagels, J. H.; Swietlicki, E.; Svenningsson, B.; Glasius, M.; Worsnop, D. R.; Riipinen, I.; Bilde, M. *Environ. Sci. Technol.* **2013**, *47*, 12123.
(102) Zardini, A. A.; Riipinen, I.; Koponen, I. K.; Kulmala, M.; Bilde, M. *J. Aerosol Sci.* **2010**, *41*, 760.
(103) Denjean, C.; Formenti, P.; Picquet-Varrault, B.; Pangui, E.; Zapf, P.; Katrib, Y.; Giorio, C.; Tapparo, A.; Monod, A.; Temime-Roussel, B.; Decorse, P.; Mangeney, C.; Doussin, J. F. *Atmos. Chem. Phys. Discuss.* **2014**, *14*, 10543.
(104) Denjean, C.; Formenti, P.; Picquet-Varrault, B.; Camredon, M.; Pangui, E.; Zapf, P.; Katrib, Y.; Giorio, C.; Tapparo, A.; Temime-Roussel, B.; Monod, A.; Aumont, B.; Doussin, J. F. *Atmos. Chem. Phys.* **2015**, *15*, 883.
(105) Power, R. M.; Reid, J. P. *Rep. Prog. Phys.* **2014**, *77*, 074601.
(106) Reid, J. P.; Meresman, H.; Mitchem, L.; Symes, R. *Int. Rev. Phys. Chem.* **2007**, *26*, 139.
(107) Symes, R.; Sayer, R. M.; Reid, J. P. *Phys. Chem. Chem. Phys.* **2004**, *6*, 474.
(108) Hunt, O. R.; Ward, A. D.; King, M. D. *Phys. Chem. Chem. Phys.* **2015**, *17*, 2734.
(109) Schaefer, T.; Schindelka, J.; Hoffmann, D.; Herrmann, H. *J. Phys. Chem. A* **2012**, *116*, 6317.
(110) Schaefer, T.; Van Pinxteren, D.; Herrmann, H. *Environ. Sci. Technol.* **2015**, *49*, 343.
(111) Monod, A.; Chebbi, A.; Durand-Jolibois, R.; Carlier, P. *Atmos. Environ.* **2000**, *34*, 5283.

DOI: 10.1021/cr500447k
Chem. Rev. 2015, 115, 4259−4334

(112) Monod, A.; Chevallier, E.; Durand-Jolibois, R.; Doussin, J.; Picquet-Varrault, B.; Carlier, P. *Atmos. Environ.* **2007**, *41*, 2412.
(113) Renard, P.; Reed Harris, A. E.; Rapf, R. J.; Ravier, S.; Demelas, C.; Coulomb, B.; Quivet, E.; Vaida, V.; Monod, A. *J. Phys. Chem. C* **2014**, *118*, 29421.
(114) Kameel, F. R.; Hoffmann, M. R.; Colussi, A. J. *J. Phys. Chem. A* **2013**, *117*, 5117.
(115) Schöne, L.; Herrmann, H. *Atmos. Chem. Phys.* **2014**, *14*, 4503.
(116) Seinfeld, J. H.; Pandis, S. N. *Atmospheric Chemistry and Physics: From Air Pollution to Climate Change*; John Wiley & Sons, Inc.: Hoboken, NJ, 2006.
(117) Tost, H.; Jöckel, P.; Kerkweg, A.; Pozzer, A.; Sander, R.; Lelieveld, J. *Atmos. Chem. Phys.* **2007**, *7*, 2733.
(118) Bower, K. N.; Choularton, T. W.; Gallagher, M. W.; Beswick, K. M.; Flynn, M. J.; Allen, A. G.; Davison, B. M.; James, J. D.; Robertson, L.; Harrison, R. M.; Hewitt, C. N.; Cape, J. N.; McFadyen, G. G.; Milford, C.; Sutton, M. A.; Martinsson, B. G.; Frank, G.; Swietlicki, E.; Zhou, J.; Berg, O. H.; Mentes, B.; Papaspiropoulos, G.; Hansson, H. C.; Leck, C.; Kulmala, M.; Aalto, P.; Väkevä, M.; Berner, A.; Bizjak, M.; Fuzzi, S.; Laj, P.; Facchini, M. C.; Orsi, G.; Ricci, L.; Nielsen, M.; Allan, B. J.; Coe, H.; McFiggans, G.; Plane, J. M. C.; Collett, J. L., Jr.; Moore, K. F.; Sherman, D. E. *Tellus, Ser. B* **2000**, *52*, 750.
(119) Collett, J. L., Jr.; Herckes, P. Cloud Chemistry. In *Encyclopedia of Atmospheric Sciences*; Holton, J., Pyle, J., Curry, J. A., Eds.; Academic Press: New York, 2003.
(120) Wobrock, W.; Schell, D.; Maser, R.; Jaeschke, W.; Georgii, H. W.; Wieprecht, W.; Arends, B. G.; Mols, J. J.; Kos, G. P. A.; Fuzzi, S.; Facchini, M. C.; Orsi, G.; Berner, A.; Solly, I.; Kruisz, C.; Svenningsson, I. B.; Wiedensohler, A.; Hansson, H. C.; Ogren, J. A.; Noone, K. J.; Hallberg, A.; Pahl, S.; Schneider, T.; Winkler, P.; Winiwarter, W.; Colvile, R. N.; Choularton, T. W.; Flossmann, A. I.; Borrmann, S. *J. Atmos. Chem.* **1994**, *19*, 3.
(121) Brüggemann, E.; Gnauk, T.; Mertes, S.; Acker, K.; Auel, R.; Wieprecht, W.; Möller, D.; Collett, J. L., Jr.; Chang, H.; Galgon, D.; Chemnitzer, R.; Rüd, C.; Junek, R.; Wiedensohler, W.; Herrmann, H. *Atmos. Environ.* **2005**, *39*, 4291.
(122) Wieprecht, W.; Acker, K.; Mertes, S.; Collett, J. L., Jr.; Jaeschke, W.; Bruggemann, E.; Möller, D.; Herrmann, H. *Atmos. Environ.* **2005**, *39*, 4267.
(123) Guo, J.; Wang, Y.; Shen, X.; Wang, Z.; Lee, T.; Wang, X.; Li, P.; Sun, M.; Collett, J. L., Jr.; Wang, W.; Wang, T. *Atmos. Environ.* **2012**, *60*, 467.
(124) Li, P.; Li, X.; Yang, C.; Wang, X.; Chen, J.; Collett, J. L., Jr. *Atmos. Environ.* **2011**, *45*, 4034.
(125) Straub, D. J.; Hutchings, J. W.; Herckes, P. *Atmos. Environ.* **2012**, *47*, 195.
(126) Yue, Y.; Niu, S.; Zhao, L.; Zhang, Y.; Xu, F. *Pure Appl. Geophys.* **2012**, *169*, 2231.
(127) Kim, Y.; Sievering, H.; Boatman, J.; Wellman, D.; Pszenny, A. *J. Geophys. Res.: Atmos.* **1995**, *100*, 23027.
(128) Sander, R.; Crutzen, P. J. *J. Geophys. Res.* **1996**, *101*, 9121.
(129) Keene, W. C.; Sander, R.; Pszenny, A. A. P.; Vogt, R.; Crutzen, P. J.; Galloway, J. N. *J. Aerosol Sci.* **1998**, *29*, 339.
(130) Fridlind, A. M.; Jacobson, M. Z. *J. Geophys. Res.* **2000**, *105*, 17.
(131) von Glasow, R.; Sander, R. *Geophys. Res. Lett.* **2001**, *28*, 247.
(132) Li, S.-M.; Macdonald, A. M.; Strapp, J. W.; Lee, Y. N.; Zhou, X. L. *J. Geophys. Res.* **1997**, *102*, 21.
(133) Pathak, R. K.; Louie, P. K. K.; Chan, C. K. *Atmos. Environ.* **2004**, *38*, 2965.
(134) Stelson, A. W.; Seinfeld, J. H. *Environ. Sci. Technol.* **1981**, *15*, 671.
(135) Volkamer, R.; San Martini, F.; Molina, L. T.; Salcedo, D.; Jimenez, J. L.; Molina, M. J. *Geophys. Res. Lett.* **2007**, *34*, L19807.
(136) Pathak, R. K.; Wu, W. S.; Wang, T. *Atmos. Chem. Phys.* **2009**, *9*, 1711.
(137) Cheng, S. H.; Yang, L. X.; Zhou, X. H.; Xue, L. K.; Gao, X. M.; Zhou, Y.; Wang, W. X. *Atmos. Environ.* **2011**, *45*, 4631.
(138) Yao, X.; Ling, T. Y.; Fang, M.; Chan, C. K. *Atmos. Environ.* **2007**, *41*, 382.
(139) Hennigan, C. J.; Izumi, J.; Sullivan, A. P.; Weber, R. J.; Nenes, A. *Atmos. Chem. Phys.* **2015**, *15*, 2775.
(140) Scheinhardt, S.; Müller, K.; Spindler, G.; Herrmann, H. *Atmos. Environ.* **2013**, *74*, 102.
(141) Meng, Z.; Seinfeld, J. H.; Saxena, P.; Kim, Y. P. *Aerosol Sci. Technol.* **1995**, *22*, 111.
(142) Ludwig, J.; Klemm, O. *Water, Air, Soil Pollut.* **1990**, *49*, 35.
(143) Seinfeld, J. H. *Atmospheric Chemistry and Physics of Air Pollution*; John Wiley & Sons, Inc.: New York, 1986.
(144) Ganor, E.; Levin, Z.; Pardess, D. *Atmos. Environ., Part A* **1993**, *27*, 1821.
(145) San Martini, F. M.; Dunlea, E. J.; Volkamer, R.; Onasch, T. B.; Jayne, J. T.; Canagaratna, M. R.; Worsnop, D. R.; Kolb, C. E.; Shorter, J. H.; Herndon, S. C.; Zahniser, M. S.; Salcedo, D.; Dzepina, K.; Jimenez, J. L.; Ortega, J. M.; Johnson, K. S.; McRae, G. J.; Molina, L. T.; Molina, M. J. *Atmos. Chem. Phys.* **2006**, *6*, 4889.
(146) Clegg, S. L.; Brimblecombe, P.; Wexler, A. S. *J. Phys. Chem. A* **1998**, *102*, 2155.
(147) Ruzmaikin, A.; Aumann, H. H.; Manning, E. M. *J. Atmos. Sci.* **2014**, *71*, 2516.
(148) Stubenrauch, C. J.; Rossow, W. B.; Kinne, S.; Ackerman, S.; Cesana, G.; Chepfer, H.; Di Girolamo, L.; Getzewich, B.; Guignard, A.; Heidinger, A.; Maddux, B. C.; Menzel, W. P.; Minnis, P.; Pearl, C.; Platnick, S.; Poulsen, C.; Riedi, J.; Sun-Mack, S.; Walther, A.; Winker, D.; Zeng, S.; Zhao, G. *Bull. Am. Meteorol. Soc.* **2013**, *94*, 1031.
(149) Wylie, D.; Jackson, D. L.; Menzel, W. P.; Bates, J. J. *J. Clim.* **2005**, *18*, 3021.
(150) Pruppacher, H. R.; Jaenicke, R. *Atmos. Res.* **1995**, *38*, 283.
(151) Carlton, A. G.; Turpin, B. J. *Atmos. Chem. Phys.* **2013**, *13*, 10203.
(152) Zhang, K.; O'Donnell, D.; Kazil, J.; Stier, P.; Kinne, S.; Lohmann, U.; Ferrachat, S.; Croft, B.; Quaas, J.; Wan, H.; Rast, S.; Feichter, J. *Atmos. Chem. Phys.* **2012**, *12*, 8911.
(153) Jacobson, M. Z. *J. Geophys. Res.: Atmos.* **2001**, *106*, 1551.
(154) Adams, P. J.; Seinfeld, J. H.; Koch, D. M. *J. Geophys. Res.: Atmos.* **1999**, *104*, 13791.
(155) Metzger, S.; Dentener, F.; Krol, M.; Jeuken, A.; Lelieveld, J. *J. Geophys. Res.: Atmos.* **2002**, *107*, ACH 17.
(156) Schuster, G. L.; Lin, B.; Dubovik, O. *Geophys. Res. Lett.* **2009**, *36*, L03814.
(157) Ammann, M.; Cox, R. A.; Crowley, J. N.; Jenkin, M. E.; Mellouki, A.; Rossi, M. J.; Troe, J.; Wallington, T. J. *Atmos. Chem. Phys.* **2013**, *13*, 8045.
(158) Davidovits, P.; Kolb, C. E.; Williams, L. R.; Jayne, J. T.; Worsnop, D. R. *Chem. Rev.* **2011**, *111*, PR76.
(159) Sander, R. *Atmos. Chem. Phys. Discuss.* **2014**, *14*, 29615.
(160) Sander, R. *Surv. Geophys.* **1999**, *20*, 1.
(161) Raventos-Duran, T.; Camredon, M.; Valorso, R.; Mouchel-Vallon, C.; Aumont, B. *Atmos. Chem. Phys.* **2010**, *10*, 7643.
(162) Compernolle, S.; Müller, J. F. *Atmos. Chem. Phys.* **2014**, *14*, 2699.
(163) Compernolle, S.; Müller, J. F. *Atmos. Chem. Phys.* **2014**, *14*, 12815.
(164) Saxena, P.; Hildemann, L. *J. Atmos. Chem.* **1996**, *24*, 57.
(165) Doussin, J. F.; Monod, A. *Atmos. Chem. Phys.* **2013**, *13*, 11625.
(166) Buxton, G. V.; Greenstock, C. L.; Helman, W. P.; Ross, A. B. *J. Phys. Chem. Ref. Data* **1988**, *17*, 513.
(167) Buley, A. L.; Norman, R. O. C.; Pritchett, R. J. *J. Chem. Soc. B* **1966**, *0*, 849.
(168) Seidler, F.; von Sonntag, C. *Z. Naturforsch., B: Chem. Sci.* **1969**, *24*, 780.
(169) Burchill, C. E.; Perron, K. M. *Can. J. Chem.* **1971**, *49*, 2382.
(170) Bansal, K. M.; Gratzel, M.; Henglein, A.; Janata, E. *J. Phys. Chem.* **1973**, *77*, 16.
(171) Steenken, S.; Davies, M. J.; Gilbert, B. C. *J. Chem. Soc., Perkin Trans. 2* **1986**, *7*, 1003.

DOI: 10.1021/cr500447k
Chem. Rev. 2015, 115, 4259−4334

(172) Alfassi, Z. B.; Khaikin, G. I.; Johnson, R. D., III; Neta, P. *J. Phys. Chem.* **1996**, *100*, 15961.
(173) Baugh, P. J.; Moore, J. S.; Norris, A. F.; von Sonntag, C. *Radiat. Phys. Chem.* **1982**, *20*, 215.
(174) Fischer, H. *Mol. Phys.* **1965**, *9*, 149.
(175) Fitchett, M.; Gilbert, B. C.; Willson, R. L. *J. Chem. Soc., Perkin Trans. 2* **1988**, 673.
(176) Frey, P. A. *Chem. Rev.* **1990**, *90*, 1343.
(177) Gilbert, B. C.; King, D. M.; Thomas, C. B. *J. Chem. Soc., Perkin Trans. 2* **1982**, *2*, 169.
(178) Gilbert, B. C.; King, D. M.; Thomas, C. B. *Carbohydr. Res.* **1984**, *125*, 217.
(179) Gilbert, B. C.; Norman, R. O. C.; Larkin, J. P. *J. Chem. Soc., Perkin Trans. 2* **1972**, *6*, 794.
(180) Gilbert, B. C.; Stell, J. K. *J. Chem. Soc., Perkin Trans. 2* **1990**, *8*, 1281.
(181) Glushonok, G. K.; Glushonok, T. G.; Edimecheva, I. P.; Shadyro, O. I. *High Energy Chem.* **1999**, *33*, 364.
(182) Jiang, D.; Barata-Vallejo, S.; Golding, B. T.; Ferreri, C.; Chatgilialoglu, C. *Org. Biomol. Chem.* **2012**, *10*, 1102.
(183) Kosobutskii, V. S. *High Energy Chem.* **2006**, *40*, 277.
(184) Petryaev, E. P.; Pavlov, A. V.; Shadyro, O. I. *Zh. Org. Khim.* **1984**, *20*, 29.
(185) Schuchmann, H. P.; von Sonntag, C. *Z. Naturforsch., B: J. Chem. Sci.* **1984**, *39*, 217.
(186) Toraya, T. *Chem. Rev.* **2003**, *103*, 2095.
(187) Beckwith, A. L. J.; Crich, D.; Duggan, P. J.; Yao, Q. W. *Chem. Rev.* **1997**, *97*, 3273.
(188) Beckwith, A. L. J.; Duggan, P. J. *J. Chem. Soc., Perkin Trans. 2* **1992**, *10*, 1777.
(189) Cozens, F. L.; Lancelot, S. F.; Schepp, N. P. *J. Org. Chem.* **2007**, *72*, 10022.
(190) Xu, L. B.; Newcomb, M. *J. Org. Chem.* **2005**, *70*, 9296.
(191) Wang, T.; Liu, Z.; Wang, W.; Ge, M. *Atmos. Environ.* **2012**, *56*, 58.
(192) Feng, J.; Möller, D. *J. Atmos. Chem.* **2004**, *48*, 217.
(193) Olson, A. R.; Simonson, J. M. *J. Chem. Phys.* **1949**, *17*, 1167.
(194) Ali, H. M.; Iedema, M.; Yu, X. Y.; Cowin, J. P. *Atmos. Environ.* **2014**, *89*, 731.
(195) Gamsjäger, H.; Lorimer, J. W.; Salomon, M.; Shaw, D. G.; Tomkins, R. *Pure Appl. Chem.* **2010**, *82*, 1137.
(196) Weisenberger, S.; Schumpe, A. *AIChE J.* **1996**, *42*, 298.
(197) Masterto, W.; Lee, T. P. *J. Phys. Chem.* **1970**, *74*, 1776.
(198) Millero, F. J.; Huang, F.; Laferiere, A. L. *Geochim. Cosmochim. Acta* **2002**, *66*, 2349.
(199) Graziano, G. *Chem. Phys. Lett.* **2011**, *505*, 26.
(200) Graziano, G. *J. Chem. Eng. Data* **2009**, *54*, 464.
(201) Pitzer, K. S. *Activity Coefficients in Electrolyte Solutions*; CRC Press: Boca Raton, FL, 1991.
(202) Ruckenstein, E.; Shulgin, I. *Ind. Eng. Chem. Res.* **2002**, *41*, 4674.
(203) Ip, H. S. S.; Huang, X. H. H.; Yu, J. Z. *Geophys. Res. Lett.* **2009**, *36*, L01802.
(204) Tilgner, A.; Herrmann, H. *Atmos. Environ.* **2010**, *44*, 5415.
(205) Tilgner, A.; Bräuer, P.; Wolke, R.; Herrmann, H. *J. Atmos. Chem.* **2013**, *70*, 221.
(206) Shen, H.; Anastasio, C. *Atmos. Chem. Phys.* **2011**, *11*, 9671.
(207) Shen, H.; Anastasio, C. *Atmos. Environ.* **2012**, *46*, 665.
(208) Arakaki, T.; Anastasio, C.; Kuroki, Y.; Nakajima, H.; Okada, K.; Kotani, Y.; Handa, D.; Azechi, S.; Kimura, T.; Tsuhako, A.; Miyagi, Y. *Environ. Sci. Technol.* **2013**, *47*, 8196.
(209) Prausnitz, J. M.; Lichtenthaler, R. N.; de Azevedo, E. G. *Molecular Thermodynamics of Fluid-Phase Equilibria*; Prentice Hall: Upper Saddle River, NJ, 1998.
(210) Li, J.; Polka, H.-M.; Gmehling, J. *Fluid Phase Equilib.* **1994**, *94*, 89.
(211) Yan, W. D.; Topphoff, M.; Rose, C.; Gemhling, J. *Fluid Phase Equilib.* **1999**, *162*, 97.
(212) Ming, Y.; Russell, L. M. *AIChE J.* **2002**, *48*, 1331.
(213) Raatikainen, T.; Laaksonen, A. *Atmos. Chem. Phys.* **2005**, *5*, 2475.
(214) Topping, D. O.; McFiggans, G. B.; Coe, H. *Atmos. Chem. Phys.* **2005**, *5*, 1205.
(215) Zaveri, R. A.; Easter, R. C.; Wexler, A. S. *J. Geophys. Res.: Atmos.* **2005**, *110*, D02201.
(216) Erdakos, G. B.; Asher, W. E.; Seinfeld, J. H.; Pankow, J. F. *Atmos. Environ.* **2006**, *40*, 6410.
(217) Clegg, S. L.; Kleeman, M. J.; Griffin, R. J.; Seinfeld, J. H. *Atmos. Chem. Phys.* **2008**, *8*, 1057.
(218) Zuend, A.; Marcolli, C.; Booth, A. M.; Lienhard, D. M.; Soonsin, V.; Krieger, U. K.; Topping, D. O.; McFiggans, G.; Peter, T.; Seinfeld, J. H. *Atmos. Chem. Phys.* **2011**, *11*, 9155.
(219) Zuend, A.; Marcolli, C.; Luo, B. P.; Peter, T. *Atmos. Chem. Phys.* **2008**, *8*, 4559.
(220) Shrivastava, M.; Fast, J.; Easter, R.; Gustafson, W., Jr.; Zaveri, R. A.; Jimenez, J. L.; Saide, P.; Hodzic, A. *Atmos. Chem. Phys.* **2011**, *11*, 6639.
(221) Wolke, R.; Sehili, A. M.; Simmel, M.; Knoth, O.; Tilgner, A.; Herrmann, H. *Atmos. Environ.* **2005**, *39*, 4375.
(222) Herrmann, H.; Tilgner, A.; Barzaghi, P.; Majdik, Z.-T.; Gligorovski, S.; Poulain, L.; Monod, A. *Atmos. Environ.* **2005**, *39*, 4351.
(223) Rusumdar, A. J. Treatment of non-ideality in the multiphase model SPACCIM and investigation of its influence on tropospheric aqueous phase chemistry. Ph.D. Dissertation, Brandenburg University of Technology, Cottbus, Germany, 2013.
(224) Bartels-Rausch, T.; Jacobi, H. W.; Kahan, T. F.; Thomas, J. L.; Thomson, E. S.; Abbatt, J. P. D.; Ammann, M.; Blackford, J. R.; Bluhm, H.; Boxe, C.; Domine, F.; Frey, M. M.; Gladich, I.; Guzmán, M. I.; Heger, D.; Huthwelker, T.; Klán, P.; Kuhs, W. F.; Kuo, M. H.; Maus, S.; Moussa, S. G.; McNeill, V. F.; Newberg, J. T.; Pettersson, J. B. C.; Roeselová, M.; Sodeau, J. R. *Atmos. Chem. Phys.* **2014**, *14*, 1587.
(225) Zellner, R.; Exner, M.; Herrmann, H. *J. Atmos. Chem.* **1990**, *10*, 411.
(226) Chu, L.; Anastasio, C. *J. Phys. Chem. A* **2005**, *109*, 6264.
(227) Kwon, B. G.; Kwon, J. H. *J. Ind. Eng. Chem.* **2010**, *16*, 193.
(228) Chu, L.; Anastasio, C. *Environ. Sci. Technol.* **2007**, *41*, 3626.
(229) Roca, M.; Zahardis, J.; Bone, J.; El-Maazawi, M.; Grassian, V. H. *J. Phys. Chem. A* **2008**, *112*, 13275.
(230) Goldstein, S.; Rabani, J. *J. Am. Chem. Soc.* **2007**, *129*, 10597.
(231) Mack, J.; Bolton, J. R. *J. Photochem. Photobiol., A* **1999**, *128*, 1.
(232) Mark, G.; Korth, H.-G.; Schuchmann, H.-P.; von Sonntag, C. *J. Photochem. Photobiol., A* **1996**, *101*, 89.
(233) Sharpless, C. M.; Linden, K. G. *Environ. Sci. Technol.* **2001**, *35*, 2949.
(234) Madsen, D.; Larsen, J.; Jensen, S. K.; Keiding, S. R.; Thøgersen, J. *J. Am. Chem. Soc.* **2003**, *125*, 15571.
(235) Svoboda, O.; Kubelová, L.; Slavíček, P. *J. Phys. Chem. A* **2013**, *117*, 12868.
(236) Anastasio, C.; Chu, L. *Environ. Sci. Technol.* **2009**, *43*, 1108.
(237) Feng, Y. G.; Smith, D. W.; Bolton, J. R. *J. Environ. Eng. Sci.* **2007**, *6*, 277.
(238) Guan, Y. H.; Ma, J.; Li, X. C.; Fang, J. Y.; Chen, L. W. *Environ. Sci. Technol.* **2011**, *45*, 9308.
(239) Riordan, E.; Minogue, N.; Healy, D.; O'Driscoll, P.; Sodeau, J. R. *J. Phys. Chem. A* **2005**, *109*, 779.
(240) Minero, C.; Maurino, V.; Bono, F.; Pelizzetti, E.; Marinoni, A.; Mailhot, G.; Carlotti, M. E.; Vione, D. *Chemosphere* **2007**, *68*, 2111.
(241) Kang, N.; Anderson, T. A.; Rao, B.; Jackson, W. A. *Environ. Chem.* **2009**, *6*, 53.
(242) Hullar, T.; Anastasio, C. *Atmos. Chem. Phys.* **2011**, *11*, 7209.
(243) Charbouillot, T.; Brigante, M.; Deguillaume, L.; Mailhot, G. *Photochem. Photobiol.* **2012**, *88*, 32.
(244) Arakaki, T.; Kuroki, Y.; Okada, K.; Nakama, Y.; Ikota, H.; Kinjo, M.; Higuchi, T.; Uehara, M.; Tanahara, A. *Atmos. Environ.* **2006**, *40*, 4764.
(245) Weller, C.; Tilgner, A.; Bräuer, P.; Herrmann, H. *Environ. Sci. Technol.* **2014**, *48*, 5652.

DOI: 10.1021/cr500447k
Chem. Rev. 2015, 115, 4259−4334

(246) Jin, L.; Zhang, P. Y.; Shao, T.; Zhao, S. L. *J. Hazard. Mater.* **2014**, *271*, 9.
(247) Liu, D. D.; Xiu, Z. M.; Liu, F.; Wu, G.; Adamson, D.; Newell, C.; Vikesland, P.; Tsai, A. L.; Alvarez, P. J. *J. Hazard. Mater.* **2013**, *262*, 456.
(248) Vu, T. T. A.; Hou, L. W.; Wang, B. B.; Deng, N. S. *Res. J. Chem. Environ.* **2010**, *14*, 93.
(249) Ou, X. X.; Zhang, F. J.; Wang, C.; Wuyunna. *Asian J. Chem.* **2012**, *24*, 3314.
(250) Xiao, D. X.; Guo, Y. G.; Lou, X. Y.; Fang, C. L.; Wang, Z. H.; Liu, J. S. *Chemosphere* **2014**, *103*, 354.
(251) Ou, X.; Wang, C. X.; Zhang, F.; Quan, X.; Ma, Y.; Liu, H. *Front. Environ. Sci. Eng. China* **2010**, *4*, 157.
(252) Wang, Z. H.; Chen, C. C.; Ma, W. H.; Zhao, J. C. *J. Phys. Chem. Lett.* **2012**, *3*, 2044.
(253) Wang, Z. H.; Song, W. J.; Ma, W. H.; Zhao, J. C. *Prog. Chem.* **2012**, *24*, 423.
(254) Weller, C.; Horn, S.; Herrmann, H. *J. Photochem. Photobiol., A* **2013**, *255*, 41.
(255) Weller, C.; Horn, S.; Herrmann, H. *J. Photochem. Photobiol., A* **2013**, *268*, 24.
(256) Goldstein, S.; Rabani, J. *J. Photochem. Photobiol., A* **2008**, *193*, 50.
(257) Hatchard, C. G.; Parker, C. A. *Proc. R. Soc. London, Ser. A* **1956**, *235*, 518.
(258) Nicodem, D. E.; Aquilera, O. M. V. *J. Photochem.* **1983**, *21*, 189.
(259) Long, Y.; Charbouillot, T.; Brigante, M.; Mailhot, G.; Delort, A. M.; Chaumerliac, N.; Deguillaume, L. *Atmos. Environ.* **2013**, *77*, 686.
(260) Pozdnyakov, I. P.; Wu, F.; Melnikov, A. A.; Grivin, V. P.; Bazhin, N. M.; Chekalin, S. V.; Plyusnin, V. F. *Russ. Chem. Bull.* **2013**, *62*, 1579.
(261) Pozdnyakov, I. P.; Kolomeets, A. V.; Plyusnin, V. F.; Melnikov, A. A.; Kompanets, V. O.; Chekalin, S. V.; Tkachenko, N.; Lemmetyinen, H. *Chem. Phys. Lett.* **2012**, *530*, 45.
(262) Glebov, E. M.; Pozdnyakov, I. P.; Grivin, V. P.; Plyusnin, V. F.; Zhang, X.; Wu, F.; Deng, N. *Photochem. Photobiol. Sci.* **2011**, *10*, 425.
(263) Borer, P.; Hug, S. J. *J. Colloid Interface Sci.* **2014**, *416*, 44.
(264) Tofan-Lazar, J.; Al-Abadleh, H. A. *Environ. Sci. Technol.* **2014**, *48*, 394.
(265) Tofan-Lazar, J.; Situm, A.; Al-Abadleh, H. A. *J. Phys. Chem. A* **2013**, *117*, 10368.
(266) Wentworth, G. R.; Al-Abadleh, H. A. *Phys. Chem. Chem. Phys.* **2011**, *13*, 6507.
(267) Witt, M. L. I.; Skrabal, S.; Kieber, R.; Willey, J. *J. Atmos. Chem.* **2007**, *58*, 89.
(268) Carraher, J. M.; Pestovsky, O.; Bakac, A. *Dalton Trans.* **2012**, *41*, 5974.
(269) Wang, Z. H.; Liu, J. S. *Catal. Today* **2014**, *224*, 244.
(270) Epstein, S. A.; Nizkorodov, S. A. *Atmos. Chem. Phys.* **2012**, *12*, 8205.
(271) Epstein, S. A.; Tapavicza, E.; Furche, F.; Nizkorodov, S. A. *Atmos. Chem. Phys.* **2013**, *13*, 9461.
(272) Maron, M. K.; Takahashi, K.; Shoemaker, R. K.; Vaida, V. *Chem. Phys. Lett.* **2011**, *513*, 184.
(273) Eugene, A. J.; Xia, S. S.; Guzman, M. I. *Proc. Natl. Acad. Sci. U.S.A.* **2013**, *110*, E4274.
(274) Griffith, E. C.; Carpenter, B. K.; Shoemaker, R. K.; Vaida, V. *Proc. Natl. Acad. Sci. U.S.A.* **2013**, *110*, E4276.
(275) Reed Harris, A. E.; Ervens, B.; Shoemaker, R. K.; Kroll, J. A.; Rapf, R. J.; Griffith, E. C.; Monod, A.; Vaida, V. *J. Phys. Chem. A* **2014**, *118*, 8505.
(276) Larsen, M. C.; Vaida, V. *J. Phys. Chem. A* **2012**, *116*, 5840.
(277) Lignell, H.; Epstein, S. A.; Marvin, M. R.; Shemesh, D.; Gerber, R. B.; Nizkorodov, S. *J. Phys. Chem. A* **2013**, *117*, 12930.
(278) Galbavy, E. S.; Ram, K.; Anastasio, C. *J. Photochem. Photobiol., A* **2010**, *209*, 186.
(279) Albinet, A.; Minero, C.; Vione, D. *Chemosphere* **2010**, *80*, 753.
(280) Lignell, H.; Hinks, M. L.; Nizkorodov, S. A. *Proc. Natl. Acad. Sci. U.S.A.* **2014**, *111*, 13780.
(281) Zakon, Y.; Halicz, L.; Gelman, F. *Environ. Sci. Technol.* **2013**, *47*, 14147.
(282) Dallin, E.; Wan, P.; Krogh, E.; Gill, C.; Moore, R. M. *J. Photochem. Photobiol., A* **2009**, *207*, 297.
(283) Sun, Y. L.; Zhang, Q.; Anastasio, C.; Sun, J. *Atmos. Chem. Phys.* **2010**, *10*, 4809.
(284) Yu, L.; Smith, J.; Laskin, A.; Anastasio, C.; Laskin, J.; Zhang, Q. *Atmos. Chem. Phys.* **2014**, *14*, 13801.
(285) Smith, J. D.; Sio, V.; Yu, L.; Zhang, Q.; Anastasio, C. *Environ. Sci. Technol.* **2014**, *48*, 1049.
(286) Vione, D.; Maurino, V.; Minero, C.; Duncianu, M.; Olariu, R.-I.; Arsene, C.; Sarakha, M.; Mailhot, G. *Atmos. Environ.* **2009**, *43*, 2321.
(287) Li, Y. J.; Huang, D. D.; Cheung, H. Y.; Lee, A. K. Y.; Chan, C. K. *Atmos. Chem. Phys.* **2014**, *14*, 2871.
(288) Gan, D.; Jia, M.; Vaughan, P. P.; Falvey, D. E.; Blough, N. V. *J. Phys. Chem. A* **2008**, *112*, 2803.
(289) Rayne, S.; Forest, K.; Friesen, K. J. *Environ. Int.* **2009**, *35*, 425.
(290) Nielsen, C. J.; Herrmann, H.; Weller, C. *Chem. Soc. Rev.* **2012**, *41*, 6684.
(291) Kwon, B. G.; Kim, J. O.; Namkung, K. C. *Sci. Total Environ.* **2012**, *437*, 237.
(292) Bonn, B.; von Kuhlmann, R.; Lawrence, M. G. *Geophys. Res. Lett.* **2004**, *31*, 4.
(293) Betterton, E. A.; Hoffmann, M. R. *Environ. Sci. Technol.* **1988**, *22*, 1415.
(294) Marklund, S. *Acta Chem. Scand.* **1971**, *25*, 3517.
(295) Zhou, X.; Lee, Y. N. *J. Phys. Chem.* **1992**, *96*, 265.
(296) Kooijman, P. L.; Ghijsen, W. L. *Recl. Trav. Chim. Pays-Bas* **1947**, *66*, 205.
(297) Greenzaid, P.; Luz, Z.; Samuel, D. *J. Am. Chem. Soc.* **1967**, *89*, 756.
(298) Sørensen, P. E. *Acta Chem. Scand.* **1972**, *26*, 3357.
(299) Yaylayan, V. A.; Harty-Majors, S.; Ismail, A. A. *Carbohydr. Res.* **1998**, *309*, 31.
(300) Wasa, T.; Musha, S. *Bull. Univ. Osaka Prefect., Ser. A* **1970**, *19*, 169.
(301) Sørensen, P. E.; Bruhn, K.; Lindelov, F. *Acta Chem. Scand., Ser. A* **1974**, *28*, 162.
(302) Bruice, P. Y. *Organic Chemistry*; Pearson Education: Upper Saddle River, NJ, 2004.
(303) Lee, A. K. Y.; Zhao, R.; Li, R.; Liggio, J.; Li, S. M.; Abbatt, J. P. *Environ. Sci. Technol.* **2013**, *47*, 12819.
(304) Lakowicz, J. R. *Principles of Fluorescence Spectroscopy*; Springer: Luxemburg, 2007.
(305) Graber, E. R.; Rudich, Y. *Atmos. Chem. Phys.* **2006**, *6*, 729.
(306) Zheng, G.; He, K.; Duan, F.; Cheng, Y.; Ma, Y. *Environ. Pollut.* **2013**, *181*, 301.
(307) Sharpless, C. M.; Aeschbacher, M.; Page, S. E.; Wenk, J.; Sander, M.; McNeill, K. *Environ. Sci. Technol.* **2014**, *48*, 2688.
(308) Sun, L. N.; Chen, H. M.; Abdulla, H. A.; Mopper, K. *Environ. Sci.: Processes Impacts* **2014**, *16*, 757.
(309) Canonica, S.; Hellrung, B.; Wirz, J. *J. Phys. Chem. A* **2000**, *104*, 1226.
(310) Canonica, S.; Kohn, T.; Mac, M.; Real, F. J.; Wirz, J.; von Gunten, U. *Environ. Sci. Technol.* **2005**, *39*, 9182.
(311) Giese, B.; Napp, M.; Jacques, O.; Boudebous, H.; Taylor, A. M.; Wirz, J. *Angew. Chem., Int. Ed.* **2005**, *44*, 4073.
(312) Vione, D.; Maurino, V.; Minero, C.; Pelizzetti, E.; Harrison, M. A. J.; Olariu, R. I.; Arsene, C. *Chem. Soc. Rev.* **2006**, *35*, 441.
(313) Canonica, S.; Jans, U.; Stemmler, K.; Hoigne, J. *Environ. Sci. Technol.* **1995**, *29*, 1822.
(314) Zepp, R. G.; Baughman, G. L.; Schlotzhauer, P. F. *Chemosphere* **1981**, *10*, 109.
(315) Zepp, R. G.; Baughman, G. L.; Schlotzhauer, P. F. *Chemosphere* **1981**, *10*, 119.
(316) Zepp, R. G.; Schlotzhauer, P. F.; Simmons, M. S.; Miller, G. C.; Baughman, G. L.; Wolfe, N. L. *Fresenius' J. Anal. Chem.* **1984**, *319*, 119.

DOI: 10.1021/cr500447k
Chem. Rev. 2015, 115, 4259−4334

(317) Zepp, R. G.; Schlotzhauer, P. F.; Sink, R. M. *Environ. Sci. Technol.* **1985**, *19*, 74.
(318) Sumner, A. J.; Woo, J. L.; McNeill, V. F. *Environ. Sci. Technol.* **2014**, *48*, 11919.
(319) Monge, M. E.; Rosenørn, T.; Favez, O.; Müller, M.; Adler, G.; Riziq, A. A.; Rudich, Y.; Herrmann, H.; George, C.; D'Anna, B. *Proc. Natl. Acad. Sci. U.S.A.* **2012**, *109*, 6840.
(320) Aregahegn, K. Z.; Nozière, B.; George, C. *Faraday Discuss.* **2013**, *165*, 123.
(321) Rossignol, S.; Aregahegn, K. Z.; Tinel, L.; Fine, L.; Nozière, B.; George, C. *Environ. Sci. Technol.* **2014**, *48*, 3218.
(322) Alvarez, E. G.; Wortham, H.; Strekowski, R.; Zetzsch, C.; Gligorovski, S. *Environ. Sci. Technol.* **2012**, *46*, 1955.
(323) Tinel, L.; Dumas, S.; George, C. *C. R. Chim.* **2014**, *17*, 801.
(324) Brigante, M.; Charbouillot, T.; Vione, D.; Mailhot, G. *J. Phys. Chem. A* **2010**, *114*, 2830.
(325) Maddigapu, P. R.; Minero, C.; Maurino, V.; Vione, D.; Brigante, M.; Charbouillot, T.; Sarakha, M.; Mailhot, G. *Photochem. Photobiol. Sci.* **2011**, *10*, 601.
(326) Wenk, J.; Eustis, S. N.; McNeill, K.; Canonica, S. *Environ. Sci. Technol.* **2013**, *47*, 12802.
(327) De Laurentiis, E.; Minella, M.; Sarakha, M.; Marrese, A.; Minero, C.; Mailhot, G.; Brigante, M.; Vione, D. *Water Res.* **2013**, *47*, 5943.
(328) Vione, D.; Minella, M.; Maurino, V.; Minero, C. *Chem.—Eur. J.* **2014**, *34*, 10590.
(329) Albinet, A.; Minero, C.; Vione, D. *Sci. Total Environ.* **2010**, *408*, 3367.
(330) Remucal, C. K. *Environ. Sci.: Processes Impacts* **2014**, *16*, 628.
(331) Calza, P.; Vione, D.; Minero, C. *Sci. Total Environ.* **2014**, *493*, 411.
(332) Clark, C. D.; de Bruyn, W.; Jones, J. G. *Mar. Pollut. Bull.* **2014**, *79*, 54.
(333) Liu, X.; Song, X.; Zhang, S.; Wang, M.; Pan, B. *Phys. Chem. Chem. Phys.* **2014**, *16*, 7571.
(334) Liang, C.; Zhao, H. M.; Deng, M. J.; Quan, X.; Chen, S. *Adv. Mater. Res.* **2014**, *926−930*, 226.
(335) Ervens, B.; Sorooshian, A.; Lim, Y. B.; Turpin, B. J. *J. Geophys. Res.: Atmos.* **2014**, *119*, 3997.
(336) Fenton, H. J. H. *J. Chem. Soc., Trans.* **1894**, *65*, 899.
(337) Walling, C. *Acc. Chem. Res.* **1975**, *8*, 125.
(338) Zepp, R. G.; Faust, B. C.; Hoigné, J. *Environ. Sci. Technol.* **1992**, *26*, 313.
(339) Christensen, H.; Sehested, K.; Løgager, T. *Radiat. Phys. Chem.* **1993**, *41*, 575.
(340) Arakaki, T.; Faust, B. C. *J. Geophys. Res.: Atmos.* **1998**, *103*, 3487.
(341) Goldstein, S.; Meyerstein, D. *Acc. Chem. Res.* **1999**, *32*, 547.
(342) Pignatello, J. J.; Liu, D.; Huston, P. *Environ. Sci. Technol.* **1999**, *33*, 1832.
(343) Valavanidis, A.; Salika, A.; Theodoropoulou, A. *Atmos. Environ.* **2000**, *34*, 2379.
(344) Gozzo, F. *J. Mol. Catal. A: Chem.* **2001**, *171*, 1.
(345) Dunford, H. B. *Coord. Chem. Rev.* **2002**, *233−234*, 311.
(346) Kremer, M. L. *J. Phys. Chem. A* **2003**, *107*, 1734.
(347) Perez-Benito, J. F. *J. Phys. Chem. A* **2004**, *108*, 4853.
(348) Willey, J. D.; Whitehead, R. F.; Kieber, R. J.; Hardison, D. R. *Environ. Sci. Technol.* **2005**, *39*, 2579.
(349) Barbusinski, K. *Ecol. Chem. Eng. S* **2009**, *16*, 347.
(350) Chevallier, E.; Durand-Jolibois, R.; Meunier, N.; Carlier, P.; Monod, A. *Atmos. Environ.* **2004**, *38*, 921.
(351) See, S. W.; Wang, Y. H.; Balasubramanian, R. *Environ. Res.* **2007**, *103*, 317.
(352) von Gunten, U. *Water Res.* **2003**, *37*, 1443.
(353) Kilpatrick, M. L.; Herrick, C. C.; Kilpatrick, M. *J. Am. Chem. Soc.* **1956**, *78*, 1784.
(354) Hewes, C. G.; Davison, R. R. *AIChE J.* **1971**, *17*, 141.
(355) Hoigné, J.; Bader, H. *Water Res.* **1976**, *10*, 377.
(356) Staehelin, J.; Hoigné, J. *Environ. Sci. Technol.* **1982**, *16*, 676.
(357) Staehelin, J.; Hoigné, J. *Environ. Sci. Technol.* **1985**, *19*, 1206.
(358) Tomiyasu, H.; Fukutomi, H.; Gordon, G. *Inorg. Chem.* **1985**, *24*, 2962.
(359) Sotelo, J. L.; Beltran, F. J.; Benitez, F. J.; Beltran-Heredia, J. *Ind. Eng. Chem. Res.* **1987**, *26*, 39.
(360) Chen, Z. M.; Wang, H. L.; Zhu, L. H.; Wang, C. X.; Jie, C. Y.; Hua, W. *Atmos. Chem. Phys.* **2008**, *8*, 2255.
(361) Wan, L. K.; Peng, J.; Lin, M. Z.; Muroya, Y.; Katsumura, Y.; Fu, H. Y. *Radiat. Phys. Chem.* **2012**, *81*, 524.
(362) Huang, D.; Zhang, X.; Chen, Z. M.; Zhao, Y.; Shen, X. L. *Atmos. Chem. Phys.* **2011**, *11*, 7399.
(363) Schöne, L.; Schindelka, J.; Szeremeta, E.; Schaefer, T.; Hoffmann, D.; Rudzinski, K. J.; Szmigielski, R.; Herrmann, H. *Phys. Chem. Chem. Phys.* **2014**, *16*, 6257.
(364) Zhang, X.; Chen, Z. M.; Zhao, Y. *Atmos. Chem. Phys.* **2010**, *10*, 9551.
(365) Richards-Henderson, N. K.; Hansel, A. K.; Valsaraj, K. T.; Anastasio, C. *Atmos. Environ.* **2014**, *95*, 105.
(366) Minakata, D.; Song, W.; Crittenden, J. *Environ. Sci. Technol.* **2011**, *45*, 6057.
(367) Ervens, B.; Gligorovski, S.; Herrmann, H. *Phys. Chem. Chem. Phys.* **2003**, *5*, 1811.
(368) Teraji, T.; Arakaki, T. *Chem. Lett.* **2010**, *39*, 900.
(369) Swancutt, K. L.; Dail, M. K.; Mezyk, S. P.; Ishida, K. P. *Chemosphere* **2010**, *81*, 339.
(370) Prasanthkumar, K. P.; Suresh, C. H.; Aravindakumar, C. T. *J. Phys. Chem. A* **2012**, *116*, 10712.
(371) Mezyk, S. P.; Razavi, B.; Swancutt, K. L.; Cox, C. R.; Kiddle, J. J. *J. Phys. Chem. A* **2012**, *116*, 8185.
(372) Sanchez-Polo, M.; Daiem, M. M. A.; Ocampo-Perez, R.; Rivera-Utrilla, J.; Mota, J. J. *Sci. Total Environ.* **2013**, *463*, 423.
(373) Wu, M.-H.; Liu, N.; Xu, G.; Ma, J.; Tang, L.; Wang, L.; Fub, H.-Y. *Radiat. Phys. Chem.* **2011**, *80*, 420.
(374) An, T.; Gao, Y.; Li, G.; Kamat, P. V.; Peller, J.; Joyce, M. V. *Environ. Sci. Technol.* **2014**, *48*, 641.
(375) Wen, G.; Ma, J.; Liu, Z.-Q.; Zhao, L. *J. Hazard. Mater.* **2011**, *195*, 371.
(376) Ayatollahi, S.; Kalniņa, D.; Song, W.; Turks, M.; Cooper, W. J. *Radiat. Phys. Chem.* **2013**, *92*, 93.
(377) Zona, R.; Solar, S.; Sehested, K. *Radiat. Phys. Chem.* **2012**, *81*, 152.
(378) Venu, S.; Naik, D. B.; Sarkar, S. K.; Aravind, U. K.; Nijamudheen, A.; Aravindakumar, C. T. *J. Phys. Chem. A* **2013**, *117*, 291.
(379) Charbouillot, T.; Brigante, M.; Mailhot, G.; Maddigapu, P. R.; Minero, C.; Vione, D. *J. Photochem. Photobiol., A* **2011**, *222*, 70.
(380) Osiewała, L.; Socha, A.; Wolszczak, M.; Rynkowski, J. *Radiat. Phys. Chem.* **2013**, *87*, 71.
(381) Solar, S.; Getoff, N.; Zona, R.; Solar, W. *Radiat. Phys. Chem.* **2011**, *80*, 932.
(382) Biswal, J.; Paul, J.; Naik, D. B.; Sarkar, S. K.; Sabharwald, S. *Radiat. Phys. Chem.* **2013**, *85*, 161.
(383) Antonopoulou, M.; Evgenidou, E.; Lambropoulou, D.; Konstantinou, I. *Water Res.* **2014**, *53*, 215.
(384) Chelme-Ayala, P.; El-Din, M. G.; Smith, D. W.; Adams, C. D. *Water Res.* **2011**, *45*, 2517.
(385) Jeong, J.; Jung, J.; Cooper, W. J.; Song, W. *Water Res.* **2010**, *44*, 4391.
(386) Karpel Vel Leitner, N.; Roshani, B. *Water Res.* **2010**, *44*, 2058.
(387) Luo, X.; Zheng, Z.; Greaves, J.; Cooper, W. J.; Song, W. *Water Res.* **2012**, *46*, 1327.
(388) Özcan, A.; Şahin, Y.; Oturan, M. A. *Water Res.* **2013**, *47*, 1470.
(389) Ruggeri, G.; Ghigo, G.; Maurino, V.; Minero, C.; Vione, D. *Water Res.* **2013**, *47*, 6109.
(390) Shu, Z.; Bolton, J. R.; Belosevic, M.; El Din, M. G. *Water Res.* **2013**, *47*, 2881.
(391) Wojnárovits, L.; Takács, E. *Radiat. Phys. Chem.* **2014**, *96*, 120.
(392) Wu, C.; Linden, K. G. *Water Res.* **2010**, *44*, 3585.

DOI: 10.1021/cr500447k
Chem. Rev. 2015, 115, 4259−4334

(393) Yang, W.; Abdelmelek, S. B.; Zheng, Z.; An, T.; Zhang, D.; Song, W. *Water Res.* **2013**, *47*, 6558.
(394) Yu, H.; Nie, E.; Xu, J.; Yana, S.; Cooper, W. J.; Song, W. *Water Res.* **2014**, *47*, 1909.
(395) Anastasio, C.; McGregor, K. G. *Atmos. Environ.* **2001**, *35*, 1079.
(396) Vione, D.; Falletti, G.; Maurino, V.; Minero, C.; Pelizzetti, E.; Malandrino, M.; Ajassa, R.; Olariu, R. I.; Arsene, C. *Environ. Sci. Technol.* **2006**, *40*, 3775.
(397) Brezonik, P. L.; Fulkerson-Brekken, J. *Environ. Sci. Technol.* **1998**, *32*, 3004.
(398) Haag, W. R.; Hoigné, J. *Chemosphere* **1985**, *14*, 1659.
(399) Katsoyiannis, I. A.; Canonica, S.; von Gunten, U. *Water Res.* **2011**, *45*, 3811.
(400) Neta, P.; Huie, R. E. *J. Phys. Chem.* **1986**, *90*, 4644.
(401) *NIST Solution Kinetics Database Version 3.0*; National Institute of Science and Technology: Gaithersburg, MD, 1998.
(402) Weller, C.; Herrmann, H. *Atmos. Res.* **2015**, *151*, 64.
(403) Elias, G.; Mincher, B. J.; Mezyk, S. P.; Muller, J.; Martin, L. R. *Radiat. Phys. Chem.* **2011**, *80*, 554.
(404) Liggio, J.; Li, S. M.; McLaren, R. *Environ. Sci. Technol.* **2005**, *39*, 1532.
(405) Nozière, B.; Dziedzic, P.; Córdova, A. *J. Phys. Chem. A* **2009**, *113*, 231.
(406) Minerath, E. C.; Elrod, M. J. *Environ. Sci. Technol.* **2009**, *43*, 1386.
(407) De Haan, D. O.; Corrigan, A. L.; Smith, K. W.; Stroik, D. R.; Turley, J. J.; Lee, F. E.; Tolbert, M. A.; Jimenez, J. L.; Cordova, K. E.; Ferrell, G. R. *Environ. Sci. Technol.* **2009**, *43*, 2818.
(408) Yasmeen, F.; Sauret, N.; Gal, J.-F.; Maria, P.-C.; Massi, L.; Maenhaut, W.; Claeys, M. *Atmos. Chem. Phys.* **2010**, *10*, 3803.
(409) Sakugawa, H.; Kaplan, I. R.; Tsai, W. T.; Cohen, Y. *Environ. Sci. Technol.* **1990**, *24*, 1452.
(410) Anastasio, C.; Faust, B. C.; Allen, J. M. *J. Geophys. Res.: Atmos.* **1994**, *99*, 8231.
(411) Guo, J.; Tilgner, A.; Yeung, C.; Wang, Z.; Louie, P. K. K.; Luk, C. W. Y.; Xu, Z.; Yuan, C.; Gao, Y.; Poon, S.; Herrmann, H.; Lee, S.; Lam, K. S.; Wang, T. *Environ. Sci. Technol.* **2014**, *48*, 1443.
(412) Möller, D. *Atmos. Environ.* **2009**, *43*, 5923.
(413) Schumb, W. C.; Satterfield, C. N.; Wentworth, R. L. *Hydrogen Peroxide*; Reinhold Publishing Corp.: New York, 1955.
(414) Carlton, A. G.; Turpin, B. J.; Lim, H. J.; Altieri, K. E.; Seitzinger, S. *Geophys. Res. Lett.* **2006**, *33*, L0682.
(415) Dunicz, B. L.; Perrin, D. D.; Style, D. W. G. *Trans. Faraday Soc.* **1951**, *47*, 1210.
(416) Satterfield, C. N.; Case, L. C. *Ind. Eng. Chem.* **1954**, *46*, 998.
(417) *The Chemistry of the Carbonyl Group*; Zabicky, J., Ed.; Interscience Publishers: London, 1970; Vol. *2*.
(418) Blank, O.; Finkenbeiner, H. *Ber. Dtsch. Chem. Ges.* **1898**, *31*, 2979.
(419) Carlton, A. G.; Turpin, B. J.; Altieri, K. E.; Seitzinger, S.; Reff, A.; Lim, H.-J.; Ervens, B. *Atmos. Environ.* **2007**, *41*, 7588.
(420) Zhang, X.; Chen, Z. M.; Wang, H. L.; He, S. Z.; Huang, D. M. *Atmos. Environ.* **2009**, *43*, 4465.
(421) Claeys, M.; Wang, W.; Ion, A. C.; Kourtchev, I.; Gelencser, A.; Maenhaut, W. *Atmos. Environ.* **2004**, *38*, 4093.
(422) Stefan, M. I.; Bolton, J. R. *Environ. Sci. Technol.* **1999**, *33*, 870.
(423) Leitzke, A.; Reisz, E.; Flyunt, R.; von Sonntag, C. *J. Chem. Soc., Perkin Trans. 2* **2001**, *5*, 793.
(424) Amels, P.; Elias, H.; Wannowius, K.-J. *J. Chem. Soc., Faraday Trans.* **1997**, *93*, 2537.
(425) Bardouki, H.; Bacellos da Rosa, M.; Mihalopoulos, N.; Palm, W.-U.; Zetzsch, C. *Atmos. Environ.* **2002**, *36*, 4627.
(426) Sehested, K.; Corfitzen, H.; Holcman, J.; Fischer, C. H.; Hart, E. J. *Environ. Sci. Technol.* **1991**, *25*, 1589.
(427) Staehelin, J.; Buhler, R. E.; Hoigne, J. *J. Phys. Chem.* **1984**, *88*, 5999.
(428) Muñoz, F.; von Sonntag, C. *J. Chem. Soc., Perkins Trans. 2* **2000**, *10*, 2029.
(429) von Sonntag, C.; von Gunten, U. *Chemistry of Ozone in Water and Wastewater Treatment: from Basic Principles to Application*; IWA Publishing: London, 2012.
(430) Turan-Ertas, T.; Gurol, M. D. *Chemosphere* **2002**, *47*, 293.
(431) Zimin, Y. S.; Trukhanova, N. V.; Gerchikov, A. Y.; Butasova, E. M.; Zubairova, E. A. *Kinet. Catal.* **2000**, *41*, 745.
(432) Zimin, Y. S.; Trukhanova, N. V.; Rafikova, G. M.; Komissarov, V. D. *Kinet. Catal.* **1998**, *39*, 467.
(433) Lee, C.; Yoon, J.; von Gunten, U. *Water Res.* **2007**, *41*, 581.
(434) Pedersen, T.; Sehested, K. *Int. J. Chem. Kinet.* **2001**, *33*, 182.
(435) Leitzke, A.; von Sonntag, C. *Ozone Sci. Eng.* **2009**, *31*, 301.
(436) King, M. D.; Thompson, K. C.; Ward, A. D.; Pfrang, C.; Hughes, B. R. *Faraday Discuss.* **2008**, *137*, 173.
(437) Mvula, E.; von Sonntag, C. *Org. Biomol. Chem.* **2003**, *1*, 1749.
(438) Ramseier, M. K.; von Gunten, U. *Ozone Sci. Eng.* **2009**, *31*, 201.
(439) Beltrán, F. J.; Rodriguez, E. M.; Romero, M. T. *J. Hazard. Mater.* **2006**, *138*, 534.
(440) Leitzke, A.; Flyunt, R.; Theruvathu, J. A.; von Sonntag, C. *Org. Biomol. Chem.* **2003**, *1*, 1012.
(441) Dowideit, P.; von Sonntag, C. *Environ. Sci. Technol.* **1998**, *32*, 1112.
(442) Zhong, L.; Kuo, C.-H. *Chin. J. Chem. Eng.* **2000**, *8*, 272.
(443) Poznyak, T.; Vivero, J. *Ozone Sci. Eng.* **2005**, *27*, 447.
(444) Muñoz, F.; von Sonntag, C. *J. Chem. Soc., Perkins Trans. 2* **2000**, *4*, 661.
(445) Bin, A. K.; Machniewski, P.; Wolyniec, J.; Pienczakowska, A. *Ozone Sci. Eng.* **2013**, *35*, 489.
(446) Beltrán, F. J.; García-Araya, J. F.; Rivas, F. J.; Alvarez, P.; Rodríguez, E. *Ozone Sci. Eng.* **2000**, *22*, 167.
(447) Benner, J.; Salhi, E.; Ternes, T.; von Gunten, U. *Water Res.* **2008**, *42*, 3003.
(448) Jans, U. Radikalbildung aus Ozon in atmosphärischen Wassern-Einfluss von Licht, gelösten Stoffen und Rußpartikeln. Ph.D. Dissertation, ETH Zürich, Switzerland, 1996.
(449) Peter, A.; von Gunten, U. *Environ. Sci. Technol.* **2007**, *41*, 626.
(450) Ning, B.; Graham, N. J. D.; Zhang, Y. P. *Chemosphere* **2007**, *68*, 1163.
(451) Nagarnaik, P. M.; Desai, I.; Boulanger, B. In *World Environmental and Water Congress*; Patterson, C. L.; Struck, S. D.; Murray, D. J., Jr., Eds.; American Society of Civil Engineers: Cincinnati, OH, 2013; Vol. *4*.
(452) Deborde, M.; Rabouan, S.; Duguet, J.-P.; Legube, B. *Environ. Sci. Technol.* **2005**, *39*, 6086.
(453) Shen, J.-M.; Chen, Z.-l.; Xu, Z.-Z.; Li, X.-Y.; Xu, B.-B.; Qi, F. *J. Hazard. Mater.* **2008**, *152*, 1325.
(454) Beltrán, F. J.; Encinar, J. M.; Alonso, M. A. *Ind. Eng. Chem. Res.* **1998**, *37*, 25.
(455) Li, B.; Xu, X.; Zhu, L. *J. Chem. Technol. Biotechnol.* **2009**, *84*, 167.
(456) Kuosa, M.; Laari, A.; Solonen, A.; Haario, H.; Kallas, J. *Chem. Eng. Sci.* **2009**, *64*, 2332.
(457) Qiu, Y.; Zappi, M. E.; Kuo, C.-H.; Fleming, E. C. *J. Environ. Eng.* **1999**, *125*, 441.
(458) Benitez, F. J.; Beltrán-Heredia, J.; Acero, J. L.; Rubio, F. J. *J. Hazard. Mater.* **2000**, *79*, 271.
(459) Hoigné, J.; Bader, H. *Water Res.* **1983**, *17*, 173.
(460) Sharma, V. K.; Graham, N. J. D. *Ozone Sci. Eng.* **2010**, *32*, 81.
(461) Hoigné, J.; Bader, H. *Water Res.* **1983**, *17*, 185.
(462) Lee, Y.; von Gunten, U. *Water Res.* **2012**, *46*, 6177.
(463) Sung, M.; Huang, C. P. *J. Hazard. Mater.* **2007**, *141*, 140.
(464) Schumacher, J.; Pi, Y. Z.; Jekel, M. *Water Sci. Technol.* **2004**, *49*, 305.
(465) Rice, R. G. *Ozone Sci. Eng.* **1996**, *18*, 477.
(466) Pratarn, W.; Pornsiri, T.; Thanit, S.; Tawatchai, C.; Wiwut, T. *Chin. J. Chem. Eng.* **2011**, *19*, 76.
(467) Pera-Titus, M.; García-Molina, V.; Baños, M. A.; Giménez, J.; Esplugas, S. *Appl. Catal., B* **2004**, *47*, 219.
(468) Kim, K. W.; Rhee, D. S. *Adv. Mater. Res.* **2014**, *937*, 620.
(469) Jin, X.; Peldszus, S.; Huck, P. M. *Water Res.* **2012**, *46*, 6519.

DOI: 10.1021/cr500447k
Chem. Rev. 2015, 115, 4259−4334

(470) Ikehata, K.; Gamal El-Din, M.; Snyder, S. A. *Ozone Sci. Eng.* **2008**, *30*, 21.
(471) Clayden, J.; Greeves, N.; Warren, S.; Wothers, P. *Organic Chemistry*; Oxford University Press: New York, 2001.
(472) Wurtz, M. A. *Bull. Soc. Chim. Fr.* **1872**, *17*, 436.
(473) Jang, M.; Lee, S.; Kamens, R. M. *Atmos. Environ.* **2003**, *37*, 2125.
(474) Jang, M.; Czoschke, N. M.; Lee, S.; Kamens, R. M. *Science* **2002**, *298*, 814.
(475) Tolocka, M. P.; Jang, M.; Ginter, J. M.; Cox, F. J.; Kamens, R. M.; Johnston, M. V. *Environ. Sci. Technol.* **2004**, *38*, 1428.
(476) Czoschke, N. M.; Jang, M. *Atmos. Environ.* **2006**, *40*, 5629.
(477) Gao, S.; Ng, N. L.; Keywood, M.; Varutbangkul, V.; Bahreini, R.; Nenes, A.; He, J. W.; Yoo, K. Y.; Beauchamp, J. L.; Hodyss, R. P.; Flagan, R. C.; Seinfeld, J. H. *Environ. Sci. Technol.* **2004**, *38*, 6582.
(478) Kroll, J. H.; Ng, N. L.; Murphy, S. M.; Varutbangkul, V.; Flagan, R. C.; Seinfeld, J. H. *J. Geophys. Res.: Atmos.* **2005**, *110*, D23207.
(479) Duncan, J. L.; Schindler, L. R.; Roberts, J. T. *J. Phys. Chem. B* **1999**, *103*, 7247.
(480) Imamura, T.; Akiyoshi, H. *Geophys. Res. Lett.* **2000**, *27*, 1419.
(481) Esteve, W.; Nozière, B. *J. Phys. Chem. A* **2005**, *109*, 10920.
(482) Nozière, B.; Voisin, D.; Longfellow, C. A.; Friedli, H.; Henry, B. E.; Hanson, D. R. *J. Phys. Chem. A* **2006**, *110*, 2387.
(483) Casale, M. T.; Richman, A. R.; Elrod, M. J.; Garland, R. M.; Beaver, M. R.; Tolbert, M. A. *Atmos. Environ.* **2007**, *41*, 6212.
(484) Nozière, B.; Esteve, W. *Atmos. Environ.* **2007**, *41*, 1150.
(485) Lee, A. K. Y.; Li, Y. J.; Lau, A. P. S.; Chan, C. K. *Aerosol Sci. Technol.* **2008**, *42*, 992.
(486) Li, Y. J.; Lee, A. K. Y.; Lau, A. P. S.; Chan, C. K. *Environ. Sci. Technol.* **2008**, *42*, 7138.
(487) Zhao, J.; Levitt, N. P.; Zhang, R. Y. *Geophys. Res. Lett.* **2005**, *32*, L09802.
(488) Garland, R. M.; Elrod, M. J.; Kincaid, K.; Beaver, M. R.; Jimenez, J. L.; Tolbert, M. A. *Atmos. Environ.* **2006**, *40*, 6863.
(489) Nozière, B.; Dziedzic, P.; Córdova, A. *Phys. Chem. Chem. Phys.* **2010**, *12*, 3864.
(490) Nozière, B.; Córdova, A. *J. Phys. Chem. A* **2008**, *112*, 2827.
(491) Nozière, B.; Dziedzic, P.; Córdova, A. *Geophys. Res. Lett.* **2007**, *34*, L21812.
(492) Sedehi, N.; Takano, H.; Blasic, V. A.; Sullivan, K. A.; De Haan, D. O. *Atmos. Environ.* **2013**, *77*, 656.
(493) Baigrie, L. M.; Cox, R. A.; Slebocka-Tilk, H.; Tencer, M.; Tidwell, T. T. *J. Am. Chem. Soc.* **1985**, *107*, 3640.
(494) Zhang, Q.; Anastasio, C. *Atmos. Environ.* **2003**, *37*, 2247.
(495) Chan, K. M.; Huang, D. D.; Li, Y. J.; Chan, M. N.; Seinfeld, J. H.; Chan, C. K. *J. Atmos. Chem.* **2013**, *70*, 1.
(496) Chan, L. P.; Chan, C. K. *Aerosol Sci. Technol.* **2011**, *45*, 872.
(497) Williams, M. B.; Michelsen, R. R. H.; Axson, J. L.; Iraci, L. T. *Atmos. Environ.* **2010**, *44*, 1145.
(498) Drozd, G. T.; McNeill, V. F. *Environ. Sci.: Processes Impacts* **2014**, *16*, 741.
(499) Nguyen, T. B.; Roach, P. J.; Laskin, J.; Laskin, A.; Nizkorodov, S. A. *Atmos. Chem. Phys.* **2011**, *11*, 6931.
(500) Song, C.; Gyawali, M.; Zaveri, R. A.; Shilling, J. E.; Arnott, W. P. *J. Geophys. Res.: Atmos.* **2013**, *118*, 11741.
(501) De Haan, D. O.; Corrigan, A. L.; Tolbert, M. A.; Jimenez, J. L.; Wood, S. E.; Turley, J. J. *Environ. Sci. Technol.* **2009**, *43*, 8184.
(502) Nguyen, T. B.; Lee, P. B.; Updyke, K. M.; Bones, D. L.; Laskin, J.; Laskin, A.; Nizkorodov, S. A. *J. Geophys. Res.: Atmos.* **2012**, *117*, D01207.
(503) Nozière, B.; Esteve, W. *Geophys. Res. Lett.* **2005**, *32*, L03812.
(504) Powelson, M. H.; Espelien, B. M.; Hawkins, L. N.; Galloway, M. M.; De Haan, D. O. *Environ. Sci. Technol.* **2014**, *48*, 985.
(505) Nguyen, T. B.; Laskin, A.; Laskin, J.; Nizkorodov, S. A. *Faraday Discuss.* **2013**, *165*, 473.
(506) Bones, D. L.; Henricksen, D. K.; Mang, S. A.; Gonsior, M.; Bateman, A. P.; Nguyen, T. B.; Cooper, W. J.; Nizkorodov, S. A. *J. Geophys. Res.: Atmos.* **2010**, *115*, D05203.
(507) Phillips, S. M.; Smith, G. D. *Environ. Sci. Technol. Lett.* **2014**, *1*, 382.
(508) Hawkins, L. N.; Baril, M. J.; Sedehi, N.; Galloway, M. M.; De Haan, D. O.; Schill, G. P.; Tolbert, M. A. *Environ. Sci. Technol.* **2014**, *48*, 2273.
(509) Schill, G. P.; De Haan, D. O.; Tolbert, M. A. *Environ. Sci. Technol.* **2014**, *48*, 1675.
(510) Barsanti, K. C.; Pankow, J. F. *Atmos. Environ.* **2005**, *39*, 6597.
(511) Barsanti, K. C.; Pankow, J. F. *Atmos. Environ.* **2004**, *38*, 4371.
(512) Tong, C. H.; Blanco, M.; Goddard, W. A.; Seinfeld, J. H. *Environ. Sci. Technol.* **2006**, *40*, 2333.
(513) Krizner, H. E.; De Haan, D. O.; Kua, J. *J. Phys. Chem. A* **2009**, *113*, 6994.
(514) DePalma, J. W.; Horan, A. J.; Hall, W. A.; Johnston, M. V. *Phys. Chem. Chem. Phys.* **2013**, *15*, 6935.
(515) Hall, W. A.; Johnston, M. V. *J. Am. Soc. Mass Spectrom.* **2012**, *23*, 1097.
(516) Liggio, J.; Li, S. M. *J. Geophys. Res.: Atmos.* **2006**, *111*, D24303.
(517) Ziemann, P. J. *J. Phys. Chem. A* **2003**, *107*, 2048.
(518) Ziemann, P. J.; Atkinson, R. *Chem. Soc. Rev.* **2012**, *41*, 6582.
(519) Lim, Y. B.; Ziemann, P. J. *Phys. Chem. Chem. Phys.* **2009**, *11*, 8029.
(520) Aimanant, S.; Ziemann, P. J. *Aerosol Sci. Technol.* **2013**, *47*, 979.
(521) Jia, L.; Xu, Y. F. *Aerosol Sci. Technol.* **2014**, *48*, 1.
(522) Kua, J.; Galloway, M. M.; Millage, K. D.; Avila, J. E.; De Haan, D. O. *J. Phys. Chem. A* **2013**, *117*, 2997.
(523) Nguyen, T. B.; Laskin, J.; Laskin, A.; Nizkorodov, S. A. *Environ. Sci. Technol.* **2011**, *45*, 6908.
(524) Kundu, S.; Fisseha, R.; Putman, A. L.; Rahn, T. A.; Mazzoleni, L. R. *Atmos. Chem. Phys.* **2012**, *12*, 5523.
(525) Ortiz-Montalvo, D. L.; Lim, Y. B.; Perri, M. J.; Seitzinger, S. P.; Turpin, B. J. *Aerosol Sci. Technol.* **2012**, *46*, 1002.
(526) Guthrie, J. P. *Can. J. Chem.* **1975**, *53*, 898.
(527) Kua, J.; Krizner, H. E.; De Haan, D. O. *J. Phys. Chem. A* **2011**, *115*, 1667.
(528) Azofra, L. M.; Alkorta, I.; Elguero, J.; Toro-Labbé, A. *J. Phys. Chem. A* **2012**, *116*, 8250.
(529) Kroll, J. H.; Seinfeld, J. H. *Atmos. Environ.* **2008**, *42*, 3593.
(530) Ingold, C. *Structure and Mechanism in Organic Chemistry*; Cornell University Press: Ithaca, NY, 1969.
(531) Hilal, S. H. Estimation of Hydrolysis Rate Constants of Carboxylic Acid Ester and Phospahte Ester Compounds in Aqueous Systems from Molecular Structure by SPARC, 2006.
(532) Larson, R. A.; Weber, E. J. *Reaction Mechanisms in Environmental Organic Chemistry*; Lewis Publishers CRC Press: Boca Raton, FL, 1994.
(533) Barsanti, K. C.; Pankow, J. F. *Atmos. Environ.* **2006**, *40*, 6676.
(534) Lee, D. G.; Yan, Y. F.; Chandler, W. D. *Anal. Chem.* **1994**, *66*, 32.
(535) Mabey, W.; Mill, T. *J. Phys. Chem. Ref. Data* **1978**, *7*, 383.
(536) Surratt, J. D.; Murphy, S. M.; Kroll, J. H.; Ng, N. L.; Hildebrandt, L.; Sorooshian, A.; Szmigielski, R.; Vermeylen, R.; Maenhaut, W.; Claeys, M.; Flagan, R. C.; Seinfeld, J. H. *J. Phys. Chem. A* **2006**, *110*, 9665.
(537) Hamilton, J. F.; Lewis, A. C.; Reynolds, J. C.; Carpenter, L. J.; Lubben, A. *Atmos. Chem. Phys.* **2006**, *6*, 4973.
(538) Szmigielski, R.; Surratt, J. D.; Vermeylen, R.; Szmigielska, K.; Kroll, J. H.; Ng, N. L.; Murphy, S. M.; Sorooshian, A.; Seinfeld, J. H.; Claeys, M. *J. Mass Spectrom.* **2007**, *42*, 101.
(539) Zhang, H.; Surratt, J. D.; Lin, Y. H.; Bapat, J.; Kamens, R. M. *Atmos. Chem. Phys.* **2011**, *11*, 6411.
(540) Strollo, C. M.; Ziemann, P. J. *Atmos. Environ.* **2013**, *77*, 534.
(541) Birdsall, A. W.; Zentner, C. A.; Elrod, M. J. *Atmos. Chem. Phys.* **2013**, *13*, 3097.
(542) Galloway, M. M.; Chhabra, P. S.; Chan, A. W. H.; Surratt, J. D.; Flagan, R. C.; Seinfeld, J. H.; Keutsch, F. N. *Atmos. Chem. Phys.* **2009**, *9*, 3331.

DOI: 10.1021/cr500447k
Chem. Rev. 2015, 115, 4259−4334

(543) Kristensen, K.; Enggrob, K. L.; King, S. M.; Worton, D. R.; Platt, S. M.; Mortensen, R.; Rosenoern, T.; Surratt, J. D.; Bilde, M.; Goldstein, A. H.; Glasius, M. *Atmos. Chem. Phys.* **2013**, *13*, 3763.
(544) Raja, S.; Raghunathan, R.; Yu, X. Y.; Lee, T. Y.; Chen, J.; Kommalapati, R. R.; Murugesan, K.; Shen, X.; Qingzhong, Y.; Valsaraj, K. T.; Collett, J. L., Jr. *Atmos. Environ.* **2008**, *42*, 2048.
(545) Raja, S.; Raghunathan, R.; Kommalapati, R. R.; Shen, X. H.; Collett, J. L., Jr.; Valsaraj, K. T. *Atmos. Environ.* **2009**, *43*, 4214.
(546) Kimura, H. *J. Polym. Sci., Part A: Polym. Chem.* **1998**, *36*, 189.
(547) Jaenicke, R. *Ber. Bunsen-Ges. Phys. Chem.* **1978**, *82*, 1198.
(548) McNeill, V. F.; Woo, J. L.; Kim, D. D.; Schwier, A. N.; Wannell, N. J.; Sumner, A. J.; Barakat, J. M. *Environ. Sci. Technol.* **2012**, *46*, 8075.
(549) Klimont, Z.; Smith, S. J.; Cofala, J. *Environ. Res. Lett.* **2013**, *8*, 6.
(550) Gupta, K. S. *J. Indian Chem. Soc.* **2012**, *89*, 713.
(551) Harris, E.; Sinha, B.; van Pinxteren, D.; Schneider, J.; Poulain, L.; Collett, J. L., Jr.; D'Anna, B.; Fahlbusch, B.; Foley, S.; Fomba, K. W.; George, C.; Gnauk, T.; Henning, S.; Lee, T.; Mertes, S.; Roth, A.; Stratmann, F.; Borrmann, S.; Hoppe, P.; Herrmann, H. *Atmos. Chem. Phys.* **2014**, *14*, 4219.
(552) Harris, E.; Sinha, B.; Foley, S.; Crowley, J. N.; Borrmann, S.; Hoppe, P. *Atmos. Chem. Phys.* **2012**, *12*, 4867.
(553) Sarwar, G.; Simon, H.; Fahey, K.; Mathur, R.; Goliff, W. S.; Stockwell, W. R. *Atmos. Environ.* **2014**, *85*, 204.
(554) Gong, W. M.; Stroud, C.; Zhang, L. M. *Atmosphere* **2011**, *2*, 567.
(555) Zuo, Y. G.; Zhan, J.; Wu, T. X. *J. Atmos. Chem.* **2005**, *50*, 195.
(556) Podkrajšek, B.; Grgić, I.; Turšič, J.; Berčič, G. J. *J. Atmos. Chem.* **2006**, *54*, 103.
(557) Mudgal, P. K.; Sharma, A. K.; Mishra, C. D.; Bansal, S. P.; Gupta, K. S. *J. Atmos. Chem.* **2008**, *61*, 31.
(558) Dhayal, Y.; Chandel, C. P. S.; Gupta, K. S. *Environ. Sci. Pollut. Res.* **2014**, *21*, 7805.
(559) Dhayal, Y.; Chandel, C. P. S.; Gupta, K. S. *Environ. Sci. Pollut. Res.* **2014**, *21*, 3474.
(560) Kahan, T. F.; Ardura, D.; Donaldson, D. J. *J. Phys. Chem. A* **2010**, *114*, 2164.
(561) Jacob, D. J. *Atmos. Environ.* **2000**, *34*, 2131.
(562) Brune, W. H.; Tan, D.; Faloona, I. F.; Jaeglé, L.; Jacob, D. J.; Heikes, B. G.; Snow, J.; Kondo, Y.; Shetter, R.; Sachse, G. W.; Anderson, B.; Gregory, G. L.; Vay, S.; Singh, H. B.; Davis, D. D.; Crawford, J. H.; Blake, D. R. *Geophys. Res. Lett.* **1999**, *26*, 3077.
(563) Commane, R.; Floquet, C. F. A.; Ingham, T.; Stone, D.; Evans, M. J.; Heard, D. E. *Atmos. Chem. Phys.* **2010**, *10*, 8783.
(564) Tilgner, A.; Majdik, Z.; Sehili, A. M.; Simmel, M.; Wolke, R.; Herrmann, H. *Atmos. Environ.* **2005**, *39*, 4389.
(565) Monod, A.; Carlier, P. *Atmos. Environ.* **1999**, *33*, 4431.
(566) Stavrakou, T.; Müller, J.-F.; Boersma, K. F.; van der A, R. J.; Kurokawa, J.; Ohara, T.; Zhang, Q. *Atmos. Chem. Phys.* **2013**, *13*, 9057.
(567) Mozurkewich, M.; McMurry, P. H.; Gupta, A.; Calvert, J. G. *J. Geophys. Res.: Atmos.* **1987**, *92*, 4163.
(568) Hanson, D. R.; Burkholder, J. B.; Howard, C. J.; Ravishankara, A. R. *J. Phys. Chem.* **1992**, *96*, 4979.
(569) Thornton, J.; Abbatt, J. P. D. *J. Geophys. Res.: Atmos.* **2005**, *110*, D08309.
(570) George, I. J.; Matthews, P. S. J.; Whalley, L. K.; Brooks, B.; Goddard, A.; Baeza-Romero, M. T.; Heard, D. E. *Phys. Chem. Chem. Phys.* **2013**, *15*, 12829.
(571) Taketani, F.; Kanaya, Y.; Akimoto, H. *Atmos. Environ.* **2009**, *43*, 1660.
(572) Taketani, F.; Kanaya, Y.; Akimoto, H. *J. Phys. Chem. A* **2008**, *112*, 2370.
(573) Thornton, J. A.; Jaeglé, L.; McNeill, V. F. *J. Geophys. Res.: Atmos.* **2008**, *113*, D05303.
(574) Loukhovitskaya, E.; Bedjanian, Y.; Morozov, I.; Le Bras, G. *Phys. Chem. Chem. Phys.* **2009**, *11*, 7896.
(575) Rabani, J.; Klug-Roth, D.; Lilie, J. *J. Phys. Chem.* **1973**, *77*, 1169.
(576) Cooper, P. L.; Abbatt, J. P. D. *J. Phys. Chem.* **1996**, *100*, 2249.
(577) Taketani, F.; Kanaya, Y.; Pochanart, P.; Liu, Y.; Li, J.; Okuzawa, K.; Kawamura, K.; Wang, Z.; Akimoto, H. *Atmos. Chem. Phys.* **2012**, *12*, 11907.
(578) de Reus, M.; Fischer, H.; Sander, R.; Gros, V.; Kormann, R.; Salisbury, G.; Van Dingenen, R.; Williams, J.; Zöllner, M.; Lelieveld, J. *Atmos. Chem. Phys.* **2005**, *5*, 1787.
(579) Mao, J.; Jacob, D. J.; Evans, M. J.; Olson, J. R.; Ren, X.; Brune, W. H.; St Clair, J. M.; Crounse, J. D.; Spencer, K. M.; Beaver, M. R.; Wennberg, P. O.; Cubison, M. J.; Jimenez, J. L.; Fried, A.; Weibring, P.; Walega, J. G.; Hall, S. R.; Weinheimer, A. J.; Cohen, R. C.; Chen, G.; Crawford, J. H.; McNaughton, C.; Clarke, A. D.; Jaeglé, L.; Fisher, J. A.; Yantosca, R. M.; Le Sager, P.; Carouge, C. *Atmos. Chem. Phys.* **2010**, *10*, 5823.
(580) Liang, H.; Chen, Z. M.; Huang, D.; Zhao, Y.; Li, Z. Y. *Atmos. Chem. Phys.* **2013**, *13*, 11259.
(581) Mao, J.; Fan, S.; Jacob, D. J.; Travis, K. R. *Atmos. Chem. Phys.* **2013**, *13*, 509.
(582) Olson, J. R.; Crawford, J. H.; Chen, G.; Fried, A.; Evans, M. J.; Jordan, C. E.; Sandholm, S. T.; Davis, D. D.; Anderson, B. E.; Avery, M. A.; Barrick, J. D.; Blake, D. R.; Brune, W. H.; Eisele, F. L.; Flocke, F.; Harder, H.; Jacob, D. J.; Kondo, Y.; Lefer, B. L.; Martinez, M.; Mauldin, R. L.; Sachse, G. W.; Shetter, R. E.; Singh, H. B.; Talbot, R. W.; Tan, D. *J. Geophys. Res.: Atmos.* **2004**, *109*, D15S10.
(583) Whalley, L. K.; George, I. J.; Stone, D.; Heard, D. E. *American Geophysical Union Fall Meeting 2011 abstract #A43D-0174*; American Geophysical Union: San Francisco, CA, 2011.
(584) Whalley, L. K.; Stone, D.; George, I. J.; Mertes, S.; van Pinxteren, D.; Tilgner, A.; Herrmann, H.; Evans, M. J.; Heard, D. E. *Atmos. Chem. Phys.* **2015**, *15*, 3289.
(585) Lelieveld, J.; Crutzen, P. J. *J. Atmos. Chem.* **1991**, *12*, 229.
(586) Kanaya, Y.; Cao, R.; Kato, S.; Miyakawa, Y.; Kajii, Y.; Tanimoto, H.; Yokouchi, Y.; Mochida, M.; Kawamura, K.; Akimoto, H. *J. Geophys. Res.: Atmos.* **2007**, *112*, D11308.
(587) Sommariva, R.; Haggerstone, A.-L.; Carpenter, L. J.; Carslaw, N.; Creasey, D. J.; Heard, D. E.; Lee, J. D.; Lewis, A. C.; Pilling, M. J.; Zador, J. *Atmos. Chem. Phys.* **2004**, *4*, 839.
(588) Kanaya, Y.; Hofzumahaus, A.; Dorn, H.-P.; Brauers, T.; Fuchs, H.; Holland, F.; Rohrer, F.; Bohn, B.; Tillmann, R.; Wegener, R.; Wahner, A.; Kajii, Y.; Miyamoto, K.; Nishida, S.; Watanabe, K.; Yoshino, A.; Kubistin, D.; Martinez, M.; Rudolf, M.; Harder, H.; Berresheim, H.; Elste, T.; Plass-Duelmer, C.; Stange, G.; Kleffmann, J.; Elshorbany, Y.; Schurath, U. *Atmos. Chem. Phys.* **2012**, *12*, 2567.
(589) Stone, D.; Whalley, L. K.; Heard, D. E. *Chem. Soc. Rev.* **2012**, *41*, 6348.
(590) Taketani, F.; Kanaya, Y.; Akimoto, H. *Int. J. Chem. Kinet.* **2013**, *45*, 560.
(591) Chang, W. L.; Bhave, P. V.; Brown, S. S.; Riemer, N.; Stutz, J.; Dabdub, D. *Aerosol Sci. Technol.* **2011**, *45*, 665.
(592) Finlayson-Pitts, B. J.; Ezell, M. J.; Pitts, J. N. *Nature* **1989**, *337*, 241.
(593) Behnke, W.; Krüger, H.-U.; Scheer, V.; Zetzsch, C. *J. Aerosol Sci.* **1991**, *22*, S609.
(594) George, C.; Ponche, J. L.; Mirabel, P.; Behnke, W.; Scheer, V.; Zetzsch, C. *J. Phys. Chem.* **1994**, *98*, 8780.
(595) Behnke, W.; George, C.; Scheer, V.; Zetzsch, C. *J. Geophys. Res.: Atmos.* **1997**, *102*, 3795.
(596) Osthoff, H. D.; Roberts, J. M.; Ravishankara, A. R.; Williams, E. J.; Lerner, B. M.; Sommariva, R.; Bates, T. S.; Coffman, D.; Quinn, P. K.; Dibb, J. E.; Stark, H.; Burkholder, J. B.; Talukdar, R. K.; Meagher, J.; Fehsenfeld, F. C.; Brown, S. S. *Nat. Geosci.* **2008**, *1*, 324.
(597) Bertram, T. H.; Thornton, J. A. *Atmos. Chem. Phys.* **2009**, *9*, 8351.
(598) Roberts, J. M.; Osthoff, H. D.; Brown, S. S.; Ravishankara, A. R.; Coffman, D.; Quinn, P.; Bates, T. *Geophys. Res. Lett.* **2009**, *36*, L20808.
(599) Roberts, J. M.; Osthoff, H. D.; Brown, S. S.; Ravishankara, A. R. *Science* **2008**, *321*, 1059.
(600) Mielke, L. H.; Furgeson, A.; Osthoff, H. D. *Environ. Sci. Technol.* **2011**, *45*, 8889.

DOI: 10.1021/cr500447k
Chem. Rev. 2015, 115, 4259−4334

(601) Riedel, T. P.; Bertram, T. H.; Crisp, T. A.; Williams, E. J.; Lerner, B. M.; Vlasenko, A.; Li, S. M.; Gilman, J.; de Gouw, J.; Bon, D. M.; Wagner, N. L.; Brown, S. S.; Thornton, J. A. *Environ. Sci. Technol.* **2012**, *46*, 10463.
(602) Riedel, T. P.; Wagner, N. L.; Dubé, W. P.; Middlebrook, A. M.; Young, C. J.; Öztürk, F.; Bahreini, R.; VandenBoer, T. C.; Wolfe, D. E.; Williams, E. J.; Roberts, J. M.; Brown, S. S.; Thornton, J. A. *J. Geophys. Res.: Atmos.* **2013**, *118*, 8702.
(603) Thornton, J. A.; Abbatt, J. P. D. *J. Phys. Chem. A* **2005**, *109*, 10004.
(604) Folkers, M.; Mentel, T. F.; Wahner, A. *Geophys. Res. Lett.* **2003**, *30*, 1644.
(605) Schweitzer, F.; Mirabel, P.; George, C. *J. Phys. Chem. A* **1998**, *102*, 3942.
(606) Heal, M. R.; Harrison, M. A. J.; Cape, J. N. *Atmos. Environ.* **2007**, *41*, 3515.
(607) Thornton, J. A.; Kercher, J. P.; Riedel, T. P.; Wagner, N. L.; Cozic, J.; Holloway, J. S.; Dubé, W. P.; Wolfe, G. M.; Quinn, P. K.; Middlebrook, A. M.; Alexander, B.; Brown, S. S. *Nature* **2010**, *464*, 271.
(608) Phillips, G. J.; Tang, M. J.; Thieser, J.; Brickwedde, B.; Schuster, G.; Bohn, B.; Lelieveld, J.; Crowley, J. N. *Geophys. Res. Lett.* **2012**, *39*, L10811.
(609) Wagner, N. L.; Riedel, T. P.; Roberts, J. M.; Thornton, J. A.; Angevine, W. M.; Williams, E. J.; Lerner, B. M.; Vlasenko, A.; Li, S. M.; Dubé, W. P.; Coffman, D. J.; Bon, D. M.; de Gouw, J. A.; Kuster, W. C.; Gilman, J. B.; Brown, S. S. *J. Geophys. Res.: Atmos.* **2012**, *117*, D00V24.
(610) Young, C. J.; Washenfelder, R. A.; Roberts, J. M.; Mielke, L. H.; Osthoff, H. D.; Tsai, C.; Pikelnaya, O.; Stutz, J.; Veres, P. R.; Cochran, A. K.; VandenBoer, T. C.; Flynn, J.; Grossberg, N.; Haman, C. L.; Lefer, B.; Stark, H.; Graus, M.; de Gouw, J.; Gilman, J. B.; Kuster, W. C.; Brown, S. S. *Environ. Sci. Technol.* **2012**, *46*, 10965.
(611) Mielke, L. H.; Stutz, J.; Tsai, C.; Hurlock, S. C.; Roberts, J. M.; Veres, P. R.; Froyd, K. D.; Hayes, P. L.; Cubison, M. J.; Jimenez, J. L.; Washenfelder, R. A.; Young, C. J.; Gilman, J. B.; de Gouw, J. A.; Flynn, J. H.; Grossberg, N.; Lefer, B. L.; Liu, J.; Weber, R. J.; Osthoff, H. D. *J. Geophys. Res.: Atmos.* **2013**, *118*, 10638.
(612) Young, A. H.; Keene, W. C.; Pszenny, A. A. P.; Sander, R.; Thornton, J. A.; Riedel, T. P.; Maben, J. R. *J. Geophys. Res.: Atmos.* **2013**, *118*, 9414.
(613) Kim, M. J.; Farmer, D. K.; Bertram, T. H. *Proc. Natl. Acad. Sci. U.S.A.* **2014**, *111*, 3943.
(614) Tham, Y. J.; Yan, C.; Xue, L. K.; Zha, Q. Z.; Wang, X. F.; Wang, T. *Chin. Sci. Bull.* **2014**, *59*, 356.
(615) Simon, H.; Kimura, Y.; McGaughey, G.; Allen, D. T.; Brown, S. S.; Coffman, D.; Dibb, J.; Osthoff, H. D.; Quinn, P.; Roberts, J. M.; Yarwood, G.; Kemball-Cook, S.; Byun, D.; Lee, D. *Atmos. Environ.* **2010**, *44*, 5476.
(616) Riedel, T. P.; Bertram, T. H.; Ryder, O. S.; Liu, S.; Day, D. A.; Russell, L. M.; Gaston, C. J.; Prather, K. A.; Thornton, J. A. *Atmos. Chem. Phys.* **2012**, *12*, 2959.
(617) Simon, H.; Kimura, Y.; McGaughey, G.; Allen, D. T.; Brown, S. S.; Osthoff, H. D.; Roberts, J. M.; Byun, D.; Lee, D. *J. Geophys. Res.: Atmos.* **2009**, *114*, D00F03.
(618) Sarwar, G.; Simon, H.; Bhave, P.; Yarwood, G. *Atmos. Chem. Phys.* **2012**, *12*, 6455.
(619) Riedel, T. P.; Wolfe, G. M.; Danas, K. T.; Gilman, J. B.; Kuster, W. C.; Bon, D. M.; Vlasenko, A.; Li, S. M.; Williams, E. J.; Lerner, B. M.; Veres, P. R.; Roberts, J. M.; Holloway, J. S.; Lefer, B.; Brown, S. S.; Thornton, J. A. *Atmos. Chem. Phys.* **2014**, *14*, 3789.
(620) Sarwar, G.; Simon, H.; Xing, J.; Mathur, R. *Geophys. Res. Lett.* **2014**, *41*, 4050.
(621) Riemer, D. D.; Apel, E. C.; Orlando, J. J.; Tyndall, G. S.; Brune, W. H.; Williams, E. J.; Lonneman, W. A.; Neece, J. D. *J. Atmos. Chem.* **2008**, *61*, 227.
(622) Tanaka, P. L.; Riemer, D. D.; Chang, S. H.; Yarwood, G.; McDonald-Buller, E. C.; Apel, E. C.; Orlando, J. J.; Silva, P. J.; Jimenez, J. L.; Canagaratna, M. R.; Neece, J. D.; Mullins, C. B.; Allen, D. T. *Atmos. Environ.* **2003**, *37*, 1393.
(623) Cai, X.; Griffin, R. J. *J. Geophys. Res.: Atmos.* **2006**, *111*, D14206.
(624) Ofner, J.; Kamilli, K. A.; Held, A.; Lendl, B.; Zetzsch, C. *Faraday Discuss.* **2013**, *165*, 135.
(625) Karlsson, R. S.; Szente, J. J.; Ball, J. C.; Maricq, M. M. *J. Phys. Chem. A* **2001**, *105*, 82.
(626) Atkinson, R. *Atmos. Environ.* **2000**, *34*, 2063.
(627) Grosjean, D.; Grosjean, E.; Gertler, A. W. *Environ. Sci. Technol.* **2001**, *35*, 45.
(628) Hays, D. M.; Geron, D. C.; Linna, J. K.; Smith, D. M.; Schauer, J. J. *Environ. Sci. Technol.* **2002**, *36*, 2281.
(629) Sinreich, R.; Coburn, S.; Dix, B.; Volkamer, R. *Atmos. Chem. Phys.* **2010**, *10*, 11359.
(630) Volkamer, R.; Coburn, S.; Dix, B.; Sinreich, R. *Clivar Exchanges* **2010**, *15*, 30.
(631) Aumont, B.; Madronich, S.; Bey, I.; Tyndall, G. S. *J. Atmos. Chem.* **2000**, *35*, 59.
(632) Blando, J. D.; Turpin, B. J. *Atmos. Environ.* **2000**, *34*, 1623.
(633) Ervens, B.; George, C.; Williams, J. E.; Buxton, G. V.; Salmon, G. A.; Bydder, M.; Wilkinson, F.; Dentener, F.; Mirabel, P.; Wolke, R.; Herrmann, H. *J. Geophys. Res.: Atmos.* **2003**, *108*, 4426.
(634) Buxton, G. V.; Malone, T. N.; Salmon, G. A. *J. Chem. Soc., Faraday Trans.* **1997**, *93*, 2889.
(635) Neta, P.; Grodkowski, J.; Ross, A. B. *J. Phys. Chem. Ref. Data* **1996**, *25*, 709.
(636) Alfassi, Z.; Nielsen, O.; Wallington, T.; Benson, S.; Cohen, N.; Rhodes, C.; Hori, Y.; Getoff, N. In *The Chemistry of Free Radicals: Peroxyl Radicals*; Alfassi, Z. B., Ed.; John Wiley & Sons: West Sussex, UK, 1997.
(637) Mezyk, S. P.; Cooper, W. J.; Madden, K. P.; Bartels, D. M. *Environ. Sci. Technol.* **2004**, *38*, 3161.
(638) Ortiz-Montalvo, D. L.; Hakkinen, S. A. K.; Schwier, A. N.; Lim, Y. B.; McNeill, V. F.; Turpin, B. J. *Environ. Sci. Technol.* **2014**, *48*, 255.
(639) Arneth, A.; Schurgers, G.; Lathiere, J.; Duhl, T.; Beerling, D. J.; Hewitt, C. N.; Martin, M.; Guenther, A. *Atmos. Chem. Phys.* **2011**, *11*, 8037.
(640) Sharkey, T. D.; Wiberley, A. E.; Donohue, A. R. *Ann. Bot.* **2008**, *101*, 5.
(641) Trainer, M.; Williams, E. J.; Parrish, D. D.; Buhr, M. P.; Allwine, E. J.; Westberg, H. H.; Fehsenfeld, F. C.; Liu, S. C. *Nature* **1987**, *329*, 705.
(642) Chameides, W. L.; Fehsenfeld, F.; Rodgers, M. O.; Cardelino, C.; Martinez, J.; Parrish, D.; Lonneman, W.; Lawson, D. R.; Rasmussen, R. A.; Zimmerman, P.; Greenberg, J.; Middleton, P.; Wang, T. *J. Geophys. Res.: Atmos.* **1992**, *97*, 6037.
(643) Claeys, M.; Graham, B.; Vas, G.; Wang, W.; Vermeylen, R.; Pashynska, V.; Cafmeyer, J.; Guyon, P.; Andreae, M. O.; Artaxo, P.; Maenhaut, W. *Science* **2004**, *303*, 1173.
(644) Kanakidou, M.; Seinfeld, J. H.; Pandis, S. N.; Barnes, I.; Dentener, F. J.; Facchini, M. C.; Van Dingenen, R.; Ervens, B.; Nenes, A.; Nielsen, C. J.; Swietlicki, E.; Putaud, J. P.; Balkanski, Y.; Fuzzi, S.; Horth, J.; Moortgat, G. K.; Winterhalter, R.; Myhre, C. E. L.; Tsigaridis, K.; Vignati, E.; Stephanou, E. G.; Wilson, J. *Atmos. Chem. Phys.* **2005**, *5*, 1053.
(645) Kalberer, M.; Paulsen, D.; Sax, M.; Steinbacher, M.; Dommen, J.; Prevot, A. S. H.; Fisseha, R.; Weingartner, E.; Frankevich, V.; Zenobi, R.; Baltensperger, U. *Science* **2004**, *303*, 1659.
(646) Kroll, J. H.; Ng, N. L.; Murphy, S. M.; Flagan, R. C.; Seinfeld, J. H. *Geophys. Res. Lett.* **2005**, *32*, L18808.
(647) Kroll, J. H.; Ng, N. L.; Murphy, S. M.; Flagan, R. C.; Seinfeld, J. H. *Environ. Sci. Technol.* **2006**, *40*, 1869.
(648) Böge, O.; Miao, Y.; Plewka, A.; Herrmann, H. *Atmos. Environ.* **2006**, *40*, 2501.
(649) Kleindienst, T. E.; Edney, E. O.; Lewandowski, M.; Offenberg, J. H.; Jaoui, M. *Environ. Sci. Technol.* **2006**, *40*, 3807.
(650) Kleindienst, T. E.; Lewandowski, M.; Offenberg, J. H.; Jaoui, M.; Edney, E. O. *Geophys. Res. Lett.* **2007**, *34*, L01805.

DOI: 10.1021/cr500447k
Chem. Rev. 2015, 115, 4259−4334

(651) Nguyen, T. B.; Bateman, A. P.; Bones, D. L.; Nizkorodov, S. A.; Laskin, J.; Laskin, A. *Atmos. Environ.* **2010**, *44*, 1032.
(652) Liu, Y.; Monod, A.; Tritscher, T.; Praplan, A. P.; DeCarlo, P. F.; Temime-Roussel, B.; Quivet, E.; Marchand, N.; Dommen, J.; Baltensperger, U. *Atmos. Chem. Phys.* **2012**, *12*, 5879.
(653) Atkinson, R.; Arey, J. *Chem. Rev.* **2003**, *103*, 4605.
(654) Nölscher, A.; Butler, T.; Auld, J.; Veres, P.; Muñoz, A.; Taraborrelli, D.; Vereecken, L.; Lelieveld, J.; Williams, J. *Atmos. Environ.* **2014**, *89*, 453.
(655) Grosjean, E.; Grosjean, D. *Int. J. Chem. Kinet.* **1996**, *28*, 911.
(656) Lindinger, W.; Hansel, A.; Jordan, A. *Int. J. Mass Spectrom. Ion Processes* **1998**, *173*, 191.
(657) Gäb, S.; Turner, W. V.; Wolff, S.; Becker, K. H.; Ruppert, L.; Brockmann, K. J. *Atmos. Environ.* **1995**, *29*, 2401.
(658) Wang, H. L.; Huang, D.; Zhang, X.; Zhao, Y.; Chen, Z. M. *Atmos. Chem. Phys.* **2012**, *12*, 7187.
(659) Iraci, L. T.; Baker, B. M.; Tyndall, G. S.; Orlando, J. J. *J. Atmos. Chem.* **1999**, *33*, 321.
(660) van Pinxteren, D.; Plewka, A.; Hoffmann, D.; Müller, K.; Kramberger, H.; Svrcina, B.; Bächmann, K.; Jaeschke, W.; Mertes, S.; Collett, J. L., Jr.; Herrmann, H. *Atmos. Environ.* **2005**, *39*, 4305.
(661) Zhu, L. H.; Chen, Z. M. *Huanjing Kexue* **2005**, *26*, 83.
(662) Umschlag, T.; Herrmann, H.; Zellner, R. *Proceedings of EUROTRAC Symposium '98: Transport and Chemical Transformation in the Troposphere*; Garmisch-Partenkirchen: Germany, 1999; p 694.
(663) Buxton, G. V.; Salmon, G. A.; Williams, J. E. *J. Atmos. Chem.* **2000**, *36*, 111.
(664) Liu, Y.; Siekmann, F.; Renard, P.; El Zein, A.; Salque, G.; El Haddad, I.; Temime-Roussel, B.; Voisin, D.; Thissen, R.; Monod, A. *Atmos. Environ.* **2012**, *49*, 123.
(665) Renard, P.; Siekmann, F.; Salque, G.; Demelas, C.; Coulomb, B.; Vassalo, L.; Ravier, S.; Temime-Roussel, B.; Voisin, D.; Monod, A. *Atmos. Chem. Phys.* **2015**, *15*, 21.
(666) Paulot, F.; Crounse, J. D.; Kjaergaard, H. G.; Kuerten, A.; St Clair, J. M.; Seinfeld, J. H.; Wennberg, P. O. *Science* **2009**, *325*, 730.
(667) Surratt, J. D.; Chan, A. W. H.; Eddingsaas, N. C.; Chan, M. N.; Loza, C. L.; Kwan, A. J.; Hersey, S. P.; Flagan, R. C.; Wennberg, P. O.; Seinfeld, J. H. *Proc. Natl. Acad. Sci. U.S.A.* **2010**, *107*, 6640.
(668) Lin, Y. H.; Zhang, Z.; Docherty, K. S.; Zhang, H.; Budisulistiorini, S. H.; Rubitschun, C. L.; Shaw, S. L.; Knipping, E. M.; Edgerton, E. S.; Kleindienst, T. E.; Gold, A.; Surratt, J. D. *Environ. Sci. Technol.* **2012**, *46*, 250.
(669) Lin, Y. H.; Zhang, H.; Pye, H. O. T.; Zhang, Z.; Marth, W. J.; Park, S.; Arashiro, M.; Cui, T.; Budisulistiorini, S. H.; Sexton, K. G.; Vizuete, W.; Xie, Y.; Luecken, D. J.; Piletic, I. R.; Edney, E. O.; Bartolotti, L. J.; Gold, A.; Surratt, J. D. *Proc. Natl. Acad. Sci. U.S.A.* **2013**, *110*, 6718.
(670) Froyd, K. D.; Murphy, S. M.; Murphy, D. M.; de Gouw, J. A.; Eddingsaas, N. C.; Wennberg, P. O. *Proc. Natl. Acad. Sci. U.S.A.* **2010**, *107*, 21360.
(671) Minerath, E. C.; Schultz, M. P.; Elrod, M. J. *Environ. Sci. Technol.* **2009**, *43*, 8133.
(672) Cole-Filipiak, N. C.; O'Connor, A. E.; Elrod, M. J. *Environ. Sci. Technol.* **2010**, *44*, 6718.
(673) Eddingsaas, N. C.; VanderVelde, D. G.; Wennberg, P. O. *J. Phys. Chem. A* **2010**, *114*, 8106.
(674) Lal, V.; Khalizov, A. F.; Lin, Y.; Galvan, M. D.; Connell, B. T.; Zhang, R. *J. Phys. Chem. A* **2012**, *116*, 6078.
(675) Wang, T.-H.; Liu, Z.; Wang, W.-G.; Ge, M.-F. *Acta Phys. Chim. Sin.* **2012**, *28*, 1608.
(676) Bleier, D. B.; Elrod, M. J. *J. Phys. Chem. A* **2013**, *117*, 4223.
(677) Darer, A. I.; Cole-Filipiak, N. C.; O'Connor, A. E.; Elrod, M. J. *Environ. Sci. Technol.* **2011**, *45*, 1895.
(678) Hu, K. S.; Darer, A. I.; Elrod, M. J. *Atmos. Chem. Phys.* **2011**, *11*, 8307.
(679) Tanner, R. L.; Olszyna, K. J.; Edgerton, E. S.; Knipping, E. M.; Shaw, S. L. *Atmos. Environ.* **2009**, *43*, 3440.
(680) Budisulistiorini, S. H.; Canagaratna, M. R.; Croteau, P. L.; Marth, W. J.; Baumann, K.; Edgerton, E. S.; Shaw, S. L.; Knipping, E. M.; Worsnop, D. R.; Jayne, J. T.; Gold, A.; Surratt, J. D. *Environ. Sci. Technol.* **2013**, *47*, 5686.
(681) Lin, Y. H.; Knipping, E. M.; Edgerton, E. S.; Shaw, S. L.; Surratt, J. D. *Atmos. Chem. Phys.* **2013**, *13*, 8457.
(682) Nguyen, T. B.; Coggon, M. M.; Bates, K. H.; Zhang, X.; Schwantes, R. H.; Schilling, K. A.; Loza, C. L.; Flagan, R. C.; Wennberg, P. O.; Seinfeld, J. H. *Atmos. Chem. Phys.* **2014**, *14*, 3497.
(683) Jacobs, M. I.; Darer, A. I.; Elrod, M. J. *Environ. Sci. Technol.* **2013**, *47*, 12868.
(684) Bates, K. H.; Crounse, J. D.; St. Clair, J. M.; Bennett, N. B.; Nguyen, T. B.; Seinfeld, J. H.; Stoltz, B. M.; Wennberg, P. O. *J. Phys. Chem. A* **2014**, *118*, 1237.
(685) Chan, M. N.; Surratt, J. D.; Claeys, M.; Edgerton, E. S.; Tanner, R. L.; Shaw, S. L.; Zheng, M.; Knipping, E. M.; Eddingsaas, N. C.; Wennberg, P. O.; Seinfeld, J. H. *Environ. Sci. Technol.* **2010**, *44*, 4590.
(686) Stone, E. A.; Yang, L.; Yu, L. E.; Rupakheti, M. *Atmos. Environ.* **2012**, *47*, 323.
(687) Worton, D. R.; Surratt, J. D.; LaFranchi, B. W.; Chan, A. W. H.; Zhao, Y.; Weber, R. J.; Park, J.-H.; Gilman, J. B.; de Gouw, J.; Park, C.; Schade, G.; Beaver, M.; St. Clair, J. M.; Crounse, J.; Wennberg, P.; Wolfe, G. M.; Harrold, S.; Thornton, J. A.; Farmer, D. K.; Docherty, K. S.; Cubison, M. J.; Jimenez, J.-L.; Frossard, A. A.; Russell, L. M.; Kristensen, K.; Glasius, M.; Mao, J.; Ren, X.; Brune, W.; Browne, E. C.; Pusede, S. E.; Cohen, R. C.; Seinfeld, J. H.; Goldstein, A. H. *Environ. Sci. Technol.* **2013**, *47*, 11403.
(688) Lin, G.; Penner, J. E.; Sillman, S.; Taraborrelli, D.; Lelieveld, J. *Atmos. Chem. Phys.* **2012**, *12*, 4743.
(689) Couvidat, F.; Sartelet, K.; Seigneur, C. *Environ. Sci. Technol.* **2013**, *47*, 914.
(690) Pye, H. O. T.; Pinder, R. W.; Piletic, I. R.; Xie, Y.; Capps, S. L.; Lin, Y.-H.; Surratt, J. D.; Zhang, Z.; Gold, A.; Luecken, D. J.; Hutzell, W. T.; Jaoui, M.; Offenberg, J. H.; Kleindienst, T. E.; Lewandowski, M.; Edney, E. O. *Environ. Sci. Technol.* **2013**, *47*, 11056.
(691) Karambelas, A.; Pye, H. O. T.; Budisulistiorini, S. H.; Surratt, J. D.; Pinder, R. W. *Environ. Sci. Technol. Lett.* **2014**, *1*, 278.
(692) Berndt, T.; Böge, O.; Stratmann, F. *Atmos. Environ.* **2003**, *37*, 3933.
(693) Eddingsaas, N. C.; Loza, C. L.; Yee, L. D.; Seinfeld, J. H.; Wennberg, P. O. *Atmos. Chem. Phys.* **2012**, *12*, 6489.
(694) Iinuma, Y.; Böge, O.; Kahnt, A.; Herrmann, H. *Phys. Chem. Chem. Phys.* **2009**, *11*, 7985.
(695) Iinuma, Y.; Kahnt, A.; Mutzel, A.; Böge, O.; Herrmann, H. *Environ. Sci. Technol.* **2013**, *47*, 3639.
(696) Drozd, G. T.; Woo, J. L.; McNeill, V. F. *Atmos. Chem. Phys.* **2013**, *13*, 8255.
(697) Zhang, H.; Zhang, Z.; Cui, T.; Lin, Y.-H.; Bhathela, N. A.; Ortega, J.; Worton, D. R.; Goldstein, A. H.; Guenther, A.; Jimenez, J. L.; Gold, A.; Surratt, J. D. *Environ. Sci. Technol. Lett.* **2014**, *1*, 242.
(698) Iinuma, Y.; Müller, C.; Berndt, T.; Böge, O.; Claeys, M.; Herrmann, H. *Environ. Sci. Technol.* **2007**, *41*, 6678.
(699) Surratt, J. D.; Gómez-González, Y.; Chan, A. W. H.; Vermeylen, R.; Shahgholi, M.; Kleindienst, T. E.; Edney, E. O.; Offenberg, J. H.; Lewandowski, M.; Jaoui, M.; Maenhaut, W.; Claeys, M.; Flagan, R. C.; Seinfeld, J. H. *J. Phys. Chem. A* **2008**, *112*, 8345.
(700) Romero, F.; Oehme, M. *J. Atmos. Chem.* **2005**, *52*, 283.
(701) Ma, Y.; Chen, J.; Wang, L. *Prog. Chem.* **2012**, *24*, 2277.
(702) Szmigielski, R. Chemistry of organic sulfates and nitrates in the urban atmosphere. In *Disposal of Dangerous Chemicals in Urban Areas and Mega Cities*; Barnes, I., Rudziński, K. J., Eds.; Springer: Dordrecht, 2013.
(703) Minerath, E. C.; Casale, M. T.; Elrod, M. J. *Environ. Sci. Technol.* **2008**, *42*, 4410.
(704) Chan, A. W. H.; Galloway, M. M.; Kwan, A. J.; Chhabra, P. S.; Keutsch, F. N.; Wennberg, P. O.; Flagan, R. C.; Seinfeld, J. H. *Environ. Sci. Technol.* **2009**, *43*, 4647.
(705) Zhang, H.; Worton, D. R.; Lewandowski, M.; Ortega, J.; Rubitschun, C. L.; Park, J.-H.; Kristensen, K.; Campuzano-Jost, P.; Day, D. A.; Jimenez, J. L.; Jaoui, M.; Offenberg, J. H.; Kleindienst, T.

DOI: 10.1021/cr500447k
Chem. Rev. 2015, 115, 4259−4334

E.; Gilman, J.; Kuster, W. C.; de Gouw, J.; Park, C.; Schade, G. W.; Frossard, A. A.; Russell, L.; Kaser, L.; Jud, W.; Hansel, A.; Cappellin, L.; Karl, T.; Glasius, M.; Guenther, A.; Goldstein, A. H.; Seinfeld, J. H.; Gold, A.; Kamens, R. M.; Surratt, J. D. *Environ. Sci. Technol.* **2012**, *46*, 9437.
(706) Rudziński, K. J.; Gmachowski, L.; Kuznietsova, I. *Atmos. Chem. Phys.* **2009**, *9*, 2129.
(707) Nozière, B.; Ekström, S.; Alsberg, T.; Holmström, S. *Geophys. Res. Lett.* **2010**, *37*, L05806.
(708) Tolocka, M. P.; Turpin, B. *Environ. Sci. Technol.* **2012**, *46*, 7978.
(709) Nguyen, Q. T.; Kristensen, T. B.; Hansen, A. M. K.; Skov, H.; Bossi, R.; Massling, A.; Sørensen, L. L.; Bilde, M.; Glasius, M.; Nøjgaard, J. K. *J. Geophys. Res.: Atmos.* **2014**, *119*, 5011.
(710) Hansen, A. M. K.; Kristensen, K.; Nguyen, Q. T.; Zare, A.; Cozzi, F.; Nøjgaard, J. K.; Skov, H.; Brandt, J.; Christensen, J. H.; Ström, J.; Tunved, P.; Krejci, R.; Glasius, M. *Atmos. Chem. Phys.* **2014**, *14*, 7807.
(711) Tao, S.; Lu, X.; Levac, N.; Bateman, A. P.; Nguyen, T. B.; Bones, D. L.; Nizkorodov, S. A.; Laskin, J.; Laskin, A.; Yang, X. *Environ. Sci. Technol.* **2014**, *48*, 10993.
(712) He, Q.-F.; Ding, X.; Wang, X.-M.; Yu, J.-Z.; Fu, X.-X.; Liu, T.-Y.; Zhang, Z.; Xue, J.; Chen, D.-H.; Zhong, L.-J.; Donahue, N. M. *Environ. Sci. Technol.* **2014**, *48*, 9236.
(713) Lin, P.; Yu, J. Z.; Engling, G.; Kalberer, M. *Environ. Sci. Technol.* **2012**, *46*, 13118.
(714) Ma, Y.; Xu, X.; Song, W.; Geng, F.; Wang, L. *Atmos. Environ.* **2014**, *85*, 152.
(715) Kundu, S.; Quraishi, T. A.; Yu, G.; Suarez, C.; Keutsch, F. N.; Stone, E. A. *Atmos. Chem. Phys.* **2013**, *13*, 4865.
(716) Staudt, S.; Kundu, S.; Lehmler, H.-J.; He, X. R.; Cui, T. Q.; Lin, Y. H.; Kristensen, K.; Glasius, M.; Zhang, X. L.; Weber, R. J.; Surratt, J. D.; Stone, E. A. *Atmos. Environ.* **2014**, *94*, 366.
(717) Hatch, L. E.; Creamean, J. M.; Ault, A. P.; Surratt, J. D.; Chan, M. N.; Seinfeld, J. H.; Edgerton, E. S.; Su, Y.; Prather, K. A. *Environ. Sci. Technol.* **2011**, *45*, 8648.
(718) Olson, C. N.; Galloway, M. M.; Yu, G.; Hedman, C. J.; Lockett, M. R.; Yoon, T.; Stone, E. A.; Smith, L. M.; Keutsch, F. N. *Environ. Sci. Technol.* **2011**, *45*, 6468.
(719) De Haan, D. O.; Tolbert, M. A.; Jimenez, J. L. *Geophys. Res. Lett.* **2009**, *36*, L11819.
(720) Hamilton, J. F.; Baeza-Romero, M. T.; Finessi, E.; Rickard, A. R.; Healy, R. M.; Peppe, S.; Adams, T. J.; Daniels, M. J. S.; Ball, S. M.; Goodall, I. C. A.; Monks, P. S.; Borrás, E.; Muñoz, A. *Faraday Discuss.* **2013**, *165*, 447.
(721) Kampf, C. J.; Jakob, R.; Hoffmann, T. *Atmos. Chem. Phys.* **2012**, *12*, 6323.
(722) Trainic, M.; Abo Riziq, A.; Lavi, A.; Flores, J. M.; Rudich, Y. *Atmos. Chem. Phys.* **2011**, *11*, 9697.
(723) Laskin, A.; Smith, J. S.; Laskin, J. *Environ. Sci. Technol.* **2009**, *43*, 3764.
(724) Debus, H. *Justus Liebigs Ann. Chem.* **1858**, *107*, 199.
(725) Updyke, K. M.; Nguyen, T. B.; Nizkorodov, S. A. *Atmos. Environ.* **2012**, *63*, 22.
(726) Shapiro, E. L.; Szprengiel, J.; Sareen, N.; Jen, C. N.; Giordano, M. R.; McNeill, V. F. *Atmos. Chem. Phys.* **2009**, *9*, 2289.
(727) Yu, X.; Shi, C.; Ma, J.; Zhu, B.; Li, M.; Wang, J.; Yang, S.; Kang, N. *Atmos. Environ.* **2013**, *81*, 475.
(728) Geddes, S.; Zahardis, J.; Petrucci, G. A. *J. Atmos. Chem.* **2009**, *63*, 187.
(729) Azar, C.; Lindgren, K.; Larson, E.; Möllersten, K. *Clim. Change* **2006**, *74*, 47.
(730) Gibbins, J.; Chalmers, H. *Energy Policy* **2008**, *36*, 4317.
(731) Qiu, C.; Zhang, R. *Phys. Chem. Chem. Phys.* **2013**, *15*, 5738.
(732) Wang, Y.; Zhang, J.; Marcotte, A. R.; Karl, M.; Dye, C.; Herckes, P. *Atmos. Res.* **2014**, *151*, 72.
(733) Poste, A. E.; Grung, M.; Wright, R. F. *Sci. Total Environ.* **2014**, *481*, 274.
(734) Morris, C. E.; Sands, D. C.; Bardin, M.; Jaenicke, R.; Vogel, B.; Leyronas, C.; Ariya, P. A.; Psenner, R. *Biogeosciences* **2011**, *8*, 17.
(735) Després, V. R.; Alex, H. J.; Burrows, S. M.; Hoose, C.; Safatov, A. S.; Buryak, G.; Fröhlich-Nowoisky, J.; Elbert, W.; Andreae, M. O.; Pöschl, U.; Jaenicke, R. *Tellus, Ser. B* **2012**, *64*, 15598.
(736) Burrows, S. M.; Elbert, W.; Lawrence, M. G.; Pöschl, U. *Atmos. Chem. Phys.* **2009**, *9*, 9263.
(737) Christner, B. C.; Cai, R.; Morris, C. E.; McCarter, K. S.; Foreman, C. M.; Skidmore, M. L.; Montross, S. N.; Sands, D. C. *Proc. Natl. Acad. Sci. U.S.A.* **2008**, *105*, 18854.
(738) Jaenicke, R. *Science* **2005**, *308*, 73.
(739) Burrows, S. M.; Butler, T.; Jöckel, P.; Tost, H.; Kerkweg, A.; Pöschl, U.; Lawrence, M. G. *Atmos. Chem. Phys.* **2009**, *9*, 9281.
(740) Möhler, O.; Georgakopoulos, D. G.; Morris, C. E.; Benz, S.; Ebert, V.; Hunsmann, S.; Saathoff, H.; Schnaiter, M.; Wagner, R. *Biogeosciences* **2008**, *5*, 1425.
(741) Möhler, O.; DeMott, P. J.; Vali, G.; Levin, Z. *Biogeosciences* **2007**, *4*, 1059.
(742) Diehl, K.; Wurzler, S. *Atmos. Environ.* **2010**, *44*, 4622.
(743) Sattler, B.; Puxbaum, H.; Psenner, R. *Geophys. Res. Lett.* **2001**, *28*, 239.
(744) Amato, P.; Ménager, M.; Sancelme, M.; Laj, P.; Mailhot, G.; Delort, A.-M. *Atmos. Environ.* **2005**, *39*, 4143.
(745) Amato, P.; Demeer, F.; Melaouhi, A.; Fontanella, S.; Martin-Biesse, A. S.; Sancelme, M.; Laj, P.; Delort, A.-M. *Atmos. Chem. Phys.* **2007**, *7*, 4159.
(746) Vaïtilingom, M.; Amato, P.; Sancelme, M.; Laj, P.; Leriche, M.; Delort, A. M. *Appl. Environ. Microbiol.* **2010**, *76*, 23.
(747) Vaïtilingom, M.; Attard, E.; Gaiani, N.; Sancelme, M.; Deguillaume, L.; Flossmann, A. I.; Amato, P.; Delort, A.-M. *Atmos. Environ.* **2012**, *56*, 88.
(748) Vaïtilingom, M.; Deguillaume, L.; Vinatier, V.; Sancelme, M.; Amato, P.; Chaumerliac, N.; Delort, A.-M. *Proc. Natl. Acad. Sci. U.S.A.* **2013**, *110*, 559.
(749) Kourtev, P. S.; Hill, K. A.; Shepson, P. B.; Konopka, A. *Atmos. Environ.* **2011**, *45*, 5399.
(750) Herlihy, L. J.; Galloway, J. N.; Mills, A. L. *Atmos. Environ.* **1987**, *21*, 2397.
(751) Ariya, P. A.; Nepotchatykh, O.; Ignatova, O.; Amyot, M. *Geophys. Res. Lett.* **2002**, *29*, 34.
(752) Deguillaume, L.; Leriche, M.; Amato, P.; Ariya, P. A.; Delort, A.-M.; Pöschl, U.; Chaumerliac, N.; Bauer, H.; Flossmann, A. I.; Morris, C. E. *Biogeosciences* **2008**, *5*, 1073.
(753) Husárová, S.; Vaïtilingom, M.; Deguillaume, L.; Traikia, M.; Vinatier, V.; Sancelme, M.; Amato, P.; Matulová, M.; Delort, A.-M. *Atmos. Environ.* **2011**, *45*, 6093.
(754) Vaïtilingom, M.; Charbouillot, T.; Deguillaume, L.; Maisonobe, R.; Parazols, M.; Amato, P.; Sancelme, M.; Delort, A. M. *Atmos. Chem. Phys.* **2011**, *11*, 8721.
(755) DeLeon-Rodriguez, N.; Lathem, T. L.; Rodriguez-R, L. M.; Barazesh, J. M.; Anderson, B. E.; Beyersdorf, A. J.; Ziemba, L. D.; Bergin, M.; Nenes, A.; Konstantinidis, K. T. *Proc. Natl. Acad. Sci. U.S.A.* **2013**, *110*, 2575.
(756) Boucher, O.; Randall, D.; Artaxo, P.; Bretherton, C.; Feingold, G.; Forster, P.; Kerminen, V.-M.; Kondo, Y.; Liao, H.; Lohmann, U.; Rasch, P.; Satheesh, S. K.; Sherwood, S.; Stevens, B.; Zhang, X. Y. In *Climate Change 2013: The Physical Science Basis. Contribution of Working Group I to the Fifth Assessment Report of the Intergovernmental Panel on Climate Change*; Stocker, T. F., Qin, D., Plattner, G.-K., Tignor, M., Allen, S. K., Boschung, J., Nauels, A., Xia, Y., Bex, V., Midgley, P. M., Eds.; Cambridge University Press: Cambridge, United Kingdom and New York, NY, 2013.
(757) Biermann, A.; Engel, A.; Riebesell, U. *J. Plankton Res.* **2014**, *36*, 658.
(758) Sett, S.; Bach, L. T.; Schulz, K. G.; Koch-Klavsen, S.; Lebrato, M.; Riebesell, U. *PLoS One* **2014**, *9*, e88308.
(759) Riahi, K.; Rao, S.; Krey, V.; Cho, C. H.; Chirkov, V.; Fischer, G.; Kindermann, G.; Nakicenovic, N.; Rafaj, P. *Clim. Change* **2011**, *109*, 33.

DOI: 10.1021/cr500447k
Chem. Rev. 2015, 115, 4259−4334

(760) Czerny, J.; Schulz, K. G.; Boxhammer, T.; Bellerby, R. G. J.; Buedenbender, J.; Engel, A.; Krug, S. A.; Ludwig, A.; Nachtigall, K.; Nondal, G.; Niehoff, B.; Silyakova, A.; Riebesell, U. *Biogeosciences* **2013**, *10*, 3109.
(761) Mueller, M. N.; Lebrato, M.; Riebesell, U.; Barcelos e Ramos, J.; Schulz, K. G.; Blanco Ameijeiras, S.; Sett, S.; Eisenhauer, A.; Stoll, H. M. *Biogeosciences* **2014**, *11*, 1065.
(762) Engel, A.; Piontek, J.; Grossart, H.-P.; Riebesell, U.; Schulz, K. G.; Sperling, M. *J. Plankton Res.* **2014**, *36*, 641.
(763) Brussaard, C. P. D.; Noordeloos, A. A. M.; Witte, H.; Collenteur, M. C. J.; Schulz, K. G.; Ludwig, A.; Riebesell, U. *Biogeosciences* **2013**, *10*, 719.
(764) Zhang, Q.; Jimenez, J. L.; Worsnop, D. R.; Canagaratna, M. *Environ. Sci. Technol.* **2007**, *41*, 3213.
(765) Benedict, K. B.; Lee, T.; Collett, J. L. *Atmos. Environ.* **2012**, *46*, 104.
(766) Navarro, J. C. A.; Smolander, S.; Struthers, H.; Zorita, E.; Ekman, A. M. L.; Kaplan, J. O.; Guenther, A.; Arneth, A.; Riipinen, I. *J. Geophys. Res.: Atmos.* **2014**, *119*, 6867.
(767) Sofen, E. D.; Alexander, B.; Kunasek, S. A. *Atmos. Chem. Phys.* **2011**, *11*, 3565.
(768) Raes, F.; Liao, H.; Chen, W. T.; Seinfeld, J. H. *J. Geophys. Res.: Atmos.* **2010**, *115*, D12121.
(769) Isaksen, I.; Granier, C.; Myhre, G.; Berntsen, T.; Dalsøren, S.; Gauss, M.; Klimont, Z.; Benestad, R.; Bousquet, P.; Collins, W.; Cox, T.; Eyring, V.; Fowler, D.; Fuzzi, S.; Jöckel, P.; Laj, P.; Lohmann, U.; Maione, M.; Monks, P. S.; Prevot, A. S. H.; Raes, F.; Richter, A.; Rogenerud, B.; Schulz, M.; Schindell, D.; Stevenson, D. S.; Storelmo, T.; Wang, W. C.; van Weele, M.; Wird, M.; Wuebbles, D. *Atmos. Environ.* **2009**, *43*, 5138.
(770) Barth, M. C.; Rasch, P. J.; Kiehl, J. T.; Benkovitz, C. M.; Schwartz, S. E. *J. Geophys. Res.: Atmos.* **2000**, *105*, 1387.
(771) Rodhe, H. *Nature* **1999**, *401*, 223.
(772) Wuebbles, D. J.; Grant, K. E.; Connell, P. S.; Penner, J. E. *JAPCA* **1989**, *39*, 22.
(773) Emmons, L. K.; Carroll, M. A.; Hauglustaine, D. A.; Brasseur, G. P.; Atherton, C.; Penner, J.; Sillman, S.; Levy, H.; Rohrer, F.; Wauben, W. M. F.; VanVelthoven, P. F. J.; Wang, Y.; Jacob, D.; Bakwin, P.; Dickerson, R.; Doddridge, B.; Gerbig, C.; Honrath, R.; Hübler, G.; Jaffe, D.; Kondo, Y.; Munger, J. W.; Torres, A.; Volz-Thomas, A. *Atmos. Environ.* **1997**, *31*, 1851.
(774) *HALIPP: Heterogeneous and Liquid Phase Processes*; Warneck, P., Ed.; Springer: New York, 2000.
(775) *Transport and Chemical Transformation of Pollutants in the Troposphere: An Overview of the Work of EUROTRAC*; Borrell, P., Borrell, P. M., Eds.; Springer: Berlin, 2012.
(776) Ehn, M.; Thornton, J. A.; Kleist, E.; Sipilä, M.; Junninen, H.; Pullinen, I.; Springer, M.; Rubach, F.; Tillmann, R.; Lee, B.; Lopez-Hilfiker, F.; Andres, S.; Acir, I.-H.; Rissanen, M.; Jokinen, T.; Schobesberger, S.; Kangasluoma, J.; Kontkanen, J.; Nieminen, T.; Kurtén, T.; Nielsen, L. B.; Jørgensen, S.; Kjaergaard, H. G.; Canagaratna, M. R.; Dal Maso, M.; Berndt, T.; Petäjä, T.; Wahner, A.; Kerminen, V.-M.; Kulmala, M.; Worsnop, D. R.; Wildt, J.; Mentel, T. F. *Nature* **2014**, *506*, 476.

DOI: 10.1021/cr500447k
Chem. Rev. 2015, 115, 4259−4334